UNIVERSITÉ DE STRASBOURG

ÉCOLE DOCTORALE Physique et Chimie-Physique

ICPEES- Institut de Chimie et Procédés pour l'Energie, l'Environnement et la Santé (UMR 7515)

THÈSE présentée par :

Murielle Oster

Soutenue le : **19 novembre 2014**

Pour obtenir le grade de : **Docteur de l'université de Strasbourg**

Discipline/ Spécialité : Chimie des Matériaux

Elaboration of functional cyclodextrin based nanofibres for biomedical applications

RAPPORTEURS :

M. Frédéric BOSSARD	Professeur des universités, Université de Grenoble
M. Bernard MARTEL	Professeur des universités, Université de Lille 1

EXAMINATEURS :

M. Jean-François LUTZ	Directeur de recherche (CNRS), ICS Strasbourg
M. Gerhard WENZ	Professeur des universités, Universität des Saarlandes

THÈSE dirigée par :

M. Guy SCHLATTER	Professeur des universités, Université de Strasbourg

A mes parents;

A Paul;

A mes frères.

Remerciements

Cette thèse a été réalisée à l'Institut de Chimie et Procédés pour l'Energie, l'Environnement et la Santé (ICPEES, UdS, ECPM, CNRS UMR 7515) à Strasbourg sous la direction du Professeur Guy Schlatter et sous la supervision du Docteur Anne Hébraud. Ces travaux ont été financés par l'Agence Nationale pour la Recherche (ANR, FibRotaxanes, ANR Blanc 2011).

Je tiens très sincèrement à remercier le Professeur Guy Schlatter et le Docteur Anne Hébraud pour leur aide tout au long de ces trois années. Merci pour leurs conseils qui m'ont permis d'avancer et de résoudre les quelques petits tracas rencontrés. Le sujet qu'ils ont accepté de me confier s'est avéré être très intéressant et plein de découvertes surprenantes. Merci pour leur disponibilité tout au long de ces travaux et pour la rédaction des différents papiers et de ce manuscrit. Ce fut la présentation de Guy, il y a maintenant quelques années de cela, qui m'avait donné envie d'étudier les polymères et m'avait montré toutes les applications possibles avec ces macromolécules. Sa passion et son aisance à décrire les polymères (en donnant mes cheveux « non coiffés » en exemple comme représentation imagée de l'organisation des chaines polymériques) étant très communicatives, j'ai toujours voulu aller plus loin et apprendre plus au sujet des polymères. Un grand merci également à Anne pour m'avoir rappelé sans cesse que tout irait bien et que je stressais beaucoup trop. Merci aussi de m'avoir accompagnée à Saclay et d'avoir pédalé avec moi au milieu des lapins.

Je tiens à exprimer ma gratitude aux Professeur Bernard Martel (Université Lille 1, Lille) et Professeur Frédéric Bossard (Université de Grenoble, Grenoble) pour avoir accepté de juger ce travail de thèse. J'exprime également ma reconnaissance au Professeur Gerhard Wenz qui nous a fait l'honneur de venir évaluer ces travaux lors de la soutenance. Je tiens également à remercier le Directeur de Recherche Jean-François Lutz (Institut Charles Sadron, Strasbourg) de m'avoir fait l'honneur de présider mon jury de thèse.

Je remercie très vivement Monsieur Christophe Fajolles pour toutes nos discussions autour des cyclodextrines et de leur chimie pour avancer au mieux dans ce projet. Merci d’avoir toujours répondu présent lorsque nous avions besoin d’éclaircissements concernant les pseudo-polyrotaxanes ou la chimie des cyclodextrines.

J’exprime également ma gratitude au Professeur Luc Avérous et au Docteur Eric Pollet pour leur implication et leur soutien dans ce projet de thèse. Ils ont su me faire part de leurs expériences et de leurs connaissances concernant la chimie des polymères.

Je remercie également nos partenaires sur le projet relatif à l’electrospinning des polysaccharides et des polyélectrolytes : le Professeur Pierre Schaaf (INSERM 1121, Strasbourg), le Docteur Fouzia Boulmedais (Institut Charles Sadron), le Docteur Philippe Lavalle (INSERM 1121, Strasbourg). Je remercie tout particulièrement le Docteur Lydie Séon (Institut Charles Sadron, Strasbourg) pour ses analyses biologiques et les tests qu’elle a réalisé pour moi en plus de ses propres travaux de thèse.

Je n’oublie pas non plus nos collaborateurs suisses, le Docteur Fintan Moriarty et le Docteur David Eglin, avec qui nous avons discuté d’une nouvelle application pour nos matériaux. Merci pour leurs précieux conseils sur les produits antibactériens et les applications qui visent à réduire les infections.

Je remercie très chaleureusement le Docteur Sébastien Gallet pour ses précieux conseils, pour m’avoir guidée et souvent dépannée face à des complications de synthèse. Nos longues discussions de chimie et de mécanismes réactionnels m’ont souvent éclairée et permis d’avancer. Merci également d’avoir été mes mains pendant une certaine période et de m’avoir montré qu’il est très facile de rattraper ses erreurs d’accidents de rotavap et de tout nettoyer en un rien de temps sans en mettre partout… Grâce à toi les tâches quotidiennes du laboratoire n’étaient plus des corvées mais un nouveau style de vie.

Je tiens également à remercier les Docteur Michel Schmitt, Docteur Sylvette Chasserot-Golaz et Monsieur Thierry Dintzer pour leur aide lors des analyses RMN, des analyses de microscopie confocale à fluorescence et des analyses par diffraction des rayons-X.

Je n’oublie pas les personnes qui ont contribué, à leur manière, de près ou de loin à ce projet. Un grand merci à Mac et Gyver pour m’avoir toujours aidée et dépannée face à des problèmes informatiques ou mécaniques. Merci de m’avoir supportée avec le sourire quand je venais vous embêter avec mes problèmes d’ordis, de courant, d’écrous ou d’aiguilles… Malheureusement, votre superbe affiche va encore devoir rester sur cette porte quelques mois. Je tiens également à remercier Chheng pour son aide au laboratoire et pour nos nombreuses discussions cuisines et « Tupperware » le midi. J'ai beaucoup appris et surtout gouté de la cuisine asiatique grâce à toi. Merci aussi à Catherine (le petit rayon de soleil) pour nos discussions du matin qui m'ont souvent donné le sourire et m'ont permis de bien démarrer ma journée. Je ne t'en veux plus d'avoir voulu m'abandonner au supermarché l'an dernier lors des courses de Noël. Je tiens encore à remercier Chheng et Catherine pour leur aide lors du pot de thèse et d'être de vraies mamans pour les thésards toute l'année (avec les réprimandes et les coups de pieds au cul qui vont avec). Je tiens également à remercier Monsieur Charles pour ses précieux conseils et sa sagesse (toujours avec le sourire) qui m'ont beaucoup servi notamment pour la rédaction de ce manuscrit. Merci également pour votre aide, vos relectures et nos discussions relatives à la chimie. Je remercie également Nicolas pour avoir su me faire sursauter dans les couloirs et dans le bureau (sur ma chaise) pendant trois ans et de m'avoir malgré tout donné de bons conseils au fil de la thèse (non, je n'ai vraiment pas peur de toi). Merci également à Sabine et Romain pour nos petites discussions culturelles toujours très instructives.

Ce travail n'aurait pas été complet sans l'aide des stagiaires sur le projet « pansements ». Merci donc à Safa et Dhikra.

Mais une thèse n'est rien sans les thésards et les post docs qui nous forment, nous encouragent et nous soutiennent. Je remercie donc de tout cœur les Filles pour leur soutien, leur encouragement, leur bonne humeur, leurs sourires et leurs rires souvent communicatifs. Merci donc à Stéphanie pour les expressions hors normes que tu savais si bien placer; merci à Patty pour ton super coaching lors de la rédaction et tes « arrêtes tes conneries maintenant »; merci à Camille pour les madeleines et les tablettes Milka qui étaient là au parfait moment et pour tes détours à l'esplanade pour me dépanner; merci à la rousse, Marie, pour ses câlins et ses craquages enflammés; et merci à Alice, même si tu m'as fait peur au début, j'ai appris à t'apprécier et maintenant j'aime beaucoup soulever le paquet avec toi tous les jeudis. Sans vous, les Filles, je ne pense pas que j'aurais tenu ou même beaucoup ri lors de la rédaction. Merci pour vos relectures et vos corrections de dernières minutes. Merci encore Marie d'être restée un vendredi soir pour relier mes manuscrits avec moi. Tes tarifs ne sont peut-être pas raisonnables mais le service est parfait. Je remercie aussi Ibrahim, mon pauvre binôme de bureau, qui a dû me supporter, moi et mes crises de folie, pendant ces trois ans, jours après jours. Merci pour tes encouragements et tes blagues lors de la rédaction. Désolée de t'avoir fait stressé pour Ta rédaction, je suis sure que tout ira aussi très bien pour toi. Merci aussi à Mathieu, merci pour tes magnifiques pas de danse à la Patrick Swayze et ta culture musique et basketball. Je remercie aussi les garçons du 2ème: FX, Stéphane, Alex, Thibaud et Ikhram pour leurs bonnes humeurs, leurs blagues et leurs réflexions philosophiques sur la vie et l'Homme en général. Merci aux anciens thésards et post-docs qui ne sont tristement plus là maintenant : Véronica, Corinne, Véronique, Jérôme, Inès et Dam… Merci aussi aux thésardes qu'on voit un peu moins mais qu'on aimerait voir plus parce qu'on les aime bien: Flavie et Amparo. Merci aussi aux petits nouveaux Sukai, Pierre et Morgane. Je leur souhaite bon courage et j'espère qu'ils auront autant de bons souvenirs que moi au labo.

Je remercie aussi mes amis de toujours et de l'école pour leur soutien et les supers weekends/soirées passés ensemble pour décompresser. Merci à Anne-cha et Micka pour leurs nombreuses visites et la saucisse à la moutarde du dimanche matin à Münich, merci à ma Lulu pour son rire, merci à Cécile et Val pour nos sorties Culture et culinaires à Stras, merci à la bande du nouvel an : Manu, Virginie, Etienne, Amane, Benji, Joël et Alexia. Et merci aux copines d'enfance : Mélanie, Laura, Carole et Julia.

Enfin, je tiens à remercier mes parents qui nous ont toujours fait passer avant eux. Merci pour votre soutien et votre confiance en moi malgré le fait que je ne suis vraiment pas facile à vivre. Je tiens aussi à remercier mes grands frères, Sébastien et Julien ; vous m'avez toujours poussée à aller plus loin, même là où je ne pensais pas pouvoir réussir. Merci aussi à mes belles sœurs, Céline et Maélène, pour votre soutien et vos conseils aussi bien au sujet de la thèse qu'au sujet des frangins. Merci aussi à Matéo et Thibaud pour leurs rires et leurs joies de vivre, ne grandissez pas trop vite. Je remercie tout particulièrement Paul de m'avoir soutenu et supporté tout au long de cette thèse. Tu as toujours su trouver les mots pour que je ne baisse pas les bras et que je continue d'avancer. A tout moment et quelles que soient les circonstances, tu as toujours été là pour m'écouter et m'épauler.

Titre français :

Elaboration de nanofibres fonctionnelles à base de cyclodextrines pour des applications biomédicales

---

Le présent mémoire de thèse a été rédigé en langue anglaise, conformément à l'autorisation délivrée par Monsieur le Professeur Jean-Pierre Bucher, professeur des universités à l'Université de Strasbourg et directeur de l'Ecole Doctorale de Physique et Chimie-physique (ED 182), le 10 juillet 2014.

TABLE OF CONTENTS

Introduction générale 2

General Context 2

Chapter1: Bibliography

Bibliography 10

1. Cyclodextrins and their use for biomedical applications 12
  1.1. History and description 12
  1.2. Cyclodextrins chemical modification strategies 14
  1.3. Formation of host-guest complexes with small molecules 15
    1.3.1. Inclusion complexes between β-cyclodextrin and curcumin 18
    1.3.2. Inclusion complexes between β-cyclodextrin and methylene blue 19
    1.3.3. Inclusion complexes between β-cyclodextrin and antibiotics 20
  1.4. The use of polymers to form supramolecular inclusion complexes: pseudo-polyrotaxanes and polyrotaxanes 22
    1.4.1. Nomenclature 22
    1.4.2. Inclusion complexes between polymers and cyclodextrins 23
    1.4.3. Applications of cyclodextrin-polymer inclusion complexes 26
  1.5. The use of cyclodextrins as building blocks for functional and reactive materials 27

2. Elaboration of fibrous materials by electrospinning and its use for tissue engineering 29
  2.1. Tissue Engineering 29
  2.2. Electrospinning: Principles 30
    The influence of solution parameters 32
    The influence of processing parameters 33
  2.3. Electrospun membranes for tissue engineering 35
  2.4. Poly(ε-caprolactone) based membranes for biomedical applications 37
    2.4.1. Physico-chemical properties of poly(ε-caprolactone) 37
    2.4.2. Poly(ε-caprolactone) based fibres for tissue engineering 38
  2.5. Elaboration of cyclodextrin inclusion complexes based fibres 41
    2.5.1. Cyclodextrin based fibres 41
    2.5.2. Fibrous mats based on polyrotaxanes of cyclodextrins and polymers 42

Chapter2: Synthesis of cyclodextrin based inclusion complexes

Synthesis of cyclodextrin inclusion complexes 46

1. Encapsulation of single molecules 48

1.1. Curcumin and methylene blue inclusion complexes for wound dressing applications 48
  1.1.1. Inclusion complexes between curcumin and β-cyclodextrin 48
  1.1.2. Inclusion complexes between methylene blue and β-CD 54
1.2. Vancomycin and gentamicin for infection treatments 57

2. Synthesis of poly(ε-caprolactone) based polyesters presenting different architectures 63
2.1. Ring Opening Polymerization of lactones by organocatalysis 63
2.2. Synthesis of well-defined four-branched polyesters 65
2.3. Synthesis of an asymmetric four-branched polymer 69
2.4. Synthesis of a block copolymer PCL-PPG-PCL 73

3. Formation of poly(ε-caprolactone) based pseudo-polyrotaxanes 76
3.1. Synthesis of α-cyclodextrin based pseudo-polyrotaxanes 76
3.2. Synthesis of β-cyclodextrin based star pseudo-polyrotaxanes 89

CONCLUSION 92

Chapter3: The use of cyclodextrins for drug encapsulation in fibrous wound dressings

The use of cyclodextrins for drug encapsulation in fibrous wound dressings 98

1. Polyelectrolyte complexes: description and their applications for biomedical materials 100

2. Preparation of electrospun membranes based on the chitosan/ carboxymethyl cellulose polyelectrolyte complex 105
2.2. Materials and description of the polyelectrolyte based solutions 105
2.3. Coaxial core:shell CMC:CHI fibres 108

3. Influence of the chemical and physical crosslinking on the electrospun fibres 118
3.1. Crosslinking of electrospun membranes with sodium periodate 118
3.2. Physical crosslinking of the fibres in an environmental chamber 121

4. Elaboration of methylene blue loaded and polyelectrolyte complex based electrospun fibres 124

5. First biological evaluations of the processed membranes 126
5.1. Description of the disc diffusion tests 126
5.2. Antibacterial assessment of the electrospun membranes 127
5.3. Drug release kinetic study 129

Conclusion 132

Chapter4: The use of cyclodextrins for the surface functionalization of pseudo-polyrotaxane based fibres

The use of cyclodextrins for the surface functionalization of pseudo-polyrotaxane based fibres 138

1. Elaboration of electrospun fibrous membranes 140
  1.1. Elaboration of blend fibres....140
  1.2. Elaboration of core: shell PCL: pPR fibres....142
    1.2.1. Elaboration and characterization of core/shell fibres 143
    1.2.2. General comparison between all the electrospun PCL:pPR core:shell fibres 149
  1.3. Characterization of the electrospun membranes 150
    1.3.1. XRD analysis.... 150
    1.3.2. Water contact angle measurements 152
    1.3.3. Mechanical properties of the core:shell membranes 153

2. Chemical functionalization of the fibre surface 156
  2.1. Grafting of fluorescein isothiocyanate 156

CONCLUSION 162

General conclusion and perspectives

CONCLUSION 168

PERSPECTIVES....172

Materials and Methods

1. Materials 178

2. Measurements....180
  2.1.NMR....180
  2.2.SEC 180
  2.3.FITR spectroscopy 181
  2.4.TGA 181
  2.5.DSC....181
  2.6.XRD 181
  2.7.SEM....181
  2.8.SANS 182
  2.9.Mechanical tensile testing....183
  2.10.Water contact angle....183
  2.11.Fluorescent confocal microscopy 184
  2.12.Stability against water test....184
  2.13.UV-Vis spectrophotometer....184

3. Synthesis 186
3.1. Synthesis of methylene blue and curcumin inclusion complexes (adapted from reference 32) 186
3.2. Synthesis of vancomycin and gentamicin based inclusion complexes 187
3.3. Synthesis of four-branched poly(ε-caprolactone) star-PCL derived from pentaerythritol ..188
3.4. Esterification of the end hydroxyl groups of star-PCL with succinic anhydride to obtain star-PCL-COOH 189
3.5. Amidation of the end groups of the star-PCL-COOH to obtain asym-PCL.......................190
3.6. Synthesis of a block copolymer (PCL-PPG-PCL) initiated by poly(propylene glycol) (PPG) and catalysed by TBD..191
3.7. Preparation of α-cyclodextrin star-pPR using star-PCL 192
3.8. Synthesis of α-cyclodextrin lin-pPR using a 10 kg.mol^{-1} commercial linear PCL..............193
3.9. Synthesis of α-cyclodextrin mik-pPR using asym-PCL 194
3.10. Synthesis of β-cyclodextrin copo-pPR derived from the block copolymer PCL-PPG-PCL... 195
3.11. Grafting of fluorescein isothiocyanate (FITC) onto the fibres surface 196

4.Electrospinning 197
4.1. Electrospinning of polyelectrolyte based fibres for wound dressing applications..............197
4.1.1. Coaxial electrospinning 197
4.1.2. Blend electrospinning.. 198
4.2. Electrospinning of polyester and pseudo-polyrotaxanes...200
4.2.1. Blend electrospinning.. 200
4.2.2. Coaxial electrospinning 201

5.Physical crosslinking in an environmental chamber 203

6.Biological evaluation..204
6.1.Determination of the minimal inhibitory concentration 204
6.2. Agar disc diffusion test (Kirby's test)..205

7.Release kinetic study of methylene blue loaded membranes 216

References..222

Publications and Valorization..234

ABBREVIATIONS

Arg	L-arginine
Asp	L-aspartic acid
BMP-2	Bone Morphogenetic Protein
CD	Cyclodextrin
CDI	1,1'-carbonyldiimidazole
$CDCl_3$	Deuterated chloroform
CHI	Chitosan
CH_2Cl_2	Dichloromethane
CH_3CN	Acetonitrile
CMC	Carboxymethylcellulose
$CuSO_4$	Copper Sulfate
DCC	N,N'-dicyclohexylcarbodiimide
DCM	Dichloromethane
DDA	Degree of Deacetylation
DMF	Dimethylformamide
DMSO	Dimethyl sulfoxide
DMTMM	4-(4,6-Dimethoxy-1,3,5-triazin-2-yl)-4-methylmorpholinium chloride
DNA	Deoxyribonucleic acid
DP	Degree of Polymerization
DSC	Differential Scanning Calorimetry
ECM	Extracellular matrix
EGF	Epidermal growth factor
ELLA	Enzyme-linked Lectin Assay
EtOAc	Ethyl acetate
FITC	Fluorescein isothiocyanate
FTIR	Fourrier Transfrom Infrared spectroscopy
Gly	Glycine
GPC	Gas Permeation Chromatography
HA	Hydroxyapatite
HIV	Human Immunodeficiency Virus
HCl	Hydrochloric acid
HOBt	Hydroxybenzotriazole
HPLC	High Performance Liquid Chromatography
HPβCD	Hydroxypropyl-β-cyclodextrin
IC	Inclusion complex
LA	Lactic acid
MeOH	Methanol
MB	Methylene Blue
$NaIO_4$	Sodium periodate
NaPSS	Sodium poly(styrene sulfonate)
NHC	N-Heterocyclic Carbene

NMR	Nuclear Magnetic Resonance
PCL	Poly(ε-caprolactone)
PDI	Polydispersity Index
PE	Polyethylene
PEC	Polyelectrolyte Complex
PEG	Poly(ethylene glycol)
PHEA	Polyhydroxylethylactetate
PMA	Poly(methacrylic acid)
PMMA	Poly(methyl methacrylate)
PNIPAAm	Poly(N-isopropylacrylamide)
PP	Polypropylene
PPG	Poly(propylene glycol)
pPR	Pseudo-polyrotaxane
PR	Polyrotaxane
PS	Polystyrene
PVA	Poly(vinyl alcohol)
RGD	Arginylglycylaspartic acid
RH	Relative Humidity
ROP	Ring Opening Polymerization
SEC	Size Exclusion Chromatography
SEM	Scanning Electron Microscopy
TBD	1,5,7-triazabicyclodecene
TEM	Transmission Electron Microscopy
TFA	Trifluoroacetic acid
TGA	Thermal Gravimetric Analysis
THF	Tetrahydrofuran
XRD	X-Ray Diffraction
α-CD	α-cyclodextrin
β-CD	β-cyclodextrin
γ-CD	γ-cyclodextrin
δ-VL	δ-valerolactone
ε-CL	ε-caprolactone

CHEMICAL STRUCTURE OF THE MOLECULES

α-cyclodextrin	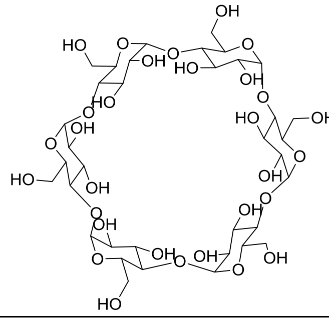
β-cyclodextrin	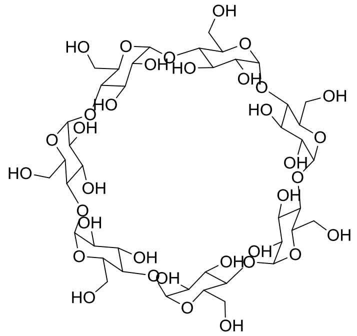
γ-cyclodextrin	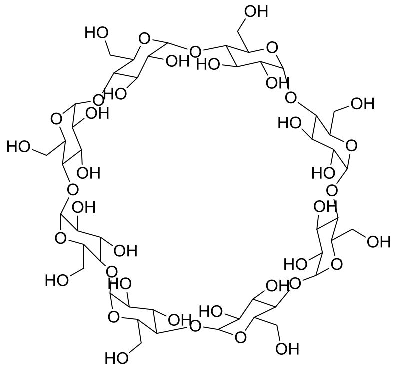
Block copolymer (PCL-PPG-PCL)	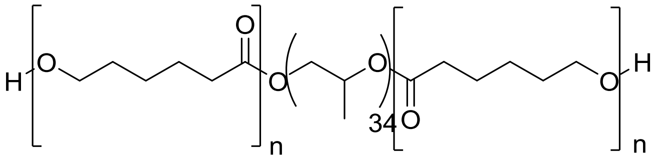
Curcumin	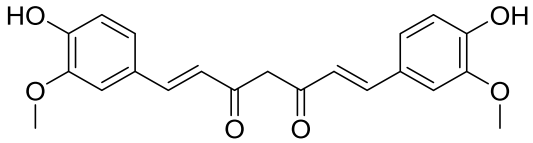
Four-branched poly(ε-caprolactone) (star-PCL)	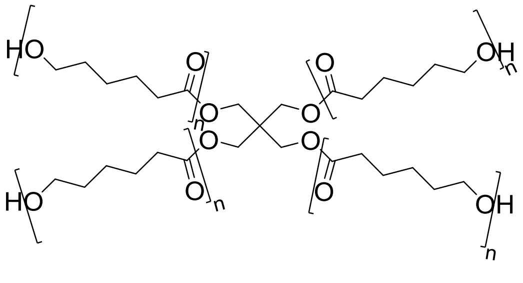

Gentamicin	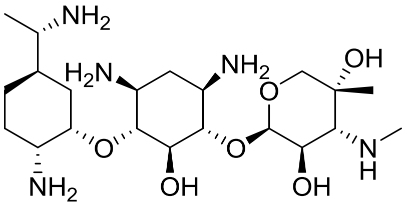
Methylene blue	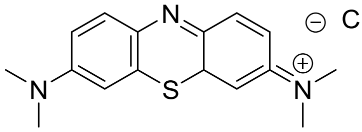
Poly(ε-caprolactone) (PCL)	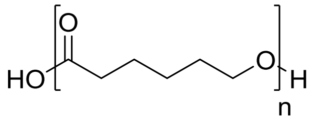
Sodium periodate	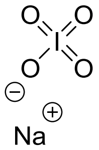
Vancomycin	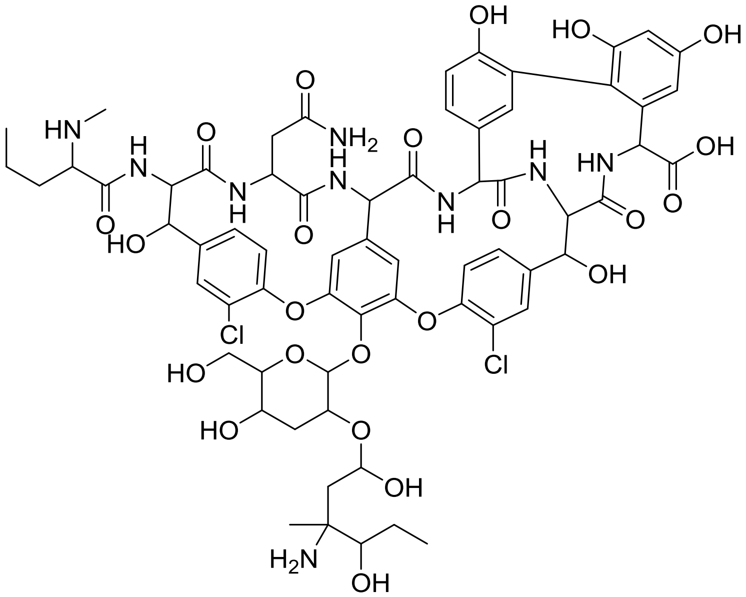

Introduction générale

Introduction générale

Depuis plusieurs siècles, d'incroyables progrès ont été réalisés dans le domaine médical. Certaines maladies ont été éradiquées et de nombreuses maladies peuvent être facilement traitées de nos jours et soignées à l'aide de vaccins, de médicaments, d'antibiotiques ou par une intervention chirurgicale. De tout temps, l'Homme a cherché à améliorer sa condition sur Terre et à prolonger son espérance de vie. Il est donc naturel que les chercheurs aient porté leur attention sur ces différents problèmes et tentent de trouver des solutions afin de développer de nouveaux traitements et de développer de nouveaux matériaux présentant des propriétés biologiques intéressantes pour supprimer les nouvelles infections et maladies.

Dans le domaine des antibiotiques, une réelle avancée a été faite dans le développement de nouveaux matériaux et la commercialisation de nouveaux types de gels, de pilules et de pansements contenant des agents antibactériens naturels ou synthétiques. Cependant de nombreux problèmes persistent, notamment le transport des agents antibactériens vers la zone infectées ou encore le contrôle de la cinétique de relargage des agents biologiques ainsi que la maitrise de l'efficacité des antibiotiques. Par ailleurs, il a été démontré ces dernières années que les bactéries présentent une nouvelle résistance face aux antibiotiques communs et très répandus ce qui ouvre la voie vers le développement de nouveaux agents antibactériens et l'élaboration de nouvelles stratégies innovantes pour réguler et moduler le relargage des antibiotiques ou agents biologiques utilisés.

De manière similaire, le domaine de l'ingénierie tissulaire a énormément évolué en quelques dizaines d'années. De nombreux progrès ont été réalisés grâce à une nouvelle approche qui consiste en l'association des connaissances dans le domaine de la biologie, des sciences des matériaux et de l'ingénierie des matériaux. Cette association des divers domaines a conduit à l'essor et au développement de nouveaux matériaux présentant un effet au long terme avec peu ou pas d'effets secondaires. En effet, les recherches menées exclusivement par les biologistes et les médecins bien que très fructueuses n'ont pas permis de développer des types de matériaux versatiles et présentant des effets modulaires.

Le but de l'ingénierie tissulaire est de réparer, régénérer ou remplacer partiellement ou totalement des organes ou tissues infectés ou endommagés en implantant des matériaux bioactifs. Bien que la majorité des échafaudages ou matrices utilisées soient de nature synthétique, ces matériaux sont activés par l'ajout d'additifs, d'agents bioactifs et de cellules saines qui vont se développer et croitre au sein du matériau. Cette association des différents domaines (Biologie cellulaire, Science des Matériaux et ingénierie des Matériaux) a permis l'élaboration de nouveaux matériaux plus résistants et adaptés à différentes maladies et symptômes. La fabrication de ce nouveau type de matrices a permis d'améliorer notre compréhension des mécanismes vivants de la reproduction et de la croissance cellulaire. Cependant de nombreux problèmes persistent et il serait intéressant de développer des matériaux versatiles adaptés à des maladies ou infections diverses. Or, comme les cellules et les tissues sont spécifiques à un organe ou une partie du corps humain, les matrices bioactives développées sont elles aussi spécifiques à ce même type d'environnement ou d'action. Ces matériaux sont donc très couteux et restent encore difficiles à élaborer. L'élaboration de matériaux versatiles et ajustables au type de cellules ou tissues permettrait de réduire les coûts économiques et temps nécessaires à la fabrication de ce type de matrice.

Ces travaux de thèses tentent de répondre à cette problématique d'ingénierie tissulaire et de développer des matériaux bio fonctionnels. Ce projet vise donc à produire des matrices fibreuses et versatiles qui peuvent être facilement fonctionnalisées.

Les cyclodextrines sont des oligosaccharides cycliques constitués de 6 à 8 unités glucose reliées entre elles. Ces dérivés du glucose ont été très utilisés pour des applications biomédicales notamment pour l'encapsulation de médicaments, de fragrances ou encore pour le relargage contrôlé de principes actifs. Lors de ce projet, des matériaux à base de cyclodextrine ont été développés en vue d'applications pansements ou d'ingénierie tissulaire (***chapitre 2***). Les cyclodextrines ont été utilisées comme points réactifs car ces oligosaccharides sont biocompatibles, biodégradables et approuvés par la FDA. De plus, les cyclodextrines ont la particularité de pouvoir former des complexes hôte/invité avec une large gamme de molécules. Ces complexes d'inclusion sont stables grâce à des interactions non covalentes et faibles de type Van der Waals ou hydrophobiques ou électrostatiques.

Ces complexes d'inclusion formés à l'aide de cyclodextrines ont été ensuite ajoutés dans des matrices polymères et électrospinnés pour l'obtention de membranes fibreuses. En effet, les matériaux fibreux présentent de nombreux avantages comme support pour des applications biomédicales telles que les pansements et l'ingénierie tissulaire. Ces matériaux fibreux présentent un grand rapport surface sur volume facilitant les échanges avec le milieu extérieur et les morphologies obtenues par electrospinning peuvent être contrôlées et peuvent imiter les structures des tissues humains. Par ailleurs, cette technique permet la mise en œuvre de nombreux polymères synthétiques mais aussi naturels à tel point qu'un nombre quasi infini de combinaison ou d'association peut désormais être envisagé et étudié. Dans le cadre de cette thèse, deux différents polysaccharides et un polyester ont été mis en œuvre par electrospinning et utilisé comme matrice polymère nécessaire afin d'obtenir les propriétés mécaniques requises pour nos applications biomédicales. De plus, ces polymères présentent une cinétique de dégradation appropriée à leur application respective.

Deux stratégies ont été étudiées lors de cette thèse afin de fonctionnaliser les matériaux fibreux à base de polymères à l'aide molécules bioactives telles que des antibiotiques ou des composés fluorescents (c.f. figure 1). La première stratégie vise à encapsuler des petites molécules dans la cavité des β-cyclodextrines et à mélanger ces complexes d'inclusion directement avec les solutions polymériques avant les expériences d'electrospinning. Ces complexes d'inclusion sont donc présents dans la composition et l'épaisseur des fibres. La seconde approche tente de fonctionnaliser la surface de fibres de polymères composée de cyclodextrines par réaction chimique. Cette seconde méthode permet donc une fonctionnalisation après l'élaboration par electrospinning des membranes fibreuses.

Ces travaux de thèse sont donc divisés en deux approches différentes qui seront présentées de manière identique dans ce mémoire.

La première stratégie vise à élaborer des matériaux pour des applications pansements. Pour préparer des matériaux avec des propriétés mécaniques améliorées et stables face aux solvants, les membranes fibreuses ont été préparées en associant deux polyélectrolytes portant des charges opposées sur leur chaine. L'association de ces polyélectrolytes conduit à la formation via des interactions non covalentes de complexes de polyélectrolytes. Pour ce type d'application, la carboxymethylcellulose et le chitosan ont été choisi car ce sont tous deux des polymères chargés qui, combinés ensemble, forment des complexes de polyélectrolytes stables. Mais ces polymères présentent également d'autres propriétés très intéressantes. La cellulose ainsi que ses dérivés tels que la carboxymethylcellulose sont abondants, peu couteux, biocompatibles, biodégradables et les propriétés mécaniques des fibres obtenues après electrospinning avec ces polysaccharides sont très bonnes. Le chitosan quant à lui est un polysaccharide naturel très abondant obtenu par déacétylation de la chitine (présente en grande quantité dans les carapaces des crustacés). Il a été démontré que le chitosan peut avoir des effets antibactériens ainsi que des propriétés de cicatrisation. Afin d'améliorer les propriétés biologiques des matériaux et prolonger l'effet antimicrobien des membranes, des complexes d'inclusion entre la β-cyclodextrine et le bleu de méthylène (un antibiotique répandu dans le commerce) ont été ajoutés et incorporés à la solution de polyélectrolytes. Le bleu de méthylène a été délibérément complexé avec la β-cyclodextrine afin de retarder le relargage du bleu de méthylène dans le milieu extérieur et ainsi augmenter les propriétés antimicrobiennes du matériau. Le but de cette partie est d'obtenir des matériaux avec de bonnes propriétés face aux bactéries *in vitro,* mais aussi, avec une efficacité prolongée sur une longue période face à un pansement standard (***chapitre 3***).

La seconde stratégie de fonctionnalisation vise à améliorer les propriétés biologiques de fibres obtenues par electrospinning par des réactions chimiques simples et rapides. Ces membranes sont principalement destinées pour des applications d'ingénierie tissulaire. Le poly(ε-caprolactone) est un polyester peu couteux, biocompatible et biodégradable. A cause de ses bonnes propriétés mécaniques et de sa cinétique de dégradation *in vivo,* ce polyester a été choisi comme matrice support pour la fabrication des membranes fibreuses destinées à l'ingénierie tissulaire. Cependant, ce polymère est inerte face aux cellules et tissues humains ; il est donc nécessaire de fonctionnaliser les fibres afin d'apporter des propriétés biologiques au matériau. Malheureusement, les modifications chimiques du poly(ε-caprolactone) sont relativement difficiles car seules les deux fonctions en bouts de chaines peuvent être modifiées par réaction chimique. En fonction de la longueur de la chaine du polymère, ces réactions de modification des bouts de chaines sont plus ou moins faciles. Ainsi, afin d'augmenter les groupes fonctionnels avec le poly(ε-caprolactone), ce polyester a été mis en contact avec la cyclodextrine pour former des auto-assemblages supramoléculaires appelés « pseudo-polyrotaxanes ». Ces supramolécules sont généralement assimilées à des colliers de perles où le polymère est apparenté à la chaine et les cyclodextrines enfilées le long de la chaine de polymère sont confondues avec les perles du collier. Dans un souci de simplicité de synthèse des différentes supramolécules, il a été décidé qu'aucune molécule encombrante ne serait greffée en bouts de chaines afin d'empêcher la perte des cyclodextrines lors de la mise en solution de ces pseudo-polyrotaxanes. Ainsi, et afin d'améliorer la stabilité des pseudo-polyrotaxanes en solution, différentes architectures de poly(ε-caprolactone) ont été synthétisées par polymérisation par ouverture de cycle de l'ε-caprolactone. Cette polymérisation s'est faite par organocatalyse avec le 1,5,7-triazabicyclo[4.4.0]dec-5-ene, car ce catalyseur peut être éliminé assez facilement lors des étapes de purification et n'est pas aussi toxique que l'octanoate d'étain utilisé de manière standard pour ce type de polymérisation. Les polymères obtenus présentent des architectures variées : linéaire, branchée et copolymère à blocs. Ces différents polyesters ont ensuite été ajoutés dans une solution aqueuse de cyclodextrines pour former les pseudo-polyrotaxanes. Après avoir caractérisé chaque supramolécule, les pseudo-polyrotaxanes ont été electrospinnés avec du poly(ε-caprolactone) pour obtenir des fibres poly(ε-caprolactone)/pseudo-polyrotaxanes avec des propriétés mécaniques appropriées pour des applications d'ingénierie tissulaire. Les fonctions hydroxyles sur la cavité externe des cyclodextrines portées par les pseudo-polyrotaxanes vont ensuite permettre la modification des membranes et le greffage de molécules bioactives spécifiques à certaines fonctions cellulaires. Les fibres ont été préparées de manière particulière afin d'assurer la présence des pseudo-polyrotaxanes, et ainsi des cyclodextrines, en surface des fibres pour faciliter les réactions de post-fonctionnalisations. Des conditions expérimentales de modification chimique ont été déterminées afin de préserver la morphologie et la structure du mat fibreux (***chapitre 4***).

Les deux approches étudiées dans ce projet de thèse sont originales dans leur utilisation des cyclodextrines. En effet, ces oligosaccharides sont utilisés comme agents réactifs et éléments essentiels pour la fonctionnalisation de matériaux fibreux pour des applications biomédicales. Ces travaux contribuent dans une certaine mesure à l'élaboration de matériaux durables, versatiles et efficaces pour des applications pansements ou d'ingénierie tissulaire.

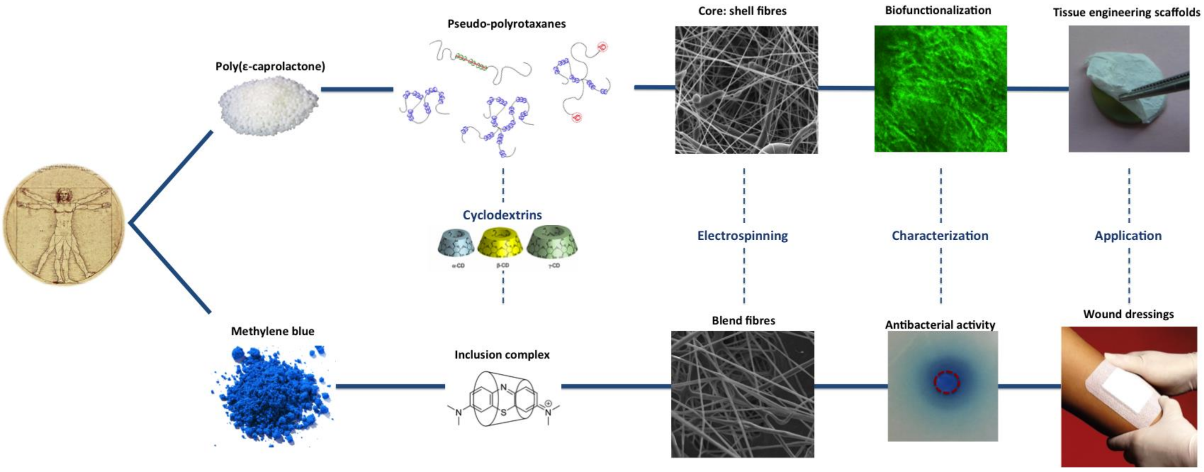
Pseudo-polyrotaxanes
Core: shell fibres
Biofunctionalization
Tissue engineering scaffolds
Poly(ε-caprolactone)
Cyclodextrins
α-CD
β-CD
γ-CD
Electrospinning
Characterization
Application
Methylene blue
Inclusion complex
N
S
N
N
Blend fibres
Antibacterial activity
Wound dressings

Figure 1. Schéma récapitulatif des deux stratégies abordées dans ces travaux de thèse.

Ce mémoire de thèse est décomposé en différents chapitres tous rédigés en anglais.

Le premier chapitre rassemble une bibliographie détaillée centrée, dans un premier temps, sur les cyclodextrines suivi d'une bibliographie sur le technique d'electrospinning.

Les différentes synthèses de complexes d'inclusion, de polymères et de pseudo-polyrotaxanes, étudiées et effectuées lors de cette thèse de doctorat sont ensuite discutées dans le second chapitre. Le détail des différentes caractérisations et les discussions autour des synthèses sont également abordés.

Le chapitre 3 se concentre sur l'élaboration de membranes fibreuses fonctionnelles à base de polysaccharides pour des applications pansements. Une étude concernant la réticulation des fibres par voie chimique et physique est également discutée. L'ajout des complexes d'inclusion entre le bleu de méthylène et la β-cyclodextrine dans les solutions de polysaccharides et leur influence sur la fabrication des fibres sont également abordés dans ce même chapitre. L'étude des propriétés antibactériennes des matériaux fibreux face aux *M.Luteus* est analysée en fin de chapitre ainsi que la cinétique de relargage du bleu de méthylène et des complexes d'inclusion.

Le chapitre 4 aborde la seconde stratégie d'utilisation des cyclodextrines par voie supramoléculaire. Les différentes études menées sur les expériences d'electrospinning ainsi que sur la caractérisation des membranes fibreuses sont détaillées. Une première approche de fonctionnalisation des mats à l'aide fluorescéine isothiocyanate est approfondie et sert de preuve du concept quant à ce type d'applications et de fonctionnalisation.

Dans un souci de clarté, il a été décidé qu'un chapitre entier serait dédié aux synthèses et expériences menées lors de ce projet de thèse et se trouve en fin de manuscrit sous l'étiquette « Materials and Methods ».

General Context

General Context

Tremendous progresses have been made in the field of medicine over the last century. Diseases that killed thousands of people are now erased and many others can be treated with commercially available, vaccines, antibiotics or surgeries. Humans always aimed to improve their condition and prolong their existence. Unfortunately, injuries and diseases have always been part of the human life. It is thus natural that many studies were carried out for the development of cures and the design of bioactive materials to fight against these various infections, injuries and diseases.

Antibiotics have evolved from the simple use of herbs, plants and oils to the development and commercialisation of new types of gels, pills and wound dressings presenting various formulations including natural and synthetic antibacterial agents. However, many issues still need to be handled such as the transport of the antibiotic to the targeted wounded areas or the control of the biomolecule antibacterial efficiency time. Additionally, it has been proven that bacteria are now able to develop some resistance toward the commonly used antibiotics. Therefore, there is a real need to find new bioagents and create innovative delivery systems for a prolonged bactericide activity.

Similarly, if a careful attention is brought to tissue engineering and reconstructive surgery, one can also see the progresses that have been achieved in only a few decades. For a long time, such issues were only the concern of biologists and doctors to resolve. However, there is now a new orientation aiming at combining different fields such as Materials Science, Material Engineering and Biology to tailor and design new materials for long-term treatments with minor side or undesirable effects. The current goal of tissue engineering is to repair or replace damaged organisms and tissues with bioactivated scaffolds. Although most of these scaffolds are synthetic, they will be implanted with healthy and active cells for the repair or reconstruction of infected tissues. Since all these various fields were interconnected, better and sustainable materials have been created. Our understanding of the mechanisms of cell development, reconstruction and healing is rapidly growing so that these new scaffolds are more effective and act faster onto the organisms. Unfortunately, several issues remain and the need for a universal type of scaffold for tissues and cells healing is still a major concern. As each cell and tissue presents its own specificities, materials have to be specifically designed and elaborated for one type of tissue and one disease or injury. It is thus extremely timeconsuming and highly expensive. It would be extremely interesting to develop a material that could be easily applicable for several damaged tissues and could be functionalised to target the particular need of different damaged tissues.

Our small contribution in this field will be discussed in the following PhD Thesis.

In this work, new cyclodextrin based materials for wound dressing and tissue engineering applications were developed (***Chapter 2***). Cyclodextrins were used as building blocks, as these cyclic oligosaccharides are biocompatible, biodegradable and FDA approved molecules. Moreover, cyclodextrins exhibit the peculiar and intriguing ability to form stable host-guest complexes with a wide range of molecules. These inclusion complexes are formed via weak interactions without the creation of covalent bonds.

These cyclodextrin based inclusion complexes were then further processed by electrospinning to elaborate fibrous membranes. Fibrous materials have proven to be appropriate scaffolds for both wound dressing and tissue engineering applications mostly due to the high surface ratio displayed by the fibres as well as for their morphology that mimics the structure of human tissues. The structure of electrospun fibres can easily be controlled. Besides, a wide range of natural and synthetic polymers can now be processed by electrospinning so that an almost infinite choice of materials and associations can be investigated. To reach the mechanical properties required for both applications, polysaccharides and poly(ε-caprolactone) were used respectively as a matrix for wound dressings and tissue engineering. These polymers also present the requisite biodegradability kinetics for their respective application field.

Two different and separate strategies were investigated to functionalise the electrospun polymer membrane with active molecules such as antibiotics (figure 1). In the first one, the antibiotics, encapsulated in β-cyclodextrin inclusion complexes were directly incorporated into the nanofibres by blending in the polymer solution before electrospinning. In the second strategy, active molecules are grafted at the surface of the nanofibres after their elaboration.

To fabricate wound dressings with enhanced mechanical properties and solvent stability, the membranes were composed of the association of two polyelectrolytes bearing opposite charges along their chains, leading to the formation of so-called polyelectrolyte complexes. Carboxymethyl cellulose and chitosan were used as they are known to form stable complexes with strong interactions. They also present several other interesting properties. Cellulose and its derivatives are abundant, cheap, biocompatible and biodegradable but they also present good mechanical properties when processed by electrospinning. Chitosan is a natural polysaccharide obtained by deacetylation of chitin (profusely found in the shells of crustaceans) that exhibits antibacterial and wound healing properties. For this type of application, inclusion complexes of methylene blue in β-cyclodextrin were used as additives within the fibres so that the release of the bioactive agents would be added to the bactericide nature of chitosan. They were also thought to favour a slower and extended release kinetic of the antibiotics in comparison to the addition of pure and free antibiotics. The overall aim of these materials was to display high efficiency properties over longer period of time *in vitro* (***Chapter 3***).

The second main target of the project was to develop versatile fibrous scaffolds for tissue engineering. For this application poly(ε-caprolactone) was chosen because of its interesting biological and mechanical properties. However, because this polymer is inert toward living tissues, it should be functionalised to become bioactive. Unfortunately, chemical modifications along the chain are difficult as only the terminal groups of the polymer can be reactive. Cyclodextrins were once again used associated to poly(ε-caprolactone) in the form of pseudo-polyrotaxanes. Pseudo-polyrotaxanes are interesting supramolecular self-assemblies composed of cyclodextrins threaded along a polymer chain. To obtain pseudo-polyrotaxanes presenting different structures and properties, the Ring Opening Polymerization of ε-caprolactone was performed using different initiators. These supramolecules were then processed with poly(ε-caprolactone) by electrospinning to elaborate polymer and pseudo-polyrotaxane fibrous membranes. The OH-functions of cyclodextrin, present in pseudo-polyrotaxanes, could then be used as reactive points on the fibre surface so that the fibrous membranes would depict specific biological properties. The fibres were elaborated so that easy and versatile chemical reactions could be achieved on the electrospun fibres while preserving the morphology and structures of the fibres (***Chapter 4***).

The strategies presented in this manuscript are original because they use cyclodextrin as a key material for the functionalization of fibrous structure for biomedical applications. This work contributes to find sustainable, versatile and efficient materials for wound dressings and tissue engineering applications.

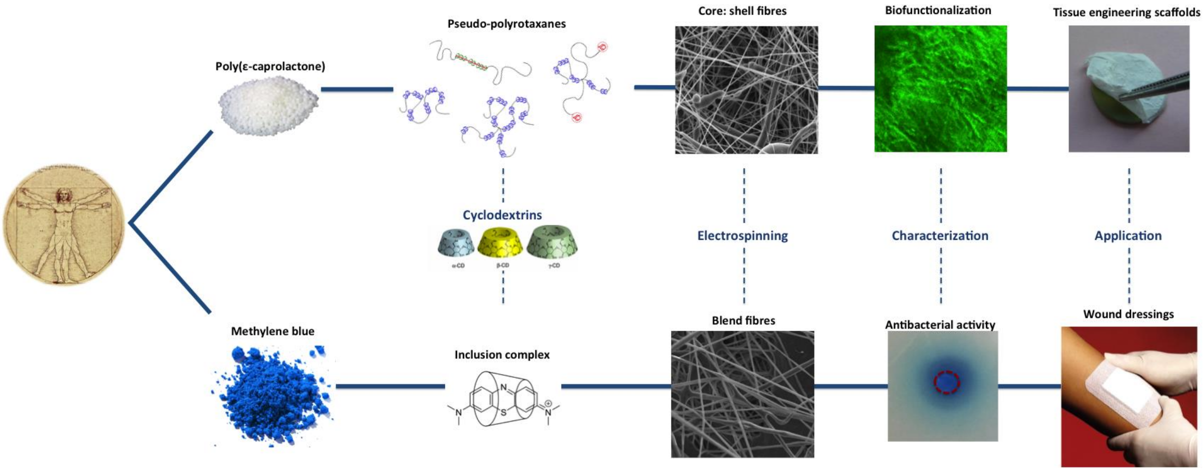
Poly(ε-caprolactone)
Pseudo-polyrotaxanes
Core: shell fibres
Biofunctionalization
Tissue engineering scaffolds
Cyclodextrins
α-CD
β-CD
γ-CD
Electrospinning
Characterization
Application
Methylene blue
Inclusion complex
Blend fibres
Antibacterial activity
Wound dressings

Figure 2. Recapitulative scheme of the different points and experiments that will be discussed in this PhD thesis

Chapter 1

Bibliography

Bibliography

To settle the basics necessary to the comprehension of the work presented in the following PhD thesis, this first chapter will detail all the various points further needed for the elaboration of the cyclodextrin based functional biomaterials.

The first part of this chapter will discuss and present the cyclodextrins and their inclusion complexes. Indeed, these cyclic oligosaccharides can form stable inclusion complexes with small molecules but also with polymers. The theory behind the interactions that rule the complex formation will also be detailed to better understand this interesting phenomenon. The study of inclusion complexes with curcumin, methylene blue, vancomycin, gentamicin and poly(ε-caprolactone) will be treated in more details as they present a particular interest in this work.

Similarly, the method used to elaborate the fibres will be explained and some theoretical points will be approached to better understand the parameters that control the morphology of the materials obtained by electrospinning. As all the electrospun materials designed in this work are thought for tissue engineering or wound dressing applications, these two types of applications will be discussed with attentions. Poly(ε-caprolactone) based fibres for biomedical applications represent a big part of our research and many studies dealing with their use and functionalization have already been done and will be shown in this chapter.

Finally, the last discussed point will handle the state of the art regarding the elaboration of fibres out of inclusion complexes whether they are inclusion complexes between cyclodextrins and small molecules or between cyclodextrins and polymers. This research is of primary interest as we aim to develop a novel type of functional supramolecular based fibres.

1. Cyclodextrins and their use for biomedical applications

1.1. History and description

Cyclodextrins (CDs) are cyclic oligosaccharides composed of α-(1-4)-linked α-D-glucopyranose repetitive units joined to form a ring. As described in figure 1.1, these native cycloamyloses present whether six, seven or eight repetitive units and are respectively called α-, β- or γ-cyclodextrins (α-CDs, β-CDs or γ-CDs).

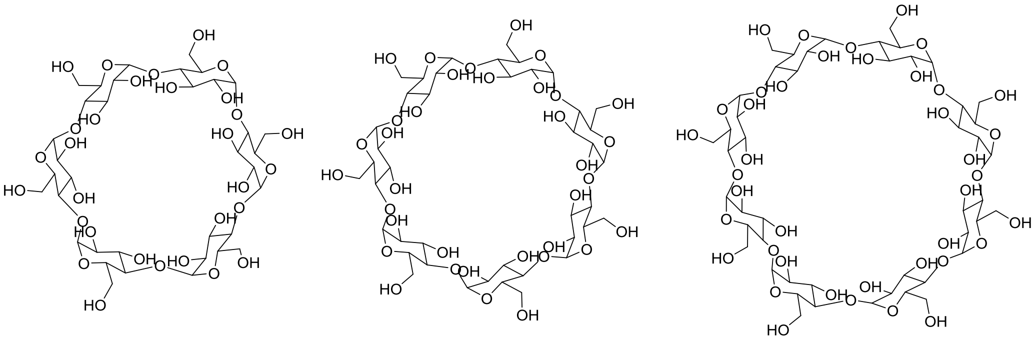

alpha-cyclodextrin
6 repetitive units

beta-cyclodextrin
7 repetitive units

gamma-cyclodextrin
8 repetitive units

Figure 1.1. Chemical structure of α-, β- and γ-cyclodextrins

They were first discovered by Villiers in 1891 as a side product of the digestion of starch by *Bacillus amylobacter*. It was first thought that they were synthesized because of the use of impure cultures and were the results of *Bacillus macerans* contamination. Because their structure was similar to cellulose, they were first named cellulosine.

In 1911, Schardinger found that *Bacillus macerans* could produce large quantities of crystalline cellulosine with two different compositions and called them α- and β-dextrins. It was only later, in 1935, that γ-CDs could be separated. The exact crystalline structures of α- and β-CDs were elucidated in 1942 by X-ray analysis and in 1948 for γ-CD[1].

Currently, CDs are still obtained by enzymatic degradation of starch by *Bacillus macerans or Alcaliphilic Bacilli* using enzymes like cyclodextrin glucosyltransferases (CGTases) and α-amylases. Interestingly, the type of enzyme used does not determine the nature of the synthesized CDs, so that after the degradation of starch each CD has been produced in various ratios. The resulting mixture presenting α-, β- and γ-CDs simultaneously will then be purified. The isolation of particular CDs can be achieved by the addition of selective precipitating agents[2]. Only the dextrorotatory enantiomers are formed and each subunit adopts the $^4C_1$ chair conformation (see figure 1.2a).

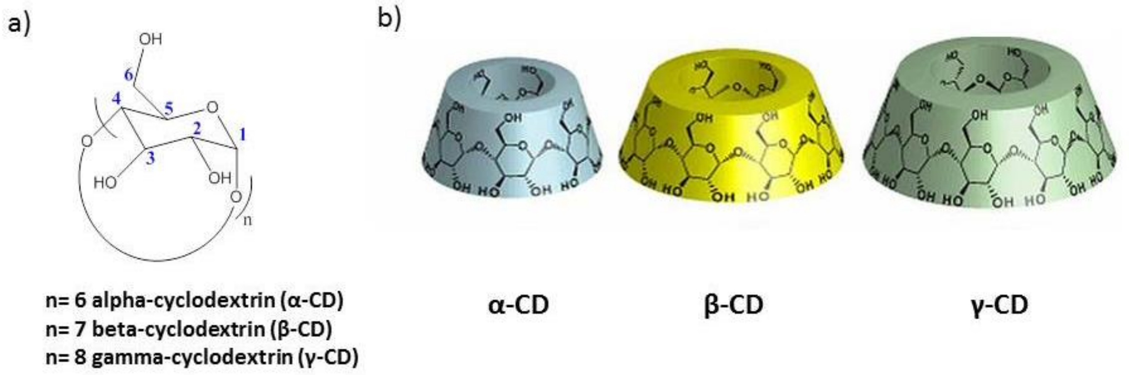
a)
OH
6
4
5
O
2
1
3
O
HO
OH
O
n
n= 6 alpha-cyclodextrin (α-CD)
n= 7 beta-cyclodextrin (β-CD)
n= 8 gamma-cyclodextrin (γ-CD)
b)
α-CD
β-CD
γ-CD

Figure 1. 2. a) Structure of the glucopyranose unit b) 3D structure of all three native cyclodextrins

CDs have a truncated cone shape with an internal hydrophobic cavity whereas the exterior cavity is hydrophilic. The small face of the cone, depicted in figure 1.2b, is composed of primary alcohol groups (OH-6) and is named primary face whereas the wider secondary face is composed of secondary alcohols (OH-2 and OH-3) on its ring. Due to the intramolecular H bonding interactions of the secondary alcohols (OH-2 and OH-3) of neighbouring units, the structure of the CDs is rigid. These interactions vary from one type of CD to the other inducing changes in the water solubility of the oligosaccharides[1]. β-CDs are the least soluble in water because these interactions are much stronger and favourable. As γ-CDs are bigger, their structure is more flexible and H-bonds formation is then harder. α-CDs are actually partially distorted and only four H-bonds can be created.[3]

As described above, the torus is stabilized by intramolecular hydrogen bonds but still flexible enough to permit considerable deviations from regular toroidal shape. Hence CDs are capable to encapsulate various molecules, ions, oils and polymers in their hydrophobic cavity[4]. The capacity to enclose molecules is directly dependent on the size of the CDs. While the height of the cavity is kept constant at 7.9 Å, the diameter of each CD varied with the number of glucopyranose units within the ring. The smallest internal diameter is found for α-CD (4.9 Å) then β-CD (6.2 Å) and γ-CD displays the biggest diameter (7.9 Å).

This peculiar property of inclusion makes them materials of choice for various applications including food packaging, flavour preservation, perfumes, drug delivery, encapsulation of volatiles and other biomedical applications.

Moreover, studies on the relative toxicity[5] of these compounds proved that they were practically nontoxic. CDs can be slightly irritating after intramuscular injection but when orally administrated, no traces of absorption can be found in the gastrointestinal tract[6].

1.2. Cyclodextrins chemical modification strategies

The presence of numerous hydroxyl functions within CDs enables to modify the native cycloamyloses. Various strategies can be considered like direct and rapid modifications. It is pretty simple but, unfortunately, some hydroxyl groups are not accessible and thus can not be modified. The second and most used route to selectively modify specific hydroxyl groups can be achieved by series of protection-deprotection. This approach is more complex but more controlled. Another strategy would be to modify the functions and then only selectively collect the targeted product by High Performance Liquid Chromatography (HPLC). This last option can be quite tough, long and is alas less effective.

CD derivatives are usually obtained by amination, etherification or esterification of the secondary and primary hydroxyl groups[1]. The OH-3 groups are the least reactive functions and can only be modified after OH-2 and OH-6 have been blocked. Numerous substituents can be added onto the CD hydroxyl functions so that mono-, di-, tri-substitutions can easily be reached. Particular precautions need to be taken for good regioselectivity.

As described, CDs are interesting molecules that have drawn a lot of attention from chemists. These biodegradable compounds can be obtained from starch according to a low cost procedure and present a low toxicity. Therefore, CDs are FDA approved molecules. These stable compounds can be modified in a regioselective manner but they can also form non-covalently bonded complexes within their cavity. For all these reasons, these Schardinger dextrins are models used for the study of weak interactions but also for the encapsulation of drugs, perfumes and flavourings.

1.3. Formation of host-guest complexes with small molecules

The formation of host-guest complexes has been known for almost a century[7]. Small molecules like chlorine, bromine and iodine were known to complex with α-dextrin. β-dextrin could encapsulate bromine and iodine whereas iodine was the only molecule known to be encapsulated by γ-CD.[8]

The use of small molecules entrapped within a CD cavity was initially performed to identify and characterize the nature of the CDs. From that point on, scientists quickly saw the potential of these structures[9] and tried to find concrete applications.[10, 11] Indeed, it was already observed that CDs could enhance the solubility, the chemical stability and the absorption of drugs.[10, 11] Since then, many studies have been published that deal with the use of CD for drug release purposes.[1, 12-16]

Interestingly enough, the formation of inclusion complexes neither forms nor breaks covalent bonds. The supramolecular structure can only be achieved when the CD cavity offers a good environment for the guest. Many different factors play an important role during the formation of inclusion complexes. A steric fit is compulsory because the cavity size of the CD needs to be appropriate to the small molecule size. During the process, high-energy water is freed to make space for the guest molecule that will be encapsulated. Finally, various interactions occur between the host and guest molecules[17] to form the inclusion complex. The stability of the host-guest complexes is attributed to hydrophobic, hydrogen, Van der Waals, coulombic or even dipole-dipole interactions depending on the nature of both the guest molecule and the CD.[2]

Connors[18] while studying the stability of CD complexes in solution, established a model detailed in equation (1) for the inclusion complexation in solution as the expression of the free energy ΔG_{comp}:

$$\Delta G_{comp} = \Delta G_{intrasolute} + \Delta G_{solvation} + \Delta G_{genmed} \qquad (1)$$

$\Delta G_{intrasolute}$ corresponds to the host-guest interactions that are whether favourable or nonexistent. As listed before, these interactions can be hydrogen bonds, dipolar, hydrophobic or Van der Waals interactions. The contribution of the solvent effect is considered in the $\Delta G_{solvation}$ term. This hydrophobic and solvent rearrangement contribution is usually unfavourable. Finally, the ΔG_{genmed} describes the general medium effect that is, the creation of a solvent cavity when the solute is dissolved. It depends on the surface area of the cavity and the solvent surface tension. The complexation phenomenon must thus largely be driven by favourable contributions of $\Delta G_{intrasolute}$ and ΔG_{genmed}.

Complexation of molecules within CD cavities can be detected in solution by circular dichroïsm, catalytic effects, dye or fluorescent agents encapsulation, isothermal titration microcalorimetry or by Nuclear Magnetic Resonance (NMR) spectroscopic shifts. NMR analyses can also determine the ratio of host over guest in the inclusion complexes. In most cases, the stoichiometry of the host over guest ratio between CDs and small molecules is 1:1. But in some cases, a 2:1 host over guest ratio is necessary to stabilize the guest molecule.[2]

The stoichiometry of the inclusion complexes has also a direct effect on the crystalline organization of solid CD complexes. When the guest molecule can be fully enclosed within the CD ring, the crystalline CD solid displays a cage-type structure as described in figure 1.3c. This behaviour is due to the presence of glucose residues on the secondary face of close CDs that reduces the cavity volume in the cage rearrangement.[17]

On the other hand, when the guest molecule is larger than the CD cavity and does not fully fit in the host ring, channel structures are produced where the CD cavities line up in order to produce a hydrophobic tube[17] as shown in figure 1.3a and 1.3b.

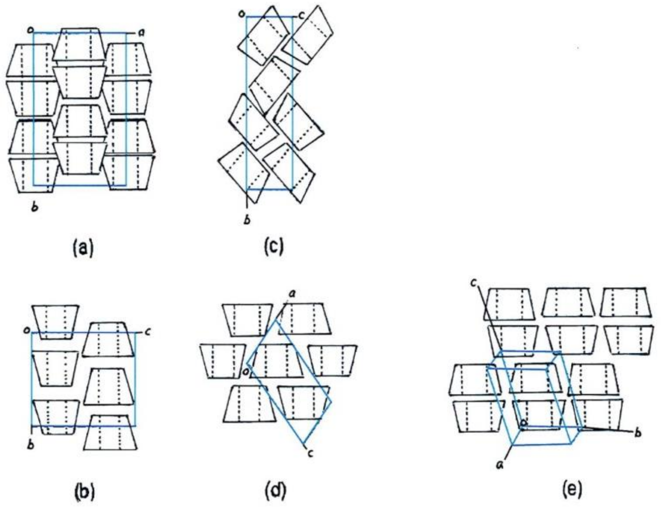

Figure 1.3. Schematic representation of the packing of cyclodextrin structures (a) head-to-head channel type, (b) head-to-tail channel structure, (c) cage type, (d) layer type and (e) layer type composed of beta-cyclodextrin dimers. (reproduction from reference 17)

As these inclusion complexes are quite stable without the need of chemical modification or grafting, various simple methods have been developed to constitute these non-covalent host-guest complexes. The most widely used method to form inclusion complexes is by co-precipitation of an aqueous CD solution with an organic solution of guest. However, some solvent such as ethanol or benzene, can also form stable interactions with the inner cavity of CDs and need to be avoided for complexation reaction. Preferentially, the solvent used for the complexation reaction should not be able to complex with CDs and has to be easily removed by evaporation. The precipitation of CD complexes occurs whether when the mixture is cooled down or when high concentrations are used so that at some point, the solubility of the host-guest complexes will be exceeded leading to the precipitation of the inclusion complexes. The precipitate is then collected by decanting, centrifugation or filtration. One major drawback to this method is the use of high amounts of water that will restrict its use for scale-up industrial applications. An alternative to reduce the amount of water used for the complexation is to encapsulate guest molecules within CDs by slurry complexation. This method is almost identical to the previous one but the CDs do not need to be completely solubilised to form inclusion complexes. Other methods such as dry mixing of powders, paste complexation, extrusion, damp mixing and heating, spray drying methods are also used for the synthesis of inclusion complexes.[4]

As said before, the CD complexes are stable but they are also reversible. Some conditions can lead to the release of the molecule encapsulated within the cavity. When the complexes are entirely dissolved in a solvent and especially water, the guest and the CD can not interact together as they are not in close proximity anymore. So the guest will be released into the solution. Likewise, in the presence of water, guest molecules can be removed from the cavity when they are displaced by water molecules. An equilibrium will be reached between free CDs, inclusion complexes and free small molecules until all the complexes will be dissolved.

In this project, we encapsulated various small molecules such as curcumin, methylene blue, vancomycin and gentamicin that are all well-known for their antimicrobial properties.

1.3.1. Inclusion complexes between *β*-cyclodextrin and curcumin

Curcumin is a natural curcuminoid found in turmeric. This natural phenol is responsible for the yellow colour of turmeric and is often used as a dye. It can be found in different tautomeric forms such as a 1,3-diketo and two equivalent enol forms (figure 1.4).

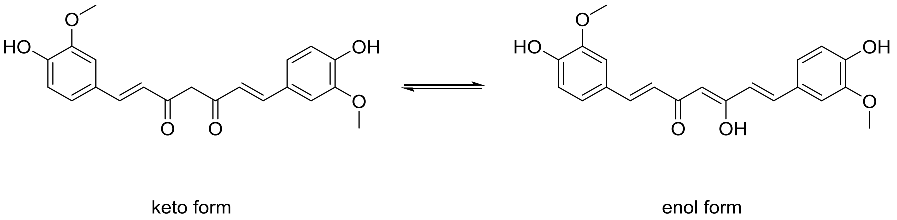

Figure 1. 4. Existing tautomeric forms of curcumin

Some studies proved the medicinal properties of curcumin. Indeed, it has been found that curcumin shows anti-inflammatory, hepatoprotective, antimicrobial, wound healing[19], anticancer, antitumor and antiviral properties.[20] The antiviral property has been exploited for the treatment of Human Immunodeficiency Virus[21] (HIV) but it has yet to be proved that curcumin has a significant effect on the virus. Its antitumor property has been applied and proved for the treatment of cancer.[22, 23] However, one major drawback is that dietary curcumin exhibited poor bioavailability during clinical phase tests. This can be explained by the fact that curcumin is highly insoluble in water (approximately 20 µg/mL).

Therefore, CDs were used to encapsulate curcumin to enhance the solubility of the curcuminoid, enhance its stability in physiological buffer and improve its biological activity. Due to the size of the curcumin molecule β-CDs and hydroxypropyl-β-CDs (HPβCDs) were used to encapsulate the curcuminoid. Several work extensively studied the resulting complexes obtained by solvent evaporation[24], by co-precipitation[25] or by freeze drying technique.[26] Several analyses were performed to identify and characterize the inclusion complexes like Fourrier Transform Infrared spectroscopy (FTIR), Raman spectroscopy, thermal analysis, X-Ray Diffraction (XRD), Scanning Electron Microscopy (SEM), and Nuclear Magnetic Resonance (NMR) analyses. According to NMR spectroscopy, the stoichiometry of β-CD:curcumin inclusion complexes was calculated to be 2:1.[25, 27]

For better anti-tumor activity, these complexes were used as such and the bioactivity of the complexes were studied *in vivo*[27]. Their anti-inflammatory effects were also evaluated and improved when compared with free curcumin[28]. These complexes were also added to polymers to form nanocarriers and their drug release properties were assessed[29]. But β-CD:curcumin inclusion complexes were also used as additives and added within poly(vinyl alcohol) (PVA) fibrous membranes[30] for wound healing, drug delivery applications and for cancer treatment.

1.3.2. Inclusion complexes between β-cyclodextrin and methylene blue

Methylene blue (MB) also known as methylthioninium chloride was first prepared in 1876 by Heinrich Caro and appears as a dark green powder at room temperature. When solubilized in a good solvent, this compound turns blue. MB displays antibacterial, antispasmodic and anti-malarial properties that have been used for decades. Due to some unpleasant side effects, MB was withdrawn and it is only recently that it attracted attention again because of its low cost.

MB has been used for various applications such as drug release[31] and for its fluorescence[32] or photolumiscence[33] properties. As MB is readily soluble in water, the complexation of β-CDs and MB has been applied to enhance the properties such as fluorescence[32] or drug release[34], but enclosed MB has also been widely used as a drug model[31]. Indeed its strong blue coloration enables good titration monitoring by UV-Visible spectroscopy[34, 35], fluorescence spectroscopy[36] or voltammetry.[37, 38]

After the inclusion complexes formation in Phosphate Buffered Saline (PBS) buffer[36-38] or distilled water[32], the stoichiometry of CD over MB within the inclusion complexes was found to be 1:1.[36, 37, 39] Figure 1.5. is a representation of the allegedly structure of the complex.

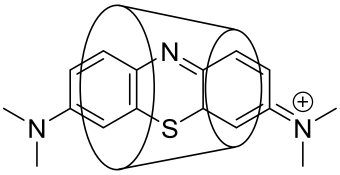

Figure 1.5. Supposed structure of the inclusion complex between methylene blue and β-cyclodextrin

1.3.3. Inclusion complexes between β-cyclodextrin and antibiotics

For this project we aim to add within our materials two different antibiotics: vancomycin and gentamicin. These two antibiotics are already commonly used and are mostly efficient against Gram-positive and Gram-negative bacteria respectively.[40, 41] So, the association of a material presenting both antibiotics will be effective regardless the nature of the bacteria.

One of the major use of CDs is for drug release[4, 13, 15] and many antibiotics have been encapsulated within their cavity: rifampin[42], novobiocin[42], ketoconazole[16], flurbiprofen[16], dexamethasone acetate[16] and vancomycin…[16, 42]

Gentamicin (figure 1.6.) is a traditional aminoglycoside antibiotic efficient toward a broad spectrum of Gram-negative bacteria[43, 44] but it displays some disadvantages such as ototoxicity (toxic for the ears) and nephrotoxicity (toxic for the kidneys). In order to kill bacteria, this antibiotic has to be in direct contact with the bacteria and destroy them by disrupting the osmosis pressure within the cells. In recent years, strategies have been developed to limit its toxicity and enhance its biological efficiency. Indeed, gentamicin has already been encapsulated within liposomes to ensure a good stability and to reduce its toxicity.[44] Nonetheless, and to the best of our knowledge, no inclusion complexes have been obtained or even synthesized between gentamicin and cyclodextrins (CDs). In this project, we supposed that encapsulating gentamicin within CDs would reduce toxicity and harmful side effects in a similar way as liposomes helped to reduce its toxic effects.

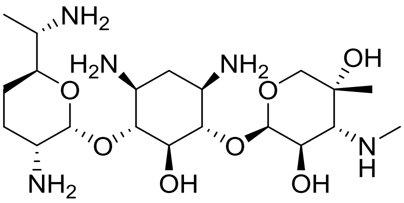

Figure 1.6. Chemical structure of gentamicin

Vancomycin (figure 1.7.) is a glycopeptide antibiotic mostly used in the case of serious infections caused by resistant Gram-positive bacteria. Vancomycin is thus an antibiotic of choice but it also presents, though to a lesser extent, ototoxicity and nephrotoxicity. Vancomycin acts on the cell walls of bacteria by inhibiting the synthesis of the wall, thus destroying the protective shell and killing the bacteria.

Despite being hydrophilic, vancomycin can interact with CDs to control its release[45] and evaluate the resulting cytotoxicity of the material.[46] Vancomycin complexes have been employed for drug delivery systems after surgical manœuvres[47, 48] and as additives in surgical implants.[45, 46, 49] Several methods of complex preparation have been used such as freeze-drying, kneading[50], solvent evaporation and spray drying.[48] Despite the thorough characterization of the resulting inclusion complexes by SEM, Thermal Gravimetric Analysis (TGA), Differential Scanning Calorimetry (DSC), FTIR and XRD, no study discusses the stoichiometry of the vancomycin/β-CD complexes.

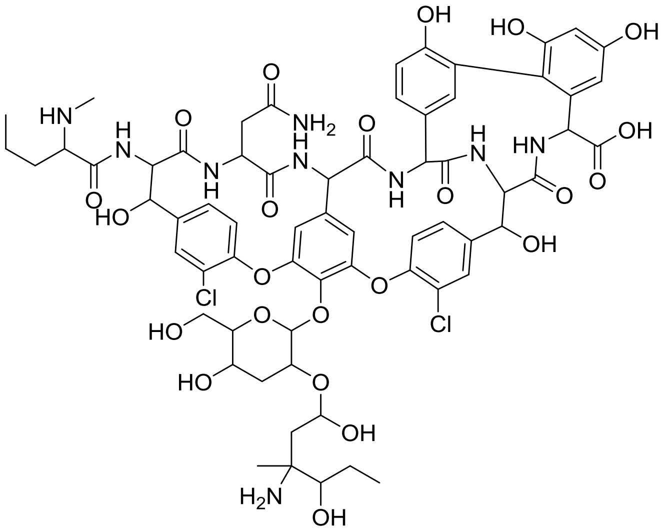

Figure 1.7. Chemical structure of vancomycin

CDs have thus proven to be useful molecules for the encapsulation of small molecules to enhance their stability, their solubility, to slow the release of drugs and thus improve the antibacterial efficiency of the molecules. Encapsulation within CD also helps to prolong the antimicrobial effect onto surfaces.

But CDs do not only display good affinities with small molecules; they also exhibit great interactions with monomers and polymers.

1.4. The use of polymers to form supramolecular inclusion complexes: pseudo-polyrotaxanes and polyrotaxanes

Although the complexation phenomenon of small molecules and antibiotics with CDs had been known for decades, it is only since 1992 that Wenz[51] and Harada[52] detailed work that inclusion complexes based on monomers or polymers has been intensively investigated. Nevertheless, the capacity of CDs to thread along polymers was already known and the first work related to the formation of a diamide and β-CD inclusion complex was reported in 1976 by Ogata et al.[53] These complexes were first referred to as "*tunnel polymers*". Also in 1976, Harada synthesized polymers presenting inclusion complexes along their side chains.[54, 55] Prior to the polymerization reaction, the monomers bearing a nitrobenzene group were entrapped within β-CD. Later, Uemura suggested a diffusion model to explain the diffusion behaviour of cyclodextrin-polymer systems.[56] He studied the ligand interactions between β-CD and poly(methacrylic acid) (PMA) or sodium poly(styrene sulfonate) (NaPSS) in aqueous solutions.

1.4.1. Nomenclature

The term "*rotaxane*"[57] stands for the Latin *rota* (wheel) and *axis* (axle) and describes a dumbbell like molecule threaded with a CD. In this particular case, the CD is entrapped and can only slide along the molecule (figure 1.8).

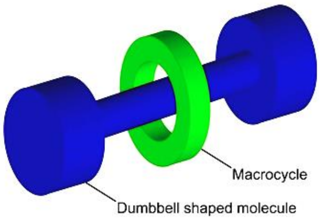

Figure 1.8. Schematic representation of a dumbbell like rotaxane (reproduction from internet)

After polymerization or when a polymer is threaded with CDs and those CDs can not be removed from the chain, the supramolecule is called polyrotaxane. Polyrotaxanes are commonly compared with pearl-necklaces, where the polymer is assimilated to the chain and the CDs to the pearls of the necklace. The bulky molecules or stoppers at the chain ends that avoid the loss of CDs are considered to be the clasp.

The term “*pseudo*-polyrotaxane” can also be used when no bulky molecules are placed at the end of the polyrotaxane (see figure 1.9).

Polyrotaxanes
Pseudo-polyrotaxanes

Figure 1.9. Commonly acknowledge structures of polyrotaxane and pseudo-polyrotaxane

1.4.2. Inclusion complexes between polymers and cyclodextrins

Many polymers[58] have been threaded along with α-, β- or γ-CDs or their derivatives over the years such as poly(ethylene glycol) (PEG)[59, 60], poly(propylene glycol (PPG)[60], poly(methyl vinyl ether)[60] , polyethylene (PE)[60], polypropylene (PP)[60], polyisobutylene[60], poly(methyl methacrylate) (PMMA)[60], poly(styrene) (PS)[61], poly(N-isopropylacrylamide) (PNIPAAm)[61], polyhydroxylethylacrylate (PHEA)[61], poly(ε-caprolactone) (PCL).[62] Block copolymers[63, 64] including Pluronics have also drawn much attention to form inclusion complexes with CDs.[65, 66] And more recently, ionic polymers have also proven to be able to form inclusion complexes with CDs as well.[2, 60]

Inclusion complexes between polymers and CDs can be formed if there are several binding sites along the polymer chain able to interact with the CD cavity. The CDs actually thread along the polymer from the end groups of the polymeric chain.[60] Similarly to the formation of small molecules inclusion complexes, the formation and stability of inclusion complexes with polymers relies on the same parameters as for small molecules. Hydrogen-bonding interactions and Van der Waals interactions are the prevailing forces that govern the formation of pseudo-polyrotaxanes. But there is also a good correlation between the sizes of the CD cavities and the cross-sectional area of the polymers.[67]

Interestingly enough and as described by Wenz in its review[2], inclusion complexes formed between polymers and CDs can be of various types as described in figure 1.10. CDs can thread along the side chains of the polymers but they can also thread along the main polymeric chain and form so-called axial inclusion complexes. Finally, inclusion complexes can also occur as additions to the main chain so that CDs are not thread along the chain but are just interacting with their appropriate binding sites onto the polymer chain.

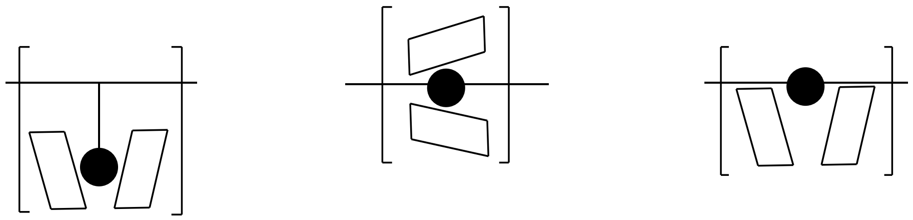

inclusion complex of side chain axial inclusion complex addition of the main chain

Figure 1.10. Schematic representation of inclusion complexes formed between polymers and cyclodextrins (reproduced from the literature 2)

These polyrotaxanes and pseudo-polyrotaxanes in comparison with their free polymer display new interesting properties. Indeed, even if the polymer is hydrophilic the resulting polyrotaxane or pseudo-polyrotaxane is most likely to be sparingly soluble in water. It is the case for most of these supramolecules, after complexation reaction with CDs. These assemblies will not be soluble in water and most organic solvent. The list of solvents that can efficiently solubilize most pseudo-polyrotaxanes and polyrotaxanes is very short and include dimethyl sulfoxide or ionic solvent.[68] Polyrotaxanes and pseudo-polyrotaxanes also show improvements in their thermal properties. They tend to support higher temperatures before degradation as the result of a synergistic effect between CDs and polymers. This can be understood by the interactions that take place between CDs and the monomer units. In a certain way, the physico-chemical properties of pseudo-polyrotaxanes tend to be similar to the one exhibited by polysaccharides.

As for inclusion complexes between small molecules and CDs, polyrotaxanes and pseudo-polyrotaxanes can also be widely characterized by NMR analysis, thermal analysis, electronic microscopy, spectroscopic methods, X-Ray crystallography, circular dichroïsm spectroscopy and scanning probe microscopy.

The property that proves the formation of inclusion complexes with polymers is the change of crystalline structure. Indeed by X-Ray diffraction, it was proven that the crystalline organization between native CDs and pseudo-polyrotaxanes or polyrotaxanes is different. Native CDs present a cage-type or herringbone crystalline structure but when threaded along polymers, the crystalline organization changes to a channel-like type structure. Steed et al. explained the reasons of these crystalline structures for inclusion complexes of small molecules[17] and it can be extrapolated that, as polymers are too long for CD cavities, tubes of inclusion complexes are thus obtained. The channel inclusion is also stabilized by intermolecular hydrogen bonds between the CD hydroxyl groups. As primary hydroxyl groups prefer interacting with primary hydroxyls and as secondary hydroxyl also preferentially interact with secondary hydroxyls, head-to-head or tail-to-tail orientations are favoured over head-to-tail columns.[67] However, in the case of α-CD complexes, both configurations can occur. For linear alkanes and α-CD based inclusion complexes head-to-head channel inclusions are formed[67] whereas for thicker guest such as hydroquinone or *p*-fluorophenol, the inclusion complexes present a head-to-tail orientation.[69]

As poly(ε-caprolactone) (PCL) is a low cost and commonly used biocompatible and biodegradable polyester, many studies have been led on inclusion complexes based on PCL and α-, β- or γ-CDs[70-73]. Due to the size of the caprolactone monomer, stable inclusion complexes could only be obtained with α- and γ-CDs.[70] In the case of β-CD, the size of the CD cavity is too big to interact with the monomer whereas in the case of γ-CDs, two chains could be threaded by a single CD cavity with proper interactions between the PCL chains and the hydroxyl groups of γ-CDs.[70] The height of CD cavity is 7.9 Å and the monomer chain length of ε-caprolactone is around 9 Å so that a 1:1 stoichiometry of CD:ε-caprolactone can be obtained.[70, 74] Several studies also proved that the molecular weight of the PCL influences the stoichiometry of the inclusion complexes between this polymer and α-CD. Indeed by increasing the molecular weight of PCL the stoichiometry of the inclusion complexes also increases so that less α-CDs or γ-CDs are threaded along the polymeric chains.[70, 75] Polyrotaxanes were also obtained but placing various polymers, e.g. poly(butyl methacrylate) and poly(N-isopropylacrylamide), at the end of the polymeric chains to avoid the CDs unthreading.[73, 76]

Star-PCL polymer could also be successfully threaded with α-CDs to obtain star-pseudo-polyrotaxanes[77, 78] that would enhance the biocompatibility of the polymer for drug delivery applications.[78]
PCL and CD based pseudo-polyrotaxanes and polyrotaxanes were developed for blood anticoagulation activity, protein absorption, protection against water and lipase molecules.[73] But the addition of PCL based polyrotaxanes into PCL also changes the degradability rate by changing the crystallinity and acts as a good enforcing filler by increasing the Young's modulus and yield strength compared with the pristine polymer.[79]

Harada once compared polyrotaxanes and pseudo-polyrotaxanes with molecular machines as "*an assembly of a distinct number of molecular components designed to perform machine-like movements in response to an appropriate external stimulus*"[60]. Indeed, it has been observed that the CDs threaded along polymer chains could rotate and slide along the chain as a response to external stimuli[60, 67]. This peculiar property was soon widely used and several supramolecules were synthesized to achieve various stimuli responsive polyrotaxanes or pseudo-polyrotaxanes.

1.4.3. Applications of cyclodextrin-polymer inclusion complexes

Polyrotaxanes and pseudo-polyrotaxanes have been the subjects of many studies over the years because they find concrete applications in various fields such as sensors, self-healing materials[80], shape memory materials[81], coatings[80], flavour preservation[17], paintings[82], adhesives[82], or biomedical applications such as artificial muscles[83], gene delivery[84], drug delivery[85], antimicrobial coatings[46], cancer therapy…[86]
In addition to form and give good stability properties to inclusion complexes, the non-covalent interactions between host and guest also lead to new properties and smart functions that permit the development of the various applications listed above.[82]

Inclusion complexes of polymers and CDs tend to form gels or self-assembled micelles in solution or solvents.[85, 87, 88] This behaviour can be really useful for drug encapsulation. The bioactive molecule or drug can be entrapped at the centre of the micelle or within the gel. The drug is then released by sol-gel transition triggered by temperature, pH or photo-irradiation.[89] Pseudo-polyrotaxanes threaded with functional CDs bearing cationic or fused-ring aromatic substituents are of particular interest as they exhibit good DNA binding ability due to the cationic and π-conjugated molecules capacity to intercalate into the grooves of DNA. These pseudo-polyrotaxanes also display low cytotoxicity and good gene transfection efficacy.[82]

Recently, Collins et al.[90] also used Pluronic (PEG-PPG-PEG triblocks) surfactant based polyrotaxanes to regulate the efflux of accumulated cholesterol from the late endosomal/lysosomal compartment in Niemann Pick C diseases models. In this study, polyrotaxanes were synthesized to boost β-CDs efficacy and improve their pharmacokinetics. Within the late endosome, the unthreading mechanism is triggered by the environment, free CDs can thus act and initiate the efflux of unesterified cholesterol.[90]

1.5. The use of cyclodextrins as building blocks for functional and reactive materials

As detailed before, inclusion complexes of small molecules and polymers within CDs were used as such for various applications as they present interesting smart properties but they were also used to functionalize surfaces, polymers or fibres in order to obtain composite materials.

Functional hybrid materials were obtained by grafting of sulphur atoms linked to β-CD to form active surfaces capable of capturing C_{60} fullerenes or biological substrates for good redox properties, antibody recognition and cell counting properties.[91] Cyclodextrin (CD) derivatives were also grafted onto gold nanoparticles to improve the separation techniques of fullerenes as they show capture-release properties by addition of solvent.[91]
Other than gold, carbon nanotubes were also widely used as templates in the construction of smart materials.[91] The CD derivatives are here grafted by aromatic substituents (e.g. pyrene substituents) onto the surface by π-π stacking. Another efficient way to form CD based nanotubes is to wrap CD-containing macromolecules or pseudo-polyrotaxanes on a carbon nanotube. As an example, cyclodextrin-chitosan conjugates could be wrapped and highly dispersed onto the multi-walled nanotubes. These functionalized nanotubes were complexed

with adamantly modified Ru complex thus forming field effect transistor sensing devices. But they can also be used to condense loose deoxyribonucleic acid (DNA) to particles of different size.[91]

CD derivatives were also synthesized and grafted onto cellulosic fabrics (Tencel®).[92] These fibres are obtained from wood pulp and are very similar to natural cotton with better breaking load, tenacity, dry elongation and a higher resistance to laundry properties. But to enhance the performances of this fabrics and to give it specific attributes, CDs were used for the encapsulation of water molecules, or fragrances or antimicrobial agents.[92]

Polymer presenting CDs as side chains[93] or end groups[94] were also synthesized to enhance the biological properties of the polymer defined as "*inert*" in regards to its biological reactivity. These materials were developed for drug encapsulation or drug uptakes purposes. To functionalize PCL, the monomers or polymer end groups were modified using propargyl groups and β-CD derivatives were grafted by click chemistry. The end group modified polymers were able to form micelles in water as only one end group was modified. The free CD cavities were oriented to the exterior of the micelles being thus free to encapsulate hydrophobic molecules such as phenolphthalein, adamantly carboxylate or umbelliferone.[94]

Using host-guest interaction between two water-soluble polymer side chains, self-healing materials were produced with interesting properties. Two different approaches were analysed to prepare self-healable gels. One approach consisted in a mixture of two polymers bearing each whether the host side chain or the guest side chain. The second approach aimed to polymerize host and guest monomers included together.[83]

In addition to being able to form inclusion complexes, CD derivatives can also polymerize and polymers capable of entrapping molecules can be obtained. Indeed when reacted with citric acid or 1,2,3,4-butanetetracarboxylic acid in the appropriate conditions, a polymer presenting alternately CD and the acid substituent is synthesized by polycondensation reaction.[95] Martel et al. grafted these CD polymers onto polyester prostheses[96, 97] by dry-curing process or incorporated into hydroxyapatite (HA) microporous materials[98] by impregnation. These polymers were used to avoid any postoperative infections by slowing the release of antibiotics and prolonging the antimicrobial effects of the prostheses or materials.[99] The CD based polymers were also grafted onto fibres for filtration[100] and depollution applications.[101]

2. Elaboration of fibrous materials by electrospinning and its use for tissue engineering

2.1. Tissue Engineering

Tissue engineering is a research field that has been developed for barely two decades. It offers new solutions for issues relative to tissue damages and infections but also to fatal side effects developed after transplantation. The interest for this new area of research has grown due to the shortage of donor tissues and organs. But besides, there is a real need to mimic nature and cellular response to avoid harmful side effects that were seen many years after organ or tissues transplants.

Basically, new and functional living tissues are fabricated using living cells that are associated with a matrix or scaffold to guide the cells development. Tissue engineering combines different scientific fields such as biology (especially stem cell biology), materials science and material engineering to form a new ensemble called regenerative medicine. The new products developed for tissue engineering aim to repair, regenerate or even replace damaged or dead human tissues with the help of human cells.

In tissue engineering, the scientific challenge lies in both the understanding of cells and the fabrication of materials to provide templates. It is only due to the interactions between material science and biology and thanks to the progresses made in each field that tissue engineering has been developed and offers new attractive solutions. There are three pillars in regenerative medicine that have to be considered to provide appropriate solutions for tissue damages or failures: the cells, the scaffolds and the signals secreted by the cells in response to the microenvironment generated by the naturally-occurring or synthetic matrix. Indeed, for the materials to be accepted and integrated within the body, the cells seeded onto the scaffolds have to proliferate but they also need to create and recreate functional structures using their innate pre-programming information and signalling. The fact that living cells are expected to normally function onto the template and are implanted instead of an inert synthetic graft is the major difference and advancement in comparison with transplantation.[102]

The scaffolds are not only synthesized using organic or inorganic compounds but they also have synergetic interactions with living tissues thanks to the bioactive molecules or agents incorporated, impregnated or grafted onto the materials. Biomolecules such as growth factors or chemotactic factors are also used to favour the cellular response and development. The engineered templates or matrices can be permanent or biodegradable but they need to be compatible with the living systems and with the living cells *in vitro* but also *in vivo*. Various systems were used as templates such as cell-seeded collagen gels, extracellular matrix or even cell self-assemblies but the most classical approach is to elaborate a polymeric scaffold. [102] Depending on the application of the material, the right tissues have to be designed with the appropriate scaffold and the required cells so that the response will be adequate to the microenvironment and the failure that needs to be taken care of. Many different tissues have been developed over the recent years such as skin, prosthetic heart valves, smooth muscles, tracheas, cartilage, ligaments and blood vessels, but also neural matrices for neural regeneration or ingrowth.[102]

In this project, we report the use of polymeric electrospun membranes as scaffolds for wound dressings, protein targeting or bone regeneration applications.

2.2. Electrospinning: Principles

Electrospinning is an effective and low cost process that aims to fabricate fibres out of an entangled polymer solution. The fibres diameters range from tens of nanometers up to a few microns. The fibres processed under high electrical field are continuously produced to form a dry non-woven mat. This method, as opposed to conventional fibre processing such as extrusion, is guided by electric charges and was reintroduced by Renecker et al.[103] in the early 1990s. This technique (figure 1.11) was already known for over a century and was completely forgotten but since two decades, it has been widely developed.[104]

The entangled polymer solution is feed out of a needle at a constant feed rate. When the solution arrives at the tip of the needle, the polymeric drop is charged because of the electric field (in the order of 1 kV/cm) generated between the needle nozzle and the collector. This field is actually induced by a difference of electric potentials between the needle and the collectors. The electrical field is then distort the charged drop and a cone, commonly called the Taylor cone is obtained. This cone is further stretched into a jet and endures looping and spiralling trajectories permitting the solvent fast evaporation. The dry fibres are collected onto collectors such as various surfaces, substrates or electrodes.[105]

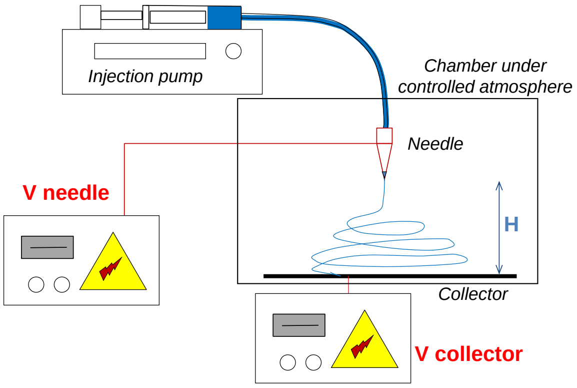

Figure 1.11. Schematic representation of the electrospinning set-up

Renecker et al.[106, 107] intensively studied and defined models to understand the complex mechanisms governing electrospinning. Several different stages were identified once the jet of polymer is formed and stretched (figure 1.12). First, a stable phase is observed, where the jet is not perturbed and linear. This phase was modelled using a Maxwell dumbbell model to describe the rheological behaviour of the polymer. But quickly after a short distance of the needle, some perturbations start and due to the electric charges present at the surface of the fibres, these perturbations become predominant. Bending instabilities force the jet to deviate and the second phase of unstable whipping movements takes place. During this phase, the solvent evaporates by convection because of the high speed of the jet and its looping motions. In each loop, the jet decreases in diameter and becomes elongated while the looping diameter increases strongly.[108, 109] During the first phase of linear stretching, the fluid jet is subjected to accelerations up to 600 m.s^{-2} and the strain rates are in the range of 1000 s^{-1}. However, the looping motion of the jet decreases the speed of the jet that is then around 1m.s^{-1}.[108]

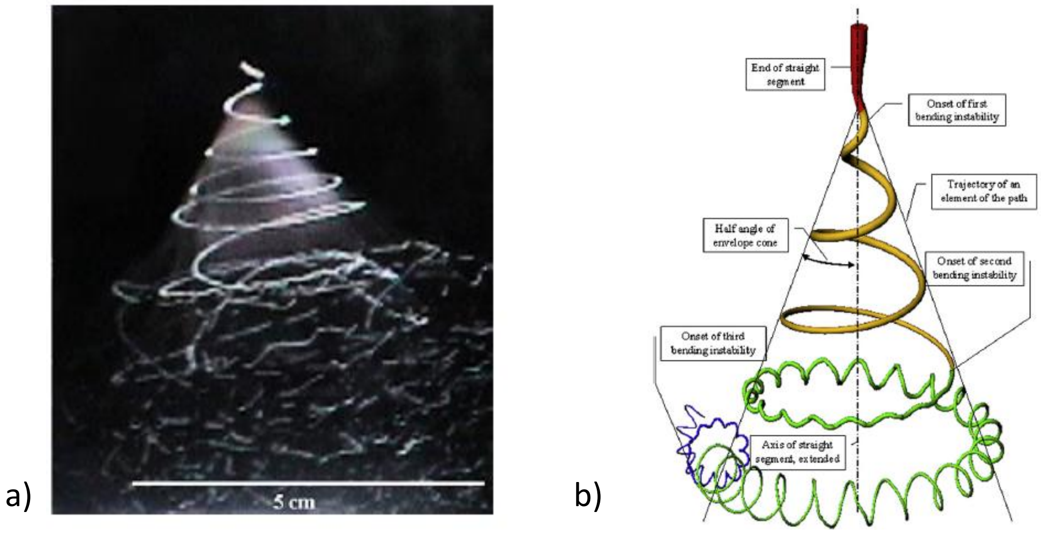
a)
5 cm
b)
End of straight segment
Onset of first bending instability
Trajectory of an element of the path
Half angle of envelope cone
Onset of second bending instability
Onset of third bending instability
Axis of straight segment, extended

Figure 1.12. a) Experimental image of an electrospun jet. b) Schematic representation by Renecker et al. and the details of each separate phase occurring during the electrospinning process (reproductions from reference [107])

The influence of solution parameters

Numerous studies deal with the electrospinning method because the so-obtained membranes present various interesting properties such as high porosity, excellent pore interconnectivity. The fibres also present high surface-to-volume ratio with small diameters. Over the years, fibres were obtained using synthetic and natural polymers but also single or blended polymers.[110]

Many researchers investigated the influence of electrospinning parameters on the fibres morphology and diameter. Hence, it is commonly known that in order to obtain fibres, a minimal solution concentration is necessary. There are certain concentration limits, at too low solution concentrations, only beads can be obtained. At higher concentrations, homogenous fibres can be processed. When further increasing the polymer solution concentration, the fibres diameter also increases.[105]

A relationship has been established between the solution concentration, the feeding rate and the surface tension and the final fibre diameter can be estimated by a power law relationship detailed as follows:

$$\phi \sim c^{\frac{1}{2}} \left(\frac{Q}{I}\right)^{2/3} \gamma^{1/3} \qquad (2)$$

where ϕ is the diameter of the fibre, c the concentration of polymer solution, Q the feed rate of the solution, I the value of electrical current and γ the surface tension of the polymer solution.[108]

If the feed rate of the polymer concentration is further increased the fibre diameter still increases but the number of defects such as beads also gets more important.

The molecular weight of polymers also plays an important role in the fabrication of fibres. Indeed, the molecular weight of polymers is tightly connected to the entanglement of the polymer and thus the viscosity of the solution. Low molecular weight polymers lead to the fabrication of beads as the viscosity of the solution is too low, whereas high molecular weight polymer solution are more viscous and thick fibres can be elaborated. It has actually been demonstrated that the product of the polymeric solution concentration time its intrinsic viscosity (connected to the polymer molecular weight) has a direct impact on the fibres diameter.[111]

The solvent determines the surface tension of the resulting polymer solution and different solvents may contribute different surface tensions. High surface tension inhibits the process of electrospinning as it generates instabilities of the jet leading to sprayed droplets. However, low surface tension will not necessary be more suitable for electrospinning. Hence, similarly to the solution concentration, surface tension determines the upper and lower boundaries of the electrospinning conditions.[105]

The conductivity of the polymeric solution also influences the fibres diameter. The polymer, the solvent used and the availability of ionizable salts determine the conductivity of the solution. By increasing the conductivity of the polymer solution, the diameter of the fibres significantly decreases whereas for low conductivity, the obtained fibres may present beads and insufficient elongation to be uniform.[105]

The influence of processing parameters

To elaborate electrospun fibres, solution parameters are not the only determining parameters that rule the aspect and size of the resulting fibres. Several processing parameters have also some influence on the resulting fibres.

The applied voltage initiates fibre formation as it induces the charges necessary on the solution for the fluid to stretch and thus for the fibres to be fabricated. There are some discussions on its effects on the fibres but, in most cases, higher voltages cause more stretching of the jet due to Coulombic forces in the solution and to a stronger electric field that lead to the fabrication of thinner fibres and faster solvent evaporation. What is certain is that at very high voltages, there is a greater probability to form beads[105].

The flow rate has in its own way a similar trend as the solution concentration. Indeed, by increasing the feed rate of the solution, the diameter of the fibres is also thicker. This can be understood as the feed rate will influence the jet velocity and the solvent evaporation rate. So it is more desirable to have lower feed rate to ensure enough solvent evaporation time within the fibre and, hence, less defect aspects of the fibres are generated[105].

The needle to collector distance has been studied as another fibre diameter and morphology controlling parameter. A certain minimal distance is required to give the solvent sufficient time to evaporate or the collected fibres will present beads. The same defects will also appear if the distance is too big because the instabilities generated will be too strong to elaborate uniform fibres.[105]

The experimental temperature and relative humidity also play significant role in the fibre morphology and collection. The temperature will impact the viscosity of the polymer solution whereas the humidity will affect the electric field and thus change the solvent evaporation conditions.[105]

In recent years, the development of new spinning devices for electrospinning was one of the main focus of research in order to fabricate bigger mats at a more efficient rate and thus gives electrospinning more industrial advantages.[108] The development of new devices and set-ups led to the extension of materials used for electrospinning processing. Indeed, not only polymers are used to fabricate fibres but also inorganic compounds (e.g. hydroxyapatite, glass, …) , metals, metal oxides, ceramics and even composite systems. The application potential of electrospun fibres has thus been multiplied because of the wide range of materials that can be processed by electrospinning.[108]

Another main subject of research was the electrospinning of well-controlled and well-defined 2D or 3D structures of fibrous membranes. Originally, aluminium foil was used as a collector, but numerous alternatives were developed such as conductive paper or cloth, wire mesh, pins and bars were used. To obtain aligned fibres, different collectors were designed such as rotating drums, rotating wheel-like bobbins, metal frames or even counter electrodes, to collect more or less parallel fibres.[105] The drums or wheels rotating at an adequate speed will permit the alignment of the fibres.

Another example of the resolution to control the deposition of fibres is that many studies deal with the elaboration of electrospun membranes onto patterned collectors to see if the deposition could be guided by the topological aspect and nature of the collectors.[112, 113] Our team particularly investigated this approach using PCL fibres onto patterned collectors[112] and studied the influence of the nature of the polymer on the structure of the fibrous mats (articles under revisions). We also established that some polymers and especially PCL, tended to self-assembled into honeycomb patterns once collected after electrospinning experiments.[114] A model was also established to understand this phenomenon and was used to better understand the deposition of fibres for different polymers. This property was then further used as an original way to self-design adequate patterned two-dimensional as well as three-dimensional membranes for tissue engineering applications.[115, 116]

2.3. Electrospun membranes for tissue engineering

As now well-established, electrospinning was used in this thesis as an approach to elaborate polymeric scaffolds appropriate for tissue engineering applications.

As already depicted in this chapter under the previous paragraph, electrospun fibres present many advantages such as high surface to volume ratio and tunable porosity that are required for tissue engineering. But fibres are also interesting as their surface is conveniently accessible and can be modified if required.[117]

Due to these multiple properties, electrospun membranes were used for various different applications such as nerve, bone, cartilage, tendon/ligament and vascular tissues reconstructions, wound dressings and drug delivery systems.[117-119]

For tissue engineering, the material of choice depends on the tissue to regenerate, the type of scaffold and its required properties but also on the time necessary for the regeneration to be completed.[120]. Biodegradable materials are often chosen although it is not compulsory for the materials to degrade after some time.[102] Nevertheless, the templates need to be biocompatible with living tissues and need to support the growth of cells. Therefore, polyesters have been widely used for this type of applications and especially polylactides, polyglycolides and PCL.[120, 121] Sometimes, two or more polymers are required to obtain adequate properties for cells to proliferate and adhere so that blends or composite systems can be electrospun. These polymers once processed by electrospinning offer the cells a good environment that mimics native extracellular matrix. Even so, polymers may not always be recognizable by cells and hence natural polymers such as cellulose, chitin, chitosan, polysaccharides, collagen, natural silk and hyaluronic acid can be preferentially electrospun for better interactions and biological properties with the living cells.[117, 120, 121] More recently electrospun proteins, peptides and even DNA were also used as matrices for tissue engineering.[122] All these materials present better cell recognition and biological properties in comparison with synthetic polymers. Yet, the processing of these materials by electrospinning has revealed to be difficult solely so that they are often mixed with synthetic polymers.[120, 122]

To improve the biological properties of the polymer based scaffolds, biomolecules were incorporated into the substrates to increase the hydrophilicity of the membranes and have a better efficiency for regenerating biofunctional tissues.[120] Different approaches can be used to incorporate bioactive agents leading to different release profiles of drugs, growth factors, genes or proteins.[120, 123] The high concentration of bioagents can be dissolved and dispersed in the polymer solution or emulsion prior to electrospinning, so that there is a good probability that some of the drug will be at the surface of the resulting fibres.[124] These mats display a burst release in the initial period of the drug release tests.[120] To have a better control over the release kinetics of the drugs, a second approach was used that consisted in the fabrication of coaxial core/shell fibres.[121] These fibres present a core incorporating the biomolecules encapsulated within a polymeric shell. The drug release then takes place whether through the aqueous pores of the shell or when the shell starts to degrade. The elaboration of core/shell fibres presents one big advantage as it protects the biomolecules from any degradation that could be induced by the electrical field during the electrospinning step.[123] Another alternative for the incorporation of bioactive agents within the scaffolds is to elaborate electrospun and electrosprayed nanomaterials. The drugs could then be electrosprayed onto electrospun membranes or sandwich-like structures could be fabricated with an alternation of non-woven fibres and electrosprayed particles.[125] This technique also enables a better control over the release of the biomolecules as they are partly of fully entrapped within the fibres.

Since the development of tissue engineering, several drugs, proteins and growth factors were incorporated into fibrous membranes to give the overall mats better biofunctionality including, bovine serum albumin, epidermal growth factor, lysozyme, bone morphogenic protein and gene, nerve growth factor, plasmid DNA encoding bone morphogenic protein, platelet-derived growth factor, plasmid DNA encoding luciferase, RNA protein segments...[123] In parallel, covalently linked molecules were also grafted onto the surface of the fibres by chemical treatments such as plasma, UV, γ-irradiation, high temperature and acid or basic solutions.[120, 126] Yet, these efficient treatments could lead to the degradation of the fibrous structures especially in the case of biodegradable polymer based fibres. Another problem is that even when the grafting is successful there is no method to quantitatively estimate the number of reacted groups on the surface.[126]

Hence there is a real need to develop materials that are biocompatible with living tissues and cells and that present interesting biofunctional properties. If for degradation time issues, an inert polymeric material is chosen as scaffold, research has to focus on a method that will functionalize fibres using soft versatile chemistry reactions in order to improve the surface biological activity of the templates while preserving the native extracellular matrix structure.

2.4. Poly(ε-caprolactone) based membranes for biomedical applications

2.4.1. *Physico-chemical properties of poly(ε-caprolactone)*

Poly(ε-caprolactone) (PCL) is low cost, biocompatible, biodegradable and FDA approved synthetic polyester. It has been used for biomedical sutures since the 1980s.[127] PCL can be degraded by microorganisms but also by hydrolysis of its ester linkage at a slow rate.[128] Its degradation rate is even slower than the one determined for polylactides. It needs two to four years to degrade *in vivo* under normal conditions. This is one of the reasons that in the late 80s, this polyester was superseded in favour of faster degradable polymers that were thought to be less harmful. But with the rise of tissue engineering, PCL was exploited again and became one of the mostly used polyester for this type of long-term applications.[129]

Additionally, PCL presents good rheological and mechanical properties. Indeed, this polyester is semi-crystalline with a glass transition temperature of -60°C and a melting temperature around 50°C depending on its crystallinity degree. Thence, PCL is always in its rubbery state at room temperature. These characteristic properties enable the polymer to be processed and formulated at low temperatures.[129] So, PCL based scaffolds can be elaborated by a wide range of technologies including gravity spinning, wet spinning, phase separation, micro particles, and electrospinning.[127]

To improve the overall properties of a PCL based material, it can be blended with a wide range of other polymers (e.g. cellulose, cellulose derivatives, poly(lactic acid), poly(lactic acid-co-glycolic acid))[129] to improve stress resistance, dye-ability and cell adhesion but when combined with starch its *in vivo* degradation rate is accelerated.[130]

However, the main disadvantage of PCL is that it is a hydrophobic polymer resulting in poor wettability and lack of cell attachment as well as uncontrolled biological interactions with the surrounding medium[127]. Fortunately, the biological interactions of this polymer with cells and tissues can be improved by incorporating biomolecules or by modifying its surface with grafted molecules or coatings.[127]

2.4.2. Poly(ε-caprolactone) based fibres for tissue engineering

As natural polymeric fibres (e.g. chitosan, collagen, gelatin) are difficult to electrospun on their own and do not reach sufficient mechanical properties[131], many synthetic polymers were used as alternative polymers. One of this widely used synthetic polymer is PCL. Many studies discuss the electrospinning of PCL and the influence of the solvent and experimental parameters on the fibres morphology.[127] Highly porous fibres with tunable pore size were obtained by electrospinning this polyester and collecting the non-woven mat in a water bath.[132] The influence of the alignment of PCL fibres on the orientation and extracellular matrix production of porcine intervertebral discs was also assessed proving that oriented fibres would strongly affect the orientation of the cells proliferating onto the mat. It also showed that highly aligned fibres had a positive effect on extracellular matrix proliferation in comparison with random fibres.[133]

The mechanical properties exhibited by PCL fibres (modulus and elasticity) are appropriate for tissue engineering applications especially for bone regeneration or vascular grafts[134]. But some studies even achieved higher strength for bone tissue engineering applications by incorporating reinforced particles such as bioactive glass[135] or hydroxyapatite (HA)[136]. More generally, Sarvestani et al. proved that the addition of nanofillers such as HA strengthen the membranes even more than the conventional macro or microscopic additives[137].

But as previously discussed, in vitro studies proved that fibrous mats based on PCL display high hydrophobicity and thus cell do not adhere onto the fibres. Fortunately, to enhance the biological activity of these polyester based membranes several methods can be used. For example, some biomolecules can easily be mixed within the polymer solution prior to electrospinning. Heparin was thus successfully incorporated within PCL fibres when mixed in a solvent mixture composed of dichloromethane/ethanol/water.[138] Several other bioactive agents (e.g. nerve growth factor, antibiotics,…) were also directly incorporated into the polymer solution and electrospun as such.[138]

Coaxial electrospinning was also used to change the surface hydrophobicity of PCL fibres. This method is easy and efficient to change the surface properties of these fibres. Our team used coaxial electrospinning to enclose PCL fibres in a gelatin based shell. HA crystals were then grown onto the surface of the fibres to obtain so-called mineralized nanofibres that favour the development of human adipose-derived stem cells.[139]

To hide the surface of PCL fibres, the membranes can be coated within solutions containing bioagents. The immobilization of BMP-2 growth factor nanoreservoirs onto fibrous PCL membranes was also performed by the Layer-by-Layer technique. This technique also enabled to reduce the concentration of growth factor incorporated within the material. The *in vitro* and *in vivo* studies proved to be very promising with a better controlled release of the drug.[124]

The surface of polyester based fibres can also be chemically modified and various surface treatments were developed including plasma treatments[140], UV-, γ-irradiation, sodium hydroxide solutions. These surface modification techniques are quite harsh and often led to the distortion of the fibres structures.

Basic solution of sodium hydroxide (NaOH) was used to generate carboxylic groups at the surface of the fibres.[129] This modified surface was then dipped in an apatite nuclei solution to obtain bone-like mat.[141, 142] NaOH treated PCL fibres were also used for vascular tissue engineering and seeded with primary endothelial cells in presence of an endothelial growth factor[143]. Despite showing good biocompatibility with living cells, NaOH treated fibres displayed faster degradation rate after six months *in vivo* compared with untreated PCL fibres.[144] Also, this treatment seems to affect the structure and reduces the porosity of the membranes.

Ma et al. also improved the surface hydrophilicity of PCL using a photo-oxidization method[145]. The membranes were preliminary soaked into a hydrogen peroxide solution under UV light. The peroxides can actually decompose and initiate, under UV irradiation, the polymerization of methacrylic acid, hydroxyethyl methacrylate or acrylamide monomers onto the surface. Hydroxyl groups could also be grafted onto the surface when the membranes are exposed to air or oxygen after their pre-treatment with peroxide solution.[145] The resulting materials demonstrate good adhesion with endothelial cells. Proteins such as Arginylglycylaspartic acid (RGD), a tripeptide containing the Arg-Gly-Asp sequence, or epidermal growth factors (EGF) were also immobilized onto PCL surface after carbonyl or amino coupling sites were created by photo-oxidization.[145]

Besides, plasma treatments have been developed. This treatment avoids the dipping of fibres into any type of solutions so that the structure has better chance to be preserved. Various types of plasma treatment have been used: oxygen, argon, nitrogen, carbon dioxide or air.[140, 146-148] Plasma treatment can easily introduce polarized groups such as hydroxyl, carboxyl, amino, sulphate on PCL surfaces depending on the gas used.[145] The selection of functionalization imparted can be varied by selection of gas plasma but also by the operating parameters (pressure, power, time, gas flow rate).[140] Plasma can be used as an alternative step to generate functional groups onto the surface of the fibres. One major drawback for this method is that all experiments have to be carried out under vacuum hence limiting the industrial exploitation of this method.[140] The hydrophilicity of plasma treated surfaces has also proven to be a non-permanent effect in some cases.[136] Additionally depending on the chosen experimental parameters, the surface of the fibres can be altered and the structure of the fibres can be lost.[147] Contradictorily and to some extent, the changes in the fibres topology and the increase in surface roughness improves the cells adhesion and proliferation.[147] Air plasma treated PCL fibres, even proved to be more efficient toward Schwann cells proliferation than core/shell poly(ε-caprolactone)/collagen scaffolds.[148]

More recently, click chemistry was investigated as a new way to easily modify PCL fibres.[149, 150] A scaffold based on α,ω-azido-poly(ε-caprolactone) fibres was electrospun and then modified. Propargylated fluorescein isothiocyanate[149], propargyl-D-galactoside[150] and propargyl-D-mannoside[150] were grafted by copper(I)-catalysed azide-alkyne cycloaddition. For carbohydrate functionalized fibres, contact angle measurements proved the increase of the hydrophilicity of the fibres. Furthermore, the bioavailability of the carbohydrates was assessed by enzyme-linked lectin assay (ELLA assay) and proved that the carbohydrates interacted with specific lectins.[150]

2.5. Elaboration of cyclodextrin inclusion complexes based fibres

2.5.1. *Cyclodextrin based fibres*

Uyar et al. have widely investigated cyclodextrin (CD) based fibres. Its early work investigated the functionalization of various polymeric fibres, such as polystyrene[151], poly(ethylene oxide)[152] or poly(methyl methacrylate)[153], with the use of CDs for the encapsulation of small molecules. CDs and polymers were mixed together and electrospun as single solutions. Their team mainly investigated applications such as filters[154, 155] or fragrance encapsulation.[156] Drug delivery systems were then later developed within their team with naproxen entrapped within β-CDs to obtain functionalized PCL fibres[157]. Additionally, allyl isothiocyanate was also successfully included into β-CD within a poly(vinyl alcohol) (PVA) matrix and the mats displayed high killing activity against both Gram positive *Staphylococcus Aureus* and Gram negative *Escheria Coli* bacteria [158].

Martel et al. prepared CD based polymers for the functionalization of polypropylene (PP)[100] and poly(ethylene terephthalate) (PET)[101] fibres. The CDs were directly polymerized onto the surface of the polymeric fibres but the cyclic oligosaccharides were not processed by electrospinning. These non-wovens were developed for metallic ion exchange[101] and pollutant absorption[100] for filtration applications.

But the major breakthrough regarding CD based fibres was achieved by Uyar et al. They were the first to electrospun non polymeric materials and obtained solid and resistant nanofibres.[159] Indeed, CDs were successfully electrospun without any polymeric matrix and present interesting mechanical properties.[160] These fibres were studied for the release of antibiotics (e.g. triclosan)[161] and may be pioneer work on the electrospinning of non-polymeric compounds.

2.5.2. Fibrous mats based on polyrotaxanes of cyclodextrins and polymers

To the best of our knowledge only a few studies deal with the electrospinning of CD based polyrotaxanes (PRs) or pseudo-polyrotaxanes (pPRs).
The first work related to this type of fibres has been related in 2006 by Araki et al.[162] Poly(ethylene glycol) (PEG) was complexed with α-CDs and, to avoid the loss of threaded CDs, adamantane stoppers were added at the end of the polymeric chain. To elaborate pure PR or PR blended with cellulose fibres, all solids were dissolved in a mixture of dimethylacetamide and lithium chloride and processed by wet spinning. No electrical field was actually used to obtain the fibres. The wet spinning process led to the precipitation of gel-like fibres in a non-solvent bath (methanol). The mechanical properties of the PR/cellulose blended fibres were assessed and compared with pure cellulose fibres. The tensile tests showed that pure PR and blended PR/cellulose scaffolds were more rigid than pure cellulose. However it seemed that pure PR fibres showed lower strength at break probably because of their low elongation rate.[162]

Later, Uyar et al. reported the first electrospinning attempt on PEG and α-CD pPR within a PEG matrix.[163] Indeed, due to the low molecular weight of PEG used, no fibres were collected when solely electrospun. The so-obtained fibres were used as a model system and characterized by X-Ray diffraction (XRD), Fourrier Transform Infra-Red spectroscopy (FTIR), Scanning Electron Microscopy (SEM) and Transmission Electron Microscopy (TEM). The presence of pPR was assessed by Fourrier Transformed Infrared spectroscopy and X-Ray diffraction (XRD) showing the characteristic channel-like threaded CDs peak at $2\theta = 20°$. A correlation between the pPR weight load within the fibres and the resulting fibres diameter could be drawn. By increasing the weight ratio of pPRs, the average fibre diameter increased and beads appeared.[163]

Katsuyama et al. also published several studies regarding the elaboration by wet-spinning of poly(ethylene glycol) and α-CD PR based fibres[164-166]. Following on from Araki et al.[162], the PR were dissolved using dimethylacetamide, lithium chloride in addition to more common organic solvent such as dimethylformamide and dimethyl sulfoxide. The fibres were thoroughly characterized and their mechanical properties prior[164] and after crosslinking[165], as well as their crystallinity[166] were studied in detail to understand the behaviour of PR fibres.

All these articles thoroughly characterize and analyse novel types of electrospun fibres based on the peculiar inclusion complexes between polymer and CDs but none actually fully realized or developed the potential of these materials.

In this PhD thesis, we will try to prove that pPR based fibres open new doors for PCL scaffold chemical modifications while preserving the porosity and extracellular matrix mimicking structure compulsory for good biological interactions.

Chapter 2

Synthesis of cyclodextrin inclusion complexes

Synthesis of cyclodextrin inclusion complexes

In this chapter, we will discuss the synthesis of all the cyclodextrin-based inclusion complexes that will be further used or functionalized for the development of biofunctional fibrous membranes.

In the first part of this chapter, we will focus on the synthesis of the inclusion complexes of small molecules developed as additives that will be incorporated into the mats. As the state of the art regarding the encapsulation of molecules has been widely detailed in the first chapter, we decided to avoid any repetitions and discuss all the synthesis and characterization of these new peculiar species. The detail of each reaction will be given as well as the results of the characterization analyses. In an attempt to clarify the purpose of each inclusion complex (IC) and better understand the choice of the antibiotic regarding their encapsulation, the syntheses of these host-guest complexes were divided into two subchapters. First curcumin and MB were used for their natural antibacterial properties. The preparation and characterization of ICs between these antibiotics and β-cyclodextrins (β-CDs) will be presented in this chapter. Although it will not be discussed here, they will be used later as additives for wound dressing applications and their properties will be studied in chapter 3. On the other hand, vancomycin and gentamicin were also let to react with β-CDs to obtain different types of adducts. These adducts were prepared for the functionalization of antibacterial materials for tissue engineering applications.

The second part deals with the synthesis of stable pseudo-polyrotaxanes (pPRs) when solubilized in dimethyl sulfoxide (DMSO). To achieve such stable supramolecular structures, our strategy was to synthesize different poly(ε-caprolactone) (PCL) based polymers presenting various architectures. PCL was chosen as it is well-known that this polyester has good biodegradable and biocompatible properties, required for tissue engineering applications. Additionally, the mechanical properties of PCL based materials are adequate for our targeted applications. Thus linear, four-branched and block copolymer polymers were synthesized by Ring Opening Polymerization (ROP) of ε-caprolactone (ε-CL). To initiate the polymerization, various polyols were used and the central block of the triblock copolymer was a commercially available poly(propylene glycol) (PPG) . An alternative to standard metal catalysed polymerization of ε-CL was used to avoid any toxicity issues relative to the use of these materials for biomedical applications. Various well-defined and tailored linear, branched and block copolymers were thus synthesized and thoroughly characterized.

The last aspect investigated in this chapter will be the synthesis and characterization of the PCL based pPRs. For the synthesis of these pPRs, α- or β-CDs were used depending on the kind of guest polymer

The physico-chemical properties exhibited by these supramolecules will be discussed in detail. Various thermal and crystalline characterizations as well as Nuclear Magnetic Resonance (NMR) analysis attested the success of the formation of ICs between CDs and the polymers. Finally, Small Angle Neutron Scattering (SANS) experiments carried out in deuterated dimethyl sulfoxide (DMSO-d_6) determined the organization of the pPRs in this solvent. DMSO will be further used for the processing of these supramolecules.

1. Encapsulation of single molecules

Four different antibiotics (e.g. curcumin, methylene blue (MB), vancomycin and gentamicin) will be encapsulated within CD cavities. Curcumin and MB based ICs were thought to be used as additives for wound dressing applications. These ICs could be incorporated into polysaccharide based membranes. On the other hand, the two synthetic antibiotics could be used for tissue engineering applications and incorporated in polyester based fibrous materials.

As these antibiotics are quite bulky, β-CD was used as encapsulating agent. β-CDs are composed of seven glucose units linked together to form a ring. The inner diameter of their cavities is appropriate for the formation of interactions with the antibiotics discussed above. α-CDs could not be used as their inner diameter was too small to allow the antibiotics as guests within their cavities.

1.1. Curcumin and methylene blue inclusion complexes for wound dressing applications

1.1.1. Inclusion complexes between curcumin and β-cyclodextrin

Curcumin is a widely known antibiotic with one major drawback: its poor solubility in water. This lack of miscibility with water leads to a lack of efficiency and the need to use additional amount of this molecule to obtain appropriate results toward bacteria. Nonetheless, when encapsulated in CD, curcumin is highly soluble. Its resulting bioavailability and antimicrobial property are then increased.

To obtain inclusion complexes between curcumin and β-CD, two different methods of complexation were tested. Both encapsulation methods were performed in solution by freeze-drying process.

The first trial was attempted in distilled water as a solvent for both the curcumin and the β-CDs[29]. The second test was done in a 50/50 v/v mixture of water and acetone.[26] Acetone was used to solubilize curcumin before the solution was poured and slowly added to the aqueous solution of β-CD. After three days, both reactions were stopped. It is interesting to point out that both reaction mixtures were still homogenous and no precipitate could be seen in the flasks. However, in the case of the reaction carried out in the 50/50 v/v mixture of water/acetone, the colour of the solution changed from yellow to orange/red. The second aqueous solution remained yellow.

Prior to the freeze drying process, acetone had to be removed by rotavapor evaporation. Both aqueous batches were then poured into glass vials and freeze-dried for a week to remove the distilled water. The same dry yellowish powders were collected when all the water was removed. No differences could be made between the two different batches of inclusion complexes.

Several characterization analyses were then carried out to identify and investigate the properties of curcumin and curcumin based ICs. After solubilizing the ICs in DMSO-d_6, ^{1}H NMR analyses were done and a 2:1 β-CD:curcumin was calculated. As initially, a 2:1 ratio of β-CD over curcumin was incorporated in the solution mixture and no purification could be performed, the same ratio was found after reaction. We supposed that, giving the reaction time and the time needed to remove all water, the curcumin had sufficient time to be entrapped within the CD cavity.[25, 27] No difference in the encapsulated ratio could be noted between the two different processes.

Thermal Gravimetric Analysis (TGA) were first conducted on the two different samples. Here again, no influence of the complexation solvents could be seen. The thermal degradation behaviour of the curcumin inclusion complexes is almost identical to the degradation of β-CD. For all samples (figure 2.1), a first weight loss below 100°C appeared corresponding to the loss of residual water. However, around 300°C encapsulated curcumin started to degrade. The degradation of β-CD started around 290°C which also proved that the cyclodextrin thermal property is even enhanced by the inclusion formation. In the case of pure curcumin, several degradation peaks could be seen starting around 200°C.

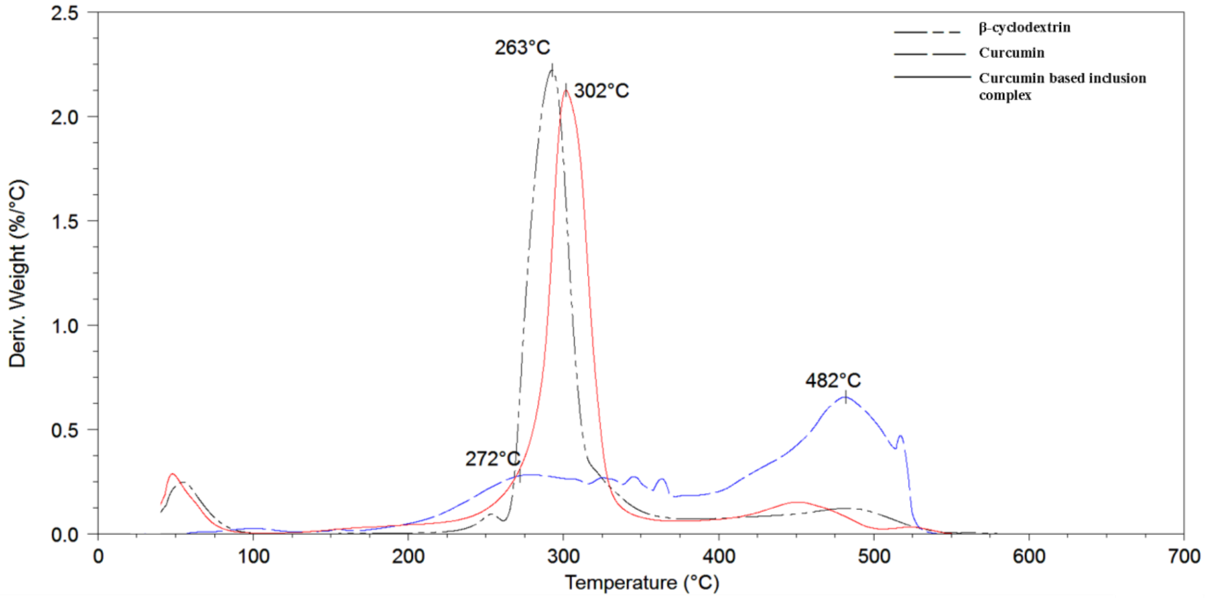

Figure 2.1. Thermal gravimetric analysis of (broken double dash) β-cyclodextrin, (long dash) curcumin and (solid) curcumin inclusion complex

Unfortunately, Differential Scanning Calorimetry (DSC) analyses could not confirm the TGA analyses as no melting temperature could be seen prior and after complexation reaction in the analysed temperature range.

To define the crystalline organization of the inclusion complexes between curcumin and β-CD, X-Ray Diffraction (XRD) was performed on the samples and compared to free curcumin, native β-CD and the physical mixture of curcumin and β-CD. The signature obtained for the two differently synthesized ICs is identical proving once again that the complex formation conditions did not influence the final signature and properties of the complexes. The signature obtained for the ICs displays numerous peaks where most of them were already seen in the signature of free curcumin. However, the inclusion complex signature is different from the XRD signature of the physical mixture of both curcumin and β-CD suggesting that the IC reaction was successful (figure 2.2).

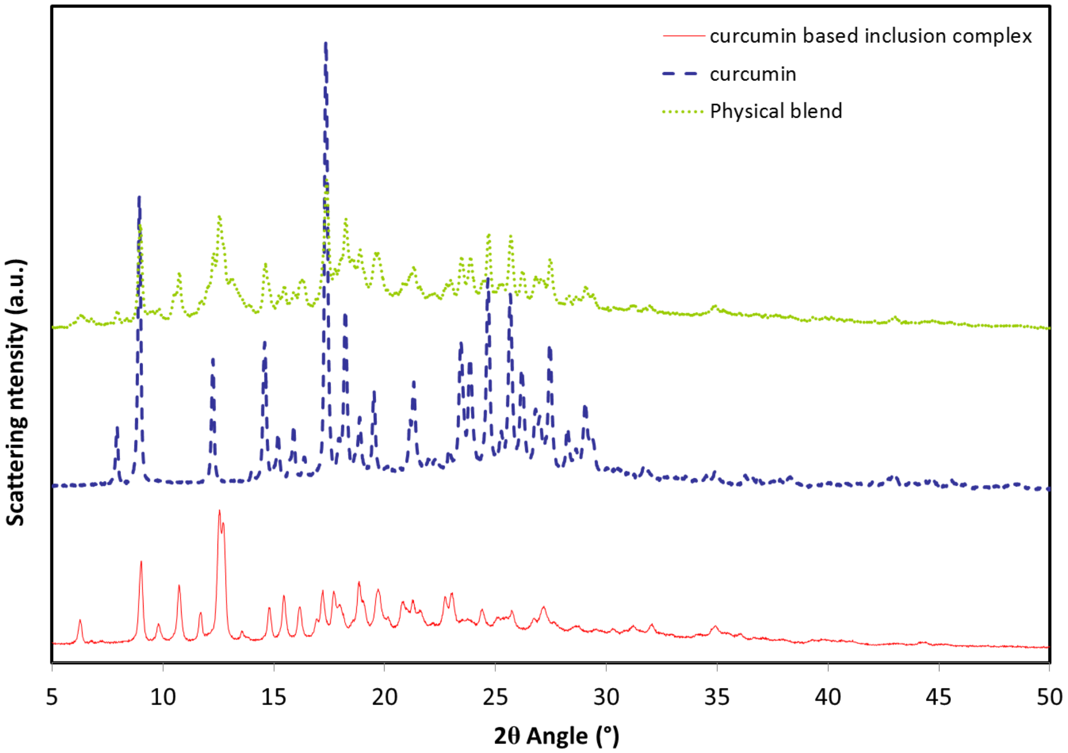

Figure 2.2. XRD spectra overlay of (- red line) β-cyclodextrin/curcumin inclusion complexes, (- blue short dash) pure curcumin and (- green dashdot) the physical blend between curcumin and β-cyclodextrin

The evaluation the Minimal Inhibitory Concentration (MIC) of curcumin and curcumin based inclusion complexes was done to determine if native curcumin or its IC derivatives display any antibacterial properties. The MIC corresponds to the lowest concentration of bioagent required to kill 100% of bacteria within a contaminated solution. Concretely, a stock solution of the material that needs to be tested is solubilized in a culture medium. In the stock solution, the introduced weight of the analysed molecule corresponds to the maximal weight that can be solubilize in the given buffer volume.

Then, several diluted solutions are prepared before the bacteria are actually added to each solution. The different diluted and contaminated flasks are then incubated at 37°C for 24 hours before the turbidity of each solution is measured. A clear solution suggests that all the bacteria were killed thanks to the antibacterial agent, whereas when the bacteria concentration was too high for the bactericide to be completely efficient, the solution becomes turbid. (see chapter 5 section 6.1 for further details)

Both native β-CD and native curcumin were also solubilized, evaluated and used as reference molecules. The synthesized ICs, the curcumin and the β-CDs were evaluated against two different types of bacteria: *M. Luteus* and *S. Aureus*.

Stock solutions were first obtained by dissolution of free curcumin, free β-CD and the two differently prepared inclusion complexes in a bacterial preculture medium. Out of these stock solutions, six different diluted solutions were prepared for each species to range concentrations between 100 and 1000 μg.mL^{-1}. The solutions were then incubated at 37°C overnight before any conclusion could be drawn.

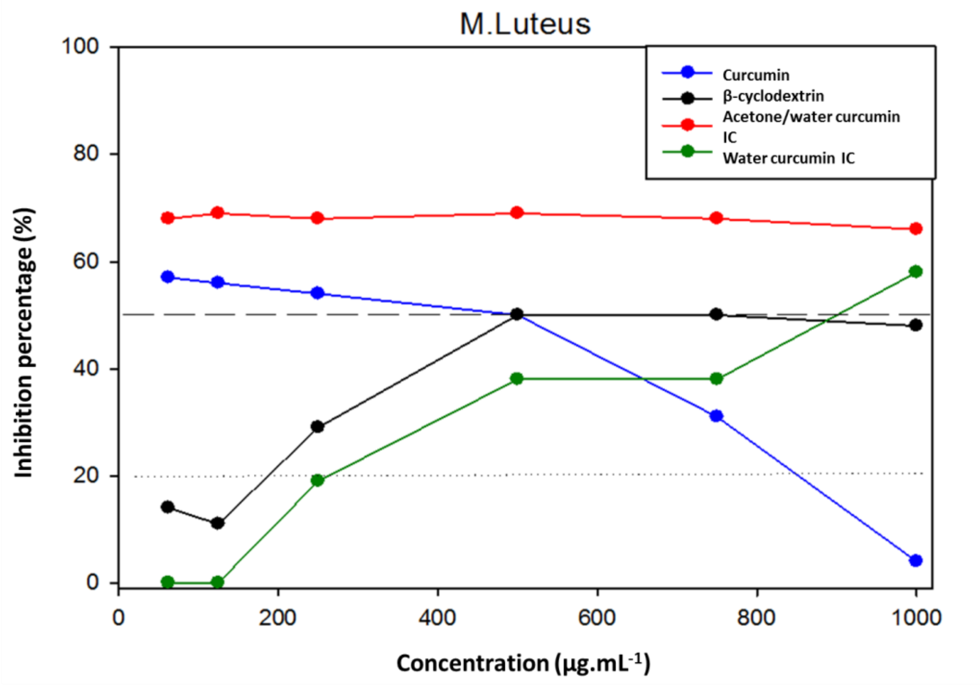

Figure 2.3. MIC determination of pure curcumin, free β-cyclodextrin and their resulting inclusion complexes against *M.Luteus*

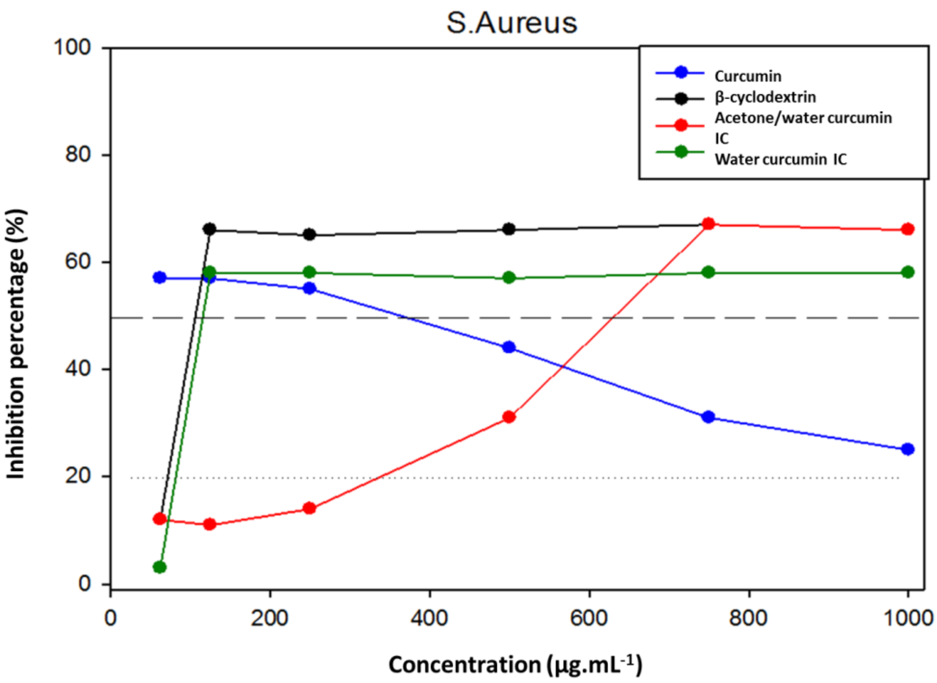

Figure 2.4. MIC determination of pure curcumin, free β-cyclodextrin and their resulting inclusion complexes against *S.Aureus*

As expected, curcumin is almost insoluble in water and thus in any biological buffer. Therefore, the MIC could not be precisely assessed (figure 2.3 and 2.4) and the results obtained are not logical and coherent. These results thus demonstrated that this antibiotic is poorly soluble in the buffer but no MIC could be determined.

Conversely, the curcumin based ICs could be solubilized and several diluted and homogenous solutions were successfully prepared and contaminated with *M.Luteus* (figure 2.3) and *S.Aureus* (figure 2.4) respectively. These series of tests further proved that the encapsulation of curcumin improved the solubility of this antibiotic.

As seen in figures 2.3 and 2.4, inclusion complexes between curcumin and β-CDs seemed to be effective toward both bacteria. However, according to our results, the maximum inhibition of the curcumin based inclusion complexes was 70%. Reaching this percentage of inhibition, a plateau was observed and the inhibition percentage did not attain 100% even when increasing the concentration of inclusion complexes in the tested solutions. This result, although unusual, could be explained by the fact that when curcumin is released from the CD cavity, a certain amount might still not be soluble in the buffer despite the enhancement of solubility induced by the CDs. The effective bactericide concentration is thus lower to the one introduced at the beginning of the test. The limit of solubility of curcumin may have been reached and so no complete inhibition could be achieved.

An influence of the IC preparation method can be seen during the MIC determination. Indeed, the behaviour of each batch of inclusion complexes is different against both types of bacteria. For the ICs prepared in the water/acetone mixture, when *M.Luteus* was added to the IC based solutions, a 70% inhibition plateau is already reached for the lowest concentration. In the case of *S.Aureus* contaminated solutions, the evolution of the inhibition is more linear and a concentration of approximately 800 μg.mL^{-1} is necessary to obtain a 70% inhibition of the bacteria. In the case of the ICs prepared in water, the evolution of the inhibition percentage in regard to the IC concentration is the complete opposite of what has been seen for the IC batch prepared in water/acetone. No explanation has yet been found to explain the differences obtained for both batches of ICs.

These MIC tests thus demonstrated that the inclusion complexes improved the solubility of curcumin in a specific buffer and led to a better antibacterial activity. The inclusion complex formation process seemed to have an effect on the inhibition of bacterial growth as the two different curcumin inclusion complex batches demonstrated different behaviours toward both bacteria. However, no complete inhibition could be achieved against both bacteria suggesting that something must stop the solubilisation of curcumin within the buffer.

1.1.2. *Inclusion complexes between methylene blue and β-CD*

MB was not encapsulated within CD cavities to improve its water solubility but to slow down the release of this antimicrobial agent from the fibrous membrane and prolong the bactericide properties of the materials.

In the case of the encapsulation of MB, a stoichiometric ratio between methylene blue and β-CD has been found in the literature.[36, 37, 97] So, to synthesize these inclusion complexes, an initial 1:1 ratio of β-CD over methylene blue was incorporated in distilled water. In this case, methylene blue is highly soluble in water and no other solvent is further required to completely solubilize the antibiotic. Inspired from the literature[32], the reaction was carried out at room temperature in pure distilled water for 3 days. The reactional solution was then poured in several glass vials and freeze dried for a week to remove water. A blue crystalline powder was obtained after drying.

Similarly to curcumin inclusion complexes, ^{1}H NMR analysis was done to determine the ratio of host and guest in the inclusion complexes. Heavy water (D_2O) was used as a solvent as these inclusion complexes were still soluble in water. The cyclodextrin over methylene blue ratio was determined using integral values obtained for each compounds. A 1:6 β-CD:MB ratio was found. This result was surprising as no rinsing or purification steps were carried out to remove any unreacted β-CDs. Additionally, a 1:1 β-CD over MB ratio was initially incorporated and the same ratio was thus expected to be recovered after the complexation. Even if the MB based ICs are highly soluble in water, some IC aggregates may be formed during the inclusion reaction. These aggregates might then not be soluble in heavy water (D_2O) anymore and will then not be analysed. The calculated ratio of β-CD over MB (β-CD:MB) ratio may not be accurate.

The presence of both free and encapsulated MB could be beneficial as well in terms of antibacterial activity. Indeed, free MB will be released during the initial stages of the tests or *in vivo* studies, responding to the immediate threat of infection and to act against the bacteria in close proximity. MB based inclusion complexes will only be efficient after some time and thus provide a second antimicrobial action. The material could then display long term efficiency toward bacteria as well as an initial burst release.

The obtained MB inclusion complexes were characterised using thermal analyses such as TGA and DSC. In the temperature range used for DSC analysis, no melting or crystallisation points could be discerned for pure MB so that no conclusion could be established regarding the success of the inclusion reaction. TGA analyses (figure 2.5), through the degradation temperatures of each compound showed us that when included within β-CD cavity, MB was more resistant toward temperature as its free form. The temperature at which the inclusion complex started to degrade increased from 173°C to 323°C. The cyclodextrin cavities thus offered a good environment and act as protective thermal barriers for the enclosed molecules. This enhancement in thermal resistivity can be seen as a proof of the inclusion complexes formation.

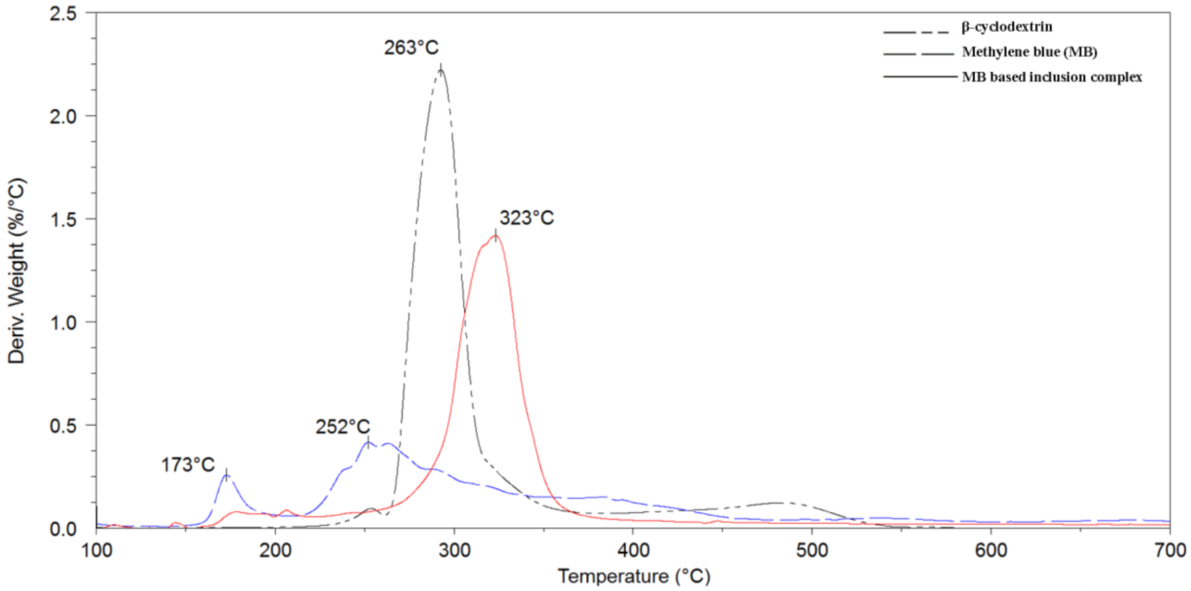

Figure 2.5. Thermal gravimetric analysis of (broken double dash) β-cyclodextrin, (long dash) methylene blue and (solid) methylene blue inclusion complex obtained in distilled water

XRD analysis (see figure 2.6) was also carried out to determine the crystalline organization of the inclusion complexes. By looking at the crystalline signals obtained in the case of free MB and β-CD/MB inclusion complexes, it was observed that the crystalline structure changed after the inclusion complexation reaction. Indeed, some peaks clearly visible in the pure MB spectrum disappeared. On the other hand, new peaks came out at 2θ = 12° or 2θ around 20-25° on the signature obtained for the inclusion complexes. This change in the crystalline signature of the compound let us think that despite the presence of free MB molecules, the IC reaction was still successful.

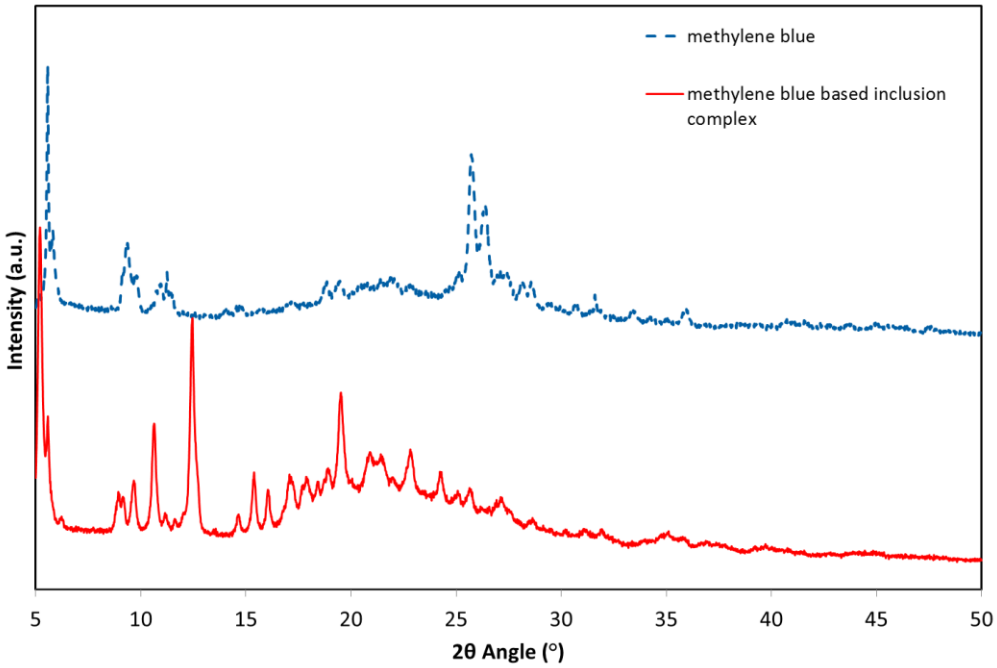

Figure 2.6. XRD spectra overlay of (red solid line) β-cyclodextrin/methylene blue inclusion complexes, (blue dash) pure methylene blue

The MIC value was also determined for MB and a minimal inhibitory concentration < 0.015 mg.mL^{-1} was determined. The determined MIC value was much lower than the one determined for curcumin or for curcumin based inclusion complexes. This means that MB is highly antibacterial and only small amounts of MB are required to obtain good bacterial inhibition. Due to a lack of time, no novel experiment was performed on the β-CD/MB inclusion complexes.

Due to the poor solubility and antibacterial efficiency of curcumin and β-CD/curcumin ICs, these curcumin based compounds were not further used for the elaboration of fibrous materials.

1.2. Vancomycin and gentamicin for infection treatments

In this project, polyester antibacterial fibres for infection treatments or tissue engineering applications were also elaborated. In order to provide antibacterial properties to these membranes, vancomycin and gentamicin were used as organisms able to kill Gram positive and Gram negative bacteria respectively. To provide good bacteria killing properties and to be efficient toward a large array of bacteria, these two antibiotics were associated. Vancomycin in particular is well-known for its high efficiency toward resistant Gram positive bacteria.[40]

To prepare vancomycin and gentamicin based complexes, β-CD was used as host molecule due to the big size of these synthetic antibiotics. As no literature has been found discussing the formation of gentamicin and β-CD inclusion complexes, the same procedure developed for vancomycin was also applied for the inclusion complex formation with gentamicin. However, due to the size and structure of the antibiotics, no inclusion complexes were obtained but interactions could be determined between the β-CD and the antibiotics. Therefore, the compounds were called adducts.

The adducts were obtained by freeze-drying process. As each antibiotic and β-CD were soluble in distilled water, the adduct was studied in distilled water and adapted from the literature.[50] The self-assembly mixture was let to stir at room temperature for seven days before being freeze-dried for a week. Initial ratios of 2:1 β-CD over antibiotic (vancomycin or gentamicin) were incorporated and no purification step was done after the dried solids were collected. An excess of β-CD molecules was introduced to ensure some interactions with the antibiotics as these molecules were bulky. The obtained solids (vancomycin and gentamicin ICs) were fluffy and in the form of closely packed needles. The final aspect of the compounds differed from the initial powdery aspect of the antibiotics. ^{1}H NMR analyses were used to determine the ratio of host and guest in the inclusion complexes. However, no ratio could be determined for these adducts due to the overlapping between numerous peaks.

Thermal analysis and especially TGA analysis gave us some information regarding the success of the formation of adducts. Similarly to the other molecules encapsulated within β-CD (e.g. curcumin, MB), an increase in the first thermal degradation temperature was noted.

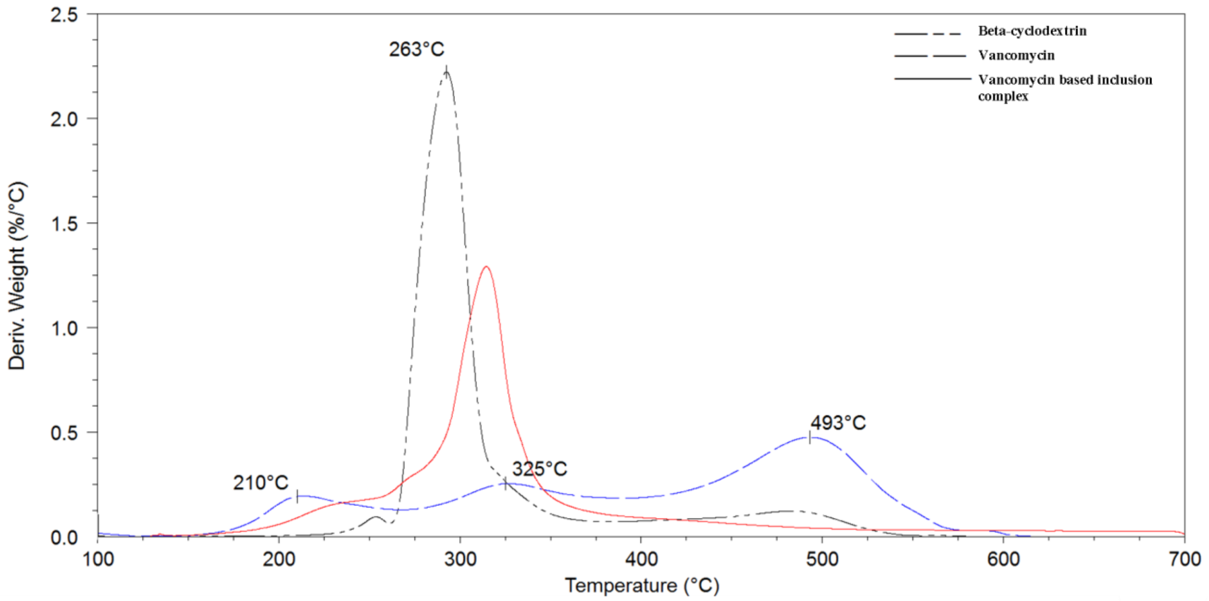

Figure 2.7. Thermal gravimetric analysis of (broken double dash) β-cyclodextrin, (long dash) vancomycin and (solid) vancomycin based adducts obtained in distilled water

Indeed, the thermal degradation profile of vancomycin showed a three-step degradation starting at 210°C. In contrast, the vancomycin based adduct first degradation temperature was around 315°C (figure 2.7) and a single thermal degradation could be seen. When interacting with the β-CD cavity, vancomycin exhibited enhanced thermal behaviour.

Additionally, the XRD signatures obtained for both vancomycin and β-CD/vancomycin adducts were different. Both native vancomycin and vancomycin based adducts are amorphous materials. Indeed, no sharp peak can be detected on the XRD spectrogram (figure 2.8); however, a small difference between the two signatures has been observed. In the case of the physical blend between β-CDs and vancomycin, a multi peak signal was obtained where the crystalline peaks of native β-CD were detected as well as the crystalline signature of vancomycin. This analysis did not confirm the results obtained by TGA.

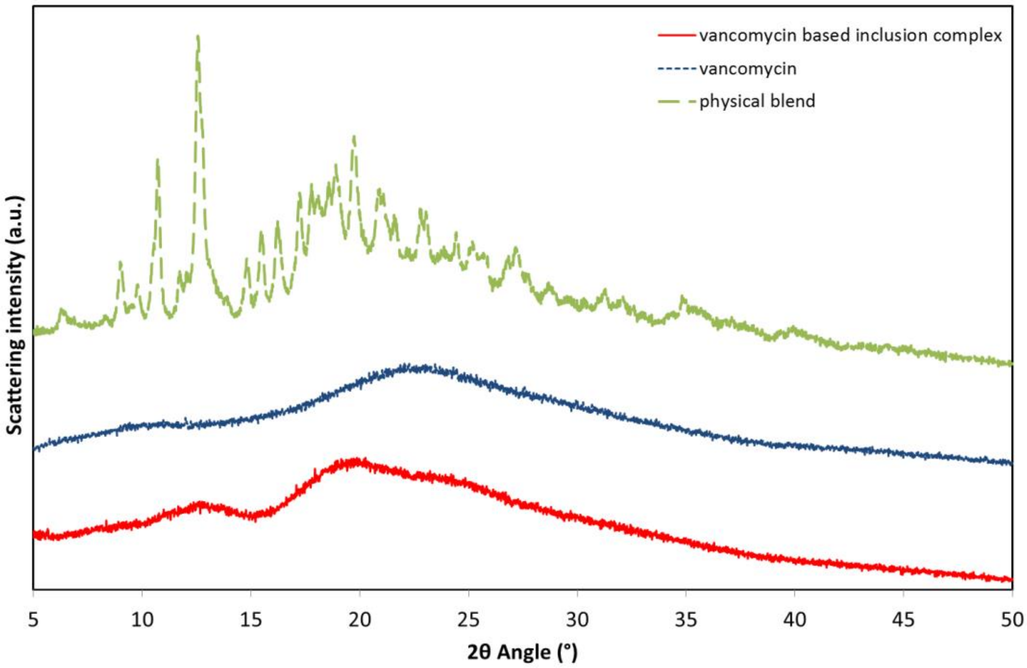

Figure 2.8. XRD spectra overlay of (- red line) β-cyclodextrin/vancomycin adducts, (- blue line) pure vancomycin and (- green line) the physical blend between vancomycin and β-CD

Gentamicin based adducts were also characterized by TGA and XRD analyses. DSC analysis was also performed and, like vancomycin, no thermal transition could be observed for pure gentamicin so that no conclusion could be drawn. As depicted in figure 2.9, the β-CD/gentamicin adducts only exhibited a single step thermal degradation at 244°C whereas the antibiotic demonstrated a two-step degradation beginning at 223°C.

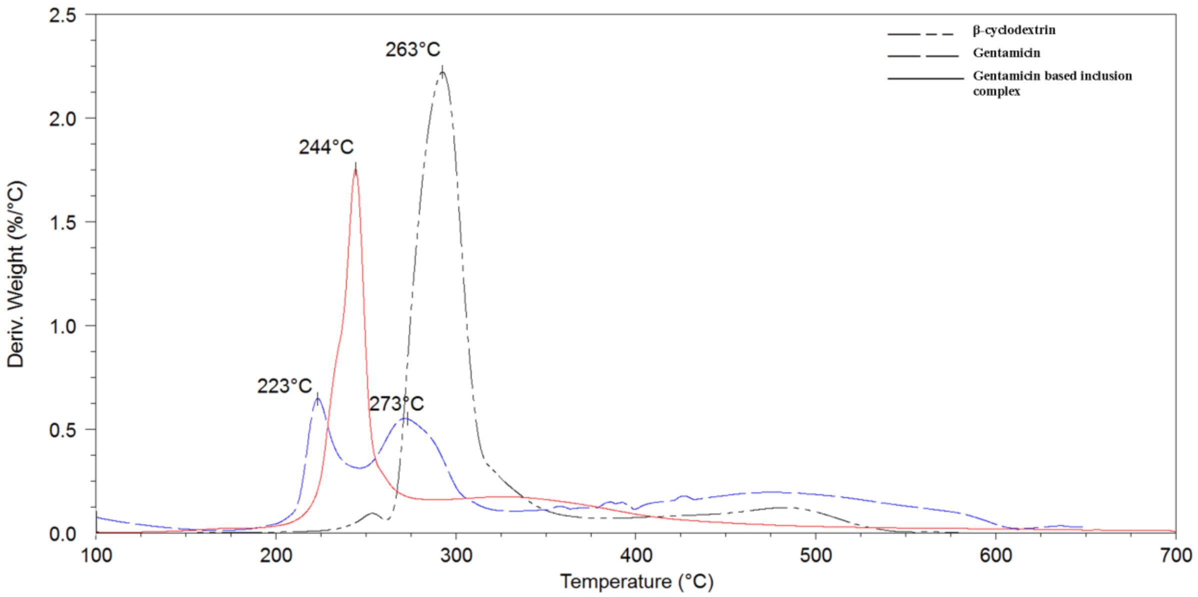

Figure 2.9. Thermal gravimetric analysis of (broken double dash) β-cyclodextrin, (long dash) gentamicin and (solid) gentamicin based inclusion complex obtained in distilled water

In order to further characterize the adducts between gentamicin and β-CD, XRD analyses were carried out and summarized in figure 2.10. It can be noted that gentamicin is amorphous as no sharp peaks are present in its XRD spectrogram. The physical blend of both compounds combined the sharp peaks of the crystalline β-CD and the amorphous signature of gentamicin. In comparison with pure gentamicin, the adducts based on this antibiotic was more crystalline and therefore, sharper peaks appeared on the XRD spectrum. The signature obtained for the adduct was also different from the blend as the crystalline peaks in the 2θ angle range between 15 and 35° were different from the ones found in the blend.

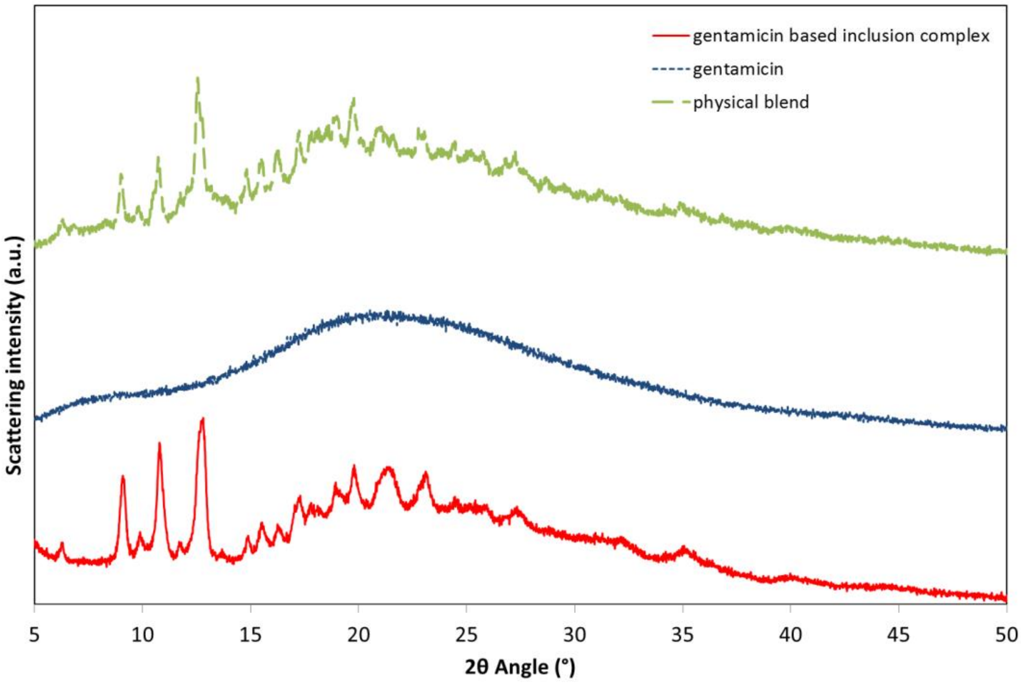

Figure 2.10. XRD spectra overlay of (- red line) β-CD/gentamicin inclusion complexes, (- blue line) pure gentamicin and (- green line) the physical blend between gentamicin and β-CD

In the case of the adducts between β-CDs and vancomycin or gentamicin, additional characterization should be done on the adduct samples to further confirm the results obtained by TGA that suggested the self-assembly of the antibiotics with the CD cavities. Isothermal titration microcalorimetry, ROESY or diffusion measurements by NMR analysis could have also been done to see the various interactions between the CDs and the antibiotics.

Inclusion complexes (ICs) and adducts of numerous molecules could be achieved by simple freeze-drying or solvent evaporation processes. Despite being soluble in the same solvent, host and guest can form stable interactions together so that the synthesized ICs and adducts present enhanced thermal properties. Moreover, when the crystalline organization of the enclosed molecule was determined, a change in the structure occurred due to the encapsulation reaction. We have now synthetized several ICs and adducts that will be further used to biofunctionalize fibrous materials whether for wound dressing applications or for tissue engineering purposes.

Curcumin based ICs will not be further used to elaborate wound dressing materials as their antibacterial evaluation demonstrated poor bactericide activity.

The adducts between β-CD and vancomycin or gentamicin have not been incorporated yet within polyester fibrous membranes and their effects on the biological properties of the overall material have not been studied.

2. Synthesis of poly(ε-caprolactone) based polyesters presenting different architectures

2.1. Ring Opening Polymerization of lactones by organocatalysis

The Ring Opening Polymerization (ROP) of lactones has become a very attractive and simple way to synthesize aliphatic polyester chains and was developed as an alternative to homo or hetero polycondensation. This type of polymerization enables to design tailor-made polyesters with high molecular weight and unimodal distributions in weight. Unfortunately, when increasing the molecular weight of the polymer, side reactions can occur such as transesterification. However, many parameters influence the polymerization such as the size of the monomer ring, the nature of the solvent, the nature of the initiator, the concentration of monomer, the temperature, if any, the type, the position and the number of substituents and the nature of the catalyst.[167]

PCL has been synthesized since 1930s by Carothers[168] and was one of the first polymer to be synthesized by ROP. Due to the high reactivity of ε-CL, the ROP of ε-CL has been the subject of many studies through polymerization by cationic, anionic, enzymatic, free radical and coordination-insertion mechanisms. At an industrial scale, high molecular weight PCL have been synthesized by a coordination-insertion mechanism with stannous octoate ($Sn(Oct)_2$) in the presence of heavy alcohol as an initiator. Solvent free systems have also been developed leading to the rapid and efficient synthesis of “green” PCL with better mechanical and rheological properties at low production cost.[169]

Due to its high reactivity and its rapid polymerization kinetics, stannous octoate ($Sn(Oct)_{2)}$ became the principal catalyst used for ROP of lactones and ε-CL. As already said, high molecular weight polymers can be obtained within several hours. Nonetheless, $Sn(Oct)_2$ proved to be a toxic material.[170] As it is difficult to remove this catalyst easily and completely from the polymer, alternatives had to be found for metal-free catalysis so that the so-synthesized polymers could be safely used for biomedical applications.

Over recent years, significant interest has been taken in the use of organocatalysts for the ROP of lactones. Nucleophilic carbenes were widely studied and consequently new compounds have emerged as powerful nucleophiles. Among these, N-Heterocyclic carbenes

(NHCs) have proved to be extremely powerful catalysts for the ROP of cyclic esters. The first NHC catalyst for living polymerization was obtained in 2002 by Hedrick and coworkers[171].
In the review of Kamber et al.[172] on the organic ROP, the authors presented the numerous advantages of amidine and guanidine organocatalysis, in particular 1,5,7-triazabicyclodec-5-ene (TBD) (figure 2.11) , as “superbases” for the opening of cyclic esters. They also reported that in comparison with other superbases, TBD had an improved activity that could be explained by the strong basic character of the molecule.

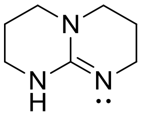

Figure 2.11. Chemical structure of 1,5,7-triazabicyclodecene

The difference of activity could also be understood as TBD compared with any other organocatalyst of the same family, possesses two accessible nitrogen atoms[173] and thus facilitates the reaction of polymerization.[174] Another interesting property of TBD is that it can form a complex with alcohols so that during the polymer purification step in cold methanol, this catalyst is removed with the alcohol. The final product will thus be freed of any catalyst. A mechanism of polymerization was suggested by Pratt et al. in 2006.[173] The suggested mechanism detailed in scheme 2.1 corresponds to the nucleophilic attack of the carbonyl group by the imine nitrogen.

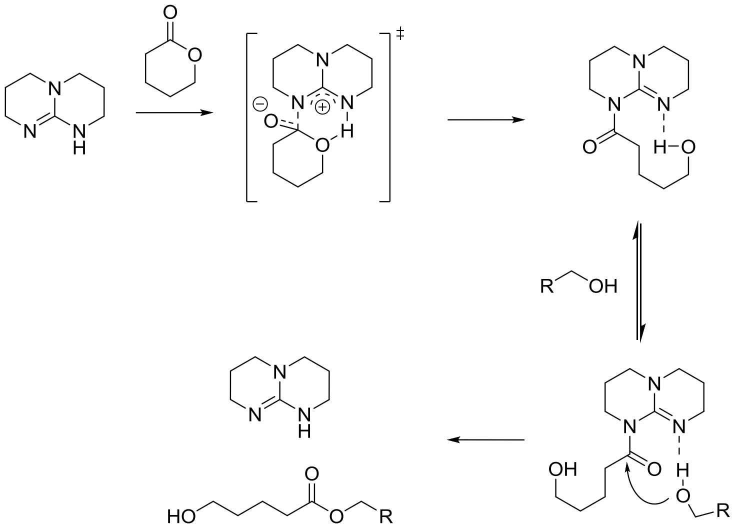

Scheme 2.1. Mechanistic pathways for the ROP of lactones with TBD suggested by Pratt et al.[173]

TBD proved to be really efficient for the ROP of lactic acid (LA) and δ-valerolactone (δ-VL) with low catalyst loading and at low monomer conversions (degree of polymerization (DP) up to 100). Aiming higher monomer conversion was more complicated as side reactions, such as transesterification, occurred.

In this project, we do not target high values of DP for the polymerization of ε-CL so that the use of TBD seems to be the most appropriate choice for metal-free catalysis for the ROP of ε-CL. Additionally, no toxicity issues will be raised by the use of TBD which is compulsory as the materials further developed with these polymers were foreseen for biomedical applications.

2.2. Synthesis of well-defined four-branched polyesters

To obtain a four-branched polymer, pentaerythritol was used as an initiator (see scheme 2.2). This molecule presents four alcohol terminal groups that will thus generate four different PCL branches. An initial [monomer]/[initiator] ratio of 100 was used so that for the polymer four branches bearing 25 monomer units would be synthesized. The good controlled character of the polymerization was demonstrated in the litterature[173, 174] and the presence of four alcohol groups with same reactivity was thought to generate a well-respected symmetrical architecture of the branched polymer.

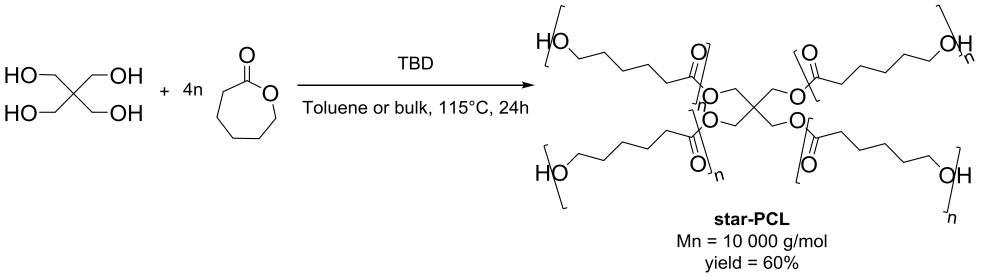

Scheme 2.2. Reaction pathway to obtain a well-controlled four-branched PCL catalyzed by TBD

Two different types of syntheses were attempted. A first set of reaction was performed in bulk and the second attempt was tried in toluene. However, in all cases, both syntheses were successful and led to polymers with similar molecular weights, structures and polydispersity index (PDI).

Both reactions were heated up to 115°C to ensure rapid and efficient conversion of ε-CL as the initiator presented four reactive groups capable to start the polymerization. To avoid any side reaction due to impurities, the glassware was perfectly dried and the syntheses were carried out under inert atmosphere. Both the monomer and the solvent were freshly distilled prior to the polymerization. The reaction was catalysed using TBD that was introduced at a 0.5 wt % in regard to the monomer content. The catalyst was only added when all the initiator and the monomers were completely solubilized and homogenously mixed. The reaction was let to stir for 24 hours before being quenched with a few drops of acetic acid. The reaction products were concentrated under vacuum and solubilized in tetrahydrofuran (THF). The so-synthesized polymers were purified by precipitation in a high volume of cold methanol. The white precipitate was collected by filtration, solubilized in THF and precipitated in cold methanol. The purification steps were done three times to ensure that all unreacted monomers were removed. The white solid was then dried under vacuum at 35°C overnight. Yields around 50 wt% were obtained each time expressing good reactivity and efficiency of the process.

To determine the structure and calculate the degree of polymerization (DP) of each branch, NMR analyses were done in deuterated acetone with a few drops of heavy water at 25°C. The mixture of deuterated solvent enabled to separate two peaks corresponding to the protons close to the hydroxyl polymer terminal functions and the protons carried by the pentaerythritol core.

^{13}C NMR analysis was also necessary to prove the structure of the branched polymer. Indeed, ^{13}C NMR analysis enabled to determine if only four branched polymers or a mixture of multi-branched polymers were synthesized. As demonstrated in figure 2.12, a single peak around 43 ppm can be seen pointing out of the baseline. According to Lang and Lu[175], the presence of a single peak in this range of displacement proved the synthesis of only four-branched polymers. If any additional peaks were to be seen in this area, a mixture of multi-branched PCL would have been formed and the ROP would not have been well-controlled.

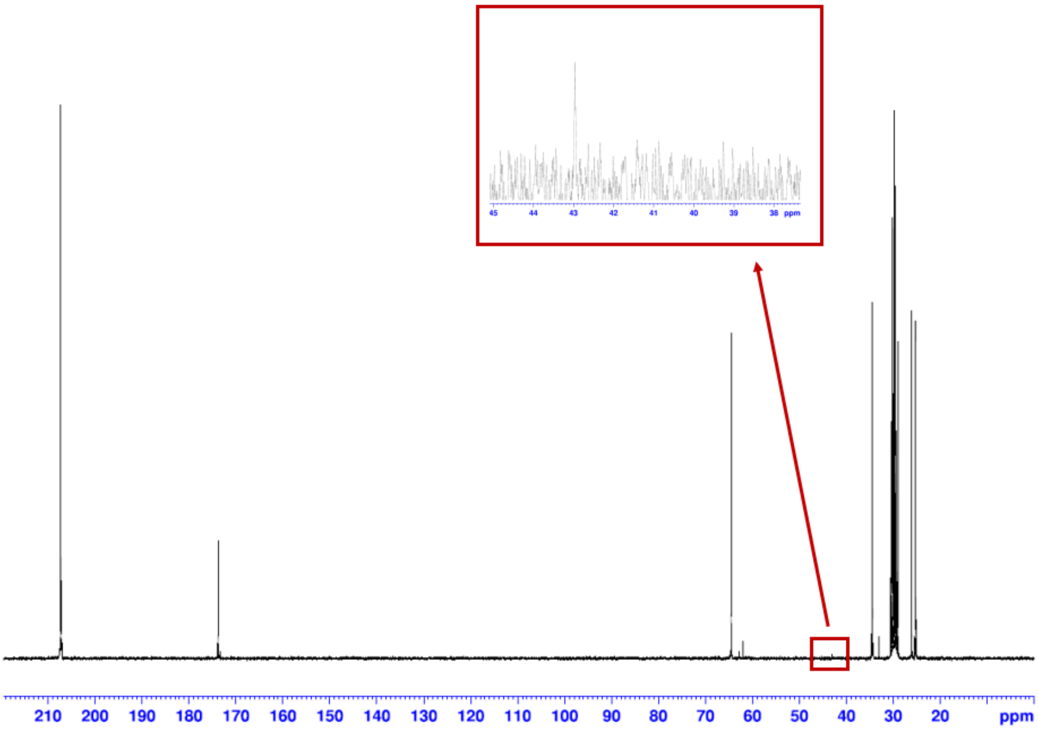

Figure 2.12. ^{13}**C NMR analysis obtained on the four-branched PCL synthesized by ROP of ε-caprolactone catalyzed by TBD in toluene. Similar spectrum was obtained for the bulk synthesis.**

As the synthesis of a four-branched polymer (called star-PCL) was confirmed, the DP per branch could be calculated using the ^{1}H NMR analysis (see figure 2.13) after identifying each peak. For the polymers synthesized in bulk and in toluene, similar DPs were found and per branch around 21 monomers were polymerized. As initially a DP of 25 was targeted, one can assumed that the polymerization reaction is yet well controlled with very limited side reactions.

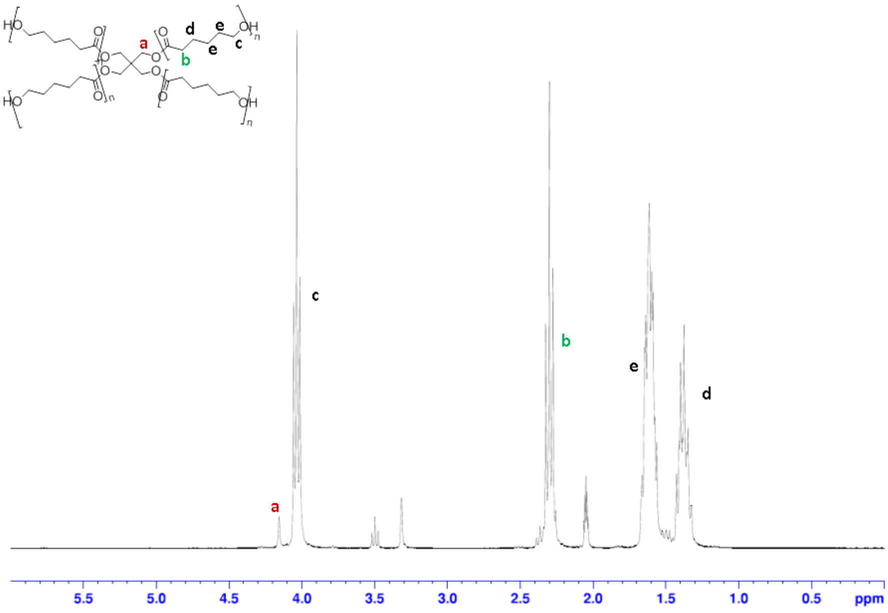

Figure 2.13. ^{1}H NMR analysis of the four-branched PCL synthesized by ROP of ε-caprolactone catalyzed by TBD in toluene. The integral values of a and b were used to determine the DP per branch of the polymer

Size Exclusion Chromatography (SEC) was also performed in chloroform to specify the PDI and thus to check the distribution in size of the polymeric chains. All the calibrations were done with a polystyrene (PS) standard. Ideally, a PDI close to one would show that the distribution in chain size is very narrow and thus that the polymer chains display similar molecular weights. Therefore, the reaction is thought to be well controlled as the polymers present the same molecular weights. On the other hand, a PDI in the range of two or more would denote random polymerization reaction with few or little control of the polymerization mechanism.

According to our SEC analyses (table 2.1), the defined PDI was 1.2 and 1.4 respectively for the bulk synthesized polymer and the one obtained in toluene. However, the Mw and Mn values are given by comparison with the PS standard. Our polymer was made of PCL and presented a branched architecture. Therefore, the Mw and Mn determined by SEC are approximate.

	Mw_{SEC} (g.mol^{-1})	Mn_{SEC} (g.mol^{-1})	Mn_{NMR} (g.mol^{-1})	PDI
Bulk synthesis	16000	13000	10000	1.2
Synthesis in toluene	16000	10000	10000	1.4

Table 2.1. Recapitulative table of the average molecular weights Mw, Mn and PDI of the synthesized four branched PCL obtained by SEC and NMR analysis

2.3. Synthesis of an asymmetric four-branched polymer

As the polymers were foreseen to form pPRs with α-CD and will be further blended with PCL to elaborate electrospun fibres, one aimed to achieve good compatibility with the PCL matrix of the fibres. Therefore, an asymmetric four-branched PCL was synthesized bearing pPR branches but also nude PCL arms.

This polymer was obtained by a two-step modification of the four-branched PCL described above. The synthesis of this peculiar polymer is described in scheme 2.3. The modification reaction parameters and conditions were first tested and optimized on a commercially available linear PCL (Mn ~530 g.mol^{-1}). The use of low molecular weight diol PCL enabled to easily characterize the end functions and see if the modifications were successful or not. These reactions will not be addressed in the following section. Besides, we will not discuss the synthesis of the four-branched PCL (called star-PCL) and its characterization as they have already been described above.

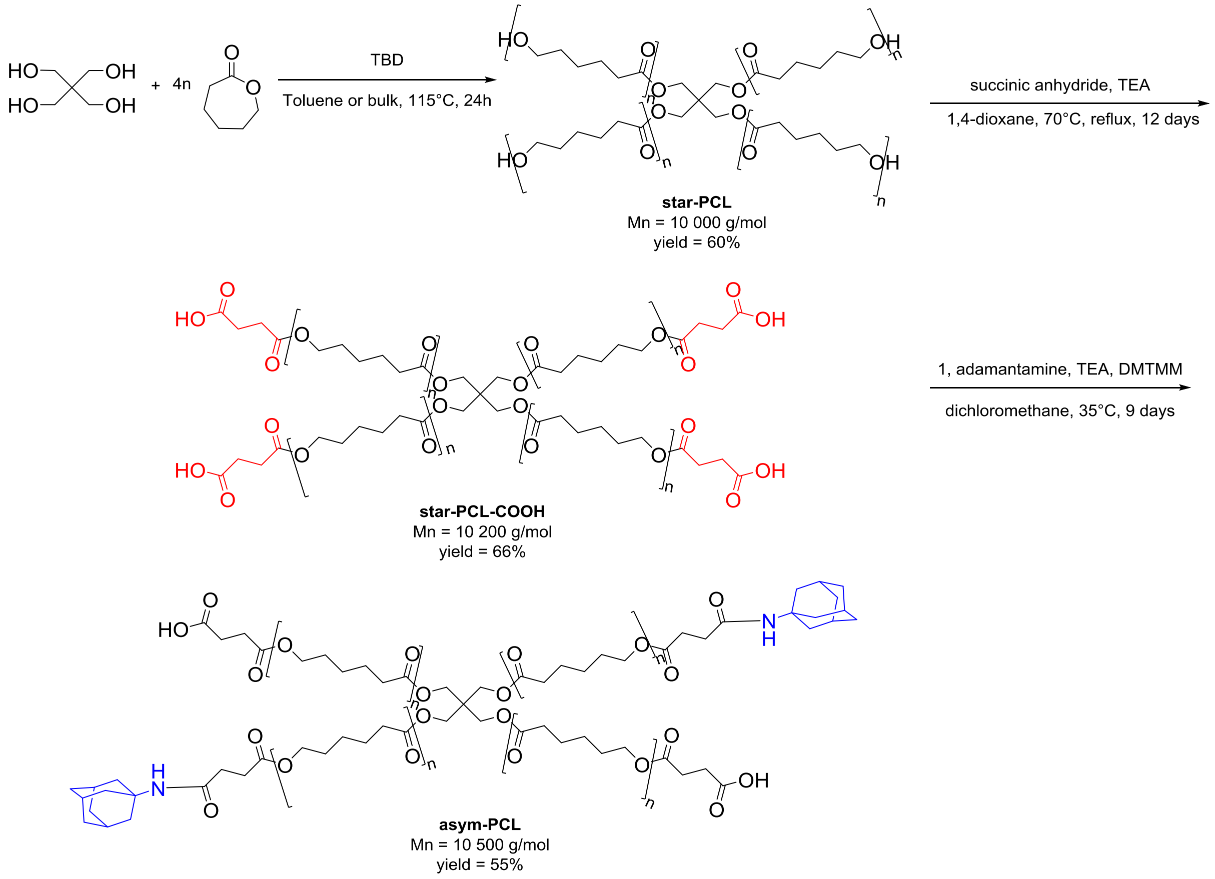
TBD
Toluene or bulk, 115°C, 24h
star-PCL
Mn = 10 000 g/mol
yield = 60%
succinic anhydride, TEA
1,4-dioxane, 70°C, reflux, 12 days
star-PCL-COOH
Mn = 10 200 g/mol
yield = 66%
1, adamantamine, TEA, DMTMM
dichloromethane, 35°C, 9 days
asym-PCL
Mn = 10 500 g/mol
yield = 55%

Scheme 2.3. Schematic representation of the synthesis of asym-PCL via a two-step end chain modification

In the first step modification, all the end groups were esterified by a reaction with a large excess of succinic anhydride in the presence of triethylamine as a catalyst in 1,4-dioxane. The reaction was carried out for 12 days at 70°C in order to allow a complete esterification of the chain ends. The reaction mixture was then concentrated by rotary evaporation and thoroughly washed by consecutive phase separation processes with ethyl acetate (EtOAc) and brine. EtOAc was used to purify the organic phase whereas brine was employed to remove triethylamine and the excess of succinic anhydride. Once the organic phase was collected all traces of water were removed using sodium sulphate (Na_2SO_4) and the solvent was removed under vacuum. ^{1}H NMR analysis (figure 2.14) was carried out in $CDCl_3$ on the yellowish oil obtained and proved the grafting of succinic anhydride at all PCL arm ends. The peak corresponding to the hydroxyl end functions of the polymer arms completely disappeared after this modification reaction.

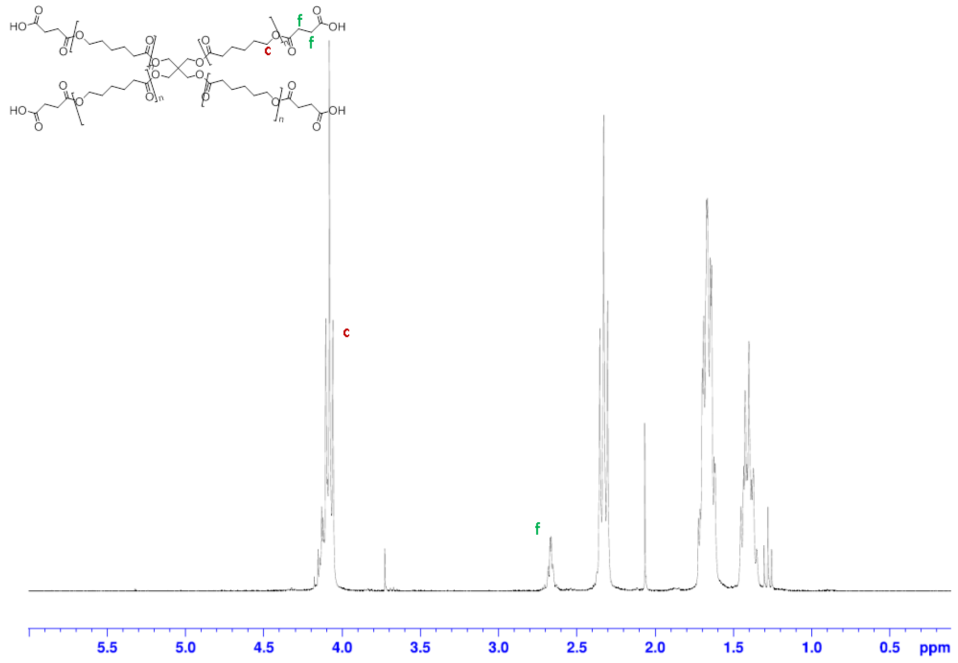

Figure 2.14. 1H NMR spectrum obtained after the esterification reaction of the star-PCL end functions. The integral values of c and f were used to determine the number of carboxyl function per branch

The star-PCL carboxylic chain-end functions were then partially modified and steric stoppers, 1-adamantine, were grafted at some chain ends. 1-adamantine is actually a well-known steric stopper usually used for the synthesis of α-CD based polyrotaxanes.[176] The aim was to partially block some branches, so that when the asymmetric polymer is let to react with α-CD s, only partial threading will be possible as some branches will not be accessible for the cyclodextrins. The resulting pPR will thus bear branches without any CD, while the other unblocked star PCL arms will present α-CD based pPRs.

The second and last modification step was the coupling of 1-adamantine. A first approach to graft 1-adamantine aimed to use N,N'-dicyclohexylcarbodiimide (DCC) and hydroxybenzotriazole (HOBt) as coupling agents to favour the grafting of the amine derivative to the carboxylic end functions. The reaction was also catalysed by triethylamine in distilled dichloromethane (CH_2Cl_2). However, once the reaction was stopped, the synthesized polymer could not be completely purified and the coupling agents (DCC and HOBt) could not be removed completely from the mixture. Thus an alternative to the use of DCC coupled had to be developed to avoid any residual coupling agent in the material.

The second developed approach was to do the reaction in the presence of 4-(4,6-dimethoxy-1,3,5-triazin-2-yl)-4-methylmorpholinium chloride hydrate (DMTMM) as single coupling agent. Indeed, DMTMM is well-known to complex with water due to its ionic nature and thus can easily be removed during the purification steps. Triethylamine was also used as a catalyst. The reaction mixture was solubilized in freshly distilled dichloromethane (CH_2Cl_2) for 9 days at 35°C under argon. An initial ratio of -NH_2 over -COOH functions of 1:2 was used to ensure a partial modification of the star-PCL arms. As previously said the aim was to block some of the branches to ensure free PCL branches and so maybe enhance the blend compatibility with PCL during the processing of fibres. Once the reaction mixture was cooled down to room temperature, the product was washed and phase separated three times with EtOAc and a 1 wt% hydrochloric acid (HCl) aqueous solution. The organic phase was collected and dried over Na_2SO_4 before the solvent was removed by rotavapor. ^{1}H NMR analysis proved the presence of 1-adamantine on half of star-PCL arms (figure 2.15). So there is a real need to let the reaction stir for several days so that a significant number of branches will be grafted with 1-adamantine. The kinetics of chain end modification is known to be slow in the case of polymers. Moreover, FTIR analysis confirmed the success of the covalent coupling by showing small peaks corresponding to the amide (-C=O and –NH functions) (figure 2.16).

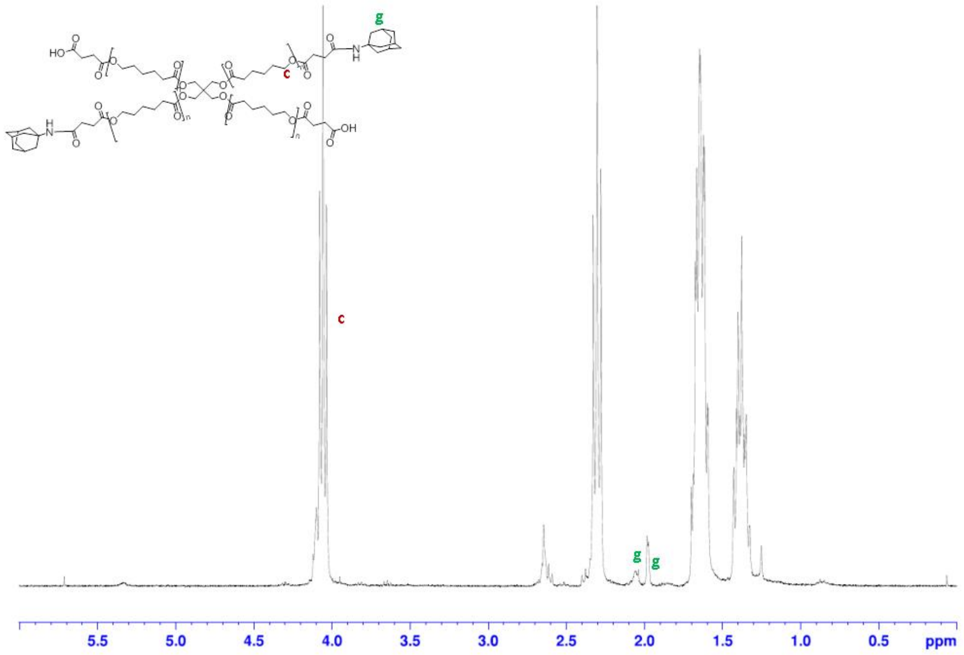

Figure 2.15. 1H NMR analysis of the asymmetrical polyester obtained after the two-step end chain modification. end functions. The integral values of c and g were used to determine the number of 1-adamantine grafted onto the star-PCL

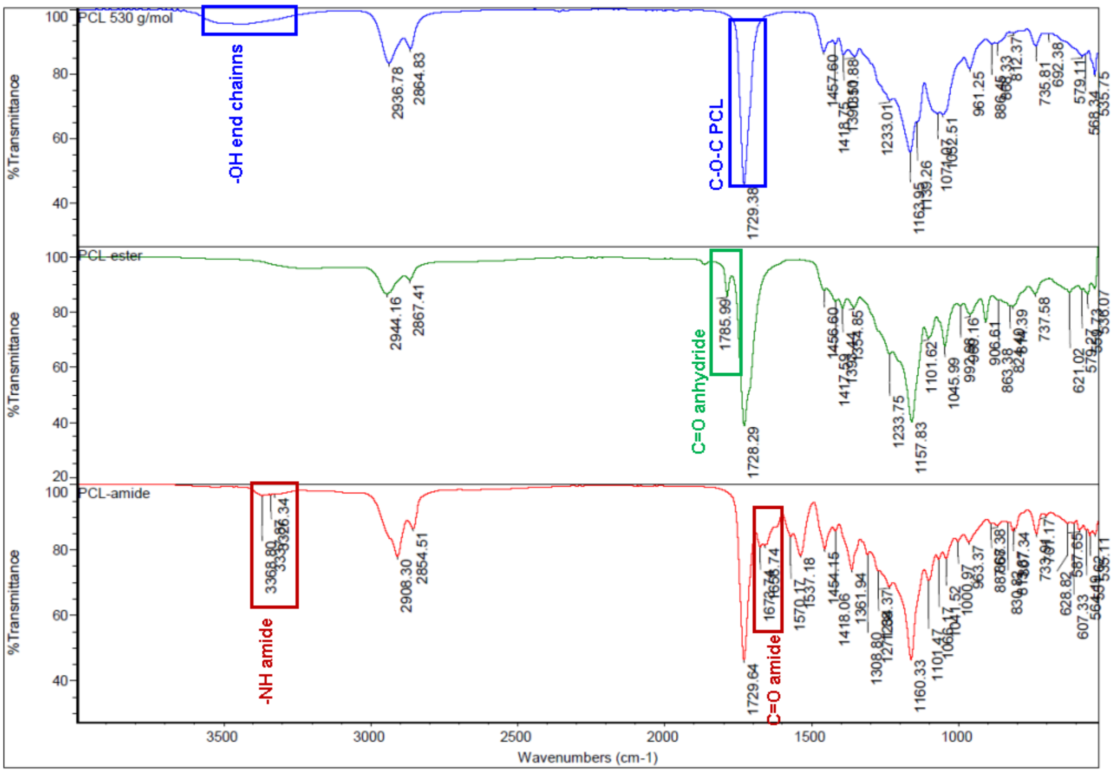

Figure 2.16. FTIR overlay of the different modification steps that were successfully achieved to modify the star-PCL and obtain the asymmetrical polyester

Following a two-step end function modification, star-PCL could be successfully modified and an asymmetric polymer (called asym-PCL) was synthesized. The NMR characterization confirmed the grafting of the chosen steric stopper, 1-adamantine, onto two branches per polymer. As this material will be further react with cyclodextrins the need for free accessible branches is compulsory and the steric stopper was not incorporated in stoichiometric ratio in regard to the carboxylic groups. The fact that the initial incorporated ratio of 1-adamantine was found in the purified product proved that the reaction time was long enough to graft all the stoppers.

2.4. Synthesis of a block copolymer PCL-PPG-PCL

The thought to synthesize a block copolymer presenting an interesting central block came as a solution to obtain PCL compatible pPRs. It was also thought that block copolymers could provide interesting and stable pPRs when in solution. The choice of the central block in the case of the triblock copolymer was not innocent. Actually, PCL is known to form pPRs with α- or γ-CDs but not with β-CDs. By choosing a polymer that would only complex with β-CDs, we ensured that the pPR will be preferentially formed onto the central block leaving two external free PCL blocks. Therefore, we decided to use poly(propylene glycol) (PPG) as a central block as the monomer structure enables stable complexation with β-CDs.[64, 90, 177]

To initiate the block copolymer, PPG with a low molecular weight (~2000 $g.mol^{-1}$) was used to obtain a triblock copolymer with a central PPG block (scheme 2.4). As the initiator presented two hydroxyl functions to initiate polymeric chains, the reaction was let to stir for 24 hours at a caprolactone concentration of 2 $mol.L^{-1}$. According to the previous kinetics study on the ROP of ε-CL initiated by ethylene glycol, 24 hours is far from enough to achieve the targeted polymer. However, the living character of the ROP enabled to prolong the reaction time without any fear of side reaction.

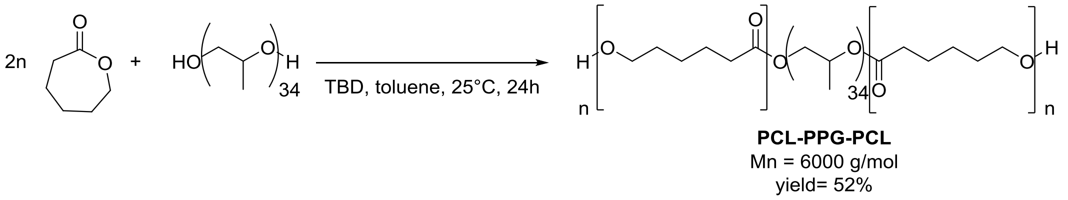

Scheme 2.4. Schematic representation of the synthesis of a triblock copolymer initiated by PPG and catalyzed by TBD

Similarly to the previous polymer syntheses, all glassware was dried and placed under inert atmosphere prior to any reactive addition. To ensure that PPG did not show any traces of water, an azeotrope between toluene and residual water potentially entrapped in the PPG oil was generated and the mixture of solvent was evaporated by rotavapor prior to the ROP. Toluene was here again distilled and immediately used. Dried ε-CL was then introduced once the PPG was solubilized in the solvent and only then TBD was added at a 0.5 wt% in regard to the monomer content. The reaction was let to stir under inert atmosphere for 24 hours before being quenched by a few drops of acetic acid. The polymer was purified by several cycles of solubilisation in THF and subsequent precipitation in cold methanol. ^1H NMR analysis in $CDCl_3$ enabled to determine the structure and the number of monomer units per block assuming that the polymerization propagation step was equivalent for each block. Initially, a ratio of [monomer]/[PPG] = 50 was incorporated to target a DP per block of 25. After synthesis, the DP determined by NMR was 52 so that each block allegedly presented a DP of 26. SEC analysis was also carried out on the polymer and a PDI value of 1.4 was found for the sample.

In the case of the synthesis of the block copolymer, the NMR (figure 2.17) and SEC analyses also proved the good control of the polymerization reaction so that the targeted block copolymer could be obtained. The particular use for this type of polymer will be seen in the next subchapter.

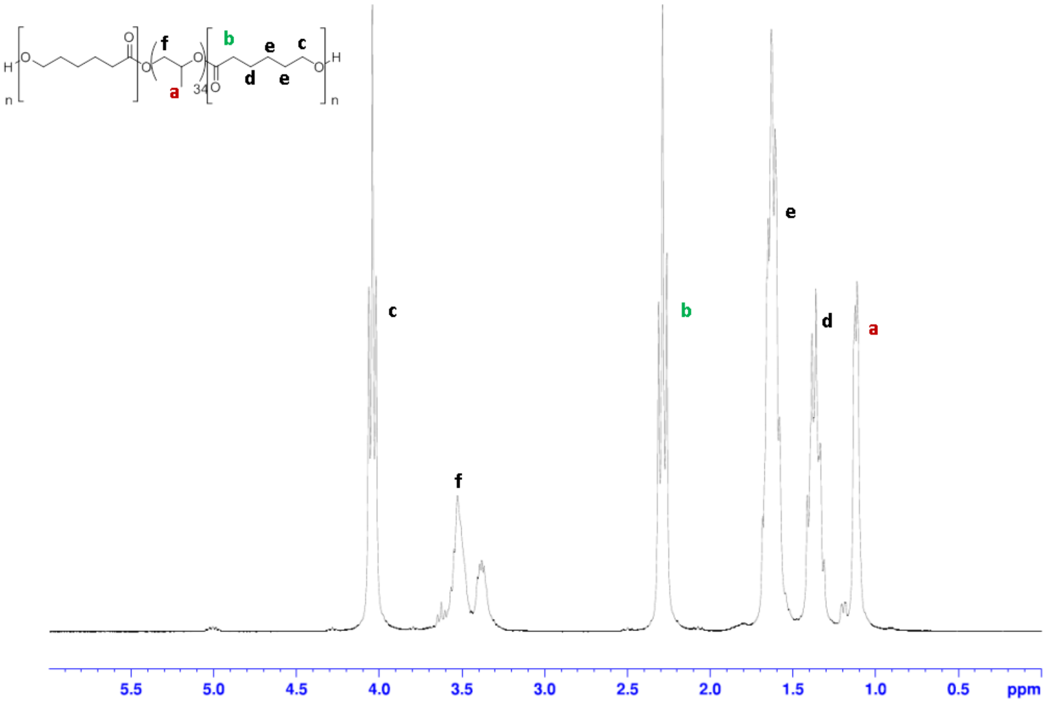

Figure 2.17. ^{1}H NMR analysis of PCL-PPG-PCL synthesized by ROP of ε-CL catalyzed by TBD in toluene. The integral values of a and b were used to determine the DP per branch of the polymer

	Mw_{SEC} (g.mol^{-1})	Mn_{SEC} (g.mol^{-1})	Mn_{NMR} (g.mol^{-1})	DP_{PCL} SEC	DP_{PCL} NMR	PDI
Block copolymer (PCL-PPG-PCL)	19200	13700	10000	32	34	1.4

Table 2.2. Recapitulative table of the synthesized block copolymer comparing the average molecular weights (Mw and Mn) and the polydispersity indexes obtained by SEC and NMR. The values display in the table correspond to the DP of PCL within the polymer so that per block there are 16 and 17 monomer units respectively according to SEC and NMR analyses

We have thus synthesized well-controlled PCL based polymers presenting various architectures: linear PCL (lin-PCL), four-branched PCL (star-PCL), an asymmetrical four-branched PCL (asym-PCL) and a block copolymer (copo-PCL).

3. Formation of poly(ε-caprolactone) based pseudo-polyrotaxanes

3.1. Synthesis of α-cyclodextrin based pseudo-polyrotaxanes

The previous lin-PCL, star-PCL and asym-PCL were used and three different pseudo-polyrotaxanes (pPRs) namely lin-pPR, star-pPR and mik-pPR were obtained using the same method of formation of inclusion complexes (ICs) (figure 2.18). This method was developed by Tonelli et al.[62] in the late 1990s. Indeed, it is well-known since Harada first article[178] on this particular subject that PCL and α-CDs can form pPRs. According to the height of the CD cavity height (7.9 Å[67]) and the extended ε-CL monomeric length (around 9Å) a stoichiometric 1:1 ratio between α-CD and ε-CL can be reached.[178]

To form pPRs, the polymer and the α-CDs were first separately solubilized in the same volume of acetone and distilled water respectively at 70°C. The initial molar quantities of monomer and α-CDs incorporated were identical so that there would be enough CDs to thread along the polymeric chains. Once each compound was dissolved, the polymer organic solution was added dropwise into the aqueous solution of α-CD. During the addition step, a white precipitate was instantly formed. Once the polymer solution was completely added into the CD solution, the reaction mixture was let to stir under reflux for 24 to 48 hours under inert atmosphere before being cooled down. The reaction was still let to stir at room temperature for several hours. After that time, the formed precipitate was filtered and collected on a sintered glass funnel. The solid was then washed with high volumes of acetone to remove unreacted PCL. The residual compound was then thoroughly washed with distilled water to remove unreacted α-CDs. The collected solid was finally dried under vacuum overnight at 40°C.

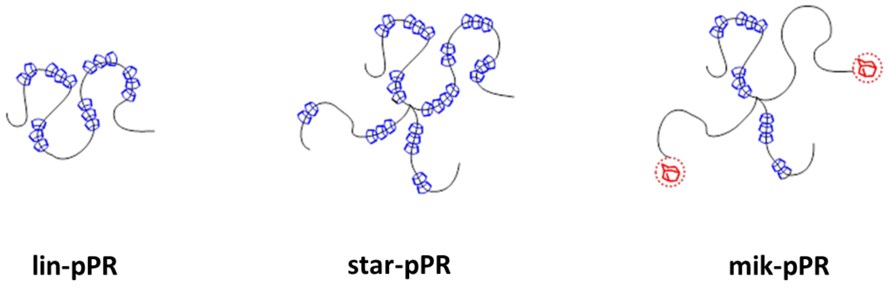

Figure 2.18. Schematic representation of the α-CD based pPRs derived from the linear PCL, star-PCL and asym-PCL

As already discussed in chapter 1, there are some relevant differences between native CDs and CDs that are threaded along polymer chains. The thermal properties and crystalline structure display significant changes prior and after complexation reaction with the polymers. In order to be able to compare the PCL and α-CDs based pPRs with each other, the various polymers used presented an equivalent molar mass M_n of 10 kg/mol. The supramolecular structure of each pPR was then studied by ^{1}H NMR, TGA, DSC and XRD.

TGA analysis enabled to determine the degradation temperatures of the nude polymers as well as the degradation temperatures exhibited by their respective pPRs. It has been observed that for all the unthreaded pure PCL polymers, the temperature of first degradation of each polyester was the same independently of their architecture. A temperature around 280°C was determined. According to the thermograms obtained by TGA, the temperature of first degradation step of the three different pPRs is higher than their respective unthreaded polymers (figure 2.19). In the case of lin-pPR, a first degradation temperature around 285°C could be measured suggesting that the PCL degradation behaviour could still be differentiated within the sample. However, the first degradation temperatures obtained for star-pPR and mik-pPR were higher than lin-pPR. An increase of approximately 20°C was determined when compared to pure PCL. These observations attest of the effective threading of CDs along the PCL chains since it has been reported that such CD threading along the polymer chains tend to enhance the polymer thermal stability[74, 179].

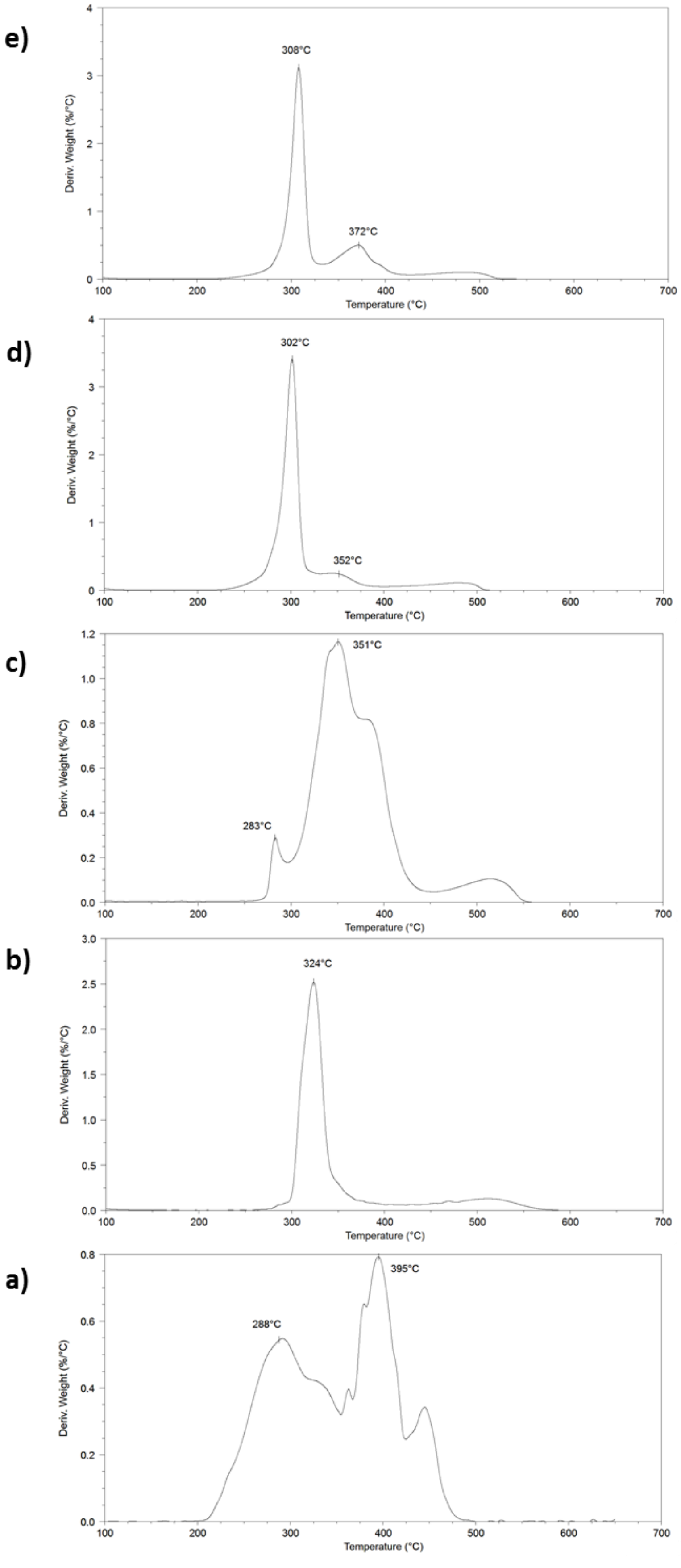

Figure 2.19. TGA thermograms overlay of a) pure PCL, b) native α-CD, c) lin-pPR, d) star-pPR and e) mik-pPR

Another thermal characterization was perfomed on each pPR and here gain, star-pPR and mik-pPR presented similar properties. On the other hand, lin-pPR displayed less pronounced supramolecular characteristics. Indeed, for lin-pPR, a melting temperature of 50°C, corresponding to the melting of pure PCL was measured by DSC whereas no thermal transition could be observed for star-pPR and mik-pPR (figure 2.20). This meant that the thermal properties of the PCL were hidden for the star-pPR and mik-pPR as opposed to lin-pPR were the thermal characteristics of neat PCL were still exhibited.

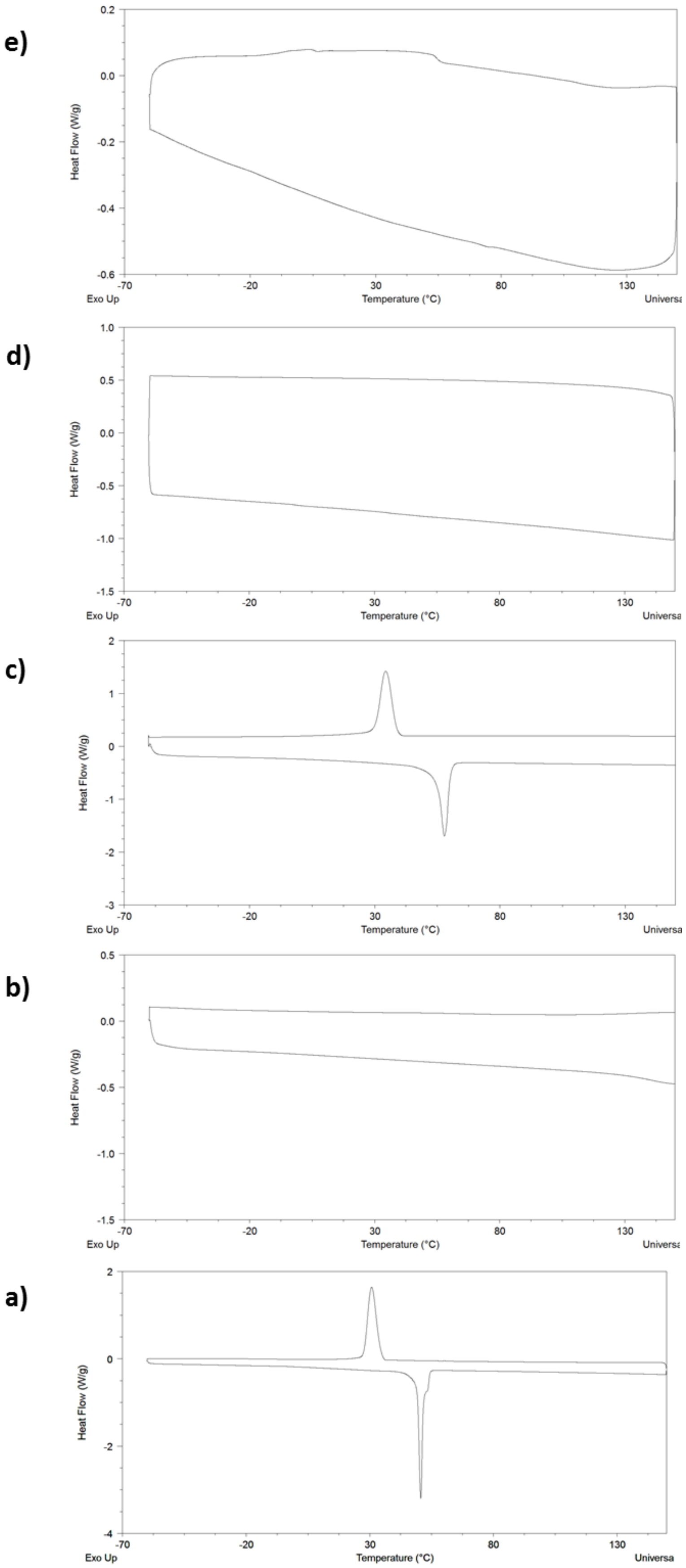

Figure 2.20. DSC thermograms overlay of a) neat PCL, b) native α-CD, c) lin-pPR, d) star-pPR and e) mik-pPR

According to these thermal analysis (TGA and DSC), the differences observed between the three pPRs suggested a dense CD coverage for both star-pPR and mik-pPR but only partial complexation for lin-pPR with a high density of uncovered PCL portions.

XRD analysis further confirmed these results. For star-pPR and mik-pPR, the characteristic peak at 2θ = 20° due to the CD channel-like crystals formed by the pPR rotaxane portions[62] is very sharp and is by far the prevailing peak. In contrast, for lin-pPR, the peaks corresponding to PCL crystal domains (i.e. the peaks corresponding to naked portions of lin-pPR uncovered by the CDs) are in this case the peaks which dominate the diffractogram (figure 2.21).

In figure 2.22, the supposed organization of star-pPR has been represented to better under their crystalline organization.

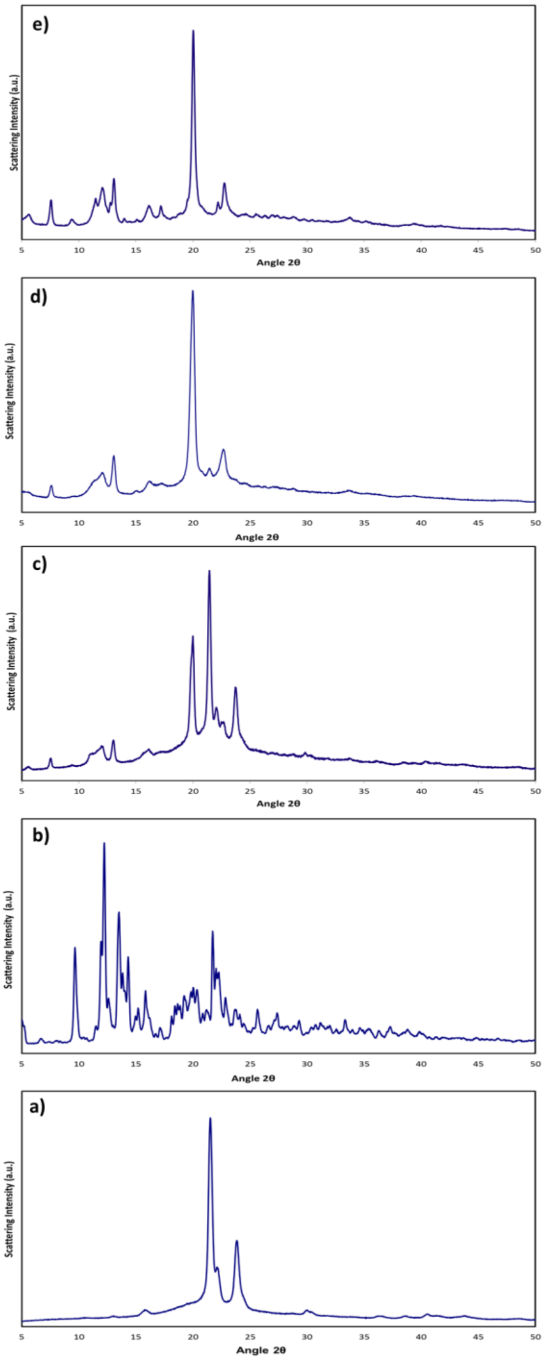

Figure 2.21. XRD overlay of a) synthesized PCL, b) native α-CD, c) lin-pPR, d) star-pPR and e) mik-pPR

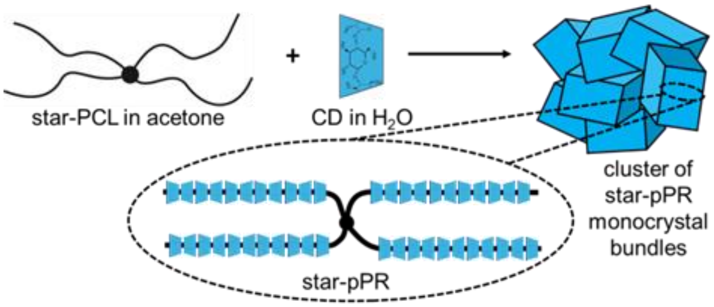

Figure 2.22. Star-pPR synthesis in the form of clusters of randomly organized monocrystalline star-pPR bundles.

To determine the complexation rate of the various pPRs, i.e. the ratio of ε-CL over α-CD (ε-CL:α-CD) within the supramolecule, ^{1}H NMR analyses were performed. Preliminary to the analysis, each pPR was solubilized in DMSO-d_6 at 50°C overnight before being analysed at 25°C by ^{1}H NMR. A second set of ^{1}H NMR analysis was performed at 80°C on both star-pPR and lin-pPR solutions and confirmed the ε-CL:α-CD ratios found at 25°C. This suggested that the first set of parameters permitted to determine with accuracy the effective complexation rates within the pPRs and no residual pPR bundle existed within the analysed solution.

The calculated ratios found for star-pPR was 2:1 ε-CL:α-CD. The ratio was not stoichiometric. This observation can be explained by the fact that for polymer chains with high molecular weights, a stoichiometric ratio for their respective pPR can not be achieved anymore[70]. For mik-pPR, the calculated ε-CL:α-CD ratio was 1:1 for the two branches that could be threaded with α-CDs. In this case, a complete complexation rate was reached. There may not have been as much steric hindrance due to the multi-branched architecture of the molecule as only two of four branches could be threaded. The lin-pPR displayed a complexation rate of 11:1 ε-CL:α-CD. The difference between multi-branched and linear pPRs was yet again significant. NMR analysis (figure 2.23) thus confirmed our previous assumption that there are big portions of lin-pPR that are not covered with α-CDs. On the other hand, star-pPR and mik-pPR complexation rates demonstrated a high number of threaded α-CDs along their arms.

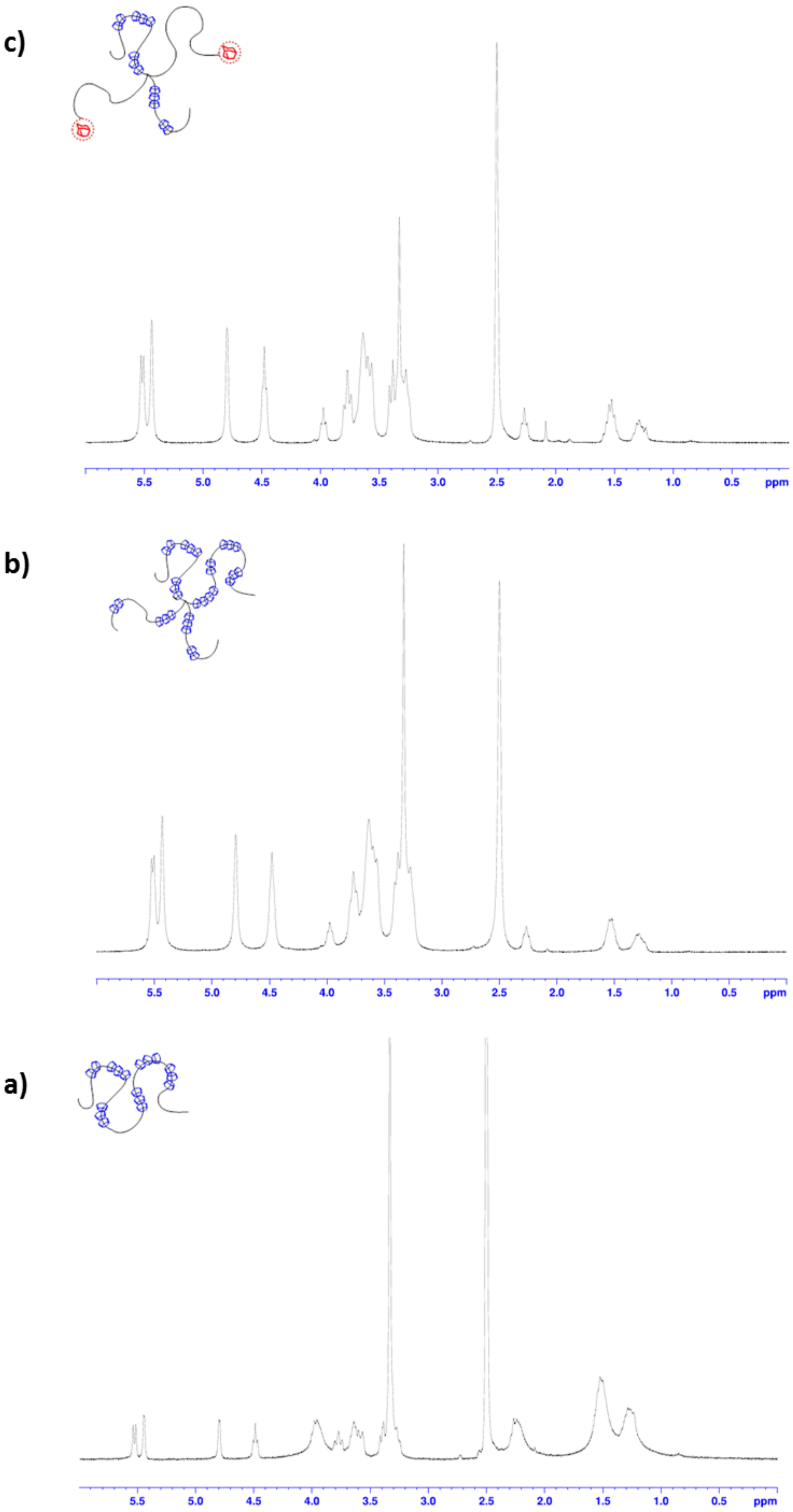

Figure 2.23. ^{1}H NMR analysis in DMSO-d$_6$ of a) lin-ppR, b) star-pPR and c)lin-pPR

The structure and the stability of the supramolecular assembly of pPRs in solvents are of prime importance for their processing by electrospinning and more generally for their use as building blocks in nanomaterials. Thus, one has to find a solvent that allows the dispersion and organization of the pPRs polycrystals clusters into nanodomains while keeping the pPR supramolecular assembly intact. Therefore, we tested different polar solvents that could potentially break the hydrogen bonding responsible for the aggregation of the pPR bundles in the clusters. Acetone, dichloromethane, chloroform, methanol, ethanol, dimethylformamide, and tetrahydrofuran were not efficient and led to white suspensions proving the presence of large aggregates. DMSO was the only solvent that led to transparent pPR suspensions without any sign of visible aggregates. However, to obtain a totally transparent solution, the mixture of pPR and DMSO needed to be heated between 30 and 35°C. Below 30°C, few aggregates were still observed. In the case of lin-pPR, a concentration $c \leq 5$ wt% was necessary to achieve the transparency of the suspension. However, when these solutions were cooled down to room temperature, they became turbid within less than an hour. In the case of star-pPR, solutions up to a concentration of 10 wt% were easily soluble and stayed transparent for several hours at room temperature.

To elucidate the structure and peculiar behaviour of star-pPR and lin-pPR in DMSO, SANS experiments were carried out in DMSO-d_6 for temperatures ranging from 35 to 50°C. In the case of lin-pPR, even at the lowest tested temperature (i.e. $T = 35$ °C), it was observed that the scattered intensity profile corresponded exactly to the sum of the profile of linear PCL chains and free CDs. This proved that CD dethreading occurred (figure 2.24). This behaviour, generally admitted for pPRs in DMSO, explained the suspension turbidity when its temperature was decreased to 20°C due to the presence of uncovered PCL chains. Indeed, observations showed that pristine PCL was not soluble in DMSO at temperature lower than 30°C and appeared as a white precipitate.

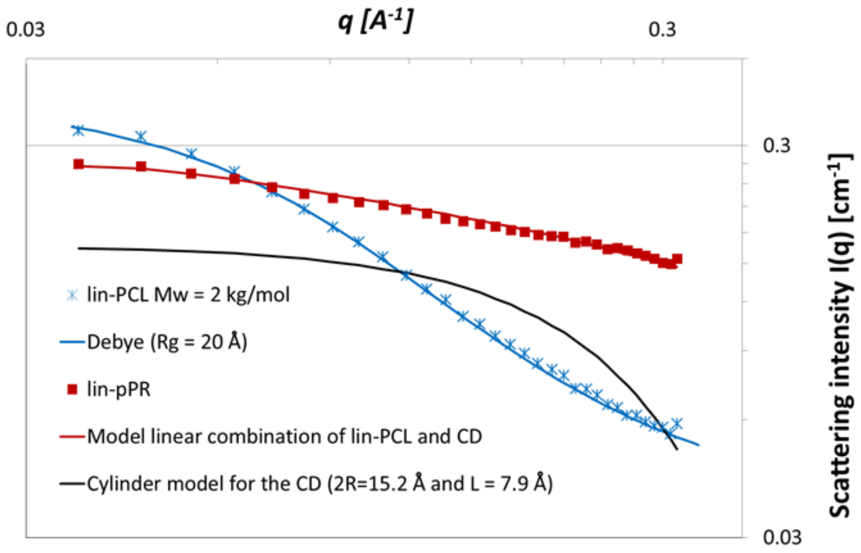

Figure 2.24. Absolute scattering intensity *I(q)* versus modulus of the scattering vector *q* obtained by SANS in DMSO-d$_6$ at 35°C for lin-PCL$_2$ (✳) of mass-average molar mass M_w = 2 kg/mol and and for the lin-pPR$_2$ (🟥) which was synthesized with this lin-PCL$_2$. The experimental data of lin-PCL$_2$ are fitted by a Debye model with a radius of gyration R$_g$ = 20 Å (blue line). The scattering intensity *I(q)* of CDs are modelled by a cylinder of diameter 2*R* = 15.2 Å and length *L* = 7.9 Å (black line). The experimental data of lin-pPR$_2$ are fitted with a model (red line) corresponding to a linear combination of the signal of CD and lin-PCL$_2$ demonstrating that complete CD dethreading occurred when lin-pPR$_2$ is solubilized in DMSO.

Star-pPRs, pristine CDs and star-PCL, as well as a blend of CDs and star-PCL directly prepared in DMSO-d$_6$ (i.e. without the complexation step) were then examined by SANS. The scattered intensity profiles obtained at 40 and 50°C are almost the same than the mixture of uncomplexed CD and PCL (figure 2.25). This result showed that for temperatures higher than 40°C, a high amount of CD dethreading occurred.

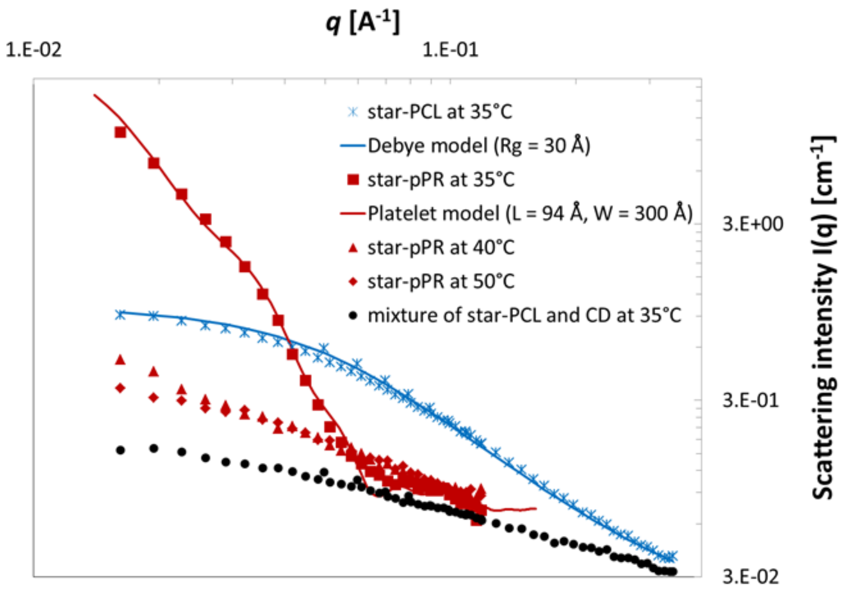

Figure 2.25. Absolute scattering intensity *I(q)* versus modulus of the scattering vector *q* obtained by SANS in DMSO-d_6 of star-PCL at 35°C (✳) and star-pPR at 35 (■), 40 (▲) and 50°C (◆) and a mixture of star-PCL and free α-CD at 35°C (●). The experimental data of star-PCL are fitted by a Debye model with a radius of gyration R_g = 30 Å (blue solid line). The experimental data of star-pPR are fitted by a parallelepiped model (red solid line) with a height L = 94 Å and a square base of width W = 300 Å.

However, at 35°C, although the suspension of star-pPR in DMSO was transparent to the eyes, an excess of scattering intensity is shown at low *q*-range suggesting aggregation of star-pPRs. Furthermore, in agreement with macroscopic observations, the scattered intensity profile was constant during more than 7 hours showing the high stability of the structures formed in DMSO at 35°C. A similar behavior was already observed for other types of pseudo-polyrotaxanes[59, 66] or polyrotaxane[180] for which lateral association between the rotaxane portions led to self-organization in nano-bundles or nano-platelets. By analogy, a parallelepiped model was used to fit the SANS data. A thickness L = 95 ± 5 Å and a lateral size W = 300 ± 100 Å allowed the fitting (figures 2.25 to 2.27). The form factor of the parallelepiped is given by:

$$\mathrm{P}(q,L,W) = \frac{2}{\pi}\int_0^{\pi/2}\int_0^{\pi/2}\left[\frac{\sin(qL/2\sin\alpha\cos\beta)}{qL/2\sin\alpha\cos\beta}\,\frac{\sin(qW/2\sin\alpha\sin\beta)}{qW/2\sin\alpha\sin\beta}\,\frac{\sin(qW/2\cos\alpha)}{qW/2\cos\alpha}\right]^2 \sin\alpha\, d\alpha\, d\beta \quad (1)$$

Knowing that the length of an α-CD is 7.9 Å and its outer diameter is 15.2 Å, the model suggests that star-pPRs are organized in the form of nanoplatelets with roughly 20 CDs in their width W and 11 aligned CDs in their thickness L. Furthermore, the L value is in agreement with the extended length of a star-PCL branch. As suggested in figure 2.27, the nanoplatelets have probably a micellar structure. The pPR channel organization prevented the CD dethreading of the inner part of the micelle, while CD dethreading of outer branches left naked PCL chains that stabilized the micelles.

By analogy, mik-pPR was assumed to behave as star-pPR in DMSO as they exhibited similar CD coverage, thermal and crystalline properties.

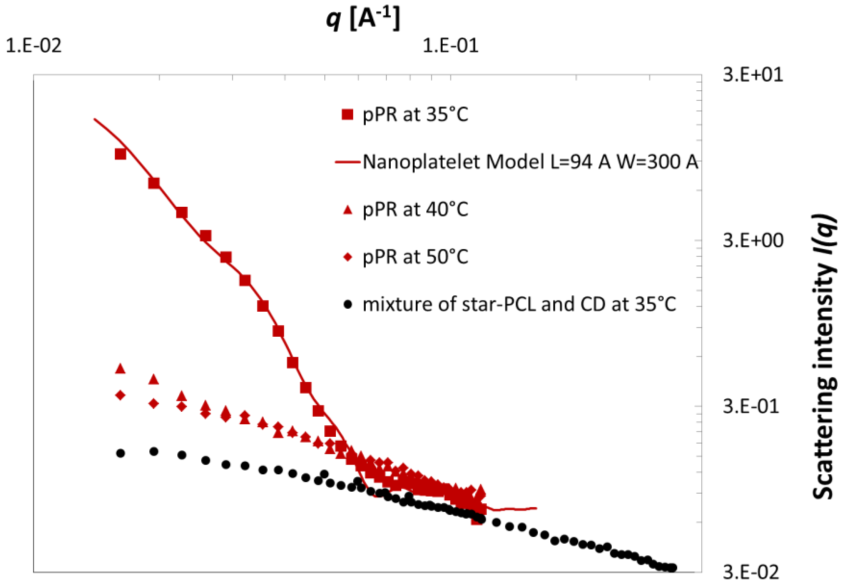

Figure 2.26. Absolute scattering intensity *I(q)* versus modulus of the scattering vector *q* obtained by SANS of star-pPR in DMSO-d$_6$. ■ star-pPR at 35°C and its fitting by a parallelepiped model with *L* = 94 Å and *W* = 300 Å (red solid line), ▲ star-pPR at 40°C, ♦ star-pPR at 50°C, ● mixture of star-PCL and free α-CD at 35°C.

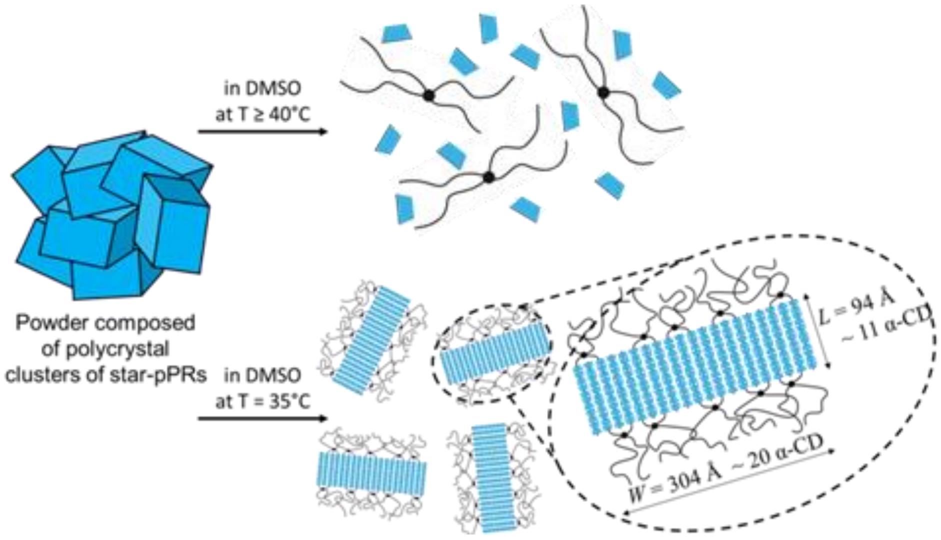
in DMSO
at T ≥ 40°C
Powder composed
of polycrystal
clusters of star-pPRs
in DMSO
at T = 35°C
L = 94 Å
~ 11 α-CD
W = 304 Å ~ 20 α-CD

Figure 2.27. Suggested structure of the star-pPR in DMSO as a function of the temperature

3.2. Synthesis of β-cyclodextrin based star pseudo-polyrotaxanes

To form pPRs based on the block copolymer (figure 2.28), β-CDs were used rather than α-CDs so that the central block would be selectively threaded with the CDs leaving the PCL blocks free of CDs. The reaction conditions were adapted from the literatures by Williamson et al.[63] and Shuai et al.[181] to successfully obtain the targeted pPR. The ratio expected between β-CDs and one monomer unit of propylene glycol is a 1:1 stoichiometric ratio.[177]

For this synthesis, the block copolymer and the β-CDs were separately solubilized in CH_2Cl_2 and DMSO at 70°C. Once both solids were completely solubilized, the polymer solution was added by dropwise addition into the aqueous β-CD solution. The reaction was further let to stir at 70°C for 3 days under argon before being cooled down to room temperature with continuous stirring. In the case of this pPR formation no solid precipitate could be seen as described in the previous subchapter. The yellow viscous solution needed to be concentrated by rotary evaporator to obtain a yellow oily cream. This cream (copo-pPR) was then further dried on a vacuum line to be more efficient toward the removal of residual entrapped solvent.

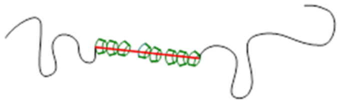

copo-pPR

Figure 2.28. Schematic representation of the β-CD based inclusion complexes elaborated with the block copolymer PCL-PPG-PCL

The so-synthesized pPR was then also characterized by TGA, XRD and NMR analyses. All these characterizations are essential to attest the success of inclusion complexation reactions. As for copo-pPR, the XRD crystalline signature was also different than for native β-CD but the peak characteristic to the threading of CDs along the PPG central block is not at 2θ = 20° but rather at 2θ = 17°.[177] There is a slight shift in the signal obtained for channel threaded β-CD in comparison with threaded α-CD. Unfortunately, no explanation has been found to understand the shift of this crystalline peak as in both cases this peak corresponds to channel-like threaded CDs. As can also be seen in figure 2.29, the peak at 2θ = 17° is quite wide. Even when dried on a vacuum line, the complete evaporation of residual DMSO is very difficult, there are still traces of the solvent in the sample that led to the observation of a wide crystalline pPR peak.

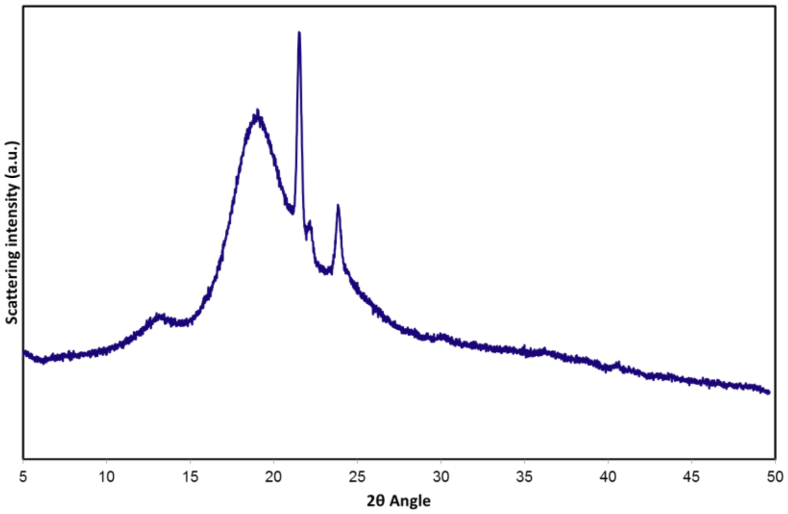

Figure 2.29. XRD spectrogram of copo-pPR

TGA analysis also confirmed the formation of copo-pPR as a shift up to a higher temperature in the first degradation temperature has been observed when comparing the nude block copolymer and the threaded pPR. The thermogram of the triblock copolymer displays multiple degradation phases starting around 200°C whereas copo-pPR exhibits fewer degradation peaks and the major degradation starts around 270°C (figure 2.30). This improvement in thermal resistivity is typical of pPRs.

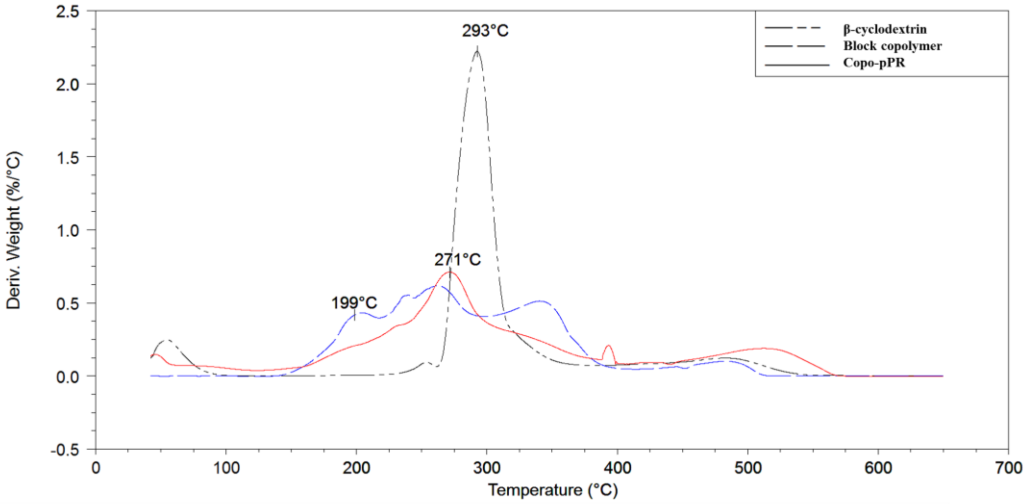

Figure 2.30. Thermal gravimetric analysis of (broken double dash) β-cyclodextrin, (long dash) the block copolymer and (solid) copo-pPR

The ^{1}H NMR analysis in DMSO-d_6 enabled to determine the stoichiometry between the propylene glycol (PG) monomer unit and β-CD. To prepare the NMR solution and to analyse the copo-pPR, the same procedure as for the α-CD based pPR was used. According to the following spectrum (figure 2.31) and hypothesizing that all CDs were threaded along the PPG central block, an average of 1.5:1 PG:β-CD ratio was calculated.

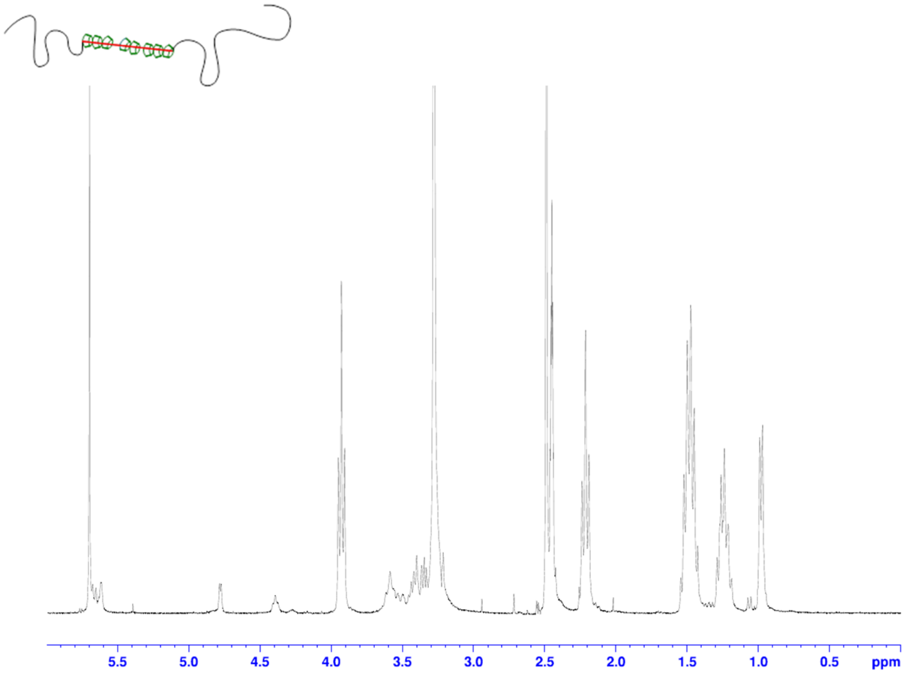

Figure 2.31. ^{1}H NMR spectrum of copo-pPR obtained in DMSO-d_6

CONCLUSION

In this chapter we demonstrated that CDs are able to form different types of inclusion complexes.

Several small molecules such as MB, curcumin, vancomycin and gentamicin were encapsulated within β-CD cavities. The use of β-CDs was necessary to obtain the weak interactions that lead to the formation of inclusion complexes. These host-guest complexes were prepared to modulate the biological properties of future electrospun materials.

Using a non-metallic organocatalyst, three different poly(ε-caprolactone) based polyesters were synthesized by ROP of ε-CL. A linear PCL (lin-PCL), a four-branched PCL (star-PCL) with similar molecular weights, and a block copolymer initiated by poly(propylene glycol) (PPG) PCL-PPG-PCL were synthesized and characterized. Star-PCL was further modified and 1-adamantine was grafted onto two of the four branches of the polyester (asym-PCL). 1-adamantine was used to enhance the compatibility between the asym-PCL pseudo-polyrotaxane derivative (mik-pPR) and the fibre polyester matrix used for tissue engineering applications.

Using a linear PCL, star-PCL and mik-PCL, well defined α-CD based pPRs were obtained and respectively called lin-pPR, star-pPR and mik-pPR. β-CD and the block copolymer were associated to form copo-pPR where the rotaxane structure is selectively formed along the PPG central part of the triblock. These four pPRs presented enhanced thermal properties in comparison with the unthreaded PCL. Their crystalline properties also varied and all displayed the characteristic peak of channel-like threaded CDs in addition to the PCL crystalline peaks. Apart from lin-pPR, the crystalline peak of threaded CDs was prevailing in the XRD spectrograms. These results suggested that in the case of lin-pPR, a low complexation rate was obtained whereas for the other pPRs, a high density of threaded CDs was achieved. ^{1}H NMR analysis further confirmed these results.

SANS experiments permitted to assess the stability of lin-pPR and star-pPR in DMSO-d_6. As opposed to lin-pPRs, the supramolecular structure of star-pPRs is stable in DMSO for several hours due to their organization in nanoplatelet clusters. It was hypothesized that naked PCL branches stabilized the external part of the micelle whereas rotaxane branches were localized in the central part and blocked by the core of the star PCL. To identify the structure of the rotaxane nanoplatelets, a parallelepiped model presenting a width of approximately ten nanometres was used to fit the SANS data. In regard to the similar thermal and crystalline properties of mik-pPR and copo-pPR, it was hypothesized that these two pPRs would present similar behaviour and nanoplatelet organization when solubilized in DMSO. Thanks to the stable nanometric organization of pPRs in DMSO, their processing by electrospinning can be considered and fibres out of pPR based solution will be prepared and studied.

Chapter 3

The use of cyclodextrins for drug encapsulation in fibrous wound dressings

The use of cyclodextrins for drug encapsulation in fibrous wound dressings

In this Chapter, the elaboration of electrospun membranes for wound dressing applications will be addressed.

Two polysaccharides were used to achieve good biocompatibility and fast degradation kinetics: chitosan and carboxymethyl cellulose. These two polysaccharides are widely used for biomedical applications due to their antibacterial and good mechanical properties respectively. Additionally, they both present ionizable charges along their backbone. Depending on the conditions used for their solubilisation, chitosan can bear NH_3^+ functions and carboxymethyl cellulose presents COO^- groups. Chitosan and carboxymethyl cellulose are thus called polyelectrolytes and are soluble in aqueous solution depending on the pH.

Polyelectrolytes bearing opposite charges can blend thanks to weak interactions that can be formed between the anions and the cations of both species. The association of polyelectrolytes via non-covalent bonds leads to the formation of so-called polyelectrolyte complexes. The closer the charge ratio gets to the stoichiometry, the stronger the resulting complexes will be and the faster their formation will be. Polyelectrolyte complexes are less soluble in water and their formation inside the nanofibres should bring water stability and increase the mechanical strength of the electrospun membrane. To detail the mechanisms that rule the formation of polyelectrolyte complexes and introduce their use for biomedical applications, a short introduction will be given in the first part of this chapter.

Two different approaches were developed to fabricate polyelectrolyte complex based fibres with chitosan and carboxymethyl cellulose. First, the carboxymethyl cellulose and chitosan were electrospun to form core:shell fibres by coaxial electrospinning. Chitosan was electrospun as the shell of the fibres so that its antibacterial properties would be more efficient when put in contact with bacteria. A second set of experiments was then carried out in which both polyelectrolytes were blended prior to the electrospinning experiments. In this case, the resulting polyelectrolyte complex solution was electrospun to obtain what will be named blend fibres. For all the fibrous membranes obtained by electrospinning, the experimental conditions were optimized and the structure of the fibres was characterized by scanning electron microscopy.

To further improve the stability of the electrospun fibres against water, the non-woven mats were crosslinked. Sodium periodate was used as a chemical agent to crosslink the polysaccharides and a second crosslinking process was developed by physically crosslinking the fibres in an environmental chamber for two weeks.

The resulting materials were prepared for wound dressing applications. In an attempt to modulate the bactericide activity of the material and prolong the release of the antibacterial agents, methylene blue (MB) or MB inclusion complexes were added within the fibres formulation. The biological activity of the various antibacterial fibrous membranes was then assessed on agar plates against *M.Luteus*. A closer look was also taken on the release kinetic of the incorporated antiseptic in a buffer at pH = 7.4 by UV-Visible spectroscopy.

Polyelectrolyte complexes: description and their applications for biomedical materials

To promote healing and prevent any further harm, wound dressings need to respond to specific requirements. Indeed, these materials need to be breathable while reducing the risks of infections. The bandages also have to stop the bleeding and start the clotting so the wound can begin to heal. Any excess of blood, plasma or any other fluid needs to be absorbed. Different types of wound dressing have been developed over the years. Foams, compressions, wraps, gauzes and tapes are still the primary materials to avoid infections.

An ideal scaffold for wound healing would present a high number of pores to absorb the excess exudate of the wounds, maintain a moist environment and enable gas exchange.[182] Electrospinning has demonstrated to be an interesting processing method for the fabrication of fibrous non-wovens for this type of applications. Indeed, electrospun fibres display high surface area and good absorbency properties. In addition, on an economical level, electrospun membranes can easily be produced according to a low cost process and shaped into various forms.

Careful consideration has been made in the use of polysaccharides for wound dressing applications and more generally for biomedical applications as they are cheap, biocompatible and biodegradable. Polysaccharides that are renewable by nature, also offer good alternatives to synthetic polymers and enable an eco-friendly processing of fibres. In this project, we used two different polysaccharides: carboxymethylcellulose and chitosan.

Carboxymethyl cellulose

Cellulose is the most abundant natural polysaccharide on earth. It is a linear polymer composed of repetitive glucose units linked by β-D-(1-4) linkages[183]. Another interesting aspect of cellulose is that it can be physically, chemically and biochemically modified to produce suitable water soluble cellulose derivatives[183] that will thus be easily miscible with a large variety of polymers and organic materials.[184] Cellulose and its derivatives, including carboxymethyl cellulose (figure 3.1), are usually used as reinforcement materials as they display strong mechanical properties.[184] They are also known for their ability to absorb water[185-187] that could be of great interest to absorb the wound exudates.

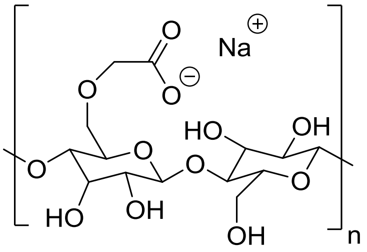

Figure 3.1. Molecular structure of carboxymethylcellulose

Chitosan

Chitosan (figure 3.2) is a natural hydrophilic cationic polysaccharide obtained by deacetylation of natural chitin[188] that is the second most abundant natural polysaccharide on earth (extracted from the shells of crustaceans). The term chitosan refers to a large group of poly(1,4-β-D-glucosamine) that differ from each other by their molecular weight (50-2000 kg.mol^{-1}) and the degree of deacetylation (DDA) (40-98%). Additionally, chitosan displays interesting biological properties such as good biocompatibility and biodegradability properties but it has also proven to exhibit antibacterial activity, low immunogenicity and wound healing properties[189]. The antimicrobial activity of chitosan is due to its cationic nature in acidic solutions. Indeed, the cations along the polymeric chains have a high affinity toward the anions of the bacterial cell wall, thereby preventing the mass transport across the cell wall[188]. Chitosan is soluble in water for pH values below its pKa (~ 6.3).

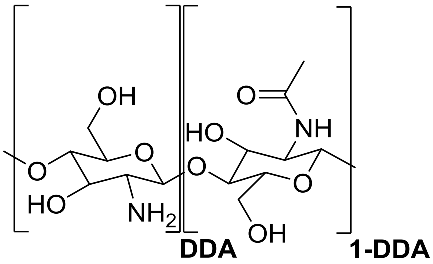

Figure 3.2. Molecular structure of chitosan

Polyelectrolyte complexes

A polyelectrolyte is a polymer bearing one or numerous fixed charges or ionizable functional groups. If the ionizable functional group is not pH dependent, the polyelectrolyte is called strong polyelectrolyte as opposed to weak polyelectrolytes where the protonation of the

ionizable functions depends on the pH value. The solubility of polyelectrolytes is driven by the electrostatic interactions between the solvent and the ionizable groups on the polymer.
Many parameters influence the conformation of the solubilized polyelectrolytes such as the affinity with the solvent, the charge density along the chain and the architecture of the charged polymer. By definition, a counterion is compulsory for the polyelectrolyte solution stability so that when solubilized, counterions are automatically released to neutralize the charges. By changing the amount of salts within the solution, the conformation of the solubilized polyelectrolytes can be altered.

Polyelectrolytes can be classified as natural bio polyelectrolytes (heparin, hyaluronic acid, chitosan…) or as synthetic polyelectrolytes (Poly(sodium 4-styrenesulfonate), poly(allylamine hydrochloride), polyvinylamine, poly(vinylsulfonic acid, sodium salt)…)[190].

Interactions between polyelectrolytes with opposite charges in aqueous media can lead to the formation of complex coacervate (phase separation containing at least two phases: one polymer-rich and one polymer-poor) or to the formation of interpolymer complexes also called polyelectrolyte complexes (PECs).[191, 192] The type of so-formed complex depends on the charge density, on the concentration of the polymers, on the ionic strength, on the temperature or on the pH. The polyelectrolytes backbones tend to repel each other as they are not compatible; nevertheless, the charge fraction on the chains determines the type of interaction going to occur between the polymers. PECs are usually stable due to electrostatic (coulombic forces) or hydrogen interactions as long as no additional salts are added within the solution to change the overall concentration of charges.

The formation of polyelectrolyte complexes (PECs) is known to be a spontaneous phenomenon[193, 194] described in figure 3.3. A high charge fraction is necessary to generate PECs thanks to the high attractive electrostatic interactions. On the other hand, a low fraction of charges will lead to the separation into two separate phases containing each mostly one of the polyelectrolyte.

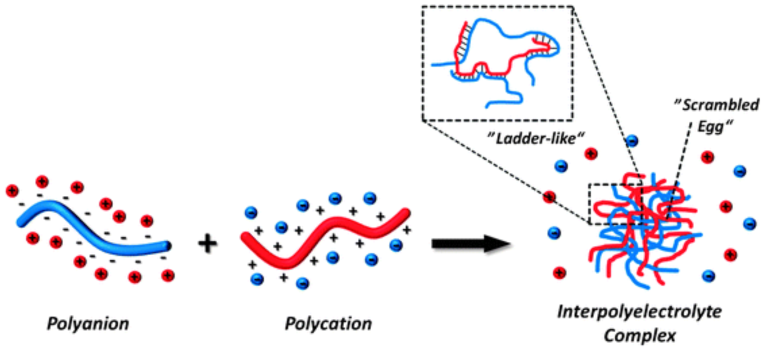

Figure 3.3. Schematic representation of the formation of polyelectrolyte complexes (reproduced from the literature [195]). The interactions between the two polyelectrolytes are represented by ladder steps.

Several experimental parameters can influence the formation of the complexes such as the ion sites, the charge density, the polyelectrolyte concentration, the pH, the ionic strength, the solvent and the temperature.

For example, electrostatic interactions can be weakened by the addition of inorganic salts into the solution resulting in the loss of the PECs already formed. Indeed, the inorganic salt will interact with the charges along the polymer chains.[194, 196] Similarly, by varying the pH during the PEC formation, the degree of ionization on a weak polyelectrolyte can be controlled.[194]

PECs have been widely used for biomedical applications such as membranes, coatings on films or fibres, for the isolation and fractionation of proteins, for the isolation of nucleic acids or for the preparation of microcapsules for drug delivery.[194, 197-199]

Electrospinning of polyelectrolytes

The electrospinning of polysaccharides has been reported over the years, and appeared to be difficult.[200] Indeed polysaccharide based solutions often present low entanglement of the polymer chains as the polysaccharide chains are very rigid.[200] The viscosity of these solutions is also often too high to be electrospun.[200] The solubility of the polysaccharide in water or organic solvents can also be a limiting[200] parameter for the elaboration of homogenous fibres. Finally, the surface tension of the solution can be very high[200] due to the ionic nature of the polysaccharide. Pure chitosan fibres were elaborated in pure acetic acid or in trifluoroacetic acid (TFA) by electrospinning.[189] However, most of the polysaccharide electrospinning related studies demonstrate the necessity to add a polymer template[201-203], that provided entanglements in the solution, or to use a surfactant[204] to obtain polysaccharide based fibres.

The same observation can be noted for cellulose and its derivatives.[200, 205] Alsberg et al.[201] demonstrated that to obtain polysaccharide based fibres, a high concentration of PEO was needed to obtain homogenous alginate based fibres. At least 30 wt% of PEO was compulsory to obtain homogenous fibres.[201]

More recently, electrospun fibres have been elaborated with polysaccharide based PECs for biomedical applications such as tissue engineering[206] or wound dressing materials.[207] At least one of the polyelectrolyte was electrospun under the high electrical field and the second oppositely charged polyelectrolyte was either dually/coaxially/blend electrospun[206, 208-211] or coated on the obtained fibres[203] to form PECs. The PEC through non-covalent interactions enhanced the good mechanical properties for the resulting fibrous membranes.[212-214] Several PEC fibres were successfully obtained based on chitosan/alginate[206, 207], chitosan/gelatin[211] or chitosan/hyaluronic acid.[203] However, the PEC formation is so fast that dual electrospinning has been developed to mix at the last instant both polyelectrolytes and avoid the formation of PEC gel at the tip of the needle.[206, 209] A second approach consisted in the formation of alginate:chitosan core:shell fibres where the core was electrospun and the shell was coated onto the existing fibres. Using this strategy, the authors electrospun alginate as the core because this polyelectrolyte could easily be electrospun and presented fewer solubility issues.[207] When both polyelectrolytes were blended and electrospun simultaneously, the effect of the ratio of positive over negative charges was investigated and demonstrated a significant influence on the electrospinnability as well as the morphology of the fibres.[208, 210, 211]

Cellulose and chitosan, despite being associated as polyelectrolyte complexes for the elaboration of reinforced films[184, 215], have not yet been used to elaborate polyelectrolyte complexes based fibres. Our contribution is thus the fabrication of resistant nanofibres using chitosan and carboxymethylcellulose that are oppositely charged and form stable polyelectrolyte complexes to give the overall fibres interesting properties.

2. Preparation of electrospun membranes based on the chitosan/ carboxymethyl cellulose polyelectrolyte complex

To obtain wound dressing fibrous materials, two different strategies were developed. Coaxial electrospinning was first tested and the carboxymethyl cellulose (CMC) and chitosan (CHI) solutions were electrospun using a coaxial needle. The core of the fibres was based on CMC to ensure good mechanical properties and CHI was used as the shell of the fibres to exhibit high antibacterial properties.

In another attempt, the two polyelectrolyte solutions were mixed together instants before the processing so that a single blend solution of PECs was electrospun to process fibres.

2.2. Materials and description of the polyelectrolyte based solutions

Determination of the charges present along the backbone of the two polysaccharides

To determine the total amount of charges along the CHI chain, ^{1}H NMR analysis (figure 3.4.) was performed and the degree of deacetylation (DDA) of the polysaccharide was calculated as follows with the integral values of the H-2(D) deacetylated proton and H-Ac, the three protons of the acetyl function.

$$DDA(\%) = \frac{H2(D)}{H2(D)\times {}^{HAc}/_{3}} \times 100 \qquad (1)$$

A degree of deacetylation (DDA) of 86% was obtained.

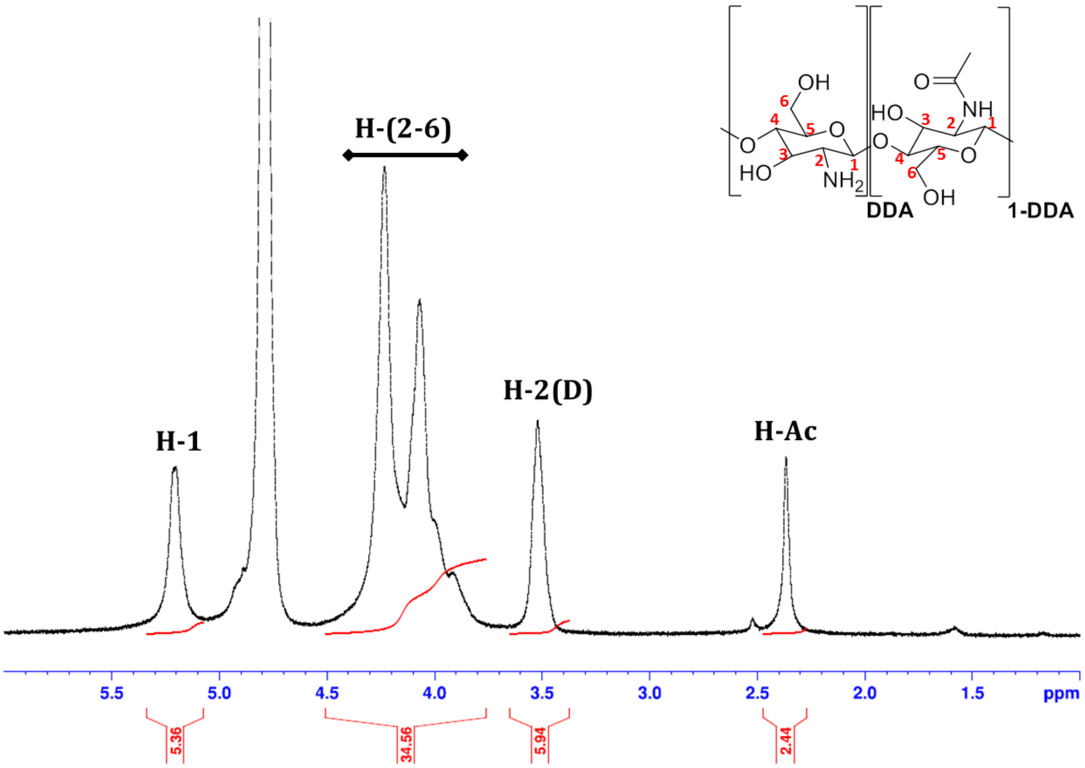

Figure 3.4. ^{1}**H NMR analysis of chitosan Chitoclear 3566 in** D_2O **at 50°C**

For CMC, the supplier provided a charge rate value of 70% in regard to the number of monomer unit per chain. This means that 70% of the monomer units were modified by addition of an ionizable group

Both values were used to determine the respective weights of polyelectrolytes that have to be introduced in each solution and thus prepare different COO^-/NH_3^+.

All the solutions were prepared 24 hours prior to any electrospinning processing and stirred at room temperature so that homogenous solutions would be electrospun.

As said in the previous subchapter, pure polysaccharide solutions can not be easily electrospun because of their low entanglement, the rigid structure of their chain or their high viscosity[200, 201]. Therefore, to obtain homogenous and regular electrospun fibres, poly(ethylene glycol) (PEO) was added within the CMC and CHI based solutions. For the wound dressing application, materials with the highest concentration of PECs were most wanted, so, the incorporated weight of PEO was kept to the minimum value required for good electrospinnability and the fabrication of homogenous fibres.

To achieve homogenous fibres, a good control over the temperature and relative humidity (RH) was necessary during the electrospinning. For RH values higher than 35%, no fibres could be obtained. The jet became really unstable. In this case, the water molecules in the atmosphere may modify the electrical field and further affect the charges already present within the polymeric jet.

Preparation of the polysaccharide solutions for coaxial electrospinning

Different charge COO^-/NH_3^+ ratios were reached to determine the conditions that lead to homogenous and regular fibres. The following ratios were targeted: 0.3, 1, 1.5, 2.2, 3.6 and 10.9.

For the coaxial electrospinning of CHI and CMC, the flow rate of the core solution was kept constant at 1 mL/h. In contrast, the flow rate of the shell solution was varied between 0.1 and 3 mL/h to adjust the COO^-/NH_3^+ ratio.

Solution of CHI:

A solution containing 1.5 wt% of CHI was dissolved in a 50/50 wt/wt mixture of formic acid/distilled water (FA/H_2O). 0.6 wt% of PEO was added to facilitate the electrospinning of this polysaccharide. Formic acid was compulsory to reach acidic conditions and thus dissolve the CHI and protonate the amine functions along the backbone.

Solution of CMC:

A 3 wt% CMC solution was prepared in pure distilled water and 1.5 wt% of PEO was added to ease the electrospinning experiments and favour the formation of homogenous fibres. Using these CHI and CMC concentrations, for identical core and shell flow rates, a stoichiometric COO^-/NH_3^+ ratio was reached.

Preparation of the polysaccharide solutions for blend electrospinning

Different charge COO^-/NH_3^+ ratios were reached to determine the conditions that lead to homogenous and regular fibres. The following ratios were targeted: 0.1, 0.3, 0.5, 0.7, 1 and 1.2.

To reach the different targeted charge ratios detailed above, the CHI solution was kept constant whereas the CMC concentration was adapted in agreement with the aimed COO^-/NH_3^+ ratio.

Solution of CHI:

For these experiments, 3 wt% CHI were dissolved in a 50/50 wt/wt FA/H_2O mixture. 1.2 wt% of PEO was added to the mixture to improve the electrospinnability of the solutions.

Solution of CMC:

The concentration of CMC was adjusted in regard to the desired COO^-/NH_3^+ ratio. CMC (between 0.5 wt% to 5.4 wt%) was solubilized in distilled water and PEO was also added to facilitate the electrospinning of the solutions. The amount of introduced PEO (between 0.25 wt% to 2.7 wt%) corresponded to half the weight of incorporated CMC. To see the exact CMC and PEO concentrations, please see the Material and Methods chapter section 4.1.

To the best of our knowledge, this is the first report of electrospun CHI/CMC/PEO based fibres. The best conditions for the coaxial and blend electrospinning of these two polyelectrolytes had thus to be found. The structure of the fibres had to be determined for each condition and the optimal parameters had to be defined.

2.3. Coaxial core:shell CMC:CHI fibres

For this set of experiments, the concentration of CHI and CMC were fixed as well as the core flow rate. The shell flow rate was adjusted to reach the targeted COO^-/NH_3^+ ratios. To see the flow rates applied to reach the targeted ratios, please refer to the Materials and Methods chapter in the electrospinning section.

The coaxial experimental set-up has been represented in figure 3.5. for the readers good understanding.

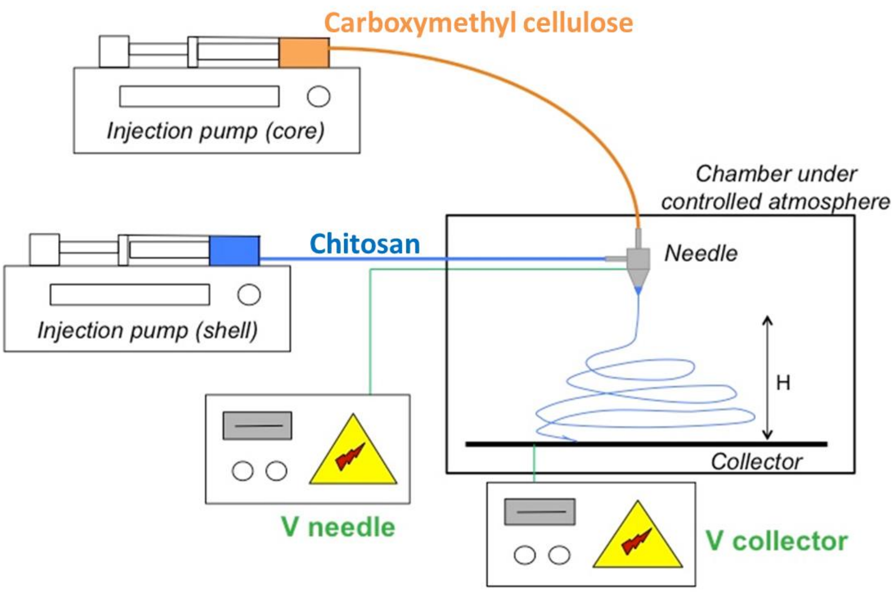
Carboxymethyl cellulose
Injection pump (core)
Chamber under controlled atmosphere
Chitosan
Needle
Injection pump (shell)
H
Collector
V needle
V collector

Figure 3.5. Schematic representation of coaxial electrospinning used to elaborate core:shell CMC:CHI fibres

With this processing method, the PEC can only starts to form at the needle tip when the two solutions come in contact. A needle to tip distance (H) of 20 cm was necessary to completely evaporate the solvents. The applied voltages at the needle and the collector had to be adapted accordingly to the CMC solution and hence to the resulting COO^-/NH_3^+ ratios.

	Core:shell fibres
$COO^-/NH_3^+ = 10.9$	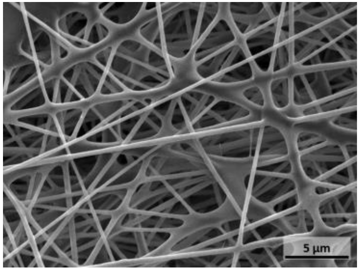
$COO^-/NH_3^+ = 3.6$	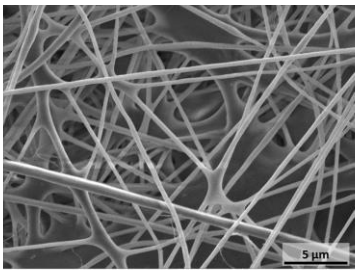
$COO^-/NH_3^+ = 2.2$	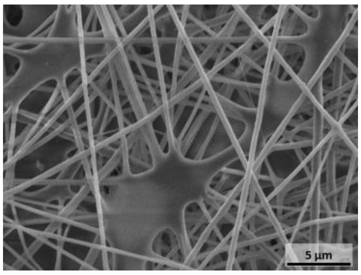
$COO^-/NH_3^+ = 1.5$	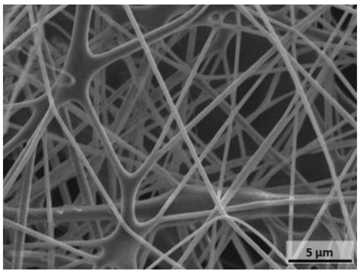
$COO^-/NH_3^+ = 1.0$	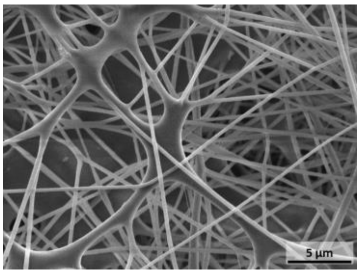
$COO^-/NH_3^+ = 0.3$	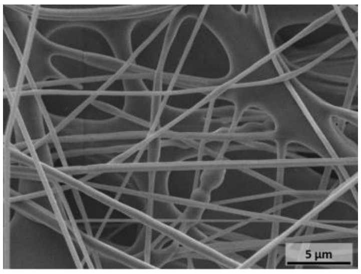

Figure 3.6. Study on the influence of the charge ratios on the fibrous structures for coaxial electrospinning

Because the concentrations of polysaccharides in solution are quite low, electrospinning times of 50 minutes were necessary to obtain a sufficient amount of deposited fibres. For all COO^-/NH_3^+ ratios ranging from 0.3 to 10.9, electrospun fibres were obtained (see figure 3.6) by applying a voltage of 25 kV at the nozzle and the voltage applied at the collector varied between -1 to -5 kV (for more detail, please see chapter 5 section 4.1.1). Many defects could be seen such as the fusion of fibres especially for the highest ratios. For these conditions, a high number of polymeric patches could be noted suggesting that the deposited fibres were not perfectly dry when collected onto the aluminium foil. Additionally, the jet was more unstable for high COO^-/NH_3^+ ratios and droplets were also collected onto the mats. For the 1 and 1.55 ratios, fewer fusion defects were observed as for these two conditions, the formation of PECs was favoured (see figure 3.6).

	COO^-/NH_3^+	Composition CMC/CHI/PEO wt/wt/wt (%)	Average fibre diameter ϕ (nm)	Standard deviation (nm)
MO LP47	**10.88**	64/3/33	370	70
MO LP48	**3.63**	58/9/33	410	100
MO LP49	**2.18**	54/14/32	390	100
MO LP50	**1.55**	50/18/32	390	100
MO LP51	**1.00**	45/23/32	340	70
MO LP52	**0.33**	27/42/31	430	130

Table 3. 1. Average diameter of the coaxially electrospun fibres in regard to the different charge ratios tested

As summarized in table 3.1., it can be noted that the fibres average diameters are in the same range regardless of the difference between the core and shell solution flow rates. In the case of coaxial electrospinning, there seem to be no or little influence of the charge ratio on the average fibre diameter measured for the so-obtained fibres. All the fibres presented an average fibre diameter around 400 ± 100 nm.

2.3. Standard electrospinning of a blend between the two polyelectrolytes

A second set of experiments was carried out in which both polyelectrolytes were blended together prior to the electrospinning-processing step. A 1:1 weight ratio of both polyelectrolyte solutions was mixed at 750 rpm with a magnetic stirrer for two minutes. The mixture was then introduced in a syringe to be electrospun. The formation of PECs being rapid, the mixing was done just instants before the electrospinning experiments. Mixing the two polyelectrolyte solutions, just before the processing, enabled to electrospun the PEC based solutions for several hours without plugging the nozzle. However, the stoichiometric COO^-/NH_3^+ ratio could not be electrospun as a PEC gel was obtained after a couple of minutes. For the other previously detailed ratios, electrospinning experiments could be carried out for 3 hours without the formation of a PEC gel. To obtain homogenous fibres, the applied voltages at the needle tip and the collector were 25/-1 kV for a distance of 20 cm. The flow rate was 1 mL/h.

	Blend fibres
$COO^-/NH_3^+ = 1.2$	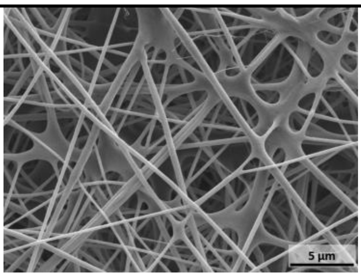
$COO^-/NH_3^+ = 1.0$	Electrospinning not possible
$COO^-/NH_3^+ = 0.7$	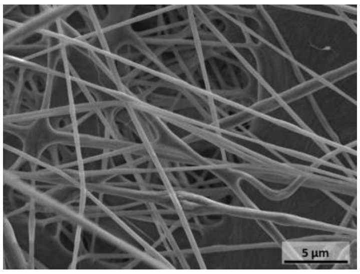
$COO^-/NH_3^+ = 0.5$	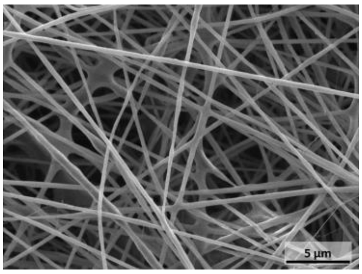
$COO^-/NH_3^+ = 0.3$	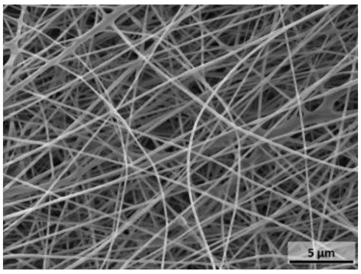
$COO^-/NH_3^+ = 0.1$	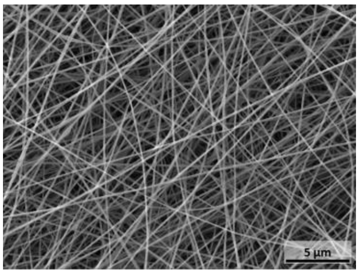

Figure 3.7. Study on the influence of the charge ratios on the fibrous structures for blend electrospinning

When comparing the overall morphology of blend electrospun membranes and the ones obtained by coaxial electrospinning (see figure 3.7. and 3.6), fewer defects (e.g. fusion, polymeric patches and beads) were observed for membranes obtained after blending. However, when the COO^-/NH_3^+ ratio got close to 1, homogenous fibres were harder to get and the stoichiometric blend could not be electrospun. For these ratios, the PECs were created more rapidly leading to the increase of the PEC viscosity and thus to the increase of the fibre diameter and the formation of beads. At the stoichiometry, the formation of PEC was so fast that the PEC agglomerated and formed a gel within several minutes.

These observations were further confirmed when measuring the average fibre diameters. As detailed in table 3.2., the average fibre diameters varied with the charge ratios. As expected, as the COO^-/NH_3^+ ratios got close to the stoichiometric ratio, the fibre diameters increased. Similarly, the standard deviation values also increased.

	COO^-/NH_3^+	**Composition CMC/CHI/PEO wt/wt/wt (%)**	**Average diameter ϕ of the fibres (nm)**	**Standard deviation (nm)**
MO LP55	**0.1**	10/61/29	170	40
MO LP59	**0.3**	23/47/30	240	60
MO LP63	**0.5**	36/43/21	360	90
MO LP67	**0.7**	37/32/31	420	130
-	**1.0**	44/24/32	-	-
MO LP36	**1.2**	45/23/32	340	110

Table 3.2. Average diameter of the blend electrospun fibres in regard to the different charge ratios tested

When comparing the two processing experiments (SEM images detailed in figure 3.6 and 3.7) for similar charge ratios (e.g. 0.1, 1 and 1.2/1.5), it can be noted that the fibres obtained by standard electrospinning of PEC blends presented fewer defects than the coaxial ones. The so-obtained blend fibres were also more regular in size and fewer beads could be observed.

These SEM images thus suggested that the mixing of the two polyelectrolyte solutions prior to the electrospinning seemed to be the best strategy for the elaboration of homogenous mats.

These materials were developed for wound dressing applications. The fibrous mats then need to be stable in water and preserve their fibrous structures. Both coaxial and blend membranes were thus immersed for 24 hours in distilled water. 2x2 cm squares of electrospun membranes were cut and immersed into 15 mL of distilled water in order to remove the PEO contained in the fibres. After 24 hours, the membranes were placed onto filter paper and let to dry under the fume cupboard (for more details see chapter 5 section 2.12).

To be able to compare the results obtained for coaxial and blend PEC based fibres, polysaccharide based membranes (namely CMC/PEO and CHI/PEO) were also immersed in distilled water for the same period of time and dried under the same conditions.

As can be seen in the SEM images (figure 3.8.a and 3.8.b), once CMC/PEO or CHI/PEO mats were soaked into water, the fibres were dissolved. Only the aluminium foil was observed after the immersion experiment. In the case of the coaxial CMC/CHI fibres (figure 3.8.c), the structure of the fibres was also lost after 24 hours and no fibres were observed by SEM after the immersion in water. For the membranes obtained after mixing both polyelectrolytes, the results obtained after the soaking in distilled water (in figure 3.8.d) demonstrated the preservation of the fibrous structure for a charge ratio close to 1. However, the fibres seemed to be flat after the treatment suggesting that their morphology was altered by water.

The difference in stability between core:shell and blend fibres can be understood by a difference of electrostatic interactions inside the two types of fibres. In the case of blend electrospinning, there is a high concentration of PECs in comparison with core:shell fibres. In the case of coaxial electrospinning, PECs could only form at the interface between the core and shell of the fibres. Hence, the surface of the fibres was composed of CHI/PEO that is less stable against water than PECs.

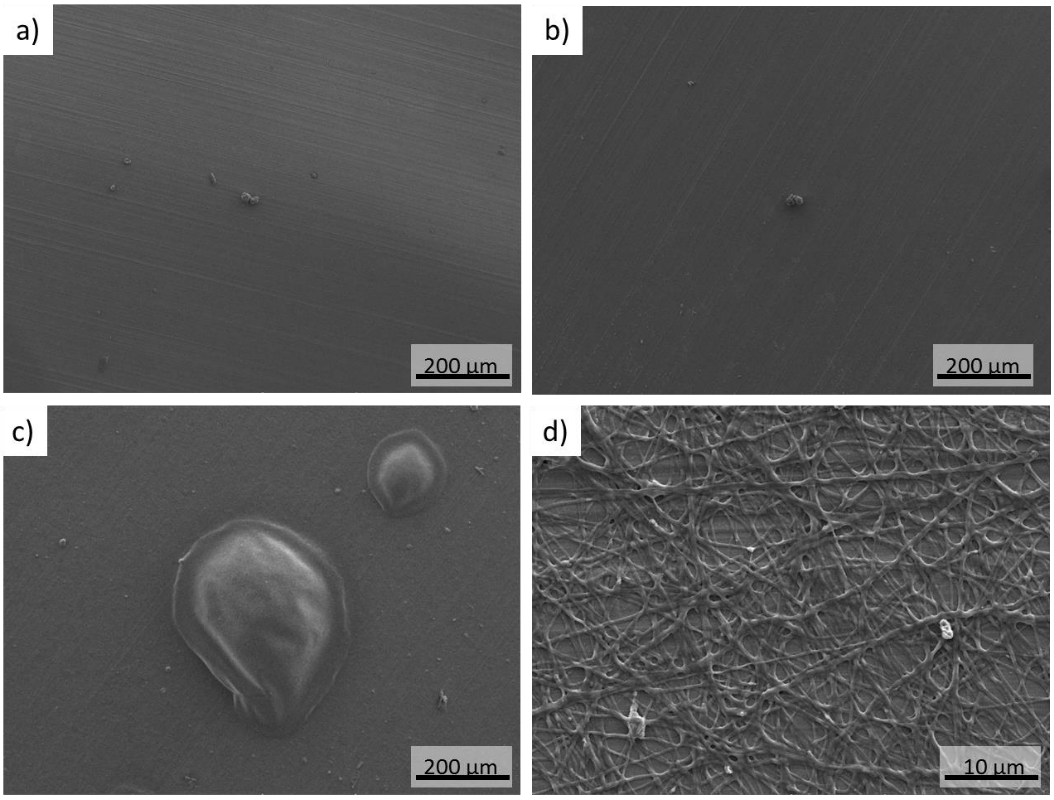

Figure 3.8. SEM images obtained on electrospun membranes a) CHI/PEO membranes, b) CMC/PEO membranes, c) core/shell CMC/CHI coaxial fibres ($COO^-/NH_3^+ = 1$) and d) CMC/CHI blend fibres ($COO^-/NH_3^+ = 1.2$) after a 24 hours immersion in distilled water.

As a conclusion, electrospun fibres based on polyelectrolyte complexes were successfully elaborated. Core:shell CMC:CHI fibres were prepared and presented numerous defects including, beads, polymeric patches and droplets on the collected mats. A blend of the two polyelectrolytes was also successfully processed by electrospinning and dryer membranes with fewer defects were obtained.

A preliminary evaluation of the stability of the electrospun membranes in water demonstrated that the CMC/PEO, CHI/PEO and core:shell CMC:CHI fibres were dissolved after 24 hours in distilled water. On the other hand, the blend fibres were maintained after a 24 hours immersion. However, fewer fibres were noted on the mat and their structure was also flattened.

Blending the two polyelectrolytes together prior to the electrospinning experiments seemed to be the best strategy to obtain stable fibres. Nonetheless, the membranes stability in water could be improved for better bioactive properties.

In the following biological evaluations and MB incorporation tests, only blend fibres presenting a COO^-/NH_3^+ ratio of 0.7 were used as PEC based electrospun membranes. This ratio was chosen as the fibres were homogenous and the charge ratio was close to the stoichiometry.

3. Influence of the chemical and physical crosslinking on the electrospun fibres

To improve the stability of the fibrous membranes in water or any physiological buffer, crosslinking experiments were carried out. Two different types of crosslinking methods were tested. Sodium periodate was used as a chemical crosslinker and mixed within the PEC based solution prior to the electrospinning experiments. Another approach aimed to physically crosslink the membranes by placing the membranes in an environmental chamber at 37°C and 25% relative humidity for two weeks.

3.1.Crosslinking of electrospun membranes with sodium periodate

Glutaraldehyde and sodium periodate are two commonly used chemical crosslinkers for biomaterials. Despite being the main crosslinker used for biomaterial applications, glutaraldehyde is highly toxic and depending on the conditions of crosslinking, this molecule can crosslink and form a film that may cover the material and mask the properties of the fabrics. Sodium periodate was rather used as its toxicity is lower than for glutaraldehyde and only small amounts of chemical agent were used.

Sodium periodate was incorporated within the CMC solutions before being blended with the CHI solution. This agent is often used to open saccharide rings between two vicinal diol groups generating two aldehyde groups (depicted in scheme 3.1). This modification of the CMC structure will further enable the chemical crosslinking between CMC and CHI when mixed together (scheme 3.2).

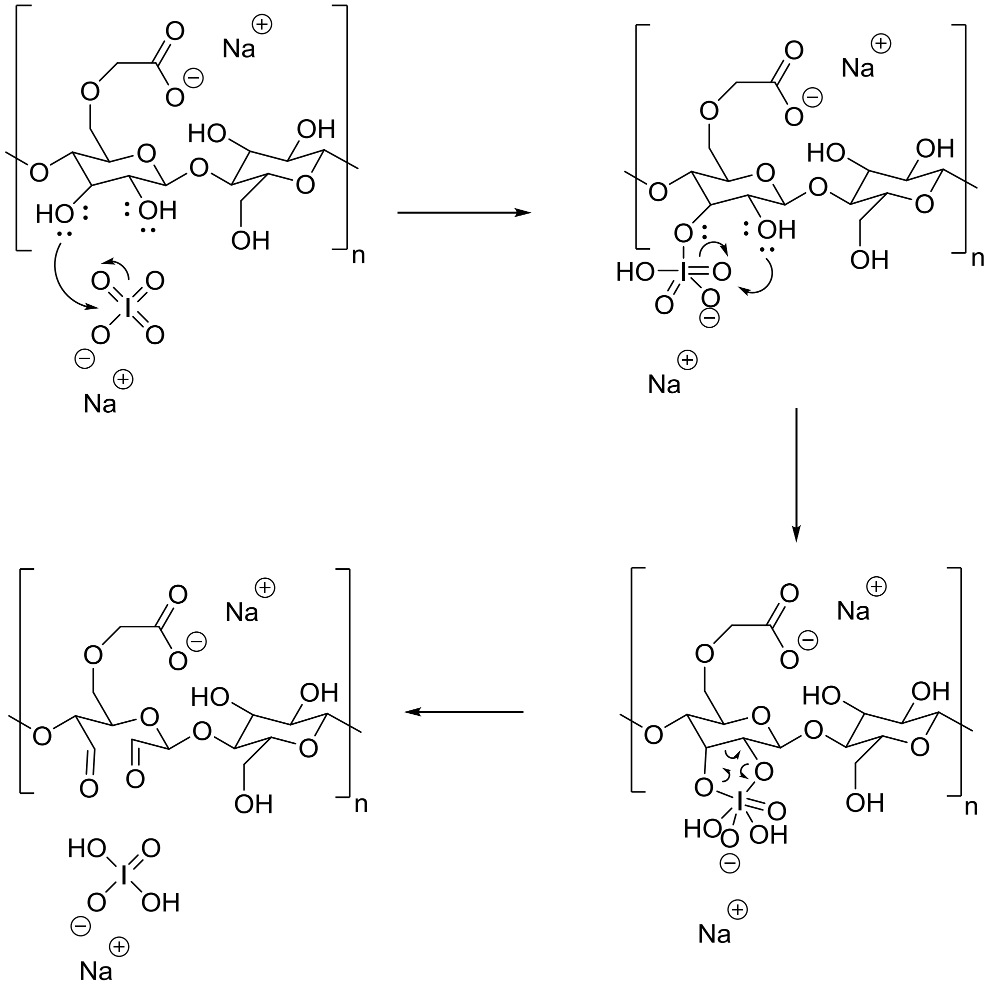

Scheme 3.1. Reaction pathway of sodium periodate on carboxymethylcellulose to activate the polysaccharide for crosslinking of the polyelectrolyte complexes[216]

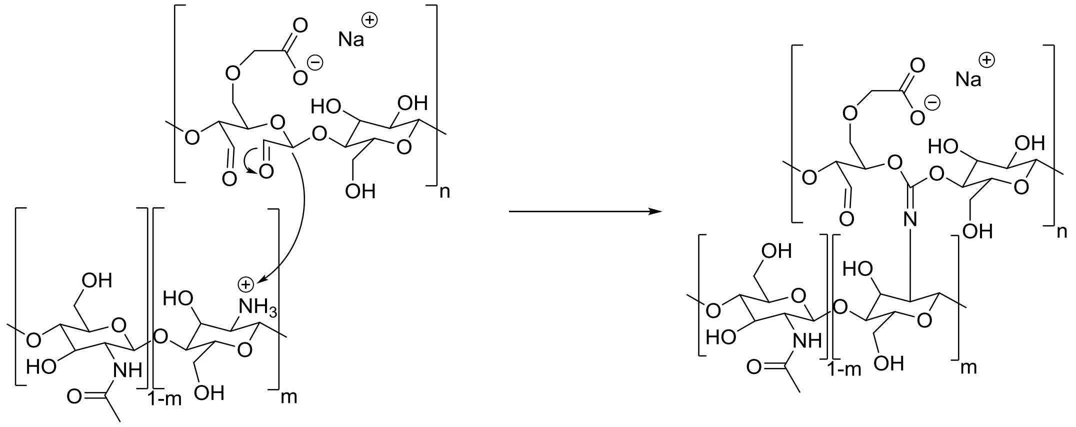

Scheme 3.2. Crosslinking mechanism between chitosan and carboxymethylcellulose after the ring opening reaction by sodium periodate

0.3 wt% of the CMC weight (corresponding to 1 IO_4^- for 335 cellulose monomer unit) was added to the CMC solution and mixed for 24 hours prior to the electrospinning experiments. As can be seen in figure 3.9.a, the fibres obtained after blend electrospinning were homogenous and the structure was highly porous. The membrane was also let to soak for 24 hours in distilled water before being dried and observed by SEM. The fibrous structure of the mat after the immersion in water was almost left unchanged (Figure 3.9.b). The polymeric patches onto the non-woven are probably composed of the PEO polymer that is soluble in water and was thus released from the fibres during the immersion in water.

This crosslinking process was thus very effective and the membrane developed a high stability in the solvent despite the decrease in porosity. Hence, this method seemed to be a method of choice for the crosslinking of these non-wovens.

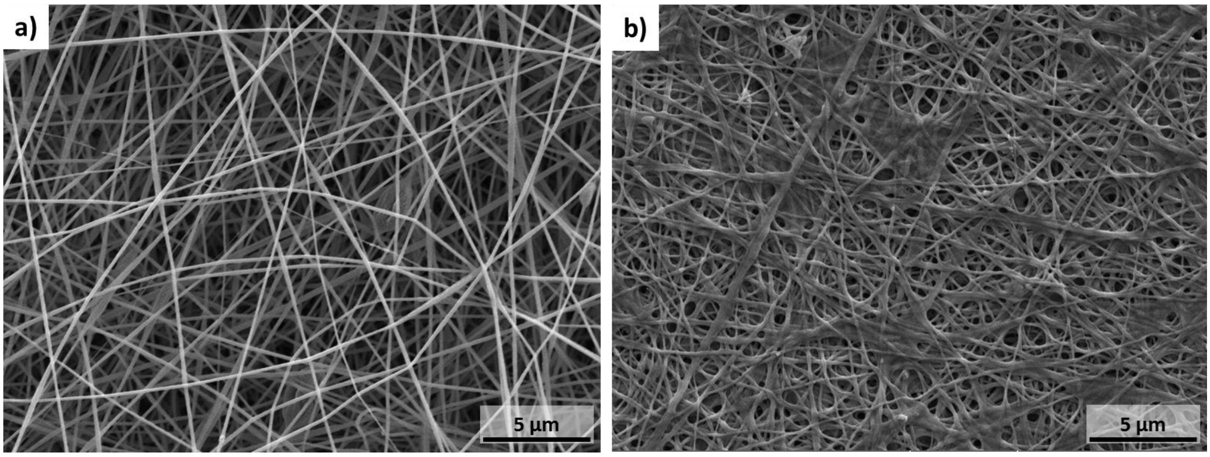

Figure 3.9. SEM images of a) blend electrospun fibres of CMC/CHI ($COO^-/NH_3^+ = 1.2$) incorporating sodium periodate and b) the same fibres after 24 hours in distilled water

As already said, the electrospun membranes were designed for wound dressing applications, and so, they will be in direct contact with human tissues. Although the crosslinking of the fibres using sodium periodate was successful, this method requires the addition of a toxic chemical agent. Therefore, another strategy was also tested to improve the stability of the fibres by physical crosslinking.

3.2.Physical crosslinking of the fibres in an environmental chamber

The electrospun membranes were placed for two weeks in an environmental chamber at 37°C and 25% RH. As PEO presents a melting temperature in the range of 40-50°C, the experimental conditions were thought to influence the mobility of the polymer backbones and thus favour some rearrangement within the fibres.

In order to test the stability of the so-obtained polysaccharide based fibres, CHI/PEO, CMC/PEO and CMC/CHI blend fibres were immersed for 24 hours in distilled water as described in chapter 5 2.12).

After this treatment, the CMC/PEO did not display any enhanced stability in water and no fibres were seen on the aluminium foil. The SEM image obtained after the passage in environmental chamber was similar as the one depicted in figure 3.8b.

On the other hand, as described in figure 3.10, the CHI/PEO fibres were preserved after the immersion in water. It is interesting to note that in figure 3.8a, the same test in water was performed on so-obtained CHI/PEO and no fibres were displayed after the soaking. So the CHI/PEO fibres after electrospinning processing were soluble in water but, after a two-weeks stay in an environmental chamber, they became stable in water.

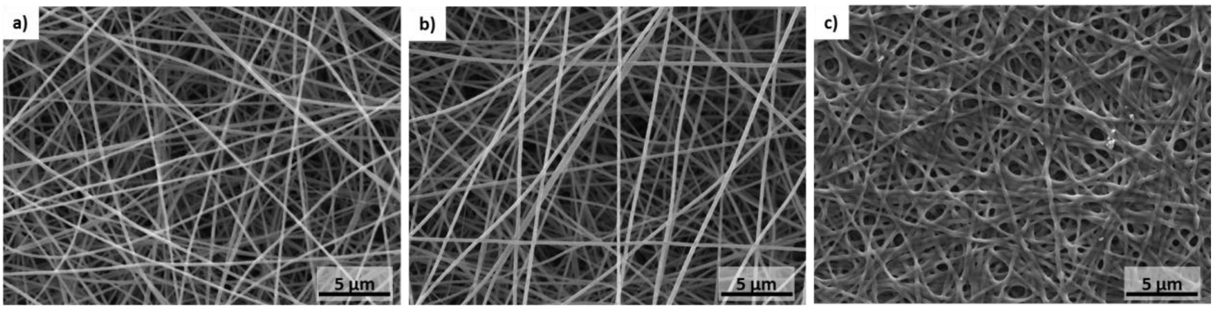

Figure 3.10. Evaluation of the fibres stability in water of a CHI/PEO membrane after physical crosslinking in an environmental chamber. a) CHI/PEO membrane, b) CHI/PEO membrane after 2 weeks at 37°C and 25% RH and c) physically crosslinked CHI membrane after 24 hours in water

To further study this phenomenon, XRD analyses were performed on the commercially available CHI powder and CHI based fibres at the different stages of processing and crosslinking.

As shown in the different diffractograms in figure 3.11., although the different products were highly amorphous, a change in the width of the crystalline peak can be seen after the incubation in the environmental chamber suggesting a change in crystallinity of the CHI. The diffractogram obtained after the two weeks in the environmental chamber (figure 3.11c) was similar to the one obtained for pristine CHI powder.

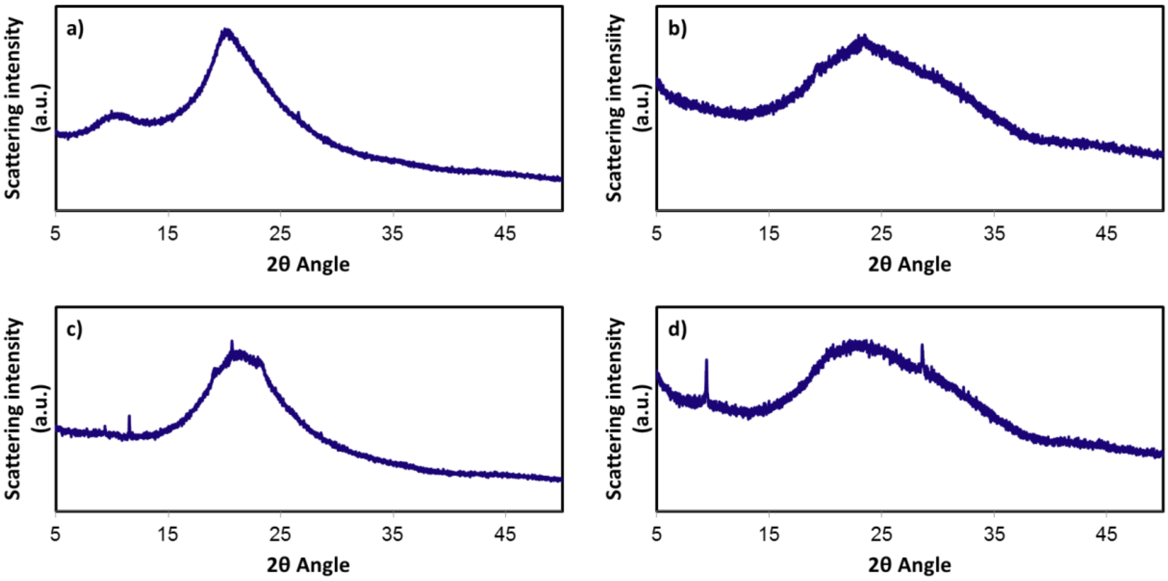

Figure 3.11. XRD thermograms obtained for a) CHI powder, b) CHI/PEO electrospun membrane, c) CHI/PEO membrane after physical crosslinking in the environmental chamber and for d) the physically crosslinked CHI/PEO membrane after 24 hours in distilled water

The XRD analyses thus seem to demonstrate that the crystallinity of CHI/PEO based fibres was improved after two weeks in an environmental chamber. This change in crystallinity may also occur for the CHI/CMC blend fibres.

For blend membranes, the SEM images confirmed that this physical crosslinking method improved the stability of the membranes in water as the fibres structure was slightly altered after immersion in water. Nevertheless, the fibres presented a slight decrease in the porosity and were flattened (see Figure 3.12). Some fibres fused together and thicker fibres were then obtained. Some polymeric patches could be seen after the immersion in water possibly due to the PEO. However, the morphology was still porous enough to ensure good exchanges between the wound and the external medium.

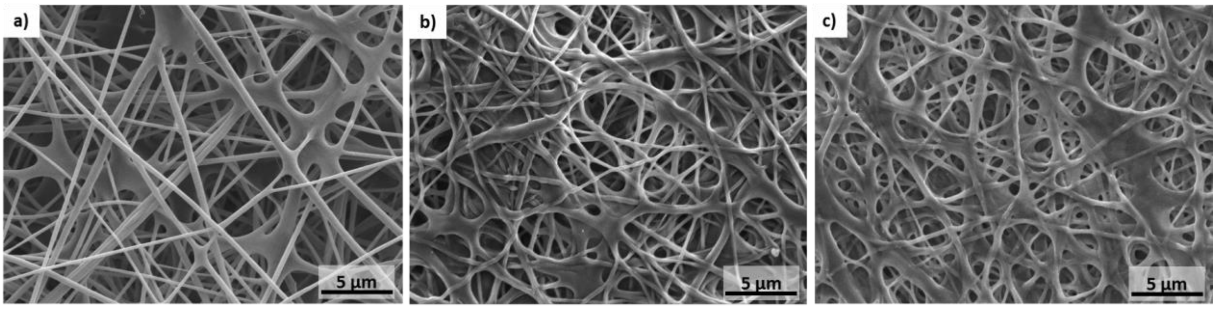

Figure 3.12. Evaluation of the water resistance of a blend CMC/CHI membrane ($COO^-/NH_3^+ = 1.2$) after physical crosslinking in an environmental chamber. a) Blend CMC/CHI membrane, b) blend CMC/CHI membrane after 2 weeks at 37°C and 25% RH and c) physically crosslinked blend CMC/CHI membrane after 24 hours in water

Physical crosslinking of CHI based fibres seem to improve the stability of the non-woven membranes in water probably because of a change in the CHI crystallinity after the passage in an environmental chamber. The change in the crystalline organization of the fibres may be induced by the temperature and humid conditions within the chamber.

4. Elaboration of methylene blue loaded and polyelectrolyte complex based electrospun fibres

Chitosan has proven to be an antibacterial polysaccharide, however, and to improve the antibacterial activity of the PEC based membranes, methylene blue (MB) was added within the fibres. MB is a cheap and efficient antibacterial agent. Inclusion complexes between methylene blue and β-cyclodextrins (β-CDs) were synthesized in chapter 2 to extend the antibacterial activity of the fibrous materials (figure 3.13). Although a 1:1 β-CD:MB complexation rate was expected, a 1:6 β-CD:MB ratio was determined by ^{1}H NMR analysis. This last complexation rate was taken into account for the calculations of methylene blue concentration.

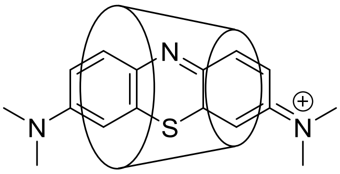

Figure 3.13. Schematic representation of the inclusion complex between methylene blue and β-cyclodextrin

Preparation of methylene blue loaded solutions

Methylene blue was added within the CHI solution and let to stir for 24 hours. 15 wt% of the CHI weight were added in the solutions. For the inclusion complexes, 17.5 wt% of the CHI weight were incorporated within the solutions and corresponded to 15 wt% of MB in regard to CHI. The CHI and MB or MB inclusion complexes (ICs) were solubilized in a 50/50 wt/wt FA/H_2O solution.

A first set of experiments was carried out to form core:shell CMC:CHI/MB or CMC:CHI/IC membranes. These coaxial fibres presented numerous defects (e.g. fusion of fibres and drops) and the collected mats were still wet. Therefore, these membranes were not further crosslinked or biologically evaluated.

Finally for methylene blue loaded non-woven mats, only $COO^-/NH_3^+ = 0.7$ blend membranes were prepared. The experimental electrospinning conditions employed for the fabrication of these fibres were the same as for standard PEC based fibres (see the electrospinning conditions detailed in chapter 5 4.1.2). Homogenous fibres were obtained by blending the

CMC, CHI and MB or MB ICs prior to the electrospinning experiments. The structure of the fibres was similar to the blend CMC/CHI fibres without adding any antibiotic.

For biological evaluation purposes, methylene blue loaded CMC/CHI blend membranes were used without being crosslinked, a second batch of mats was crosslinked using sodium periodate and the third one was physically crosslinked in an environmental chamber. The same experiments were performed for the MB inclusion complexes loaded blend CMC/CHI membranes.

For biological evaluations, a total of 12 CMC/CHI based blend fibrous membranes ($COO^-/NH_3^+ = 0.7$) were prepared as detailed in the following table:

Not crosslinked	Chemically crosslinked	Physically crosslinked
CMC/CHI	CMC/CHI + $NaIO_4$	CMC/CHI
CMC/CHI/CD	CMC/CHI/CD + $NaIO_4$	CMC/CHI/CD
CMC/CHI/MB	CMC/CHI/MB + $NaIO_4$	CMC/CHI/MB
CMC/CHI/IC	CMC/CHI/IC + $NaIO_4$	CMC/CHI/IC

Table 3.3. Recapitulative table detailing all the electrospun membranes prepared for the biological evaluations

Cyclodextrins were also added within some membrane formulations to be evaluated and used as references for the antibacterial assessment.

5. First biological evaluations of the processed membranes

All the biological evaluations were performed by L.Seon through the collaboration with Pr. P. Schaaf (INSERM, U1121) and Dr. F. Boulmedais (ICS, UPR22).

The biological evaluation of the membranes was a preliminary assessment of the antibacterial activity of the electrospun mats. CHI/PEO, core:shell CMC:CHI and blend CMC/CHI membranes were tested against M.Luteus.

5.1.Description of the disc diffusion tests

To see the exact procedure of the Kirby test, please refer to chapter 5 section 6.2.

For disc diffusion tests, bacteria are impregnated onto agar plates. The aim of the test is to evaluate the efficiency of antibiotics or materials presenting antibacterial properties. The agar plates are incubated at 37°C for several days and the diameters of bacteria free zones, the so-called inhibition zones, are regularly measured.

The zone of inhibition can easily be characterized as it corresponds to a clear circle around the disc (figure 3.14). If no inhibition zone can be measured around the disc but, when removed, no bacteria can be seen under the material, the fibrous mat still display bactericide effect without any diffusion properties.

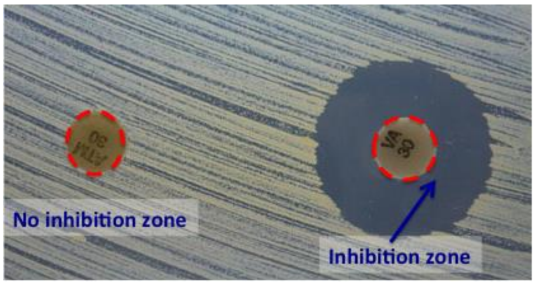

Figure 3.14. Representation of disc diffusion test results for two different samples without and with an inhibition zone

5.2. Antibacterial assessment of the electrospun membranes

The CMC/CHI based membranes were evaluated against M.Luteus and the samples were incubated at 37°C for 48 hours. CHI/PEO and CMC/CHI/CD membranes were used as controls for the evaluation of the bactericide properties.

As depicted in figure 3.15. (see also figure 3.16), none of the CMC/CHI membranes presented any antibacterial activity after 24 hours. Even the coaxial core:shell CMC:CHI membranes did not display any clear area around the disc. Although CHI has been known for its bactericide properties, it seemed that our fibrous membranes did not contain a sufficient CHI concentration to be effective toward the bacteria.

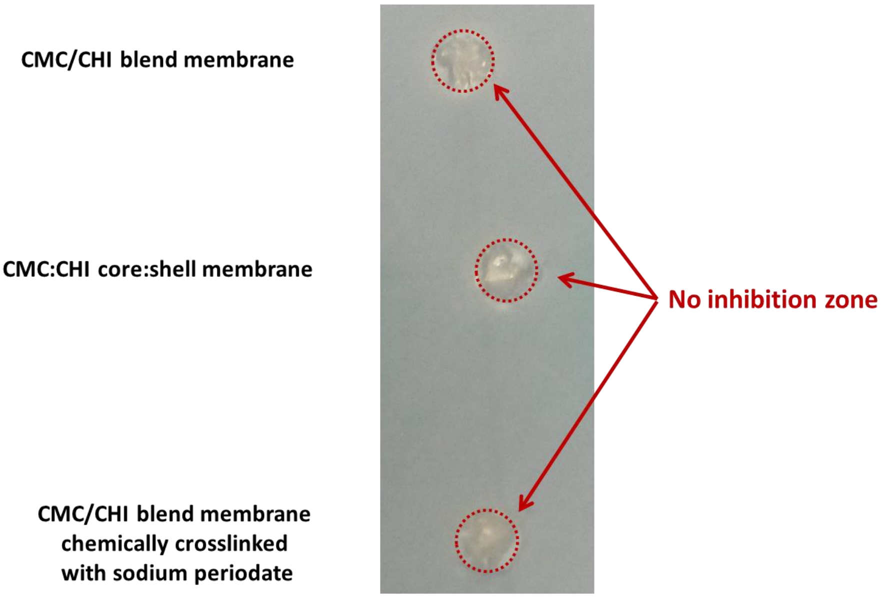
CMC/CHI blend membrane
CMC:CHI core:shell membrane
CMC/CHI blend membrane chemically crosslinked with sodium periodate
No inhibition zone

Figure 3.15. Disc diffusion results obtained on CMC/CHI based membranes. One membrane was obtained by coaxial electrospinning and the two other were the results of blend electrospinning incorporating sodium periodate or not

The various MB and MB ICs loaded blend membranes ($COO^-/NH_3^+ = 0.7$), chemically crosslinked, physically crosslinked or not crosslinked were also incubated at 37°C for 48 hours. After 18, 24 and 48 hours, the agar plates were removed from the incubator and their inhibition diameters were measured before being incubated again.

As can be seen in the following figure (Figure 3.16.), all membranes containing MB or MB ICs displayed an inhibition circle (see chapter 5 6.2). This suggested that MB and MB ICs loaded membranes exhibited an antibacterial activity. When comparing the type of crosslinking used, no conclusion could be drawn as no tendency could be seen in the diameter value measured. Whether the fibres are crosslinked or not, whether they are chemically or physically crosslinked, no improved bactericide properties were exhibited for a certain type of membrane.

A difference in the antimicrobial properties between pure MB loaded membranes and MB based ICs electrospun mats was noted. Indeed, when observing the inhibition diameters for MB loaded membranes, the inhibition zone diameter after 48 hours was smaller than the one measured at 24 hours. However, for MB ICs loaded membranes, the inhibition zone remained almost constant over the two days test. Additionally, the diameters obtained after 24 and 48 hours were big enough to prove the good bactericide properties of both types of MB loaded membranes.

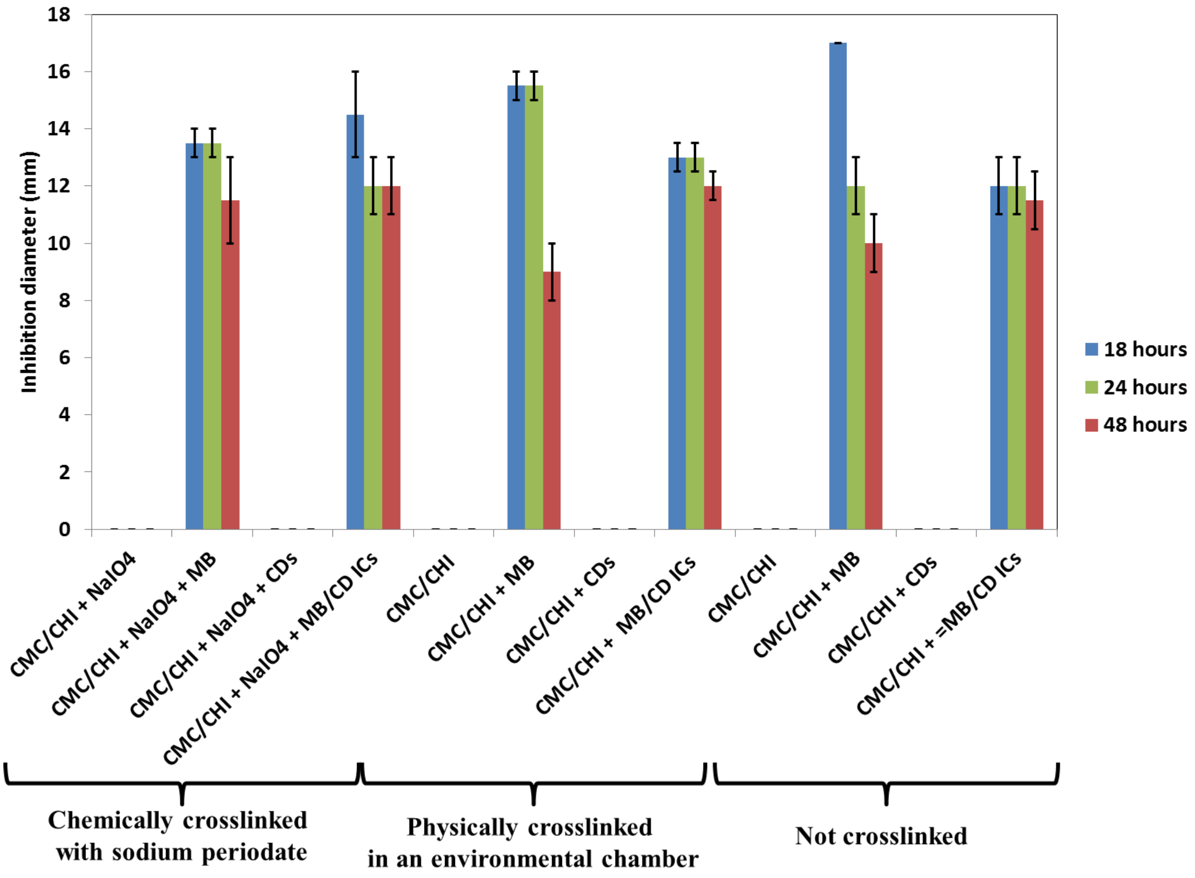

Figure 3.16. Biological evaluation of the antibacterial activity of the PEC based blend membranes (COO-/NH3+ = 1.55) against *M.Luteus* by disc diffusion test (Kirby's test)

Hence, these results suggest that the blend CMC/CHI membranes loaded with MB or MB ICs exhibit good antibacterial properties. The strategy used to crosslink the fibres did not seem to have any influence on the bactericide properties displayed by the membranes. Nonetheless, a difference between pure MB and MB IC loaded membrane was seen. After 24 hours, the antibacterial properties of pure MB loaded membranes showed smaller inhibition diameters suggesting a loss in the antibacterial activity. However, MB IC loaded membranes exhibited similar antimicrobial activity demonstrating a prolonged bactericide activity of the mats. These membranes thus seem to be promising materials for wound dressing applications.

5.3.Drug release kinetic study

To better assess the differences in drug release between MB or MB IC loaded membranes, a release kinetic study in a buffer at pH = 7.4 over several days was followed by UV-Visible spectrometry.

Preliminary studies were performed on pure MB and on MB ICs to determine the molar extinction coefficient ε_{MB} (in $L.mol^{-1}.cm^{-1}$) of pure MB and of MB within the ICs. To see the values obtained as well as the calibration curves, please see chapter 5 section 7.

To measure the MB release from the electrospun membranes, discs of blend electrospun membranes were cut and immersed in 20 mL of a pH = 7.4 buffer. At regular intervals, 0.8 mL of the solution was collected and the absorption of the buffer was measured by UV-Visible spectrometer (at λ = 640 nm for MB loaded membranes and at λ = 630 nm for MB IC loaded membranes). Knowing the absorbance value obtained and applying the value within the Beer-lambert law, the MB concentrations could be assessed. After some time, a plateau was obtained. To plot the time versus the percentage of released MB, it was hypothesized that the average concentration value at the plateau corresponded to a 100% release.

For the IC loaded membranes, the determined absorption values were supposed to be the absorption values of pure MB. Nonetheless, it could not be determined with certainty if the absorption values corresponded to the absorption of free and pure MB of if the encapsulated MB within the IC also absorbed light.

The calculated MB release percentage as a function of time obtained for MB and MB IC loaded membranes are depicted in figures 3.17a and 3.17b. For MB loaded membranes, the maximal value of released MB was achieved and a plateau was seen so that no additional MB was released in the supernatant after 4 hours. In the case of IC loaded mats, the plateau obtained for the release of MB or MB/IC was reached after 8 hours of the test. The release kinetic found for the IC loaded non-wovens was thus slower than the one displayed by pure MB loaded fibrous membranes. The encapsulation of MB hence contributed to the extension of the antibiotic release as suggested by the biological and drug release kinetic tests.

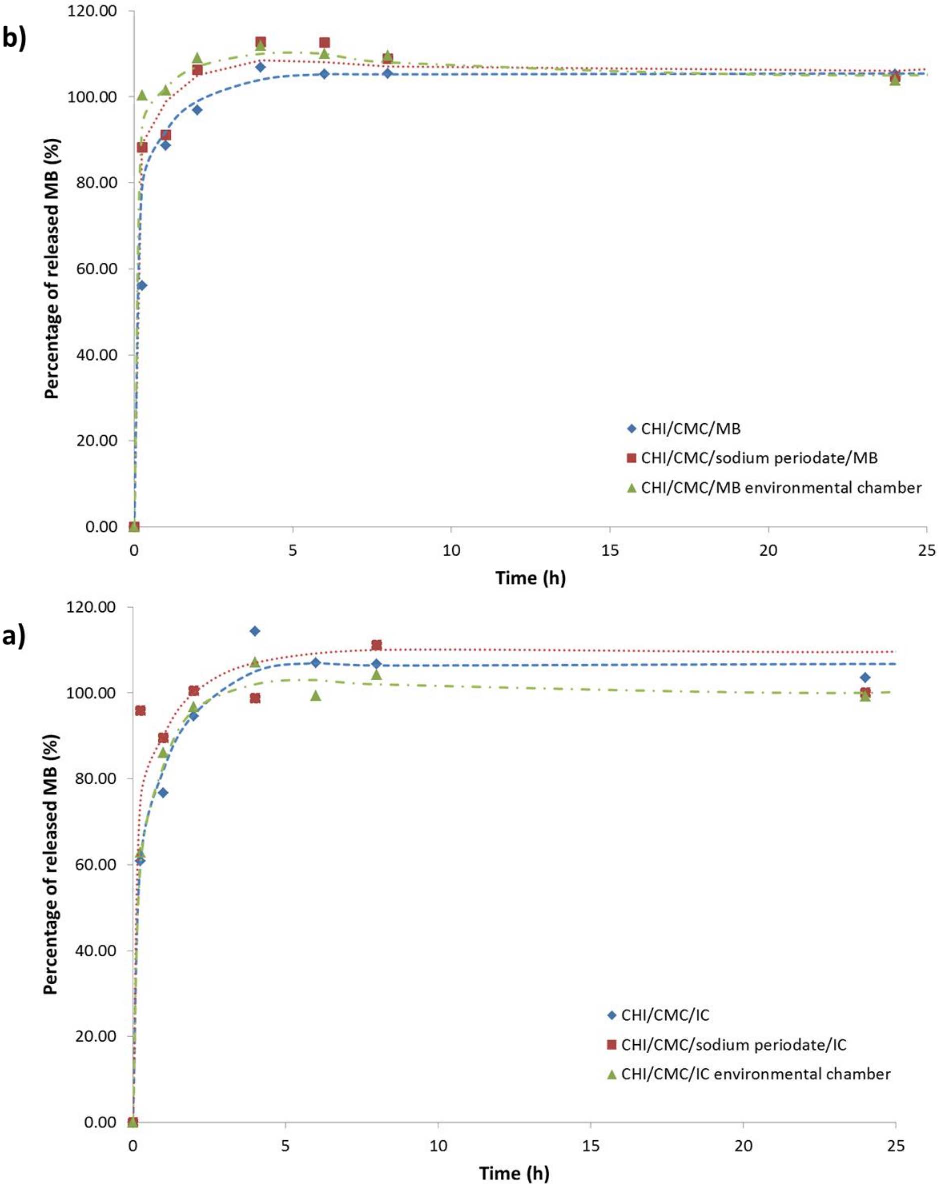

Figure 3.17. Release kinetic evaluation of a) pure methylene blue in the various blend membranes and b) of methylene blue inclusion complexes in their respective PEC based membranes. The dashed lines are given as guides to the eye.

It can be noted that after 2 to 4 hours all the MB contained in the MB loaded membranes was released in the aqueous buffer. On the other hand, for IC loaded membranes, the overall content of MB ICs was completely released after 8 hours. Although, the entire release of the antibiotic was achieved in less than 24 hours, the ICs displayed a prolonged drug release in comparison with pure MB.

The fact that the IC loaded membranes exhibited good antibacterial efficiency for 48 hours could be understood by the fact that once the ICs are released from the membranes, some time might still be needed to break the interactions between MB and β-CD.

Conclusion

We have successfully electrospun polyelectrolyte complexes based on the oppositely charged CHI and CMC and obtained two different types of fibres: coaxial core:shell fibres as well as blend PEC based fibres. PEO was added to the two polyelectrolyte solutions prior to the electrospinning experiments to enable the electrospinning of the polysaccharide solutions by improving the polymer chains entanglements and the viscosity of the solutions.

To determine the best parameters for the elaboration of homogenous fibres, the COO^-/NH_3^+ ratios were varied from 0.1 to 10.9.

For the coaxial experiments, the best results were obtained for COO^-/NH_3^+ ratios close to 1 that can be well understood by the fact that at these ratios, the formation of PEC interface is favoured.

To avoid the formation of a gel while electrospinning a blend of the two polyelectrolytes, the mixing of the two polysaccharide solutions was done instants before the processing. As opposed to core:shell fibres, the COO^-/NH_3^+ stoichiometric ratio could not be electrospun as a gel was formed within minutes. Homogenous and bead-free fibres were obtained for the other ratios. The blend mats were dryer and less fibre fusion could be seen on the membranes. These fibres presented thus fewer defects than the coaxial fibres. Due to its charge ratio close to the stoichiometry, the 0.7 COO^-/NH_3^+ ratio was used as the standard value for the elaboration of blend membranes for the biological evaluations.

To test the fibres stability in water, all membranes were immersed for 24 hours in distilled water. As the fibrous structure was not entirely preserved after the water immersion, we decided to crosslink the membranes. Two different crosslinking methods were used. Sodium periodate was added to the CMC solutions to chemically crosslink the fibrous mats. In an attempt to reinforce the membranes without the use of any chemical crosslinker, the membranes were placed for two weeks at 37°C and 25% RH in an environmental chamber. Both crosslinking processes were successful and the fibrous structure was mainly preserved after the crosslinked electrospun mats were soaked in water.

To improve the antibacterial properties of the membranes and modulate the antibacterial activity of the materials, methylene blue (MB) and its derived ICs were added to the CHI solutions. Both coaxial and blend electrospinning experiments were performed. Because of the numerous defects, only the blend CMC/CHI membranes loaded with MB or MB IC were kept for biological evaluations.

To assess the biological properties of the PEC based fibrous membranes against M. Luteus, disc diffusion tests were carried out on impregnated agar plates. The membranes were incubated at 37°C for several days to see the bactericide efficiency of the non-woven mats. Both CMC/CHI blend and CMC:CHI core:shell membranes showed no antibacterial effects against M. Luteus. The blend membranes loaded with MB or MB based ICs were highly efficient and inhibition zones were measured and presented big bacteria free diameters. The MB IC loaded membranes were especially highly bactericide and displayed good antibacterial properties for 48 hours. Drug release kinetic studies on the MB loaded membranes confirmed that the MB ICs loaded membranes exhibited a delayed and prolonged release in comparison with pure MB loaded membranes.

To further establish the antibacterial activity of these promising bandages, new biological tests need to be performed as well as *in vivo* evaluations. But first, new materials need to be prepared and crosslinked. New experiments to obtain the same charge ratios between coaxial and blend fibres need to be carried out for better comparison purposes. The mechanical properties of the polyelectrolyte complex based fibres have also to be assessed.

The use of different antibiotics such as curcumin and their respective inclusion complexes will be attempted and evaluated. The association of these natural antibiotics (curcumin and MB) could also be imagined to investigate their synergetic antimicrobial activity.

Chapter 4

The use of cyclodextrins for the surface functionalization of pseudo-polyrotaxane based fibres

The use of cyclodextrins for the surface functionalization of pseudo-polyrotaxane based fibres

The second application approached in this PhD thesis is the elaboration of biofunctional materials for tissue engineering applications. For this project, poly(ε-caprolactone) (PCL) was chosen as the electrospun polymer matrix. This polyester is a well-known biocompatible and biodegradable polymer that exhibits good mechanical properties. Hence, PCL has been used for decades for biomedical applications including tissue engineering. However, one major drawback of using PCL is that it can not easily be functionalized. To enhance the biological activity of PCL fibres, the previously discussed pseudo-polyrotaxanes (pPRs) were added as building blocks for the biofunctionalization of the non-woven mats. Indeed the presence of cyclodextrin (CD) on the pPR provides a large number of easily functionalising hydroxyl functions.

The four different pPRs prepared (see chapter 2) were separately used to elaborate electrospun scaffolds. A linear pPR (lin-pPR), a four-branched pPR (star-pPR), an asymmetric four-branched pPR (mik-pPR) and a block copolymer derived pPR (copo-pPR) (figure 4.1) were separately solubilised in DMSO to obtain solutions that could be electrospun.

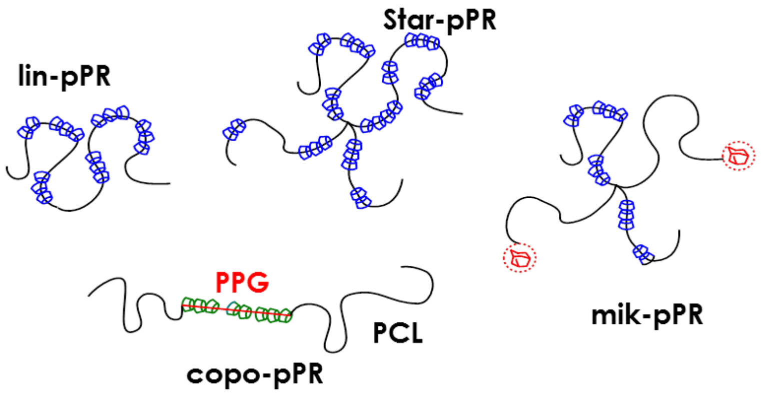

Figure 4.1. Schematic representation of the different synthesized pseudo-polyrotaxanes already detailed in chapter 2

Two different electrospinning strategies were investigated to elaborate reactive electrospun fibres. Blend solutions containing both the polymer and the pseudo-polyrotaxanes were first processed by electrospinning. To ensure the presence of hydroxyl groups at the surface of the fibres and thus ease the post chemical modification, a second attempt aimed to prepare core:shell PCL:pPR fibres. The surface properties of the fibres such as its roughness, as well as the density and homogeneity of cyclodextrin hydroxyl functions present at the surface are important parameters in order to facilitate the post-functionalization. Thus, the influence of the pPR flow rate as well as the influence of the relative humidity during the processing on the fibre morphologies were investigated.

Prior to any functionalization reaction, the presence of the pPRs within the fibres or at the surface of the fibres had to be proven. Indeed, without pPRs and especially without any CDs on the fibre surface, no bioactive molecule could be successfully grafted as PCL does not display any reactive function along its backbone. XRD and water contact angle measurements were thus carried out to characterize the fibres composition and to see if the hydrophobicity of the fibres was modified by the addition of pseudo-polyrotaxanes. Mechanical tensile tests were also performed on electrospun membranes to determine the change of mechanical properties induced by the presence of the pseudo-polyrotaxanes within the PCL based fibres.

Then, as proof of concept, fluorescein isothiocyanate was first grafted onto the obtained fibres as this molecule was very reactive and commercially available. To assess the success of the grafting reaction, confocal fluorescent microscopy images were done on each sample.

1. Elaboration of electrospun fibrous membranes

To prepare the fibrous materials, two different approaches were developed to obtain reactive fibrous membranes. First, blends of PCL and pPR were processed by simple electrospinning to obtain fibres. Secondly, core:shell PCL:pPR fibres were fabricated by coaxial electrospinning to favour the presence of the reactive functions at the surface of the fibres.

1.1.Elaboration of blend fibres

All solutions were prepared 24 hours prior to any electrospinning experiments to ensure a complete dissolution of PCL and pPRs. For these experiments, only star-pPRs were added within the solutions for the fabrication of fibres by electrospinning.

Because star-pPR and PCL do not have a common solvent, a 50/25/25 wt% mixture of dichloromethane/dimethylformamide/dimethyl sulfoxide (DCM/DMF/DMSO) was chosen among the tested solvent mixtures.

The prepared solution concentrations (see details in chapter 5 section 4.2.1. for the detailed solution preparation and electrospinning conditions) varied between 15 and 20 wt% of solid. For each solution, 5 wt% of the solid weight was composed of the star-pPRs. However, only opalescent or turbid solutions were obtained and processed by electrospinning. The electrospinning parameters were optimized until a stable jet was formed and stretched. As can be seen in figure 4.2., the membranes obtained in each case presented many defects, especially beads and fusion between neighbouring fibres. The presence of beads might be due to the low concentration of the solid used for the experiments. Nevertheless, the solid concentrations could not be further increased as the solution incorporating 20 wt% of solid was already turbid and aggregates could not be dissolved. Furthermore, the solutions became unstable during the electrospinning processing and became more turbid with time especially for the 18 wt% and 20 wt% solid solutions.

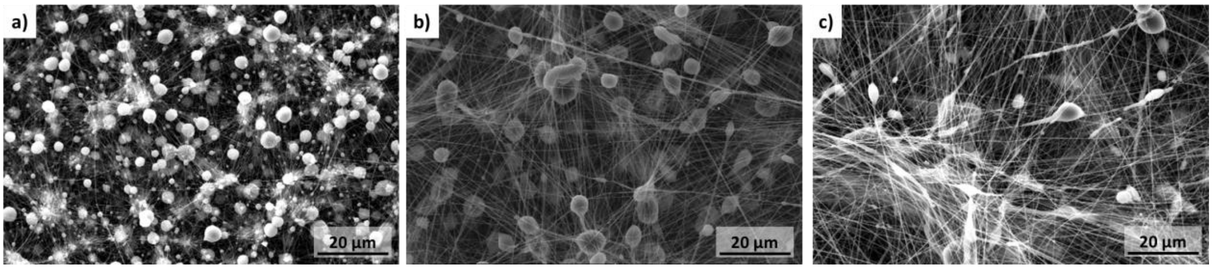

Figure 4.2. SEM images obtained after electrospinning experiments with applied voltages of 25/-5 kV at the needle and the collector for blend solutions containing a) 15 wt% of solid, b) 18 wt% of solid and c) 20 wt% of solid in total

Thus, only the 15 wt% solid solution was selected for further studies as the solution was opalescent and no aggregates could be seen within the solution. To improve the morphology of the blend fibres, the influence of the relative humidity (RH) on the fibre was investigated.

A new set of experiments was carried out where the RH was kept below 30%. As depicted in the following figure 4.3., the obtained mat presented more homogenous fibres with fewer beads. The fusion between neighbouring fibres was also enhanced as less thick fibres could be observed on the mat. Thus the RH seems to play an important role in the elaboration of electrospun fibres. Indeed, the RH will impact the evaporation of the solvents and especially the evaporation of DMSO. Moreover, this organic solvent is highly hydrophilic and will thus absorb the water molecules present in the atmosphere rather than interact with the electric charges. To a lesser extent, the water molecules will also modify the charge density within the electrical field.

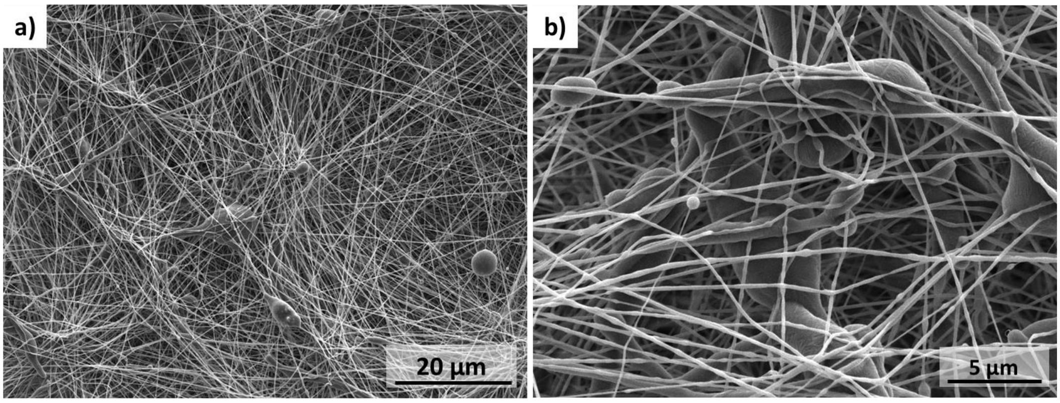

Figure 4.3. SEM images of 15 wt% solid fibres obtained at a) 3000 x magnification and b) 10 000 x magnification

XRD analysis was carried out on the blend fibres obtained under low relative humidity conditions to determine the presence of pPR within the membrane. The presence of pPRs would be noticed as a 2θ = 20° peak of threaded CDs would be seen on the spectrogram.

However, the spectrogram obtained for the blend mat did not exhibit any peak at 20° but only the characteristic peaks of crystalline PCL. Hence, no conclusion could be drawn.

Various blends of PCL and star-pPR were successfully electrospun under high electrical field. The best solubilized solution incorporating 15 wt% of solid was further studied. When decreasing the RH value within the electrospinning set-up, the morphology of the star-pPR based fibres was improved. Unfortunately the starting solution is opalescent and, during the processing, also unstable. After fabrication, the presence of star-pPR within the fibres could not be determined. Therefore, another approach to ensure the presence of pPRs and the accessibility of the hydroxyl groups has to be developed.

1.2.Elaboration of core: shell PCL: pPR fibres

Here, PCL:pPR core:shell fibres were produced by coaxial electrospinning. Knowing that electrospinning needs homogeneous polymer solutions and well-dispersed suspensions for the preparation of composite nanofibres[217], coaxial electrospinning appeared as the best strategy allowing to adapt the solvent of each polymer.

To elaborate core:shell fibres as described in the following figure 4.4, two separate core and shell solutions were prepared 24 hours prior to any electrospinning experiments (see chapter 5 section 4.2.2). Thus, for the core solution, 15 w% of PCL was solubilized in a 60/40 wt/wt mixture of DCM/DMF whereas concentrations of 5, 10 and 15 w% of pPRs in DMSO were prepared and resulted in PCL:pPR solid weight ratios in the fibres of respectively 10:1, 10:2 and 10:3.

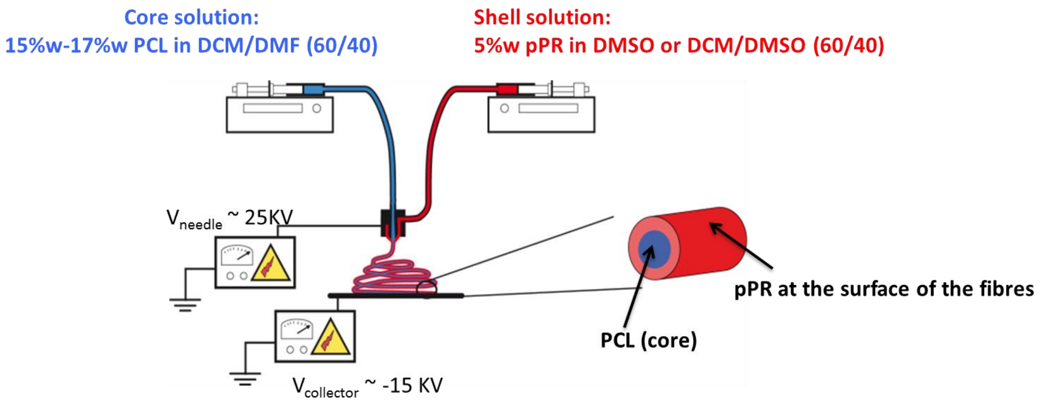
Core solution:
15%w-17%w PCL in DCM/DMF (60/40)
Shell solution:
5%w pPR in DMSO or DCM/DMSO (60/40)
V$_{needle}$ ~ 25KV
V$_{collector}$ ~ -15 KV
pPR at the surface of the fibres
PCL (core)

Figure 4.4. Schematic representation of the coaxial electrospinning set-up and a detail of the so-produced electrospun fibres

1.2.1. Elaboration and characterization of core/shell fibres

In the following work, the core:shell fibres will be described by their respective core:shell weight ratio.

The electrospinning experiments demonstrated to be sensitive to the relative humidity (RH). Using star-pPR and copo-pPR as shell solutions, experiments were carried out under different RH from 15 to 45%. With increasing RH values, macroscopic spots could be observed onto the membranes. As described in the following figure 4.5., the variations of the macroscopic structures were obvious with small changes in RH values.

This can be understood as the RH value has an influence on the evaporation of solvents. Also, with increasing RH values, there is an increase in the number of water molecules. The ions present in water will thus modify the electrical field by changing the charge density.

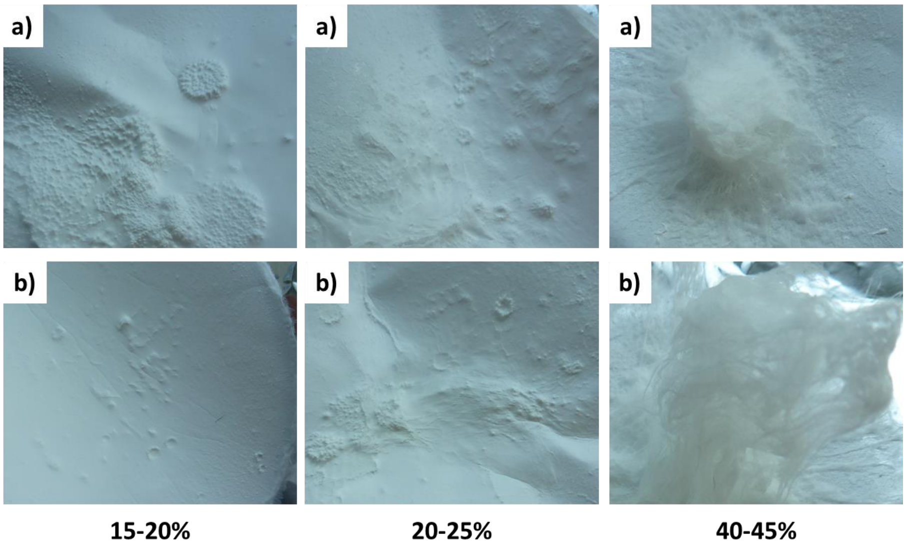

Figure 4.5. Influence of the relative humidity on the a) 10:1 core:shell PCL:star-pPR and the b) 10:1 PCL:copo-pPR

For all the electrospinning experiments, the relative humidity was then kept below 25 ± 5% RH and the temperature was around 27 ± 7°C.

First, the various pPR based fibrous membranes will be briefly described (e.g. morphology, fibre diameters…). A general comparison between the mats will then be made and general conclusions regarding their morphology will be established.

Electrospinning of the linear pPR shell solution

The lin-pPR solutions obtained after 24 hours of stirring were opalescent for concentrations higher than 5 wt%. After some time in the syringe, all the shell solutions, including the 5wt% lin-pPR solution, became turbid. These shell solutions were then not stable over long periods of time confirming the results obtained by SANS and already detailed in chapter 2.

The core:shell fibres were obtained by applying high voltages at the needle and the collector (25 kV and -10 kV respectively). The collected mats presented two populations of fibre with diameters ϕ_S and ϕ_L. The various thick and thin fibres were randomly distributed on the membranes. It was noticed that with increasing shell concentration, the number of thick fibres and fibre fusion increased (figure 4.6).

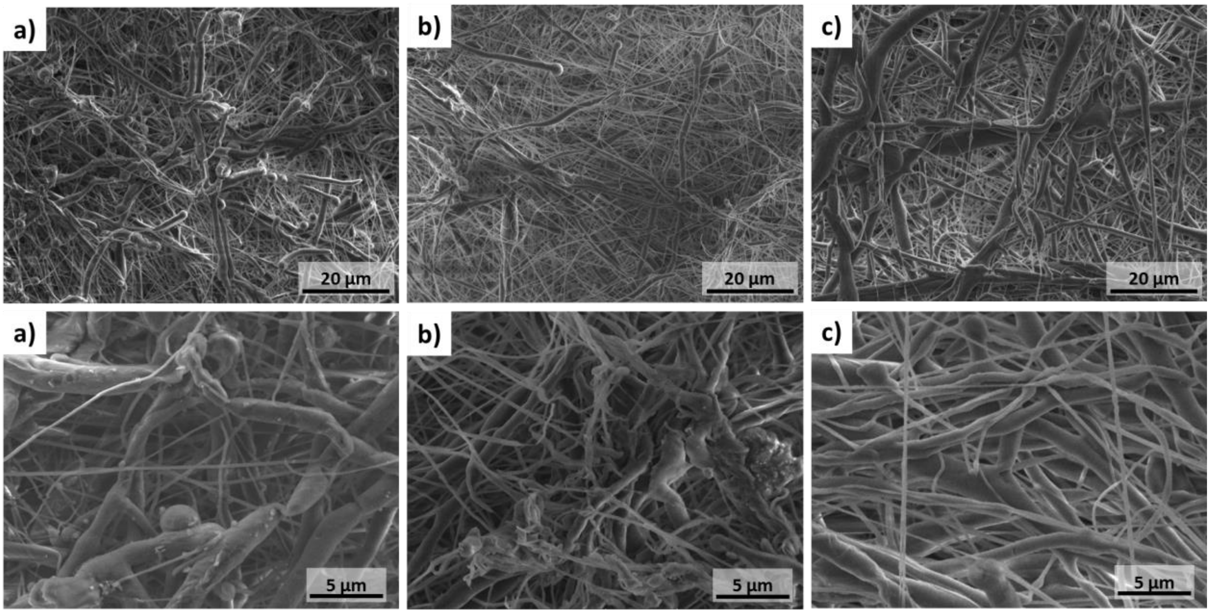

Figure 4.6. SEM images at 3000 x and 10k x magnifications of a) 10:1 PCL:lin-pPR, b) 10:2 PCL:lin-pPR and c) 10:3 PCL:lin-pPR

The following table details the diameters measured for the PCL:lin-pPR fibrous mats. When comparing the diameters obtained for each core:shell formulation, it can be seen that with increasing shell concentration, the collected fibres presented bigger diameters.

	10:1 PCL:lin-pPR	**10:2 PCL:lin-pPR**	**10:3 PCL:lin-pPR**
ϕ_S (nm)	260 ± 40	350 ± 115	426 ± 167
ϕ_L (nm)	1330 ± 480	1460 ± 380	1820 ± 610

Table 4. 1. Fibre average diameters of the core:shell PCL:lin-pPR membranes

Elaboration of core:shell fibres with copo-pPRs

Two different solutions were prepared incorporating respectively 5 wt% and 15 wt% of copo-pPR. The solid was solubilized in a mixture of DCM/DMSO (60/40 wt/wt%).

The applied voltages required to obtain a regular mat were in the same range as the previous experiments. 25 kV were applied at the needle tip and -10 kV were applied for both shell solutions.

As described in the following figure 4.7. and table 4.2., dry fibres with two diameter populations (with diameters ϕ_S and ϕ_L) were obtained for the 10:1 PCL:copo-pPR mats. This membrane was more homogenous and regular than the membranes obtained with lin-pPRs. For the 10:3 PCL:copo-pPR core: shell fibres, only thick fibres with beads were obtained. The difference in morphology can be explained as the 10:3 PCL:copo-pPR fibres were elaborated using a copo-pPR solution with aggregates that could not be dissolved.

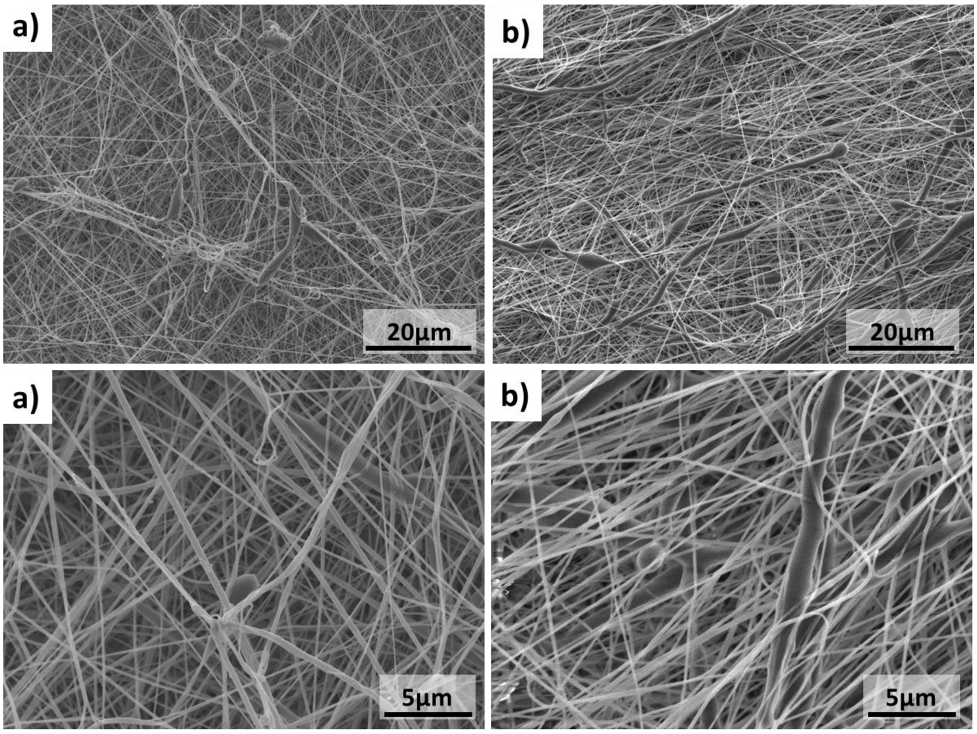

Figure 4.7. SEM images at 3000x and 10kx magnifications of a) 10:1 PCL:copo-pPR and b) 10:3 PCL:copo-pPR

	10:1 PCL:copo-pPR	**10:3 PCL:copo-pPR**
ϕ_S (nm)	270 ± 115	275 ± 80
ϕ_L (nm)	-	1400 ± 380

Table 4.2. Fibre average diameters of the core:shell PCL:copo-pPR membranes

Elaboration of core:shell fibres using star-pPR

The star-pPR solutions were prepared incorporating different concentrations ranging from 5 to 15 wt% of the synthesized star-pPR. As demonstrated in the chapter related to the synthesis of these pPRs (chapter 2), SANS experiments proved that the star-pPRs were stable over several hours for temperatures up to 35°C. As for the previous pPR based solutions, the homogenously stirred star-pPR solutions were electrospun with a PCL core solution. When increasing the star-pPR shell concentrations, the voltages applied at the collector had to be increased to obtain a stable jet and elaborate homogenous electrospun fibres. The voltage applied at the nozzle was kept constant at 25 kV and the voltage applied at the collector varied between -5 and -15 kV.

Similarly to the PCL:lin-pPR fibres, the fibres presented two populations with diameters ϕ_S and ϕ_L. The thin fibres were mainly randomly distributed onto the mat whereas the thick fibres formed bundles. The stacking of these aggregated thick fibres may be due to heterogeneous electrostatic effects occurring at the vicinity of the collector.[114]

When increasing the shell concentration, the average diameter of the thin fibres as well as the number of thick fibres (figure 4.8 and table 4.3) increased due to the formation of aggregates within the shell solution. The resulting solutions were also less stable over the processing time.

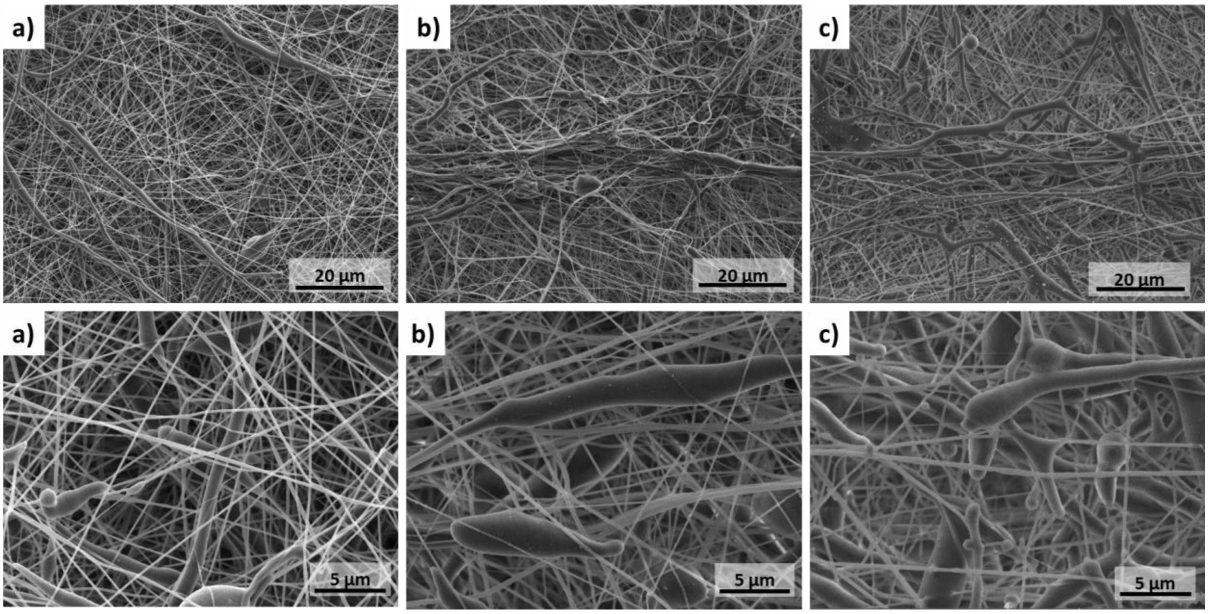

Figure 4.8. SEM images at 3000x and 10kx magnifications of a) 10:1 PCL:star-pPR, b) 10:2 PCL:star-pPR and c) 10:3 PCL:star-pPR

	10:1 PCL:star-pPR	**10:2 PCL:star-pPR**	**10:3 PCL:star-pPR**
ϕ_S (nm)	160 ± 50	220 ± 60	760 ± 260
ϕ_L (nm)	900 ± 130	1070 ± 550	2900 ± 660

Table 4.3. Fibre average diameters of the core:shell PCL:star-pPR membranes

Elaboration of core:shell fibres with mik-pPR

The mik-pPR solutions were prepared in DMSO and mik-pPR concentrations of 5 wt% and 15 wt% were used to prepare 10:1 and 10:3 PCL:mik-pPR fibres. These shell solutions were electrospun with a PCL core solution in DCM/DMF.

The following table 4.4. and figure 4.9. summarize the different morphologies and diameters obtained for the electrospun core:shell fibrous membranes. These fibrous membranes presented two diameter populations. The 10:1 PCL:mik-pPR mat was homogenous and dry. In addition to the increase in the ϕ_S and ϕ_L diameters, more defects were also encountered onto the 10:3 PCL:mik-pPR membrane. A high number of thick fibres were observed for the

10:3 PCL:mik-pPR mat probably because of the low solubility of mik-pPRs in DMSO at a high concentration.

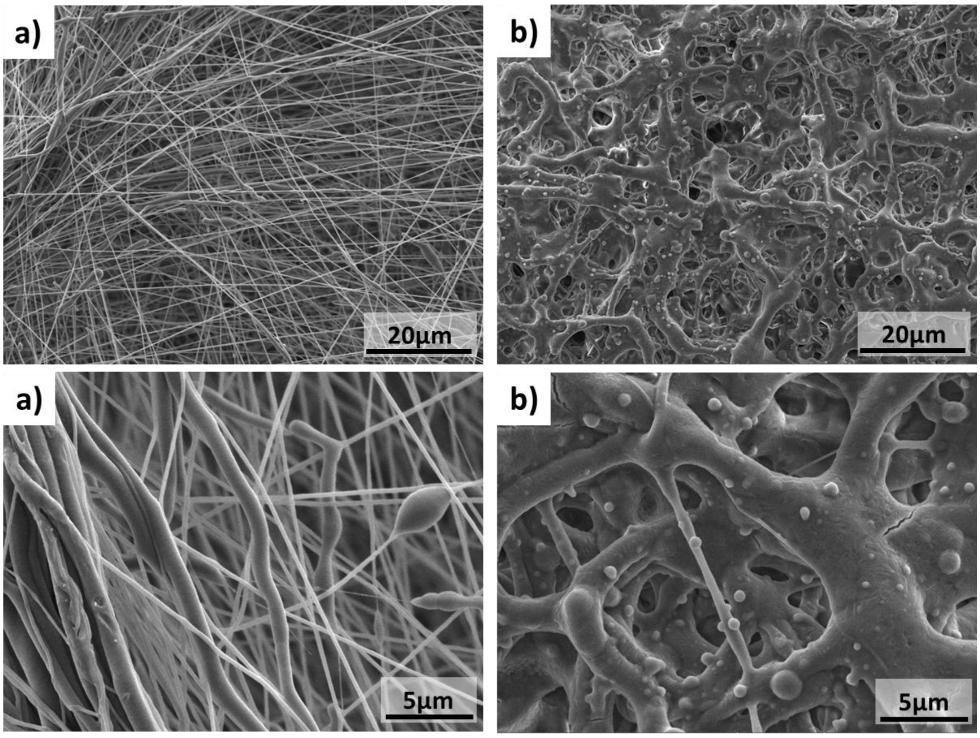

Figure 4.9. SEM images at 3000 and 10k magnifications of a) 10:1 PCL:mik-pPR and b) 10:3 PCL:mik-pPR

	10:1 PCL:mik-pPR	**10:3 PCL:mik-pPR**
ϕ_S (nm)	260 ± 50	550 ± 200
ϕ_L (nm)	980 ± 310	2250 ± 630

Table 4.4. Fibre average diameters of the core:shell PCL:mik-pPR membranes

1.2.2. General comparison between all the electrospun PCL:pPR core:shell fibres

We have thus demonstrated that for each type of PCL:pPR core:shell electrospinning experiments, fibres could be obtained. The most regular fibres were obtained for the 10:1 PCL:pPR based fibres. For the least concentrated shell solutions, the mixtures were stable over long periods of time. All the different fibrous membranes presented two populations with diameters ϕ_S and ϕ_L. When increasing the shell solution concentration, the solutions obtained after 24 hours of stirring were opalescent and many aggregates could be seen in the solution. The presence of aggregates led to the elaboration of fibres presenting many beads. Thicker fibres were also elaborated by electrospinning with these shell solutions.

The morphology and fibrous structure obtained for the 10:1 PCL:star-pPR and the 10:1 PCL:mik-pPR based fibres were homogenous and only few defects could be detected on the fibrous membranes. The fibres, obtained for the 10:1 PCL:copo-pPR core:shell conditions, were homogenous and no fusion or thick fibres were observed. The decrease in the DMSO concentration may have improved the evaporation of the solvents and thus the collection of dry and regular fibres. However, the fibres obtained using a PCL core solution and the lin-pPR shell solutions displayed many defects, especially beads and thick fibres. The high instability of the lin-pPRs, induced by the low complexation rate of CDs along the PCL when solubilized, may explain the fabrication of fibres with many defects.
Regarding the morphologies obtained for each pPR based fibres, the core:shell fibres, PCL:star-pPR, PCL:mik-pPR and PCL:copo-pPR, displayed the best fibrous structures.

Prior to any functionalization, the core:shell fibres had to be characterized and the presence of CDs bearing hydroxyl groups had to be confirmed.

1.3.Characterization of the electrospun membranes

1.3.1. XRD analysis

The core:shell electrospun membranes were characterized by XRD to see if pPRs could be detected within the fibres. The signature that was analysed for the synthesized pPRs is very characteristic of the threading of CDs along polymeric chains. In the XRD spectra obtained for the various pPRs, a predominant peak came out at $2\theta = 20°$ and $2\theta = 17°$ for the α-CD and β-CD based pPRs respectively. So, the presence of the same peaks in the electrospun membranes XRD spectrogram would prove the stability of the supramolecular structure during the processing.

The 10:1 core:shell PCL:pPR fibres were thus analysed by XRD. However, no pPR characteristic peak could be seen (see figure 4.10). Small irregularities in the baseline could be seen close to 2θ = 20° or 2θ = 17°.

A second set of analysis was then performed on the 10:3 core:shell PCL:lin-pPR, PCL:copo-pPR, PCL:star-pPR and PCL:mik-pPR membranes (figure 4.11). For the core:shell membranes based on star-pPRs and mik-pPRs, a peak could be seen at 2θ = 20°. The height of the peak corresponding to crystalline rotaxane portions was less than three times smaller than the PCL crystalline peak. This is due to the presence of a crystalline PCL peak in addition to the peak of the CD channel-like rotaxane portion. Nevertheless, the presence of star-pPR and mik-pPR was confirmed within the fibrous membranes. For the copo-pPR and lin-pPR based fibres, no peak was displayed on the analysed spectrograms. No conclusion could be drawn for PCL:copo-pPR fibres. In contrast, and as demonstrated by SANS experiments, lin-pPRs lose their supramolecular structure once solubilized in DMSO. Hence, during the electrospinning processing, lin-pPRs were not processed but a mixture of linear PCL and free CDs. No pPR structure was thus found within the fibres.

Therefore, it was hypothesized that for the 10:1 PCL:star-pPR and 10:1 PCL:mik-pPR, the pPRs were also preserved. However, the concentration of pPR was too low to be analysed. No conclusion could be made for 10:1 PCL:copo-pPR fibres. On the other hand, no pPRs were present in the 10:1 PCL:lin-pPR.

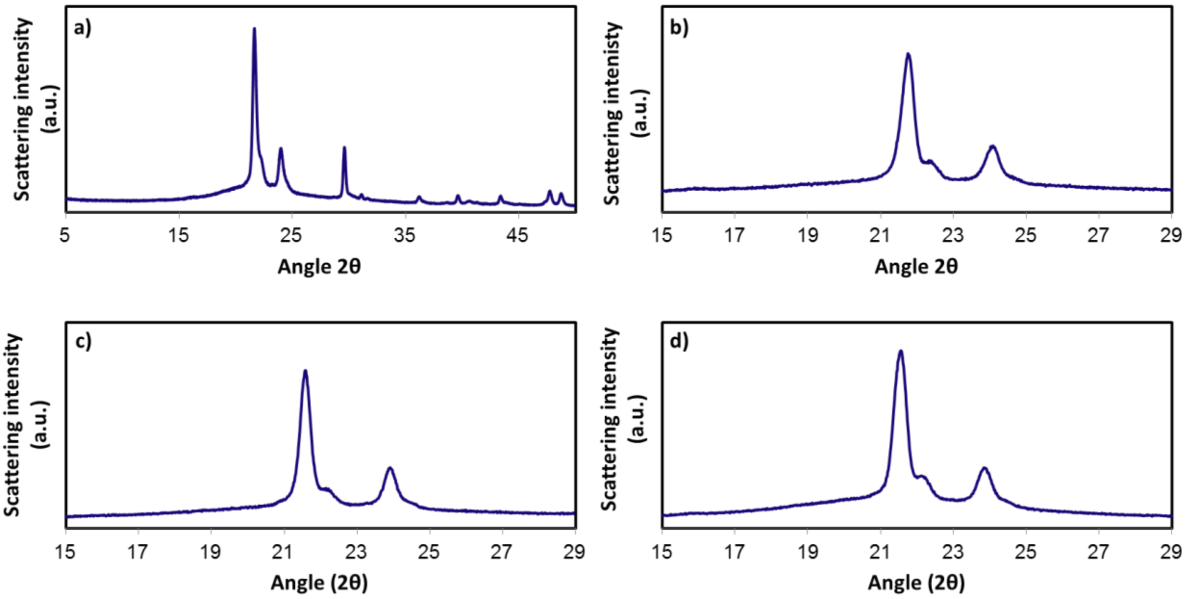

Figure 4.10. XRD spectrograms obtained in the case of the a) 10:1 PCL:lin-pPR, b) 10:1 PCL:star-pPR, c) 10:1 PCL:copo-pPR and d) 10:1 PCL:mik-pPR core:shell electrospun membranes

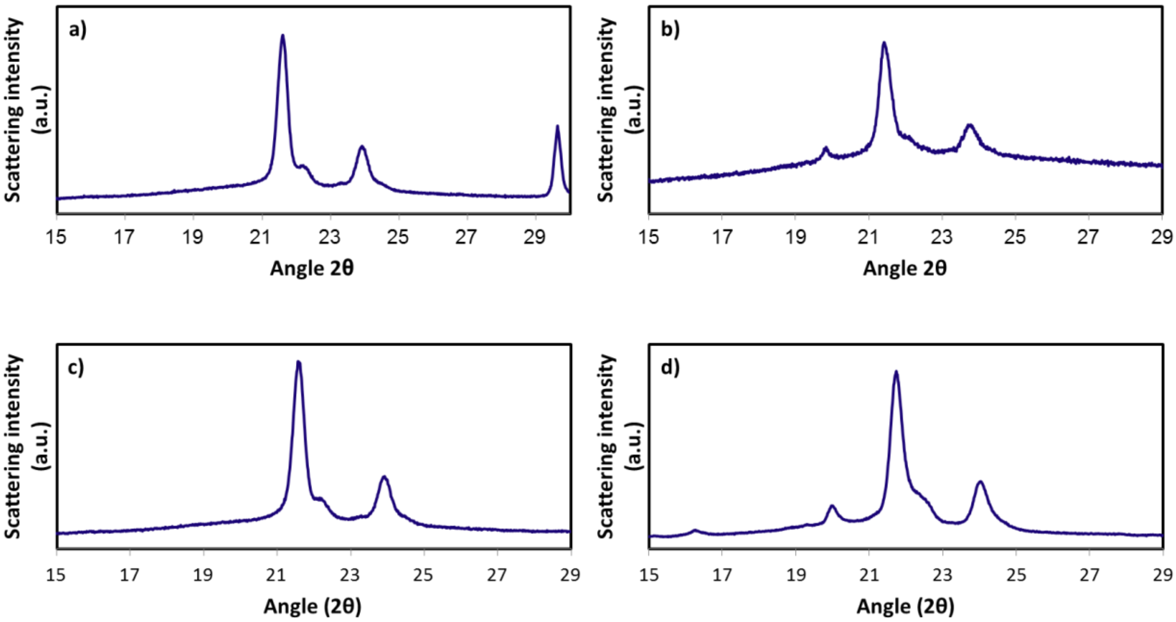

Figure 4.11. XRD spectrograms obtained in the case of the a) 10:3 PCL:lin-pPR, b) 10:3 PCL:star-pPR, c) 10:3 PCL:copo-pPR and d) 10:3 PCL:mik-pPR core:shell electrospun membranes

1.3.2. Water contact angle measurements

To determine if the addition of pPRs modified the wettability of the fibre surface, a drop of water was put on the surface of pure PCL and the various 10:1 PCL:pPR based fibres. Its contact angle was then measured (see figure 4.12).

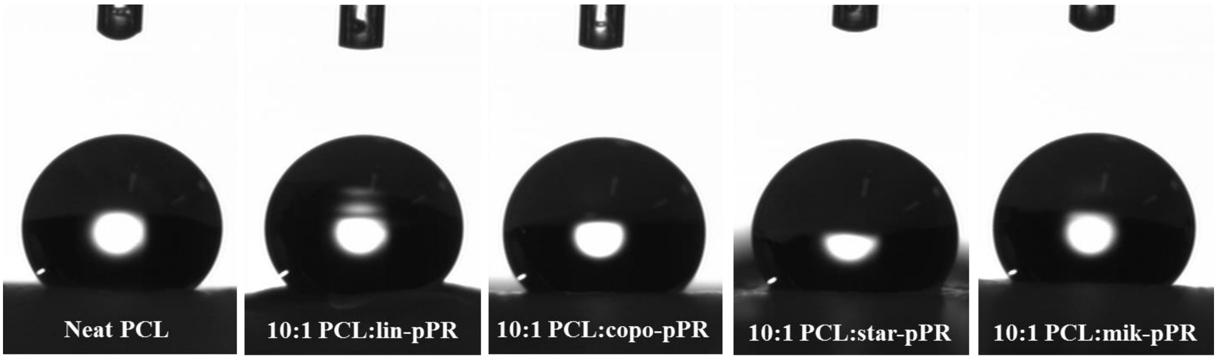

Figure 4.12. Contact angle images of the water drop onto each type of electrospun membrane

The following table 4.5. gathers all the contact angle values and surface energy interactions between the drop and the non-woven mats. As can be seen, all the PCL and pPR based membranes are highly hydrophobic.

A slight decrease in the contact angle could be observed between pure PCL and the pPR based fibres. However, this change was not significant enough to suggest that the pPR based fibres were more hydrophilic than the neat PCL fibres. No change in surface wettability was thus noted for the 10:1 PCL:pPR based fibres.

	Core:shell ratio	**Angle**	**Wettability**
neat PCL	**-**	128.74 ± 2.25	S<0, partial
PCL:lin-pPR	**10:1**	120.2 ± 2.86	S<0, partial
PCL:copo-pPR	**10:1**	121.84 ± 3.38	S<0, partial
PCL:star-pPR	**10:1**	120.06 ± 2.32	S<0, partial
PCL:mik-pPR	**10:1**	111.73 ± 4.5	S<0, partial

Table 4. 5. Recapitulative chart of the contact angle values of the different membranes

1.3.3. *Mechanical properties of the core:shell membranes*

To evaluate the mechanical properties of the electrospun membranes, a special set of electrospinning experiments was carried out to obtain stripes of the aligned fibres. Despite the collection of fibres on a rotative drum (see conditions in chapter 5 section 4.2.2), the obtained fibres were not highly aligned on the mat.

For each type of membrane, an average of ten workable tensile measurements was used to obtain good average values on the different PCL and pPR based mats. For each membrane and for appropriate comparison reasons, the values determined during the tests were adjusted in agreement with the samples respective densities.

When comparing the tensile tests results measured for one type of formulation, large differences between the Young modulus, the stress at break and the strain at break could be detected. The standard deviation values were thus important. To improve the reproducibility of the electrospinning experiments, many parameters will need to be modified to better control the morphology of the membranes.

As demonstrated in previous literature[165], fibres based on pPR or CD blended with a polymer were more rigid than the neat polymer fibres. Hence, our pPR based membranes were expected to present higher rigidity. As seen in the following table (table 4.6), the Young's moduli displayed by our pPR based electrospun membranes were higher than the one exhibited by neat PCL.

When comparing the various pPR based membranes with each other, interesting results could be noted. In the following table (table 4.6), it can be seen that 10:1 PCL:mik-pPR and 10:1 PCL:copo-pPR core:shell mats exhibited similar behaviour as neat PCL fibres. Indeed, both the elongation and stress at break values were found to be in the same range as for PCL. The values were lower than for the neat polyester but these results were very promising. On the other hand, 10:1 PCL:star-pPR and 10:1 PCL:lin-pPR fibres were highly rigid and their elongation and stress at break values were poor compared with PCL.

The differences between these pPRs could be explained as mik-pPR and copo-pPR present unthreaded portions of polymer that will thus improve the elasticity of the pPR based fibres. On the other hand, for PCL:star-pPR fibres, α-CDs were threaded along the four branches of PCL. The mat mechanical properties will thus be mainly induced by the pPRs. Therefore, the membrane was more rigid and the elongation at break was poor. In the case of the 10:1 PCL:lin-pPR membranes, the high number of defects on the core:shell membranes could explain the elongation and stress at break values.

	Core:shell ratio	**E/ρ_{app} (Pa / (g.cm^{-3}))**	**σ_r/ρ_{app} (Pa / (g.cm^{-3}))**	**ε_r (%)**
Neat PCL	**-**	$8.80.10^{7} \pm 5.02.10^{7}$	$1.45.10^{7} \pm 0.34.10^{7}$	44 ± 12
PCL:lin-pPR	**10:1**	$1.12.10^{8} \pm 5.13.10^{7}$	$5.68.10^{6} \pm 8.80.10^{5}$	8 ± 4
PCL:copo-pPR	**10:1**	$9.62.10^{7} \pm 9.27.10^{6}$	$1.90.10^{7} \pm 2.19.10^{6}$	48 ± 5
PCL:star-pPR	**10:1**	$3.39.10^{8} \pm 2.96.10^{8}$	$4{,}95.10^{6} \pm 0{,}98.10^{6}$	10 ± 9
PCL:mik-pPR	**10:1**	$6.43.10^{7} \pm 1.10.10^{7}$	$1.10.10^{7} \pm 0{,}06.10^{7}$	46 ± 5

Table 4. 6. Mechanical properties obtained for the different electrospun membranes by tensile test measurements at a constant speed

The pPR based core:shell fibres exhibited good mechanical properties although they were more rigid than pure PCL fibres. For the 10:1 PCL:copo-pPR and 10:1 PCL:mik-pPR based membranes, the fact that CDs were only partially threaded along the polyester led to the preservation of the neat PCL stress and elongation at break values. In the case of the star-pPR based fibres, the high complexation rate induced the increase in rigidity as well as the reduction of the stress and elongation at break values.

Chemical functionalization of the fibre surface

The various PCL:pPR based core:shell fibres were successfully produced and characterized. The XRD, water contact angle and mechanical tensile tests suggested that pPRs were present within the fibres. To see if the reactive hydroxyl functions were accessible at the shell of the fibres, the functionalization reaction of the fibres was attempted.

2.1. Grafting of fluorescein isothiocyanate

As proof of concept, fluorescein isothiocyanate (FITC) (figure 4.13) was used as a fluorescent reagent and directly grafted onto the hydroxyl groups of the fibres. FITC is a common organic fluorescent compound presenting a highly reactive isothiocyanate function able to react with the hydroxyl functions of the pPRs. After the modification reaction, it was compulsory that the FITC grafting was successful while preserving the fibrous structure of the mats. Indeed, two of main advantages to use electrospun materials are the high porosity of the non-woven as well as their ability to mimic the structure of living tissues. It is thus essential to keep the elementary structure of the fibre mat intact.

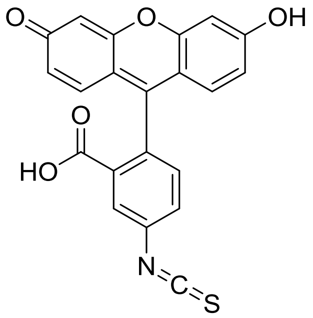

Figure 4.13. Chemical structure of fluorescein isothiocyanate

For all the grafting reactions, the reaction mixtures were kept in the dark to preserve the fluorescent properties of FITC. The electrospun membranes were let to react in a 10^{-6} mol.L^{-1} FITC organic solution. A 50/50 wt/wt mixture of acetonitrile and distilled water (CH_3CN/H_2O) was used as solvent mixture for the reaction and the solubilisation of FITC.[149]
Several preliminary attempts were made for which the time of the reaction was varied to successfully graft FITC without the degradation of the electrospun fibres. At least four hours were necessary to ensure the grafting of FITC. Under these conditions, the fibrous structure

and porosity were almost preserved. However, after 24 hours, the membranes were altered and some polymeric patches appeared on the surface of the sample.

Anhydrous copper(II) sulfate ($CuSO_4$) was used as a catalyst to see its influence on the grafting reaction kinetics. However, even without the use of any catalyst, the hydroxyl groups present on the CDs external cavities reacted rapidly with the isothiocyanate function of the FITC. It was then decided that no catalyst would be used for these reaction. The choice to work without catalyst also aimed to limit the use of metal based agents and thus avoid any later toxicity issues related to the use of coupling agents or catalysts.

The neat PCL, PCL/star-pPR blend and the various core:shell fibres, 10:1 to 10:3 of PCL:star-pPR, the 10:1 PCL:lin-pPR, 10:1 PCL:copo-pPR and 10:1 PCL:mik-pPR membranes were let to react with the fluorescent agent. After the modification reaction, the fibrous mats were heavily rinsed with a 50/50 CH_3CN/H_2O mixture until no fluorescein was recovered in the rinsing supernatant. The membranes were then let to dry and kept in the dark until further characterization.

All the reacted non-woven membranes were first observed by SEM. The following figure (figure 4.14.) shows the structure of the electrospun membranes after the grafting reaction. The neat PCL membrane, the PCL/star-pPR blend membrane and the 10:1 PCL:lin-pPR core:shell membrane were degraded by the reaction conditions as polymeric patches appeared on the surface of the mats (figure 4.14 a-c). Additionally, only few well-defined fibres could be seen on the mat. On the other hand, the 10:1 core:shell PCL:copo-pPR, 10:1 PCL:star-pPR and 10:1 PCL:mik-pPR membranes were also degraded by the solvent treatment but to a lesser extent than neat PCL (figure 4.14 d-f). The fibrous organization of the mats was still preserved. The solvent treatment seemed to have induced the agglomeration of the fibres and thus decreased the porosity between the fibres. Nonetheless these observations suggested that pPRs act as a protective shield against solvents. The fibres are thus more resistant toward the attack of organic solvent treatments.

The PCL:star-pPR core:shell fibres proved to be the most resistant fibres after modification reaction. Their structure was highly preserved and no polymeric patches were observed.

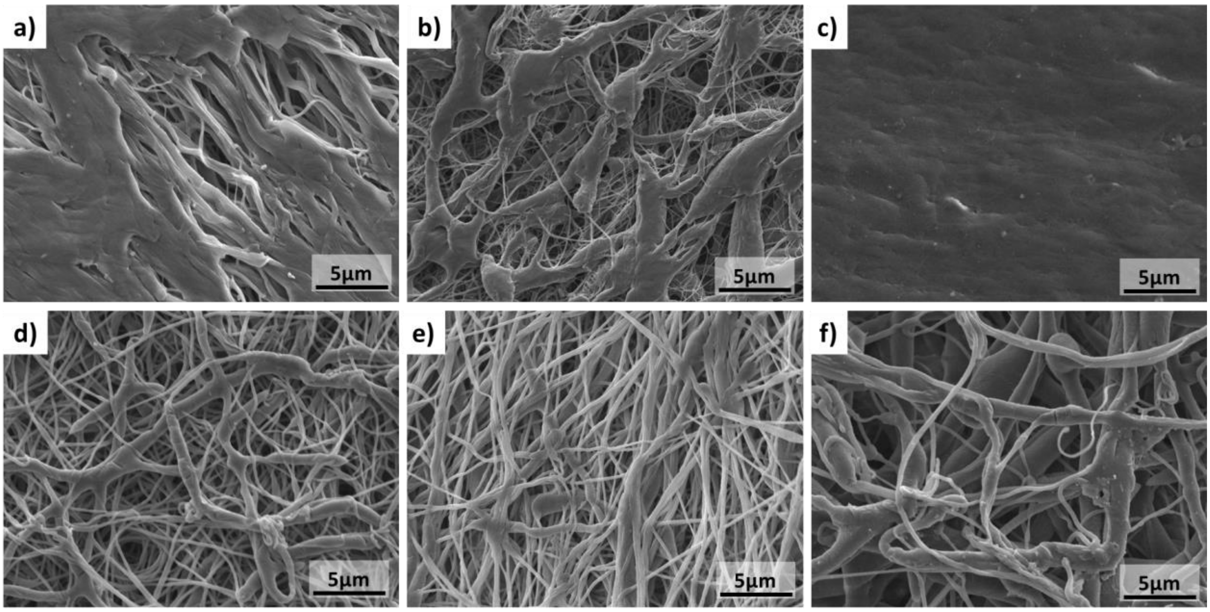

Figure 4.14. SEM images of the fibrous structures obtained after the grafting of FITC on a) neat PCL membrane, b) blend fibres, c) the 10:1 PCL:lin-pPR core:shell membrane, d) the 10:1 PCL:copo-pPR membrane, d) the 10:1 PCL:star-pPR membrane and the f) 10:1 PCL:mik-pPR membrane

Fluorescent confocal microscopy analysis was then performed on each membrane to see if the core: shell membranes display any fluorescent properties. This would thus prove the success of the FITC grafting reaction and the availability of the hydroxyl groups on the CDs. The PCL membrane did not display any fluorescent properties. Hence, no grafting reaction was possible onto a neat PCL backbone.

In the case of the fibres obtained by blending PCL and star-pPR prior to the electrospinning experiment, no fluorescence could be seen either. By blending both supramolecules prior to the electrospinning processing, only few CDs could be at the fibre surface and thus not many reactive points were accessible for the reaction with FITC. A similar observation was done for the 10:1 PCL:lin-pPR based fibres. The absence of fluorescence for lin-pPR based membranes could be explained by the CD dethreading in DMSO during electrospinning leading to the CD leaching during the FITC grafting.

However, the 10:1 PCL:copo-pPR, 10:1 PCL:star-pPR and 10:1 PCL:mik-pPR exhibited good fluorescent properties as demonstrated in figure 4.15. It can also be noted, that the fluorescence is observed on the fibres confirming the grafting onto the hydroxyl functions. No FITC seemed to be trapped within the fibre pores.

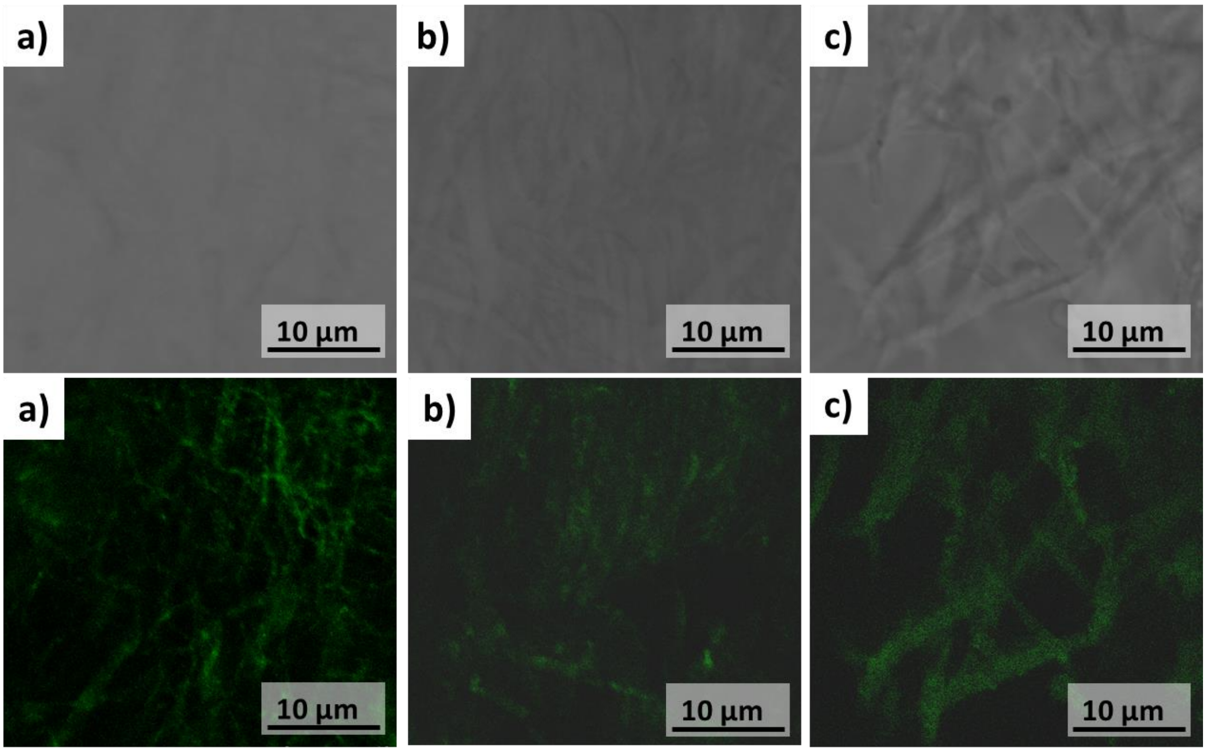

Figure 4.15.White image (top) and the corresponding fluorescent image (bottom) of the FITC functionalized fibres a) 10:1 PCL:copo-pPR, b) 10:1 PCL:star-pPR and c) 10:1 PCL:mik-pPR (analyses performed on a Leica confocal fluorescent microspcope)

For the various 10:1, 10:2 and 10:3 core:shell PCL:star-pPR ratios (figure 4.16), although no fluorescence measurements were done, it could be seen that the fluorescent signal got stronger with increasing shell concentration. The good reactivity of the CD hydroxyl groups and the good reactivity of the FITC isothiocyanate function were so confirmed.

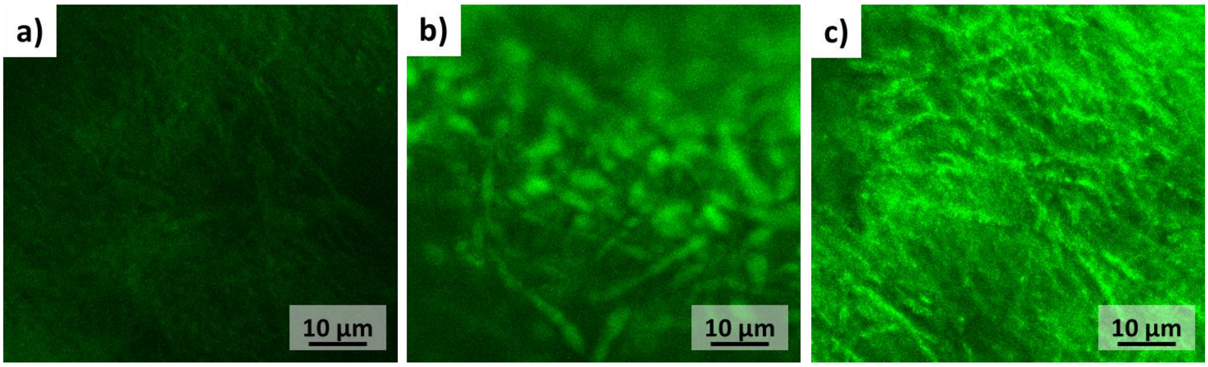

Figure 4.16. Fluorescent microscope image obtained on the fluorescent a) 10:1 PCL:star-pPR, b) 10:2 PCL:star-pPR and 10:3 PCL:star-pPR (analyses performed on a Zeiss fluorescent microscope)

Hence, FITC was successfully grafted onto pPR based fibres. The reaction conditions were optimized so that the fibrous structure of the membranes was preserved during the grafting reaction. However, the neat PCL, the PCL/pPR blend and 10:1 PCL:lin-pPR membranes were altered and polymeric patches were observed after the reaction with FITC. The confocal fluorescent microscopy analysis further demonstrated that no FITC was grafted onto the surface of these two different types of fibres.

For the 10:1 PCL:copo-pPR and 10:1 PCL:mik-pPR core:shell membranes, the fluorescent properties of each membrane were good despite the agglomeration of some fibres due to the solvent treatment. On the other hand, the PCL:star-pPR based membranes displayed excellent resistivity toward the solvents and the various PCL:star-pPR mats exhibited increasing fluorescent properties with increasing shell concentration suggesting the rapid and good availability of the CDs onto the fibres surface.

Hence, the core:shell fibres, and especially the 10:1 PCL:star-pPR, seemed to be good candidates for the biofunctionalization of PCL and pPR based fibres. FITC grafting has thus proved the concept of this project leading the way for any further functionalization.

CONCLUSION

In this chapter, PCL and pPR based membranes were processed by electrospinning according to two different strategies.

In the first strategy, both the PCL matrix and the pPRs were mixed prior to the electrospinning processing. PCL and star-pPR were solubilized in a 50/25/25 wt/wt/wt mixture of DCM/DMF/DMSO. The obtained electrospun fibres were sensitive to the relative humidity. When reducing the relative humidity, fibres with some beads and fibre fusion were elaborated under the electrical field. However, the characterization step would not allow any conclusion regarding the presence of CD within the membrane.

To simplify the solvent system and to improve the structure of the electrospun fibres, a coaxial set-up was used and core:shell fibres were prepared incorporating PCL within the core solution and pPRs as the shell solution so that the reactive hydroxyl groups would be at the surface of the fibres. Each different pPR, namely lin-pPR, copo-pPR, star-pPR and mik-pPR, was solubilized and electrospun as a shell solution. Apart from the lin-pPR derived fibres, all electrospun mats displayed homogenous and regular fibrous structure with bimodal distribution of diameter. The 10:1 core:shell membranes presented the best morphologies and structures. Nevertheless, when increasing the shell solution concentration, the electrospun fibres showed an increase in defects and numerous beads appeared on the mat. The 10:1 core:shell fibres were thus further used for the functionalization reactions.

To determine if the supramolecular assembly of pPRs was still intact, XRD analyses were performed on the different membranes. For both 10:3 PCL:star-pPR and 10:3 PCL:mik-pPR based mats, a clear peak could be seen at $2\theta = 20°$ proving the presence of pPRs within the fibrous structure. In the case of the 10:3 PCL:copo-pPR, no peak could be distinguished so that no conclusion could be drawn. Lin-pPR based membranes did not exhibit any characteristic peak of pPR. This result is in agreement with SANS experiments which demonstrated that lin-pPR were not stable when solubilised in DMSO so that only free CDs remained in the core:shell fibres.

To further characterize the influence of the presence of pPRs within the fibrous membranes, mechanical tensile tests and water contact angle measurements were performed. The results obtained for the mechanical testing suggested that the pPR based fibres were more rigid than pure PCL. Moreover, apart from copo-pPR and mik-pPR that display unthreaded PCL parts to improve their compatibility with PCL, the other PCL:pPR based core:shell fibres presented low elongation at break values. The water contact angles measured for the pPR based fibres were lower as compared with neat PCL but no significant change in hydrophobicity could be determined.

As proof of concept, FITC was grafted onto the various electrospun membranes. Once the grafting reaction parameters were optimized, it was proven that pure PCL, the PCL/star-pPR blend and the 10:1 PCL:lin-pPR membranes did not support the solvent treatment and no FITC could be grafted onto these fibres. The PCL:copo-pPR, PCL:mik-pPR and PCL:star-pPR fibres were mainly preserved after the grafting treatment. Although the size of the pores was reduced after the reaction, the fibrous structure of the mats was maintained. The 10:1 PCL:star-pPR core:shell fibres especially displayed good stability in the solvent mixture. High fluorescent intensities were observed for PCL:copo-pPR, PCL:mik-pPR and PCL:star-pPR membranes. The FITC grafting was also proven to occur onto the fibre surface. Hydroxyl functions of the CDs on pPRs thus demonstrated to be accessible and reactive when electrospun at the shell of the fibres.

These first attempts to chemically bond fluorescent molecules onto electrospun PCL and pPR based fibres paved the way toward covalent bonding reactions with a wide range of biomolecules.

General conclusion and perspectives

CONCLUSION

In this PhD work, CDs were used for the functionalization of electrospun fibrous materials. The membranes were developed for two different biomedical applications: wound dressings and tissue engineering. The ability of cyclodextrins to form host-guest complexes with various antibiotics and polymers was exploited in this project and led to the preparation of bioactive materials.

Elaboration of bioactive wound dressing materials

Wound dressing materials based on polyelectrolyte complexes (PECs) of chitosan (CHI) and carboxymethyl cellulose (CMC) were elaborated by electrospinning. The two polysaccharides were used for their good biocompatible and biodegradable properties. In addition, CMC was incorporated for its good mechanical properties whereas CHI was added as a natural antibiotic agent.

To obtain homogenous and regular fibrous mats of fibres, two different strategies were developed to obtain coaxial CMC:CHI core:shell fibres as well as blended CMC/CHI fibres. For each experiment, fibres were processed with different COO^-/NH_3^+ charge ratios. The structure of the blend fibres was more homogenous and fewer defects such as beads and fibre fusion were noted onto the membranes. However, in this case the stoichiometric charge ratio could not be electrospun as a PEC gel was formed within minutes after the two polyelectrolytes mixing. The stability of the two PEC based fibres in water was different. The core:shell fibres were dissolved due to the low electrostatic interactions inside the coaxial fibres whereas the fibrous structure of the blend membranes was maintained.

To improve the stability of the polysaccharide based fibres, the fibres were either chemically crosslinked with sodium periodate or physically crosslinked by a two-week stay in an environmental chamber.

Although chitosan is known for its antibacterial activity, methylene blue (MB) or methylene blue inclusion complexes (MB ICs) were separately incorporated in the CMC/CHI blend fibres to promote the antimicrobial activity of the fibrous mats.

The preliminary antibacterial evaluations demonstrated that no antimicrobial activity was exhibited for the various core:shell and blend CMC/CHI fibres. However, all the MB loaded membranes exhibited good bactericide properties for 48 hours. Although, no influence of the crosslinking method could be seen on the antimicrobial activity, a difference in antimicrobial property was noted between the MB loaded and IC loaded membranes. Indeed, the bactericide efficiency was higher for IC loaded non-wovens after 48 hours than for pure MB, with an identical bactericide activity as the one displayed at 24 hours. Hence, this type of membrane is highly promising as a polysaccharide based wound dressing material. The incorporation of cyclodextrin (CD) based inclusion complexes led to the extension of the antibacterial activity of the resulting material.

Elaboration of pseudo-polyrotaxane based nanofibrous materials for tissue engineering

The second aspect developed in this project was the elaboration of poly(ε-caprolactone) (PCL) based biofunctionalized fibres. PCL is an interesting biocompatible and biodegradable polyester with good mechanical properties that has been widely used for biomedical applications. However as PCL does not display any reactive functions along its chain, it is difficult to graft any biomolecule for tissue engineering applications. CDs were thus used as building blocks to form pseudo-polyrotaxanes (pPRs).
To obtain stable pPRs when solubilized in DMSO for the electrospinning processing, various PCL presenting different architectures were synthesized:

- Linear PCL
- Four-branched PCL (star-PCL)
- Asymmetrical four-branched PCL (asym-PCL)
- A block copolymer with a central poly(propylene glycol) (PPG) block (PCL-PPG-PCL)

To avoid any toxicity issues, the Ring Opening Polymerization (ROP) of ε-caprolactone was carried out using 1,5,7-Triazabicyclo[4.4.0]dec-5-ene (TBD) as non-metallic catalyst. The well-defined synthesized PCL were characterized and reacted with α-cyclodextrins (α-CD) for all of them except for the block copolymer which was complexed with β-cyclodextrin (β-CD). Four different pPRs were then obtained:

- A linear pPR (lin-pPR)
- A four-branched pPR (star-pPR)
- An miktoarm pPR (mik-pPR)
- A block pPR where the β-CDs were threaded along the central block (copo-pPR)

After the various thermal and crystalline characterizations, the formation of pPRs was successful for each PCL structure.

The stability of star-pPR and lin-pPR was studied by SANS experiments. For temperatures below 35°C, star-pPRs were very stable due to their organization in nanoplatelet clusters. In contrast, lin-pPRs that present only low CD coverage did lost their supramolecular architecture. It was hypothesized that mik-pPR and copo-pPR would present a similar behaviour as star-pPR.

Electrospinning experiments were then carried out. A first attempt aimed to process a blend of PCL and star-pPR. A mixture of 50/25/25 wt% DCM/DMF/DMSO was found to be the best solvent choice. However, only opalescent solutions were obtained showing that all species were not fully soluble. The electrospinning was sensitive to relative humidity (RH) and although the RH was kept to low values, fibrous membranes presenting many defects such as beads and fibre fusion were obtained. Even so, the presence of CDs within the fibrous mats could not be established. The subsequent attempt to functionalize the blend fibres led to the decrease of the porosity and the degradation of the fibrous structure. After FITC grafting attempt, no fluorescent properties could be observed on the resulting material suggesting that the concentration of reactive and accessible CDs was too low.

10:1 and 10:3 PCL:pPR core:shell fibres were elaborated by coaxial electrospinning. When using a PCL core solution, the resulting fibres were ensured to present suitable mechanical properties regarding potential biomedical applications while by using pPR solutions for the shell, the reactive CD hydroxyl groups were expected to be on the fibre surface in order to facilitate the post-functionalization.

For each type of pPR, fibrous membranes were obtained presenting a bimodal distribution of diameters. The thick fibres agglomerated and formed bundles probably due to heterogeneous electrostatic effects. XRD analysis confirmed the presence of pPR in the fibres for the 10:3 PCL:star-pPR and PCL:mik-pPR fibres. So, it was hypothesized that the 10:1 fibres also preserved the pPRs. However, no conclusion could be drawn for the PCL:copo-pPR.

Water contact angle measurements were also carried out on the 10:1 PCL:pPR core:shell fibres but no change in the hydrophobicity of the PCL based membranes was noted. Tensile tests demonstrated that PCL:pPR based fibres displayed enhanced rigidity in comparison with neat PCL membranes. 10:1 PCL:copo-pPR and 10:1 PCL:mik-pPR, demonstrated similar stress and elongation at break than neat PCL, problably due to a better compatibility of the pPRs with PCL due to nude PCL chain portions. On the other hand, the elongation and stress at break obtained for PCL:star-pPR and PCL:lin-pPR were poor.

As proof of concept, FITC was successfully grafted onto the surface of PCL:star-pPR, PCL:mik-pPR and PCL:copo-pPR. The structure of the fibres was mainly preserved and a slight decrease in the porosity could be detected. In contrast, PCL:lin-pPR did not exhibit any fluorescent properties. Indeed, according to SANS experiments, lin-pPRs lost their supramolecular assembly leading thus to the processing of free CDs. Those free CDs thus leached during the grafting reaction. Thus, for star-pPR, mik-pPR and copo-pPR based fibers, the rotaxane potions acted as shields toward the solvents.

The 10:1 core:shell PCL:star-pPR thus seemed to be the best candidates for the functionalization of PCL:pPR based fibres as they are very stable against solvent.

PERSPECTIVES

In this thesis we have demonstrated two possibilities to functionalize electrospun membranes for biomedical applications. The encapsulation of an active molecule as an inclusion complex with cyclodextrin and its incorporation inside the fibres allows a more or less rapid diffusion of the molecule in the environment whereas grafting the active molecule on pPRs at the surface of the fibres ensures a longer presence of the molecule in the electrospun membrane. It could thus be very interesting to combine the two strategies as a function of the targeted application.

As an example, our PCL:pPR based membranes are intended to be used as a coating of small medical implant parts (sleeves, nails...). In this case, the membranes should have bactericide properties in order to prevent infections. It is then important to have a material that will be effective at the early stages of treatment but also for a certain period of time. Moreover, bacteria display increasing resistance toward antibiotics and depending on their family, their killing mechanism is different. We will thus use the inclusion complexes of gentamicin that have been prepared. They will be included within the PCL:pPR core:shell fibres in order to provide the initial antibacterial activity. In parallel for long-term effects, vancomycin will be grafted onto the nanofibres surface via the pPRs.

Several types of active membranes will be prepared to modulate the release of the encapsulated antibiotics. A preliminary biological assessment of the fibrous membranes has to be performed to evaluate their bactericide effects. These tests will enable to develop the best type of composition for extended bacterial effects.

To achieve this objective, the grafting reaction of active molecules still has to be investigated.

Several experiments need to be carried out to develop and biofunctionalize the polyester and pPR based fibres. Different ways have been imagined and are already under study.

For the grafting of vancomycin onto the membrane, 1,1'-carbonyldiimidazole (CDI) will be used as a coupling agent between the COOH group of the vancomycin and the OH groups of the CDs.

For the grafting of bulkier bioactive molecules (e.g. proteins, polycarbohydrates), a spacer will be used to enhance the reactivity of the hydroxyl groups. *p*-phenylene diisothiocyanate that bears two isothiocyanate functions, will be used as reactive spacer as the isothiocyanate functions have already demonstrated good reactivity toward the hydroxyl functions of CDs (Chapter 4). Moreover, this spacer being rigid, it will not be able to bend and react at both ends with the CD OH groups. At the end of this first step, a reactive isothiocyanate will be available for the grafing of the biomolecule.

Finally, another biofunctionalization will be developed to graft a second type of spacer onto the PCL:pPR core:shell fibres. For this strategy, two different bicyclononyne (BCN) derivatives (figure 1) will be let to react with the cyclodextrin bearing hydroxyl groups.

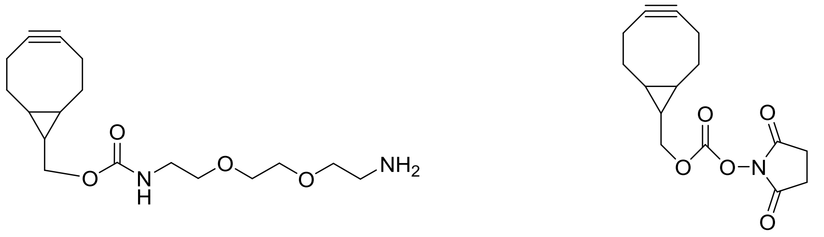

BCN amine

BCN succinimidyl ester

Figure 1. Chemical structure of the two bicyclononyne derivatives that will be used for copper-free click chemistry

The free alkyne functions will thus be further used for copper-free click chemistry and the grafting of bioactive molecules. A fluorescent dye has already been bought to optimize the chemical conditions for this two-step modification reaction before any biomolecules will be used.

Materials and Methods

1. Materials

α-cyclodextrin and β-cyclodextrin (α-CD and β-CD) were respectively obtained from Alfa Aesar and Sigma-Aldrich. Prior to any chemical reaction, these cyclic oligosaccharides were dried overnight under vacuum at 50°C.

To form the inclusion complexes between small molecules and β-CDs, methylene blue was purchased from Alfa Aesar. Vancomycin and gentamicin were purchased from Sigma-Aldrich and stored in a fridge until needed.

For the ring opening polymerizations of ε-caprolactone (ε-CL), ε-CL was dried over calcium hydride, distilled under reduced pressure and kept under an argon atmosphere over molecular sieves in a fridge. 1,5,7-triazabicyclo[4.4.0]dec-5-ene (TBD), ethylene glycol were obtained from Sigma-Aldrich. Poly(propylene glycol) (PPG) was purchased from Alfa Aesar. To remove any residual water in the commercially available PPG, an azeotrope was formed between the water contained in the PPG and distilled toluene. The azeotrope was removed by rotary evaporation. Pentaerythritol was supplied by Alfa Aesar, kept away from any moisture and light and used as received.

For the synthesis of asym-PCL, anhydride succinic, 4-(4,6-Dimethoxy-1,3,5-triazin-2-yl)-4-methylmorpholinium chloride (DMTMM), triethylamine (TEA) and 1-adamantamine were used without any preliminary purification and bought from Sigma-Aldrich.

Fluorescein isothiocyanate (FITC) obtained from Sigma-Aldrich were preserved from the light and used as such.

Two commercially available linear poly(ε-caprolactone) (PCL) with Mw ~80 000 g/mol (CAPA 6806) and Mn ~10 000 g/mol were supplied by Perstorp and Sigma-Aldrich and used as such for electrospinning experiments and the synthesis of lin-pPR respectively.

A commercially available poly(ethylene oxide) (PEO) (~2.10^6 g.mol^{-1}) was used as a polymer matrix for the electrospinning of polysaccharides and sodium periodate as a chemical crosslinker were purchased from Sigma-Aldrich and used as received. Carboxymethyl cellulose (~90 000 g.mol^{-1}) presenting a 70% backbone modification was purchased from

Sigma-Aldrich. Chitosan (Chitoclear 3566, ~200 000 $g.mol^{-1}$) with a degree of deacetylation of 96% was received from Primex and used as such.

In this work, distilled water, toluene, 1,4-dioxane, dichloromethane (CH_2Cl_2), acetone, dimethyl sulfoxide (DMSO) and acetonitrile (CH_3CN) were used for the various synthesis. Toluene (Sigma-Aldrich) was dried over sodium, distilled and directly used for the synthesis of the four-branched polyester. Acetone, N,N-dimethylformamide (DMF), dimethyl sulfoxide (DMSO) and dichloromethane (CH_2Cl_2) were all obtained from Sigma-Aldrich and, apart from acetone, they were all purified by distillation prior to use and kept in the dark under an argon atmosphere over molecular sieves. For the grafting of FITC onto the surface of the fibres, acetronitrile, commercially available from Riedel-de-Haën (Sigma-Aldrich), was used without further purification.

All the electrospinning solutions were prepared with water, formic acid (AF), dichloromethane (DCM), dimethyl sulfoxide (DMSO) and dimethylformamide (DMF) that were purchased from Sigma-Aldrich. All the organic solvents were distilled prior to the preparation of the electrospinning solutions.

For the ^1H and ^{13}C NMR analysis, deuterated DMSO (Euriso-Top) (DMSO-d_6), deuterated chloroform ($CDCl_3$), deuterium oxide (D_2O) or acetone (acetone-d_6) (Sigma-Aldrich) were used to solubilize the inclusion complexes, polymers or pseudopolyrotaxanes.

2. Measurements

2.1.NMR

^{1}H NMR and ^{13}C NMR spectroscopy was performed using a Brucker Advance 300 MHz and 400MHz Avance III HD spectrometer. Chemical shifts were referenced to the solvent values, δ = 2.50 ppm in the case of DMSO-d_6 and δ = 7.26 ppm for $CDCl_3$. All solutions were prepared several hours prior to the NMR analysis.

For the pseudopolyrotaxanes, after the synthesis purifications with water to remove free cyclodextrins and acetone to remove unthreaded PCL, all powders were solubilized at 323K in DMSO-d_6 for at least several hours to ensure the pPR decomplexation so that all molecules (i.e. CD and PCL) were isolated in the mixture. The NMR analyses were performed at 296K directly when the solutions were taken away from the heat. A second set of conditions was performed at 80°C to ensure the solubility of all the components during the characterization. As similar results were obtained at 25°C and 80°C, standard NMR analysis conditions at 25°C were kept.

2.2.SEC

Size exclusion chromatography (SEC) measurements were performed in chloroform (HPLC grade) in a Shimadzu liquid chromatograph equipped with a LC-10AD isocratic pump, a DGU-14A degasser, a SIL-10AD automated injector, a CTO-10A thermostated oven with a 5 PLGel Guard column, two PL-gel 5 MIXED-C and a 5 100 Å 300 mm-columns, and three online detectors : Shimadzu RID-10A refractive index detector, Wyatt Technologies MiniDAWN 3-angle-light scattering detector and Shimadzu SPD-M10A diode array (UV) detector.

Samples were dissolved in chloroform (at a concentration 4 mg/mL) and filtered through a 0.2 µ PTFE membrane. For all analyses the injection volume was 100 µL, the flow rate was 0.8 mL/min and the oven temperature was set at 25°C. Molecular weights and polydispersity indexes were calculated from a calibration with polystyrene standard in UV or RI detection.

2.3.FITR spectroscopy

The infrared spectra were obtained by using a Fourrier transform infrared spectrometer (FTIR) (Thermo Nicolet 380 FT-IR). The scans (64 scans) were recorded between 4000 and 400 cm^{-1} at a resolution of 4 cm^{-1}.

2.4.TGA

Thermogravimetric analyses (TGA) were performed on a TA Instrument Q5000 thermal analysis apparatus. All samples were heated under air up to 650°C at a constant rate of 10°C/min.

2.5.DSC

Differential Scanning Calorimetry (DSC) thermograms were obtained using TA Instrument Q200 apparatus. Temperatures were varied from -70°C up to 250°C at a heating rate of 10°C/min. Several Heat/cool/heat cycles were performed on the same samples. The reported melting point temperatures (T_m) were all assessed from the second heating cycle thermogram.

2.6.XRD

Crystalline organization of solids and membranes was determined by X-Ray diffraction (XRD) measurements using a Brucker D8 Advance diffractometer at a scanning rate of 1.6°/min. The detector used for the analyses was a Lynxeye photo diode and the copper source was excited under vacuum. 2θ angle values ranged from 5° to 50°.

2.7.SEM

The structure and size of the fibres were evaluated by Scanning Electron Microscopy on TESCAN Vega3 microscope. All images were obtained at 5 kV, at a 5 mm working distance, on a SE detector. Before imaging the fibres, all samples were gold sputtered using Quorum Technologies Q150RS gold sputter coater. Image J software was used to measure the diameter of the fibres. Approximately 100 measurements per sample at a 10k magnification were done and the average fibres diameter and standard deviation of the fibres were calculated with these values.

2.8.SANS

Small Angle Neutron Scattering (SANS) measurements were performed on the PAXY spectrometer at the Laboratoire Léon Brillouin (LLB, CEA Saclay, France). The first (respectively second) used configuration consisted in a sample-to-detector distance of 3 m (respectively 1 m) and a wavelength of 6 Å in both configurations. The global probed *q*-range corresponding to these configurations was $1.6*10^{-2}$ Å^{-1} $\leq q \leq$ $1.2*10^{-1}$ Å^{-1}. The signal was corrected by taking into account the contributions of the measurement cell, the solvent and incoherent background. The incoherent scattering of poly(methyl methacrylate) was used to correct the detector efficiency. Thus, the data were brought to absolute scale. The measurement cells were made of 1 mm thick quartz windows separated by a 2 mm O-ring and equipped with a cadmium boron carbide diaphragm whose hole diameter is 10 mm. DMSO-d_6 was used as the solvent during all the experiments. The temperature-regulated rack carrying the measurements cells filled with the pPR solutions was heated between 35 and 50°C depending on the experiment. After the samples were equilibrated at the targeted temperature (after 5 min), 5 min scans were recorded for several hours (up to 4 hours).

Sensitivity of small angle neutron scattering measurements in DMSO-d_6

For neutron scattering, the determinant condition for scattering to occur concerns the scattering length density of the solute with respect to the solvent.[1] The scattering length density δ_i can be estimated as follows:

$$\delta_i = \frac{a_i N_A}{V_i} \qquad (1)$$

$$a_i = \sum_m a_{i,m} \qquad (2)$$

Where the index i stands for the α-CD, the PCL or the DMSO-d_6 molecule and the index m represents the constitutive atoms of the molecule i. a_i designates the coherent diffusion length of the molecule i, N_A the Avogadro constant and V_i the molar volume of the molecule i. The so-called contrast length density v_{bi} with respect to the solvent is equal to:

$$^{v}b_i = \delta_i - \delta_{solvent} \qquad (3)$$

The obtained values are given in the Table S1. The comparison of the obtained contrast length density vbi values shows that α-CD and PCL scatter neutrons in an equivalent way in DMSO-d_6. Thus, SANS measurements are not sensitive to a particular species as far as concerns α-CD or PCL in DMSO-d_6.

i	V_i [$cm^3\ mol^{-1}$]	a_i [cm] #	δ_i [cm^{-2}]	v_{bi} [cm^{-2}]
α-CD	1944.16	1.89×10^{-11}	5.85×10^{9}	-4.69×10^{10}
PCL	105.88	1.41×10^{-13}	8.01×10^{9}	-4.47×10^{10}
DMSO-d_6	70.73	6.20×10^{-12}	5.28×10^{10}	0

#: calculated with equation (2) and reference 2

Table 5.1. SANS: Molar volume V_i, coherent diffusion length ai, scattering length density δ_i and contrast length density v_{bi} with respect to the solvent for i = α-CD, PCL and DMSO-d_6

(1) J. P. Cotton, *Journal de Physique IV* (France), **1999**, 9, 21 49 (in French).
(2) A. J. Dianoux and G. Lander, Neutron Data Booklet, OCP Science, Philadelphia (USA), **2003**.

2.9.Mechanical tensile testing

Young’s moduli and tensile strengths of the fibrous membranes were measured using the Anton Paar Physica MCR 301 rheometer with the universal extensional Fixture UXF12/CTD450. The measurements were performed on a fibrous strip presenting a constant 35 mm length and a width varying from 4 to 8 mm depending on the sample. Prior to any tensile tests, the samples were weighted and the thickness determined. The tensile speed was kept constant at 1 mm/min. Independent results from 10 fibrous strips were averaged and the standard deviations were also assessed. The apparent densities of each mat were calculated and taking into account for the evaluation of the Young’s moduli and strains at break.

2.10.Water contact angle

The static contact angles were recorded on Digidrop (GBX model ASE). The measurements were made by bringing the surface in contact with a 9 µL droplet of Milli-Q water. At least five measurements were done on each membrane to obtain an accurate average contact angle value.

2.11.Fluorescent confocal microscopy

Fluorescent properties of functionalized fibres were assessed by confocal microscopy on a Leica SP5 11 confocal microscope equipped with an oil-immersion objective lens 62x. FITC-labelled fibres were visualized by excitation of the fluorophore at λ = 488 nm. Simultaneously, images of the mats under white light were taken. In order to determine that the fluorescent properties were only due to FITC, red and blue images of the mats were also taken to eliminate the signal obtained due to the background noise.

A Zeiss confocal microscope equipped with an oil-immersion objective lens 62x was also used for the study on the influence of the shell concentration with the electrospun membranes resulting fluorescent properties. FITC-labelled fibres were visualized by excitation of the fluorophore at λ = 488nm.

2.12.Stability against water test

To test the stability of the polysaccharide based fibres against water, 2x2 cm squares of the polyelectrolyte complex based membranes were cut. The membranes were then fixed onto a cork. The cork served as a float when the membranes were immersed into 15 mL of distilled water. The membranes were placed into the water bath so that any solubilized PEO would be removed from the mat and dissolved in the water. After 24 hours, the membranes were placed onto filter paper and let to dry under an extractor hood.

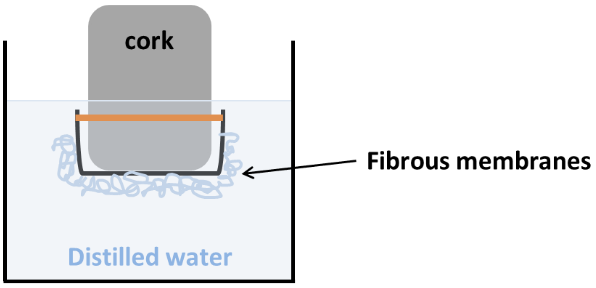

Figure 5.1. Schematic representation of the immersion of electrospun membranes in distilled water to evaluate their stability against water

2.13.UV-Vis spectrophotometer

The absorption measurements of the solutions were performed on a Shimadzu UV-Vis - 2101PC spectrophotometer. 0.8mL of the solution was collected from the reaction mixture and added in a 70-850 µL UV cells (Roth, polystyrene cells) instants before the analysis. The reference was a UV cell containing a pH = 7.4 buffer. The absorption values were taken at the maximum absorption wavelength value (λ = 653 nm for the calibration curves and λ = 643 nm for the release kinetics of the membranes)

3. Synthesis

3.1. Synthesis of methylene blue and curcumin inclusion complexes (adapted from reference 32)

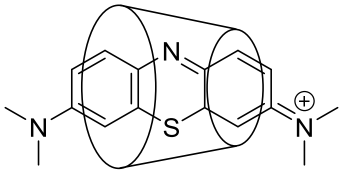

Figure 5.2. Chemical structure of the inclusion complex between methylene blue and β-cyclodextrin

In a 500 mL three-neck flask, 5.0 g of β-CD (4.41 mmol, 1 eq) were incorporated under inert atmosphere. 300 mL of distilled water were then added and the reaction mixture was stirred until the β-CD was completely solubilized. Methylene blue (1.41 g, 4.41 mmol, 1 eq) was then introduced within the aqueous solution and let to stir at room temperature for two days before transferring the reactive mixture into several 50 mL flasks. These flasks were freeze-dried for three days to remove all the distilled water. The resulting blue crystalline powder was collected and yielded 77 wt% of the total introduced weight.

^{1}H NMR (300 MHz, T = 296 K, D_2O, ppm): δ 7.34 (m, 7H), 7.03 (m, 7H), 6.77 (s, 7H), 3.86 (m, 7H), 3.76 (m, 1H), 3.54 (m, 21H), 3.09 (m, 13H).

The same procedure was followed for the synthesis of curcumin inclusion complexes in distilled water. When prepared in 1:1 acetone:water, curcumin was first solubilized in acetone and then added to the saturated aqueous solution of β-CD.

Curcumin inclusion complexes prepared in distilled water:

^{1}H NMR (300 MHz, T = 296 K, DMSO, ppm): δ 9.65 (broad peak, -OH), 7.55 (m, 2H), 7.32 (s, 2H), 7.14 (m, 2H), 6.78 (m, 4H), 6.05 (m, 1H), 5.5 (m, 14H), 4.80 (s, 7H), 3.85 (s, 6H), 3.50 (broad peak with water, 28H).

Curcumin inclusion complexes prepared in 50/50 acetone/distilled water:

^{1}H NMR (300 MHz, T = 296 K, DMSO, ppm): δ 9.66 (broad peak, -OH), 7.55 (m, 2H), 7.31 (s, 2H), 7.14 (m, 2H), 6.77 (m, 4H), 6.05 (s, 1H), 5.6 (m, 14H), 4.83 (s, 7H), 3.83 (s, 6H), 3.49 (m, 28H).

3.2. Synthesis of vancomycin and gentamicin based adducts

For both antibiotics namely vancomycin and gentamicin, the same procedure inspired from the literature was used[50].

In a 50mL two-neck flask under inert atmosphere, 0.1 g (0.07 mmol, 1 eq) of vancomycin (respectively 0.1 g (0.21 mmol, 1 eq) of gentamicin) was added to 10 mL of distilled water. The antibiotic was dissolved under vigourous stirring at room temperature. Once a clear solution was obtained, 0.15 g (0.14 mmol, 2 eq) of the β-CD (respectively 0.47 g (0.42 mmol, 2 eq) was added to the β-CD solution) was incorporated into the reaction mixture and let to stir for seven days under inert atmosphere at room temperature. After seven days, the reaction mixture was freeze-dried to remove the distilled water from the solution. A white crystalline solid was collected. The vancomycin adducts formation yielded an 85 wt% and the gentamicin adduct formation achieved 88 wt% yield.

Vancomycin adduct:

^{1}H NMR (300 MHz, T = 296 K, D_2O, ppm): δ 7.66 (s, 1H), 7.57 (s, 1H), 7.50 (m, 1H), 7.22 (m, 1H), 7.06 (s, 1H), 6.88 (m, 2H), 6.47 (m, 2H), 5.7 (m, 1H), 5.48 (s, 2H), 5.32 (m, 4H), 4.5 (s, 2H), 4.20 (s, 1H), 4.03 (m, 2H), 2.71 (s, 4H), 2.14 (s, 2H), 2.00 (m, 2H), 1.37 (s, 3H), 1.1 (m, 3H), 0.84 (m, 7H).

Gentamicin adduct:

^{1}H NMR (300 MHz, T = 296 K, D_2O, ppm): δ 5.75 (m, 1H), 5.28 (m, 2H), 4.99 (m, 46H), 3.86 (m, 190H), 3.55 (m, 100H), 2.85 (s, 6H), 2.67 (s, 1H), 2.14 (s,15H), 1.9 (m, 5H), 1.27 (m, 9H).

3.3. Synthesis of four-branched poly(ε-caprolactone) star-PCL derived from pentaerythritol (adapted from reference [173])

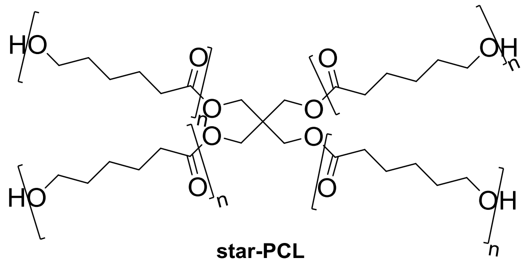

Mn = 10 000 g/mol
yield = 60%

Figure 5.3. Chemical structure of star-PCL

This reaction was performed in anhydrous conditions in order to avoid any transfer reaction due to water contamination. 0.2 g (1.47 mmol) of pentaerythritol was incorporated into a 100 mL three-neck round flask under an argon atmosphere and stirred at room temperature. Freshly distilled toluene (75 mL) was then added. 0.10 g (0.73 mmol, 1 eq) of TBD was then incorporated to the solution and let to stir until complete dissolution of the catalyst before distilled ε-CL (16.77 g, 0.15 mol, 200 eq) was incorporated. The temperature was then set to 115°C and the reaction was refluxed for 24 hours before being quenched by adding a few drops of acetic acid. The reaction was let to stir for 30 minutes while cooling down before the solution was concentrated under reduced pressure. 25 mL of tetrahydrofuran (THF) was then used to solubilize the polymer and let to precipitate in 300 mL of cold methanol (MeOH). The obtained polymer was filtered and purified again twice with THF and MeOH. The collected white solid was then vacuum dried overnight at 35°C. A 60 wt% yield of star-PCL was achieved.

^{1}H NMR (300 MHz, T = 296 K, acetone-d_6 + D_2O, ppm): δ 4.16 (s, 2H), 4.04 (t, *J* = 6.5728 Hz, 2H), 3.50 (t, *J* = 6.4378 Hz, 2H), 3.32 (s, 2H), 2.29 (m, 2H), 1.56 (m, 4H), 1.35 (m, 2H).

^{13}C NMR (300 MHz, T = 296 K, acetone-d_6 + D_2O, ppm): δ 207.3, 173.78, 64.5, 62.8, 61.9, 42.9, 34.6, 34.4, 34.2, 33.1, 26.1, 25.5, 25.2, 25.1.

3.4. Esterification of the end hydroxyl groups of star-PCL with succinic anhydride to obtain star-PCL-COOH

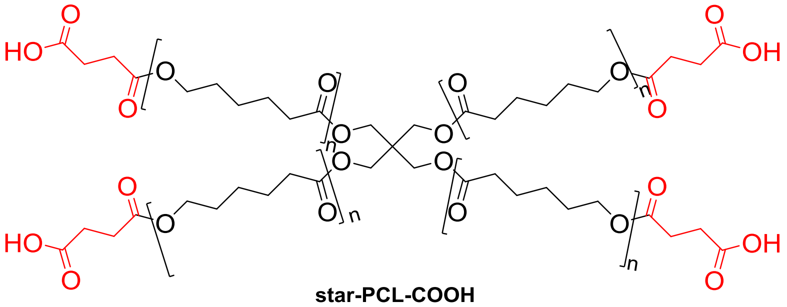

star-PCL-COOH
Mn = 10 200 g/mol
yield = 66%

Figure 5.4. Chemical structure of star-PCL-COOH

A four-branched PCL (3.0 g, 0.3 mmol, 1.3 mmol of hydroxyl functions) was dissolved in 25 mL of 1,4-dioxane under inert atmosphere. Once the polymer was completely dissolved, succinic anhydride (0.25 g, 2.47 mmol) was added as well as a few drops of triethylamine (TEA). The reaction was carried out at 70°C for 12 days before being cooled down. The resulting mixture was concentrated under reduced pressure, by evaporation. This organic phase was washed with 100 mL of ethyl acetate (EtOAc) and 100 mL of brine. After the phase separation, the aqueous and organic phases were washed three times with 50 mL of EtOAc and brine, respectively. Similarly, the resulting organic phases were then dried over sodium sulphate and filtered. The final product was concentrated at the rotary evaporator. The yellowish product yielded 66 wt%.

^{1}*H NMR (300 MHz, T = 296 K,* $CDCl_3$*, ppm):* δ 4.12 (m, 2H), 2.67 (m, 4H), 2.33 (t, *J*= 14,86 Hz, 2H), 1.65 (m, 4H), 1.41 (m, 2H).

^{13}*C NMR (300 MHz, T = 296 K,* $CDCl_3$*, ppm):* δ 174.34, 174.19, 172.82, 67.74, 65.24, 64.80, 61.04, 34.78, 34.51, 29.01, 28.90, 26.19, 25.23, 25.16, 25.09.

3.5. Amidation of the end groups of the star-PCL-COOH to obtain asym-PCL (adapted from reference [218])

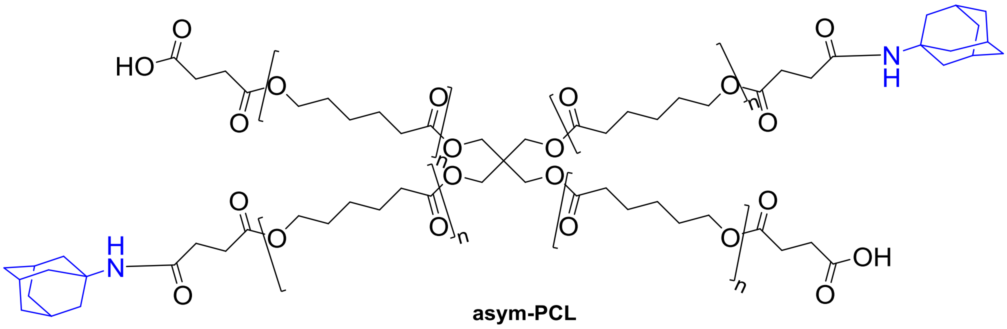

asym-PCL
Mn = 10 500 g/mol
yield = 55%

Figure 5.5. Chemical structure of asym-PCL

The esterified star-PCL (1.0 g, 0.01 mmol, 0.39 mmol of COOH functions) was added to 1-adamantine (0.03 g, 0.19 mmol, 0.5 $\text{eq}_{/\text{COOH}}$). The solids were solubilized under inert atmosphere with 18 mL of freshly distilled dichloromethane. 0.06 g of 4-(4,6-dimethoxy-1,3,5-triazin-2-yl)-4-methylmorpholinium chloride hydrate (DMTMM) was then added as well as 2mL of TEA. The reaction was carried out under stiring for 9 days at 35°C before the solution was concentrated under reduced pressure. The solid was then solubilized in 100 mL of EtOAc and phase separated with 100 mL of a 1 wt% HCl solution. The organic phase was further washed with 100 mL of 1 wt% HCl solution. Similarly, the aqueous phase was extracted three times with 100 mL of EtOAc. The organic phase was dried over sodium sulphate, filtered and collected before being concentrated at the rotavapor to obtain a white solid (yield = 86 wt%).

^{1}H NMR (300 MHz, T = 296 K, $CDCl_3$, ppm): δ 5.34 (s, NH), 4.07 (t, *J*= 6.68 Hz, 2H), 2.67 (m, 4H), 2.05 (t, *J*= 14,95 HZ, 2H), 1.64 (m, 4H), 1.36 (m, 2H).

^{13}C NMR (300 MHz, T = 296 K, $CDCl_3$, ppm): δ 173.67, 64.29, 41.78, 34.27, 28.51, 25.68, 24.73.

3.6. Synthesis of a block copolymer (PCL-PPG-PCL) initiated by poly(propylene glycol) (PPG) and catalysed by TBD (adapted from reference [173])

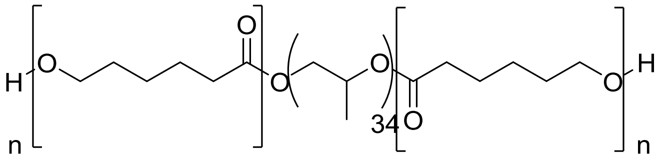

PCL-PPG-PCL
Mn = 6000 g/mol
yield= 52%

Figure 5.6. Chemical structure of the block copolymer

This reaction was performed in anhydrous conditions in order to avoid any transfer reaction due to water contamination. 0.5 g (0.25 mmol) of poly(propylene glycol) (PPG) was incorporated into a 100 mL three-neck round flask under an argon atmosphere and stirred at room temperature. Freshly distilled toluene (25 mL) was then added. 2.85 g (24.9 mmol, 200 eq) of freshly distilled ε-CL was then incorporated to the solution and let to stir until an homogenous solution was obtained. The catalyst was then added into the flask (0.02 g, 0.13 mmol, 1 eq). The temperature was then set to 25°C and the reaction was carried out for 24 hours before being quenched by adding a few drops of acetic acid. The polymer solution was then added 300 mL of cold methanol (MeOH) and the block copolymer precipitated instantly. The obtained solid was filtered and purified again twice with THF and cold MeOH. The collected white solid was then vacuum dried overnight at 35°C. A 50 wt% yield of PCL-PPG-PCL was achieved.

^{1}H NMR (300 MHz, T = 296 K, $CDCl_3$, ppm): δ 4.03 (t, *J*= 6.68 Hz, 2H), 3.55 (m, 2H), 3.38 (m, 1H), 2.29 (t, *J*= 14,95 HZ, 2H), 1.62 (m, 4H), 1.34 (m, 2H), 1.11 (m, 3H).

^{13}C NMR (300 MHz, T = 296 K, $CDCl_3$, ppm): δ 173.51, 75.53, 75.33, 75.12, 73.37, 72.87, 64.13, 34.11, 28.35, 25.53, 17.48, 17.36.

3.7. Preparation of α-cyclodextrin star-pPR using star-PCL (adapted from reference [62])

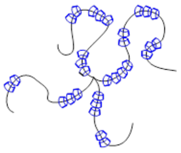

star-pPR

Figure 5.7. Schematic representation of star-pPR

In a 500 mL three-neck round flask, 100 mL of a saturated aqueous solution of α-cyclodextrin (16.82 g, 17.3 mmol) was prepared. In another round flask, 2.00 g of star-PCL (0.2 mmol of polymer corresponding to 17.5 mmol of monomer units) was dissolved in 100 mL of acetone. Once both solid were dissolved in their respective solvent, the polymer solution was added dropwise in the saturated solution of α-CD. A white precipitate was formed instantly during the addition. The mixture was then stirred for 24 hours at 70°C before being cooled down to room temperature. The white solid was filtered and washed several times with acetone or distilled water to remove any unreacted star-PCL or α-CD respectively. The so obtained pseudopolyrotaxane, star-pPR, (yield = 35 wt%) was then dried overnight in a vacuum oven at 35°C.

^{1}H NMR (300 MHz, T = 296 K, DMSO-d$_6$, ppm): δ 5.61 (d, *J*= 6.36 Hz, 6H), 5.54 (s, 6H), 4.90 (s, 6H), 4.58 (s, 6H), 4.08 (m, 2H), 3.74 (m, 18H), 2.35 (m, 2H), 1.63 (m, 4H), 1.39 (m, 2H).

^{13}C NMR (300 MHz, T = 296 K, DMSO-d$_6$, ppm): δ 171.99, 101.51, 81.79, 72.89, 71.94, 71.87, 62.93, 59.90, 32.98, 27.32, 24.41, 23.54.

3.8. Synthesis of α-cyclodextrin lin-pPR using a 10 kg.mol^{-1} commercial linear PCL (adapted from reference [62])

lin-pPR

Figure 5.8. Schematic representation of lin-pPR

In a 500 mL three-neck round flask, 100 mL of a saturated aqueous solution of α-cyclodextrin (17.12 g, 17.6 mmol) was prepared. In another round flask, 2.00 g of linear PCL (0.2 mmol of polymer corresponding to 17.5 mmol of monomer units) was dissolved in 100 mL of acetone. Once both solid were dissolved in their respective solvent, the polymer solution was added dropwise in the saturated solution of α-CD. A white precipitate was formed instantly during the addition. The mixture was then stirred for 24 hours at 70°C before being cooled down to room temperature. The white solid was filtered and washed several times with acetone or distilled water to remove any unreacted lin-PCL or α-CD respectively. The so obtained pseudopolyrotaxane, lin-pPR, (yield = 33 wt%) was then dried overnight in a vacuum oven at 35°C.

^{1}H NMR (300 MHz, T = 296 K, DMSO-d_6, ppm): δ 5.52 (d, *J*= 7.02 Hz, 6H), 5.43 (s, 6H), 4.79 (s, 6H), 4.48 (t, *J*= 5.45 Hz, 6H), 3.97 (t, *J*= 6.36 Hz, 2H), 3.67 (m, 18H), 2.26 (t, *J*= 14.35 Hz, 2H), 1.52 (m, 4H), 1.27 (m, 2H).

^{13}C NMR (300 MHz, T = 296 K, DMSO-d_6, ppm): δ 172.99, 101.52, 81.80, 72.89, 71.95, 71.87, 62.94, 59.90, 32.99, 27.32, 24.42, 23.54.

3.9. Synthesis of α-cyclodextrin mik-pPR using asym-PCL (adapted from reference [62])

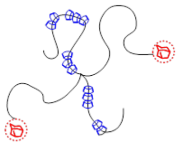

mik-pPR

Figure 5.9. Schematic representation of mik-pPR

In a 500 mL three-neck round flask, 100 mL of an aqueous solution of α-cyclodextrin (14.86 g, 15.3 mmol) was prepared. In another round flask, 2.00 g (0.19 mmol) of asym-PCL was dissolved in 100 mL of acetone. Once both solid were dissolved in their respective solvent, the polymer solution was added dropwise in the saturated solution of α-CD. A white precipitate was formed instantly. The mixture was then stirred for 48 hours at 70°C before being cooled down to room temperature. The white solid was filtered and washed several times with acetone or distilled water to remove any unreacted asym-PCL or α-CD, respectively. The so obtained pseudopolyrotaxane, mik-pPR, (yield = 24 wt%) was then dried in a vacuum oven at 35°C.

^{1}*H NMR (300 MHz, T = 296 K, DMSO-d$_6$, ppm):* δ 5.52 (d, *J*= 7.02Hz, 6H), 5.44 (s, 6H), 4.80 (s, 6H), 4.47 (m, 6H), 3.98 (m, 2H), 3.77 (m, 6H), 3,60 (m, 12H), 2.26 (m, 2H), 1.53 (m, 4H), 1.26 (m, 2H).

^{13}*C NMR (300 MHz, T = 296 K, DMSO-d$_6$, ppm):* δ 172.72, 101.96, 82.07, 73.25, 72.1, 63.47, 59.97, 33.35, 27.79, 24.88, 24.07.

3.10. Synthesis of β-cyclodextrin copo-pPR derived from the block copolymer PCL-PPG-PCL (adapted from reference [63] and [181])

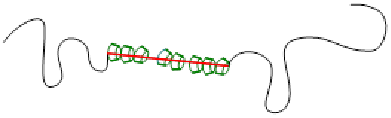

copo-pPR

Figure 5.10. Schematic representation of copo-pPR

In a 500 mL three-neck round flask, 100 mL of an aqueous solution of β-cyclodextrin (2.50 g, 2.22 mmol) was prepared. In another round flask, 2.00 g (0.2 mmol of the block copolymer corresponding to 2.22 mmol of propylene glycol monomer unit) of PCL-PPG-PCL was dissolved in 100 mL of acetone. Once both solid were dissolved in their respective solvent, the polymer solution was added dropwise in the saturated solution of α-CD. The mixture was then stirred for 24 hours at 70°C under reflux before being cooled down to room temperature. The solution was let to stir for another 24 hours at room temperature. A yellow solid could be seen at the wall of the flask. The solvents were removed by rotary evaporator for several to remove the highest amount of DMSO. The so obtained pseudo-polyrotaxane, copo-pPR, (yield = 50 wt%) was then dried further dried on a vacuum line.

^{1}H NMR (300 MHz, T = 296 K, DMSO-d_6, ppm): δ 5.75 (3, 14H), 4.88 (s, 7H), 4.03 (m, 2H), 3.66 (m, 7H), 3.35 (m, 14H), 2.32 (m, 2H), 1.58 (m, 4H), 1.34 (m, 2H), 1.08 (m, 3H).

^{13}C NMR (300 MHz, T = 296 K, DMSO-d_6, ppm): δ 121.93, 81.53, 73.03, 72.40, 72.03, 59.9, 24.07.

3.11. Grafting of fluorescein isothiocyanate (FITC) onto the fibres surface

All grafting reactions were realized according to the same procedure[149]. In order to maximize the fluorescence of FITC during the fluorescent confocal microscopy analysis, all reactions were performed in the dark. First, a 10^{-6} mol.L^{-1} stock solution of FITC was prepared in a 50/50 wt/wt mixture of acetonitrile and distilled water (CH_3CN/H_2O). Samples of electrospun membranes were cut out (~10 mg), immersed and stirred in 2 mL of a 50/50 wt/wt mixture of CH_3CN/H_2O. 1 mL of the 10^{-6} mol.L^{-1} FITC solution was then added to the reaction medium and let to react for 4 hours at room temperature. The membranes were then thoroughly rinsed with the CH_3CN/H_2O solution before being dried on filter paper. All membranes were kept in the dark until the SEM and confocal fluorescent microscopy analyses were performed.

4.Electrospinning

4.1. Electrospinning of polyelectrolyte based fibres for wound dressing applications

As said in chapter 3, chitosan (CHI) and carboxymethyl cellulose (CMC) present several ionizable functions along their backbone. However, the charge densities on each polyelectrolyte is different. In CHI, 86% of the chain monomer was deacetylated and can thus be ionizable (NH_3^+), whereas CMC exhibited 70% of modified cellulose that are now charged (COO^-).

For the electrospinning experiments, the relative humidity was kept below 40% and the temperature was between 20-25 °C.

4.1.1. Coaxial electrospinning

To determine the influence of the charge ratio on the morphology of the fibres as well as on the mechanical properties of the polyelectrolyte complex based fibres, different COO^-/NH_3^+ ratios were prepared and electrospun: 10.88, 3.63, 2.18, 1.55, 1.0, 0.33.

Preparation of chitosan solution

The solution concentration of CHI was kept constant for all the various electrospinning experiments and only the concentration of CMC was changed to reach the targeted COO^-/NH_3^+ ratios. To ionize the CHI and obtain a polyelectrolyte, formic acid (FA) was mixed with water to obtain an acidic pH. To be able to form CHI based fibres, poly(ethylene oxide) (PEO) was added and the lowest concentration was used to form mainly based polyeletrolyte fibres. Typically, a 1.5 wt% concentration of CHI was mixed with 0.6 wt% of PEO in a 50/50 wt/wt FA/water mixture. The solution was stirred at room temperature for 24 hours prior to any electrospinning experiments.

When methylene blue was added within the CHI solution, a constant 15 wt% of methylene blue in regard to the total concentration of CHI was added to the CHI solution. Both solids were solubilized in a 50/50 wt/wt FA/water mixture.

Preparation of carboxymethyl cellulose solution

The CMC solution prepared for the coaxial electrospinning was prepared so that for identical flow rates between the CMC core and the CHI shell a COO^-/NH_3^+ ratio of 1 was reached. To reach the other charge ratios detailed above, the shell flow rate was varied. For these experiments, a 3 wt% of CMC was blended with 1.5 wt% of PEO and solubilized in distilled water. This solution was also stirred for 24 hours prior to any electrospinning experiment.

Coaxial electrospinning experiments

The experiments were performed in a closed booth with a vertical set-up. To obtain core: shell fibres, the CMC solution was introduced in the syringe linked to the core of the needle whereas all CHI solutions were used as a shell. The core flow rate was kept constant at 1 mL/h (Harvard Apparatus, PHD 2000, USA). The shell flow rate varied between 0.1 and 3 mL/h (Harvard Apparatus, PHD 2000, USA) to reach the COO^-/NH_3^+ between 1 and 10.88. The applied voltages at the needle tip and the collector were 25 kV and -1 kV or -5 kV (Spellman SL10 high voltage power supplies, ± 30 kV, USA). The distance between the nozzle and the collector was kept constant at 20 cm.

4.1.2. Blend electrospinning

To determine the influence of the charge ratio on the morphology of the fibres as well as on the mechanical properties of the polyelectrolyte complex based fibres, different COO^-/NH_3^+ ratios were prepared and electrospun: 1.2, 1, 0.7, 0.5, 0.3, 0.1.

Preparation of chitosan solution

The solution concentration of CHI was kept constant for all the various electrospinning experiments. To ionize the CHI and obtained a polyelectrolyte, formic acid (FA) was mixed with water to obtain an acidic pH. To be able to form CHI based fibres, poly(ethylene oxide) (PEO) was added and the lowest concentration was used to form mainly based polyeletrolyte fibres. Typically, a 3 wt% concentration of CHI was mixed with 1.2 wt% of PEO in a 50/50 wt/wt FA/water mixture. The solution was stirred at room temperature for 24 hours prior to any electrospinning experiments.

When methylene blue and methylene blue inclusion complexes were added to the polyelectrolyte based fibres, a constant methylene blue concentration of 15 wt% (corresponding to 17.5 wt% concentration of methylene blue inclusion complex) in regard to the total amount of CHI. All solids were still solubilized in a 50/50 wt/wt FA/water 24 hours prior to the electrospinning experiments.

Preparation of carboxymethyl cellulose solution

As opposed to coaxial electrospinning, to reach the targeted COO^-/NH_3^+ ratios, the concentration of CMC varied for each solution to be combined with the CHI solution detailed above. PEO was also added for the electrospinnability of the polysaccharide solutions. The polymers were solubilized in pure distilled water.

The following table summarizes the different PEO and CMC concentrations needed to reach the targeted ratios:

COO^-/NH_3^+ ratio	CMC concentration (wt%)	PEO concentration (wt%)
0.1	0,50	0.248
0.3	1.49	0.74
0.5	2.48	1.24
0.7	3.49	1.74
1.0	5.4	2.7
1.2	6.0	3.0

Table 5.2. Recapitulative table of the different CMC and PEO concentrations used for blend electrospinning

When sodium periodate was added to chemically crosslink the electrospun fibre, 0.1 wt% in regard to the CMC concentration was added within the CMC solutions and stirred for 24 hours prior to the blending step.

Blend electrospinning of the polyelectrolyte solutions

Just instants before the electrospinning, a 50/50 wt/wt mixture of CHI and CMC solutions was blended at 750 rpm for two minutes. The polyelectrolyte blending enabled the formation of polyelectrolyte complexes (PECs) within the mixture. The reactive mixture was introduced in a 10 mL syringe and the solution was electrospun. The experiments were performed in a closed booth with a vertical set-up. These blend solutions were stable for 3 hours to allow the processing of the PECs by electrospinning.

To elaborate homogenous fibres, a distance between the nozzle and the collector of 20 cm was necessary. The flow rate of the blend solution was 1 mL/h (Harvard Apparatus, PHD 2000, USA) and the applied voltages at the needle tip and the collector were 25/-1 kV/kV (Spellman SL10 high voltage power supplies, ± 30 kV, USA) for all the different blend solutions loaded or not with methylene blue inclusion complexes.

4.2. Electrospinning of polyester and pseudo-polyrotaxanes

For solvent fast evaporation purposes, all experiments have been carried out at 27°C and the relative humidity controlled and maintained below 40%. Beyond this value, the Taylor cone and jet became unstable and the process of electrospinning was not continuous anymore.

4.2.1. Blend electrospinning

These electrospinning experiments were only prepared with star-pPRs the commercially available linear PCL (80 000 g/mol, CAPA 6806).

Preparation of the solutions

To solubilize at the same time the hydrophobic PCL and the nanoplatelets of star-pPRs, a mixture of 50/25/25 wt/wt/wt dichloromethane/dimethylformamide/dimethyl sulfoxide (DCM/DMF/DMSO) was necessary. Different blends were prepared incorporating 15 wt%, 18 wt% and 20 wt% of a mixture between linear PCL (commercially available, 80 000 g/mol, CAPA 6806) and the star-pPR. The pPR was incorporated at 5 wt% concentration in regard to the amount of PCL used. This means that for the 15 to 20 wt% concentration of solid, there was respectively 0.75 wt%, 0.9 wt% and 1wt% of supramolecules within the solution. The solutions were let to stir for several hours at 30°C before the electrospinning process. All the solutions were opalescent at best or turbid when the concentration of solid increased.

Elaboration of blend fibrous membranes by electrospinning

The fabrication of fibres was performed in a closed booth with a vertical set-up. The distance between the needle tip and the collector was varied between 20 and 30 cm. The distance between the two charged points was increased to enhance the evaporation of the solvents. The flow rate of the solution was kept constant at 1 mL/h (Harvard Apparatus, PHD 2000, USA). The applied voltage at the nozzle was maintained at 25 kV (Spellman SL10 high voltage power supplies, ± 30kV, USA) whereas the voltage at the collector was varied between -5 and -15 kV (Spellman SL10 high voltage power supplies, ± 30 kV, USA). By increasing the electrical field, a fibrous jet could be formed even for the highest solid contents.

4.2.2. Coaxial electrospinning

Preparation of the solutions

Core solution: The core and shell solutions were prepared separately 24 hours prior to the electrospinning step. The core solution was a 15 wt% solution of linear high molecular weight PCL (80 000 g/mol, CAPA 6806) dissolved in a mixture of DCM and DMF at a 60/40 ratio.

Shell solutions: lin-pPR, star-pPR and mik-pPR were dissolved in DMSO. For star-pPR and lin-pPR, three different shell concentrations were prepared: 5 wt%, 10 wt% and 15 wt%. Two different mik-pPR shell solutions of 5 wt% and 15 wt% were solubilized in DMSO. The solutions were stirred at 30 °C for several hours in an oil bath to ensure complete dissolution of the pPRs. Copo-pPR was solubilized in a mixture of DCM/DMSO (60/40 wt/wt) and two different solutions were prepared (5wt% and 15 wt%) and stirred for 24 hours at room temperature.

Elaboration of core:shell fibrous membranes by coaxial electrospinning

The experiments were performed in a closed booth with a vertical set-up. The needle and aluminium covered collector were separated from each other by 15 cm. A self-designed spinneret presenting a coaxial needle was used and the core and shell solutions were placed in 10 mL and 5 mL syringes. For the core solution, the flow rate was 1 mL/h and in the case of the shell solution, the flow rate was 0.3 mL/h (Harvard Apparatus, PHD 2000, USA). Within the processed coaxial fibres, the resulting weight ratios of PCL:star-pPR and PCL:lin-pPR are then respectively 10:1, 10:2 and 10:3. The same flow rate conditions were also applied to mik-pPR and copo-pPR solutions, leading to fibres with PCL:pPR weight ratios of 10:1 and

10:3. The applied voltages (Spellman SL10 high voltage power supplies, ± 30 kV, USA) at the needle tip and at the collector were adjusted depending on the shell solution concentrations to obtain bead-free fibres. These parameters were optimized until homogenous fibres could be spun continuously. In the case of the 5 wt% shell pPR solutions, the voltages at the tip and at the collector were 25 kV and -5 kV respectively. For the 10 wt% and 15 wt% shell pPR solutions, the applied voltages were 30 kV and -10 kV at the needle tip and the aluminium collector.

Elaboration of core:shell fibrous membranes by electrospinning for tensile test measurements

The experiments were performed in a closed booth with a horizontal set-up. The collector was a rotative drum spinning at 300 rpm speed. The needle and aluminium covered collector were separated from each other by 15cm. A self-designed spinneret presenting a coaxial needle was used and the core and shell solutions were placed in 10 mL and 5 mL syringes. For the core solution, the flow rate was 1 mL/h and in the case of the shell solution, the flow rate was 0.3 mL/h (Harvard Apparatus, PHD 2000, USA). For these experiments, neat PCL and 10:1 PCL:pPR core:shell fibres were prepared. The applied voltages (Spellman SL10 high voltage power supplies, ± 30 kV, USA) at the needle tip and at the collector were adjusted to obtain bead-free fibres. These parameters were optimized until homogenous fibres could be spun continuously. The voltages at the tip and at the collector were 25 kV and -10 kV respectively. The electrical field conditions were changed in comparison with the other parameters due to the change of set-up in the booth. Despite these conditions, the fibres were not aligned and the thickness of each stripe was measured. Small samples of 35 mm in length and 4-8 mm in width were cut to achieve the requirements and prerequisites of the Anton Paar rheometer used for the tensile tests.

5.Physical crosslinking in an environmental chamber

To physically crosslink the polyelectrolyte complex based membranes, all membranes were placed in Petri dishes and uncovered in a Climacell 111L. The conditions were set to regulate the relative humidity (RH) between 35-40% and the temperature was programmed at 37°C for two weeks. Regular controls of the conditions were done to ensure the stability of the conditions. After two weeks, the membranes were removed from the environmental chamber and covered. The membranes were kept away from moisture until needed.

6.Biological evaluation

All the biological evaluations were performed by Dr. Lydie Seon at the Institute for Biomaterials and Bioengineering, INSERM, UMR S1121, University of Strasbourg.

6.1. Determination of the minimal inhibitory concentration

Antibacterial activity of methylene blue and curcumin was assessed by using a microdilution assay on two bacterial strains: *Micrococcus luteus* (A270) and *Staphylococcus aureus* (ATCC25923).

Microbial preculture

Preparing a microbial culture consists in multiplying microbial organisms by letting them reproduce in predetermined culture.

Bacteria were precultured aerobically in a Mueller-Hinton Broth (MHB) growth medium (Merck, Darmstadt, Germany) under stirring for 18 hours at 37°C in an incubator (Tritamax 1000, Heidolph, Germany).

Antimicrobial activity assay

The antimicrobial activity was tested using a bacterial suspension with an optical density at a 620 nm wavelength (OD_{620}) of 0.001 prepared from the microbial preculture. This corresponds to about 5.10^8 cells per milliliter.

For methylene blue and curcumin, the antimicrobial tests were performed in solution. Aqueous solutions of these compounds were prepared in bacterial medium at different concentrations by dilution of a stock solution. 10 µL of these solutions were incubated in 96-well microplates (Falcon, Becton Dickinson, USA) with 90 µL of bacteria or yeast with final concentrations ranging from 1 to 100 µM of peptide. After 24 hours of incubation at 37°C under gentle stirring, the OD_{620} of the 96-well plate was measured by a microplate reader (Multiscan EX, Shangai, China). The minimal inhibitory concentration (MIC) of an antibiotic is defined as the lowest antibacterial concentration that inhibits the bacterial growth after 24 hours incubation at 37°C (± 2°C).

Several controls were used: a fresh medium without inoculation of pathogens was used to ensure sterility, a mixture of tetracycline (10 µg.mL^{-1}) and cefotaxime (0.1 µg.mL^{-1}) for antibacterial assay and a fresh inoculated culture medium without any addition was taken as negative control. Each assay was performed in triplicate and the experiments were repeated at least three times.

The normalized growth of pathogens (in %) was estimated by comparing the OD_{620} values of the antibiotic to the positive and the negative controls. The OD_{620} value of control cultures growing in the absence of antibiotics was taken as 100% growth (negative control) and the OD_{620} value of cultures growing in the presence of antibiotics (tetracycline and cefotaxime) was taken as 0% growth (positive control). Using the following equation, the normalized pathogen growth can be evaluated:

$$\text{normalized pathogen growth} = 100 \times \frac{\mathrm{OD}_{620,sample} - \mathrm{OD}_{620,\text{positive control}}}{\mathrm{OD}_{620,\text{negative control}} - \mathrm{OD}_{620,\text{positive control}}} \qquad (4)$$

6.2. Agar disc diffusion test (Kirby’s test)

Antibacterial activity of the polyelectrolyte complex (PEC) based electrospun membranes were assessed by disc diffusion test against *Micrococcus luteus* (A270).

Preparation of a test inoculum

Preparing a microbial culture consists in multiplying microbial organisms by letting them reproduce in predetermined culture.

Bacteria were precultured aerobically in a Mueller-Hinton Broth (MHB) growth medium (Merck, Darmstadt, Germany) under stirring for 18 hours at 37°C in an incubator (Tritamax 1000, Heidolph, Germany). A bacteria concentration 5.10^8 cells per milliliter was reached and necessary for the disc diffusion test. The concentration of the test inoculum was measured by optical density at a 620 nm wavelength (OD_{620}) and had to reach a value of 0.001.

Preparation of the agar plates

The Petri dishes containing the broth were prepared before the testing according to a standard procedure using Tryptic Soy Broth (TSB).

For the test, the agar plates were taken out of the freezer and warmed up in the incubator for 20 minutes.

Using a swab that was previously immersed in the test inoculum, the bacteria were evenly distributed onto the agar plate surface. To do so, the swab was lightly applied onto the surface and slightly rubbed so that all the top of the agar was covered. The plates were then turned (60° rotation) and the swab as well. It was then again slightly applied onto the all surface of the broth. This was done a third time to ensure that the entire surface was covered.

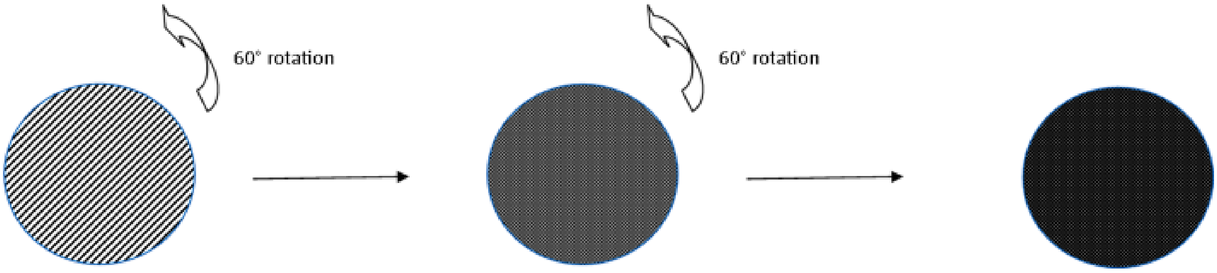

Figure 5. 11. Schematic representation of the preparation of the agar plates with the microbial preculture

Once the agar plates were contaminated with the microbial preculture and the inoculum was impregnated within the broth, small discs (8 mm in diameter) of the electrospun membranes were placed on the surface of the agar plates. Approximately 6 discs per agar plates were tested at the same time. Duplicates of each membrane were used for the Kirby's test as well as positive and negative references. Once the membranes were put in contact with the bacteria, the agar plates were covered and inverted before being incubated at 37°C (± 2°C) for 24 hours.

After these 24 hours, the agar plates were removed from the incubator and the zone of bacterial inhibition was measured under and around each fibrous discs. The membranes were replaced on their spot and the agar plates were incubated for another 24 hours before the diameter of inhibition was measured once again.

Disc diffusion tests results obtained for the various CMC/CHI blend based membranes

N°	**Type of membrane**
1	CHI + NaIO4
2	CHI + NaIO4 + MB
3	CHI + NaIO4 + CD
4	CHI + NaIO4 + MB/CD IC
5	CHI environmental chamber
6	CHI + MB environmental chamber
7	CHI + CD environmental chamber
8	CHI + MB/CD IC environmental chamber
9	CHI
10	CHI + MB
11	CHI + CD
12	CHI + MB/CD IC
13	CMC/CHI + NaIO4
14	CMC/CHI + NaIO4 + MB
15	CMC/CHI + NaIO4 + CD
16	CMC/CHI + NaIO4 + MB/CD IC
17	CMC/CHI environmental chamber
18	CMC/CHI + MB environmental chamber
19	CMC/CHI + CD environmental chamber
20	CMC/CHI + MB/CD IC environmental chamber
21	CMC/CHI
22	CMC/CHI + MB
23	CMC/CHI + CD
24	CMC/CHI + MB/CD IC

Results at 24hours

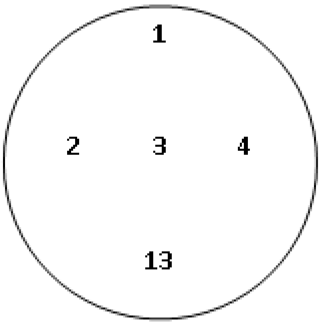

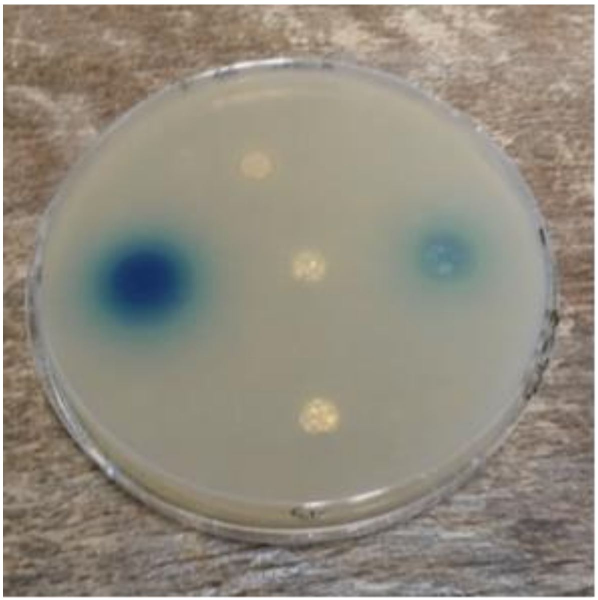

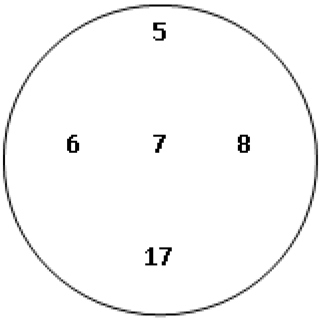

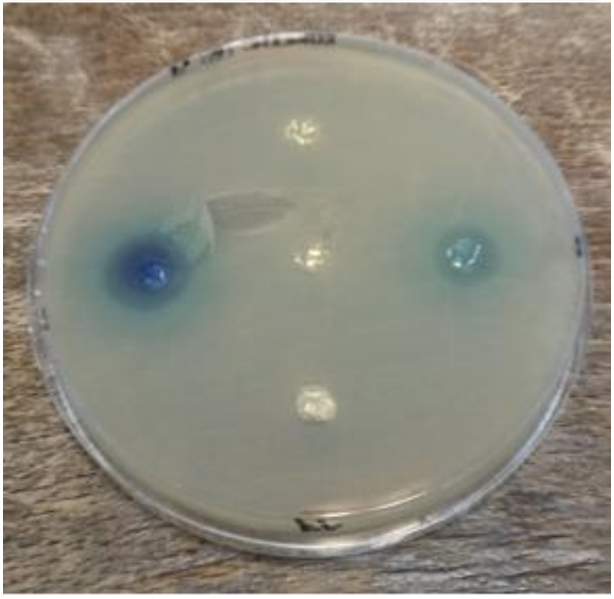

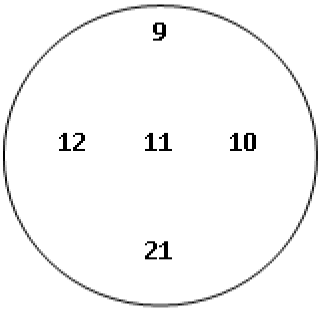
9
12
11
10
21

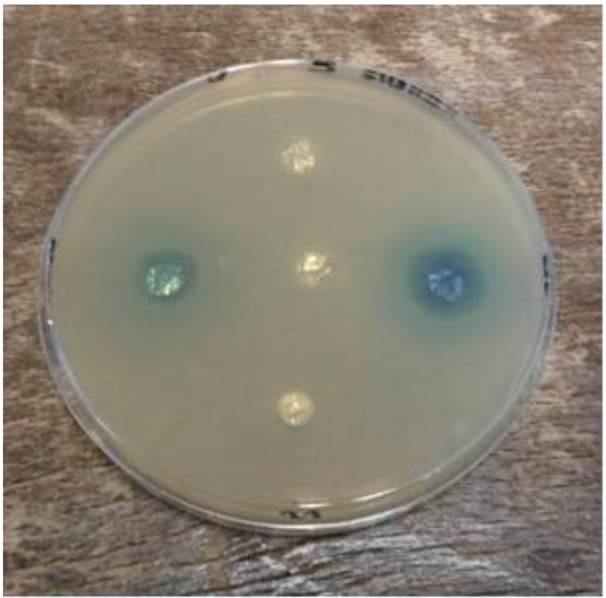

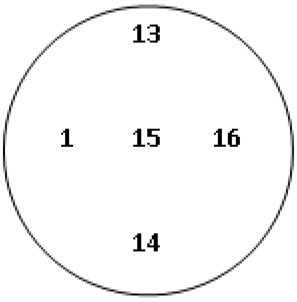
13
1
15
16
14

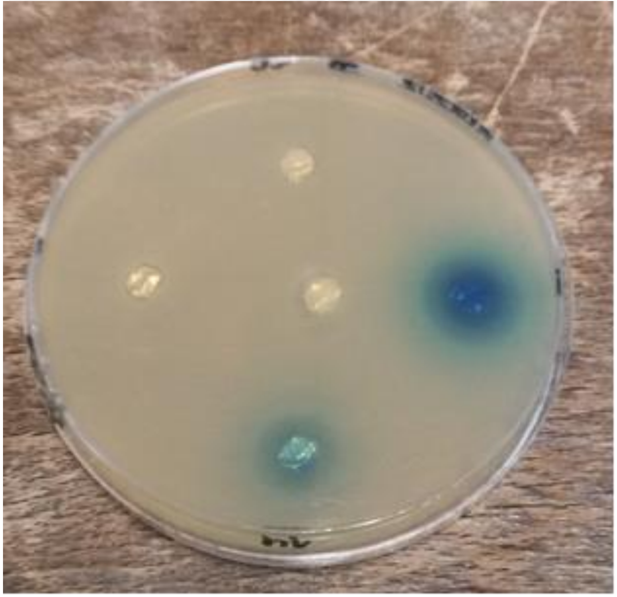

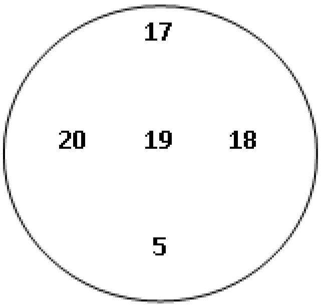
17
20
19
18
5

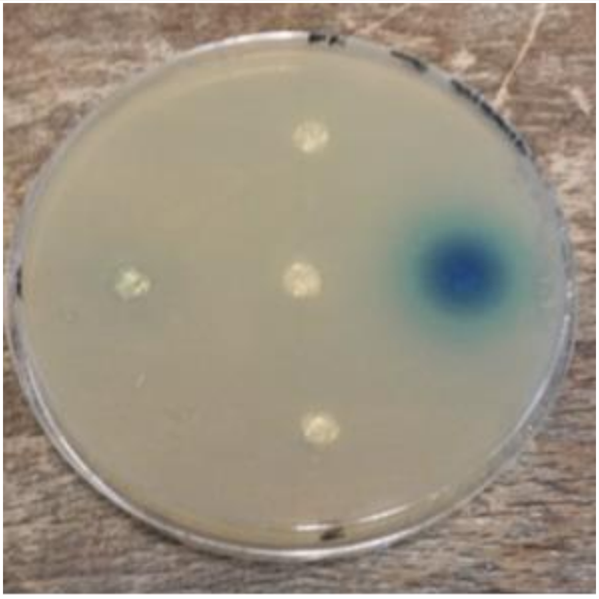

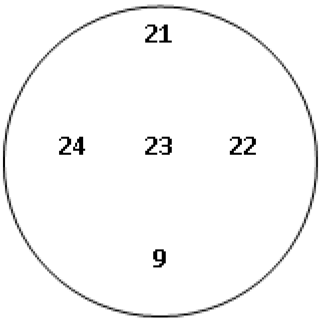
21
24
23
22
9

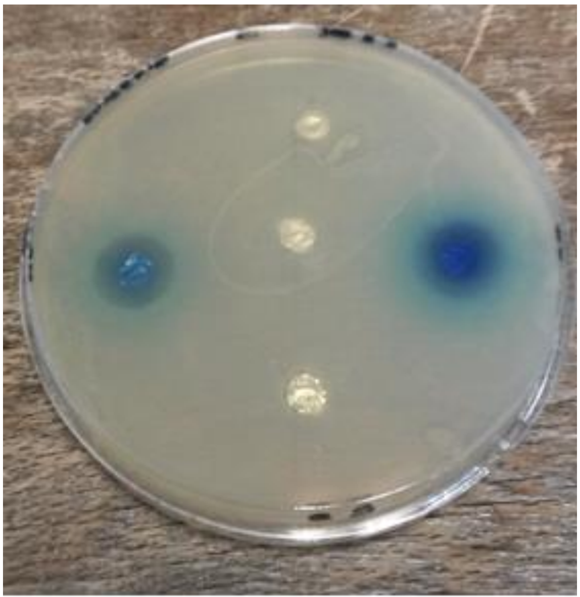

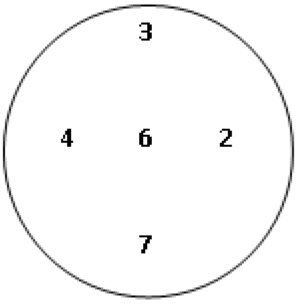
3
4
6
2
7

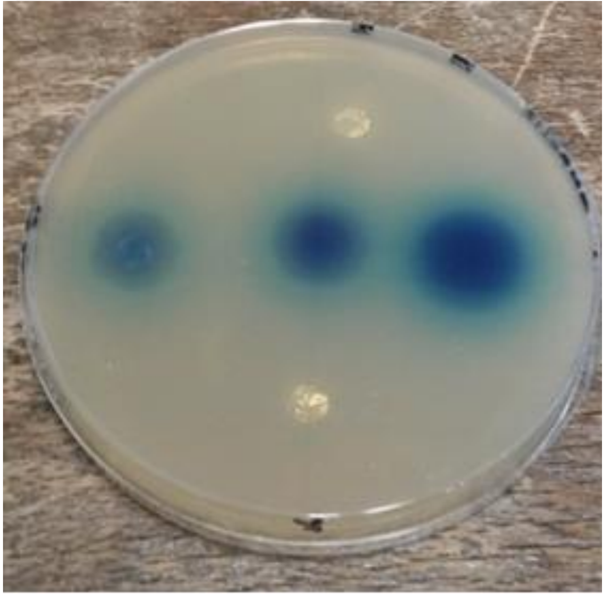

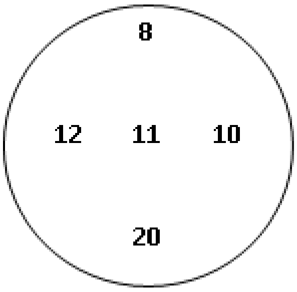
8
12
11
10
20

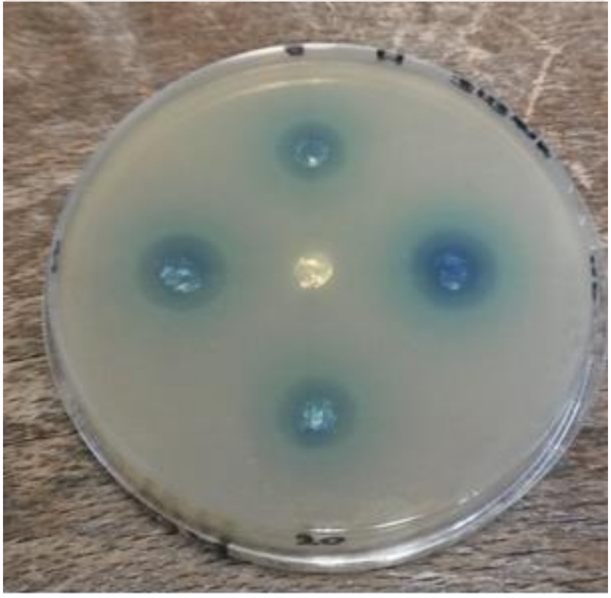

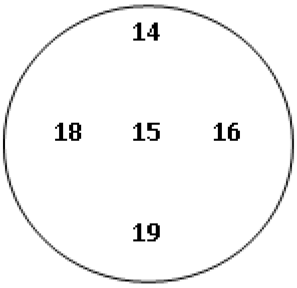
14
18
15
16
19

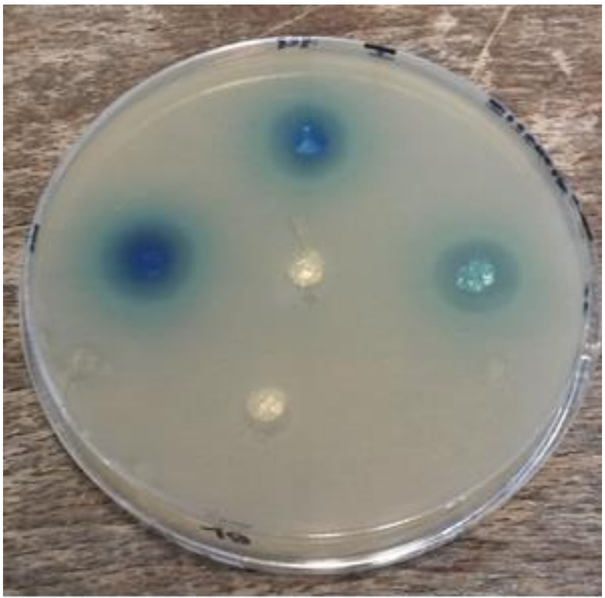

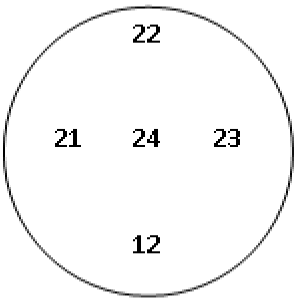
22
21
24
23
12

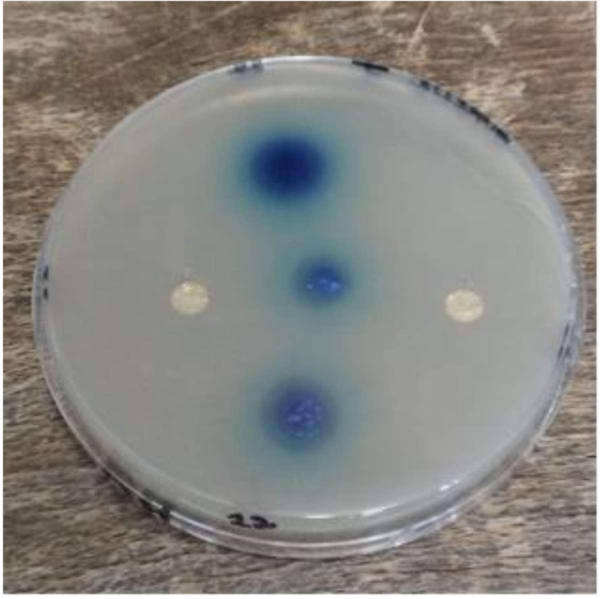

Results at 48 hours:

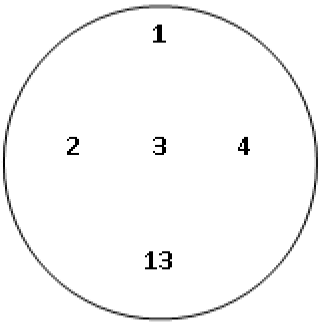

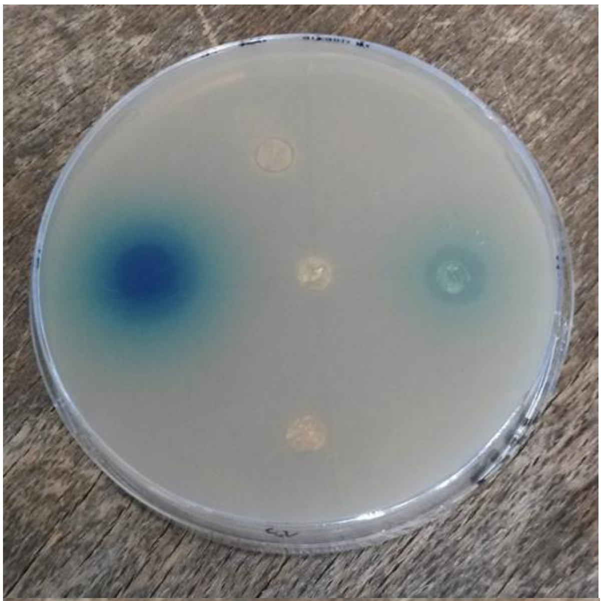

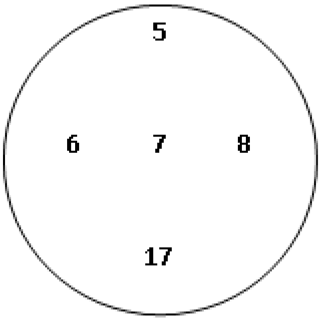

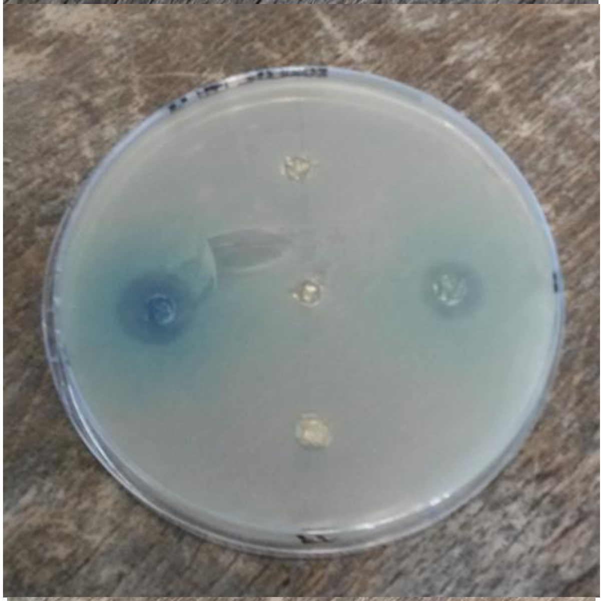

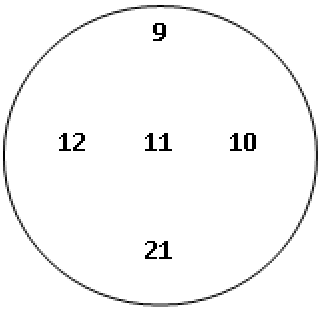

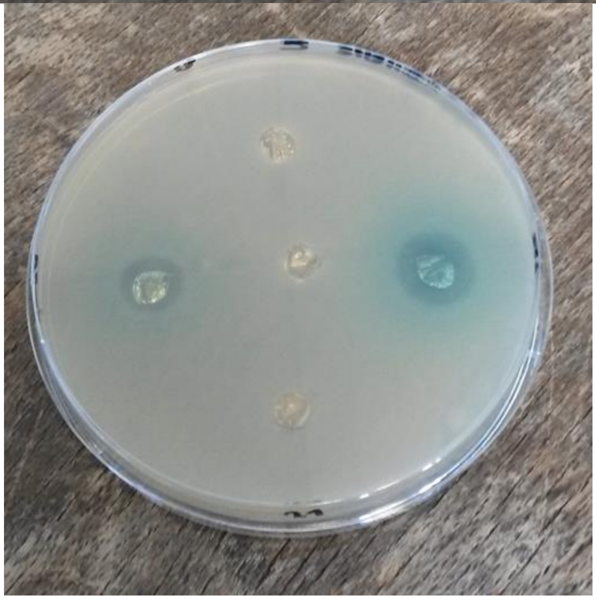

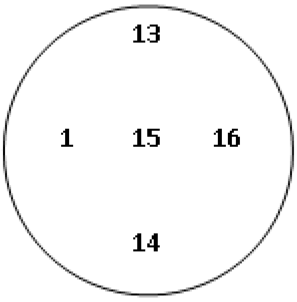
13
1
15
16
14

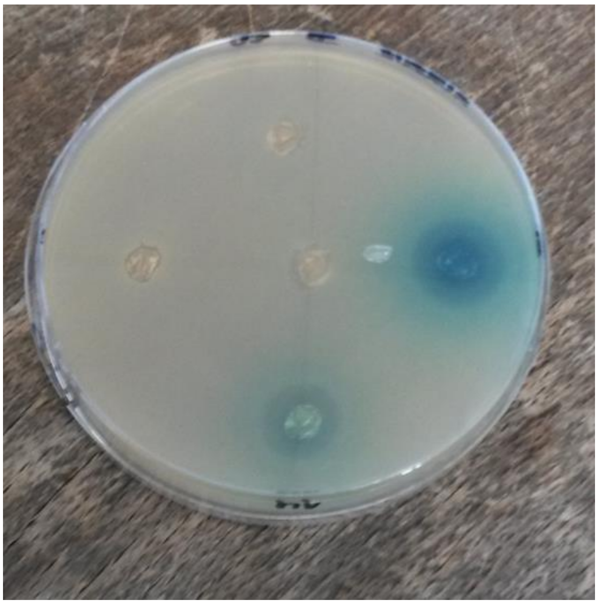

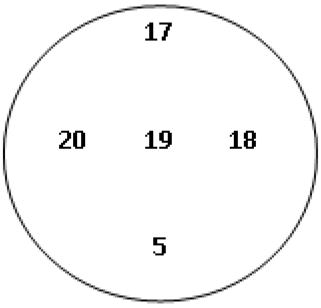
17
20
19
18
5

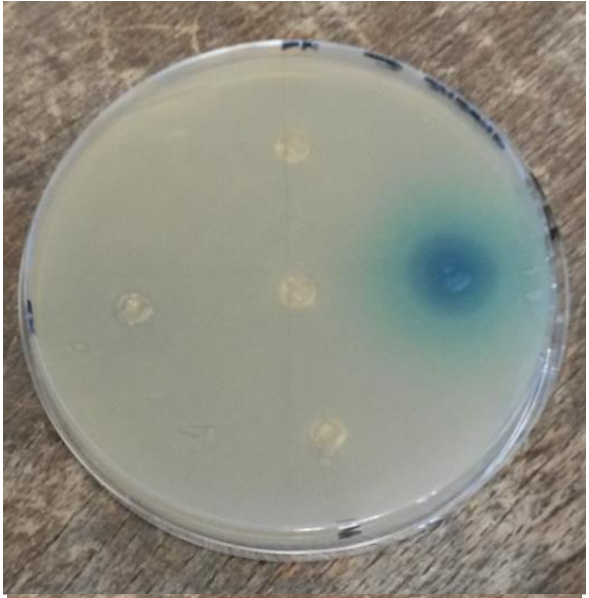

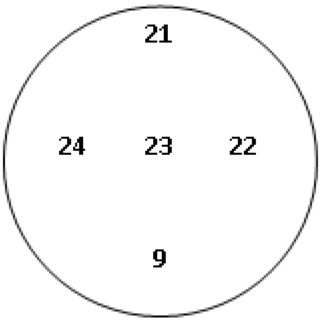
21
24
23
22
9

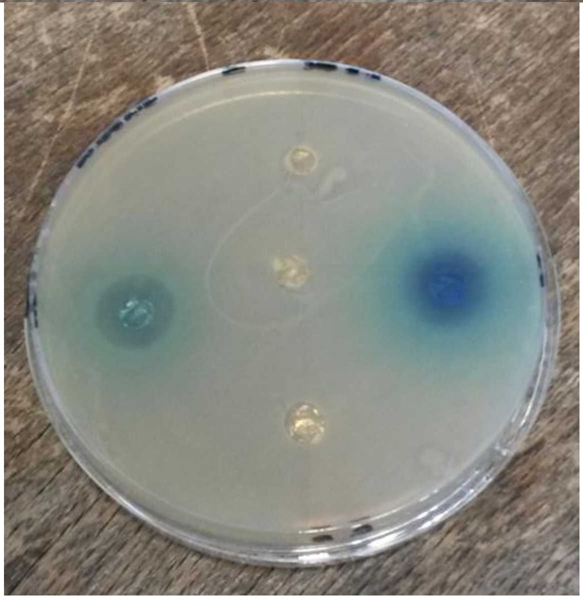

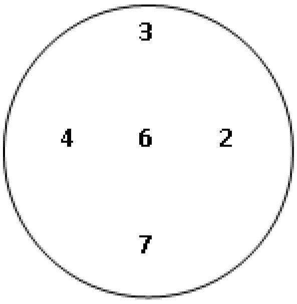
3
4
6
2
7

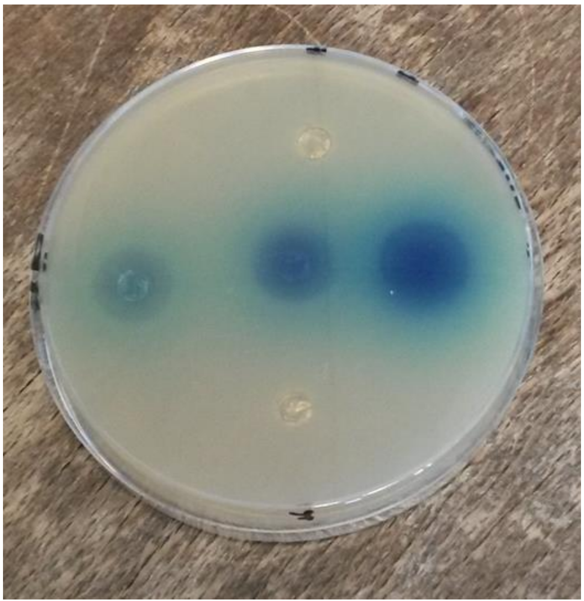

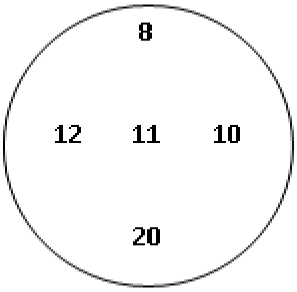
8
12
11
10
20

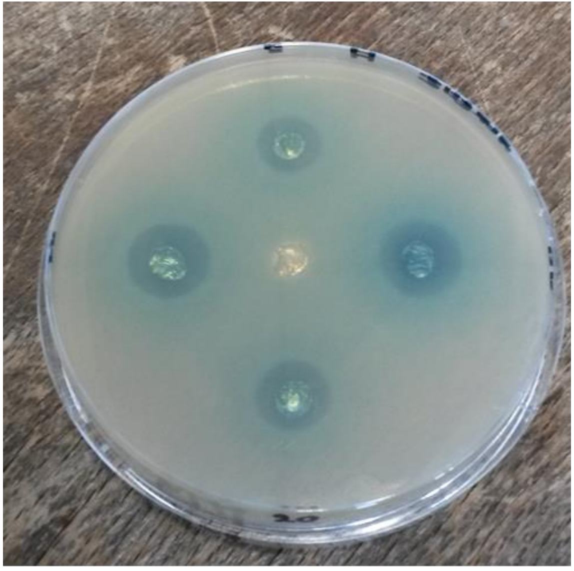
20

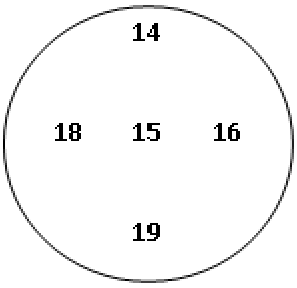
14
18
15
16
19

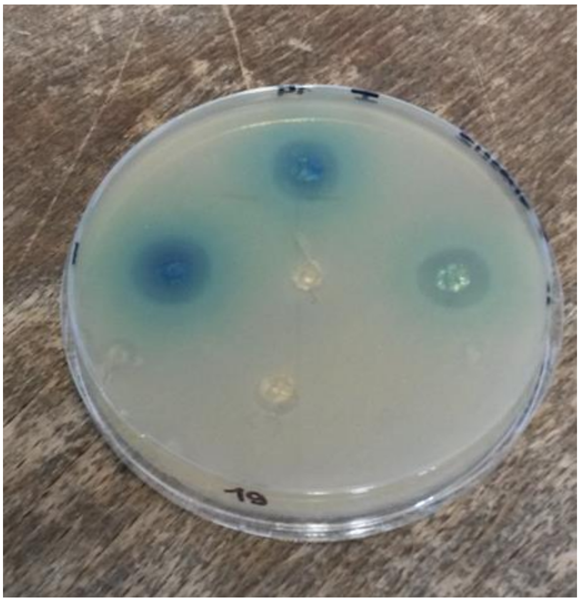
19

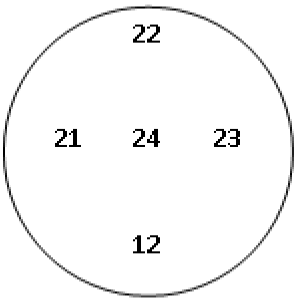
22
21
24
23
12

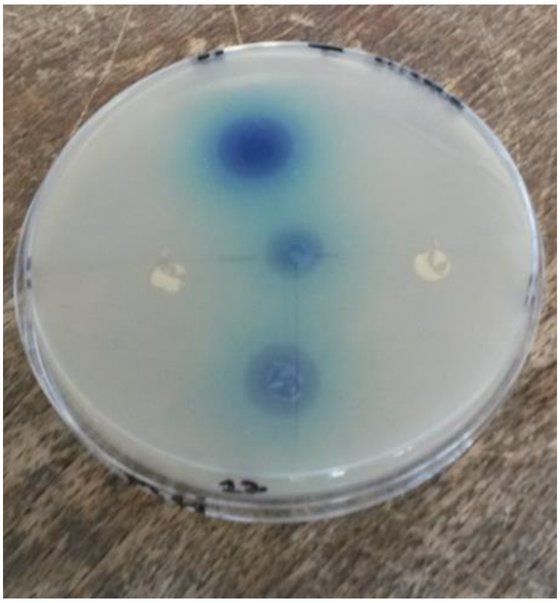

7.Release kinetic study of methylene blue loaded membranes

To evaluate the kinetics of methylene blue release from the polysaccharide membranes, the absorbance of the antibiotic in ionic buffer solutions was measured with a UV-Visible spectrophotometer (Shimadzu, UV-2101 PC).

To evaluate the release of methylene blue form the electrospun membranes, whether they were encapsulated in cyclodextrins or not, two calibration lines were first established to determine the molar extinction coefficient of pure methylene blue and methylene blue encapsulated in β-cyclodextrin.

Determination of the molar extinction coefficient of methylene blue

The calibration curves were established by preparing multiple solutions with different methylene blue or methylene blue inclusion complex concentrations in a pH=7.4 buffer. The absorption of each solution was measured for different wavelength λ (λ = 614.5, 633, 653 and 663 nm). The solutions concentration versus absorption was then plotted.

The molar extinction coefficient of methylene blue (native or encapsulated) was determined as being part of the slope. According to the Beer-Lambert law:

$$A = \varepsilon \times l \times c \qquad (5)$$

Where A is the absorption value measured with the UV-Vis spectrophotometer, l is the pathlength through the sample, c its concentration and ε is the molar extinction coefficient of methylene blue. The UV cells (Roth, polystyrene (PS), 70-850 µL cells) used for these experiments exhibited a 1 cm pathlength.

The following calibration curves were obtained:

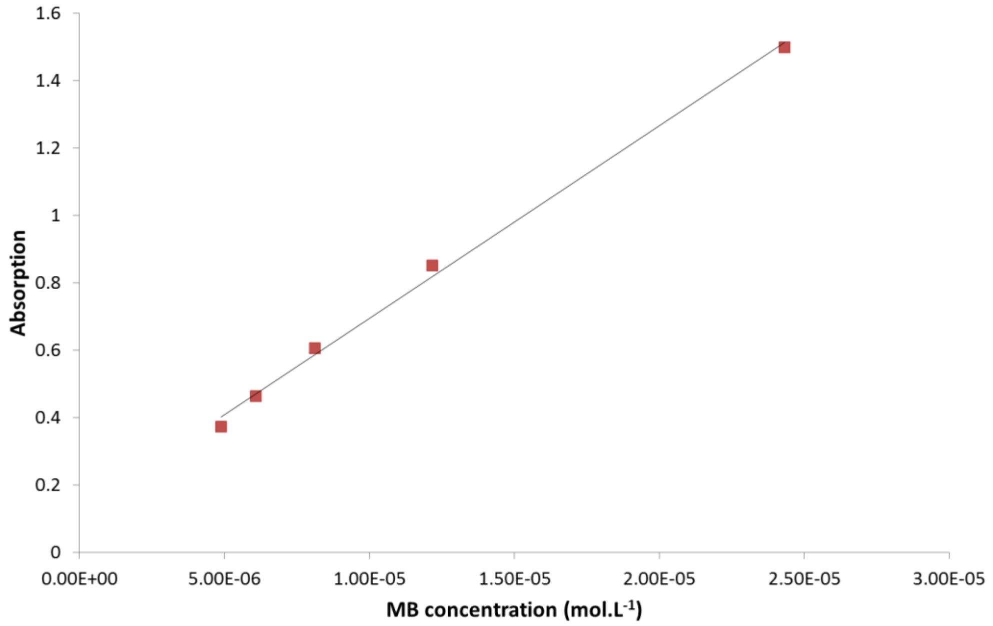

Figure 5.12. Calibration line of the absorption of methylene blue in a pH=7.4 ionic buffer

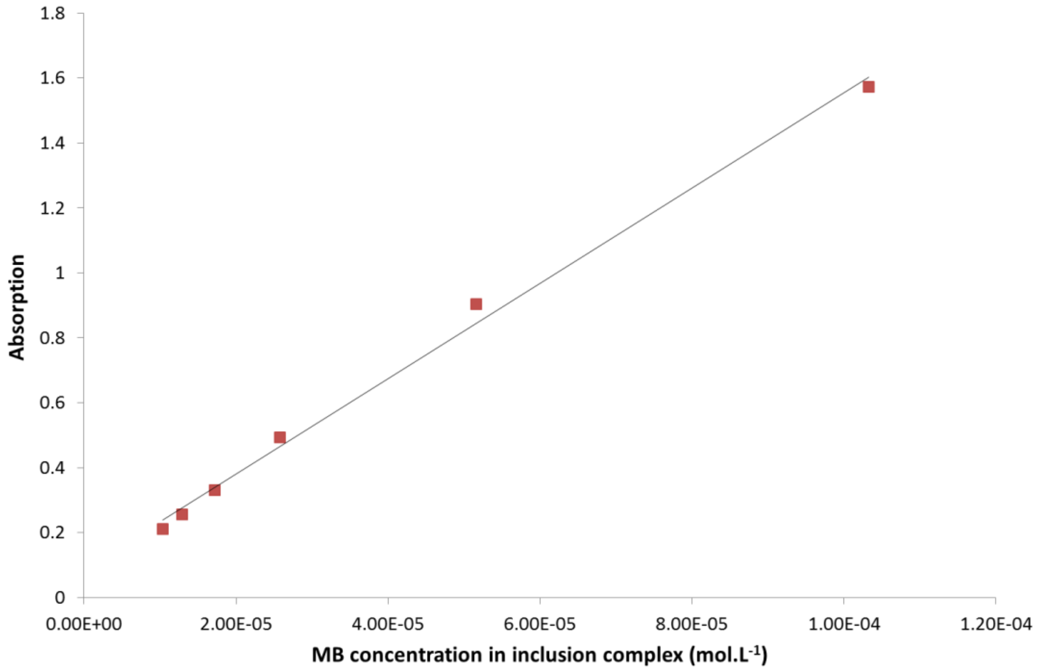

Figure 5.13. Calibration line of the absorption of methylene blue inclusion complex in a pH=7.4 ionic buffer

The following table details the average calculated molar extinction coefficient (ε_{MB}) of methylene blue when used as such and when encapsulated in β-cyclodextrin:

	ε_{MB} (L.mol^{-1}.cm^{-1})
Pure methylene blue	52 590
Encapsulated methylene blue	13 490

Table 5.3. Molar extinction coefficients determined for pure methylene blue and methylene blue inclusion complexes

Release kinetic study of the polyelectrolyte complex (PEC) based membranes

For these tests, small discs of the PEC based membranes with a 1.6 cm diameter were cut and immersed in 20 mL of the ionic buffer at pH=7.4. Methylene blue and methylene blue inclusion complexes were then released within the buffer. The amount of methylene blue was determined by absorption measurements by UV-Vis spectroscopy. The selected wavelength for the absorption was around λ= 640 nm.

At regular time intervals, 0.8 mL of the supernatant was removed and analysed. Using the Beer-Lambert law and the previously calculated molar absorption coefficients, the concentration of methylene blue was determined and thus the amount of methylene blue in the buffer. The release kinetic study was performed over 5 days.

References

References

1. Zafar, N.; Fessi, H.; Elaissari, A. *International Journal of Pharmaceutics* **2014,** 461, (1-2), 351-366.
2. Wenz, G. *Angewandte Chemie (International Edition in English)* **1994,** 33, (8), 803-822.
3. Szejtli, J. *Chemical Reviews* **1998,** 98, (5), 1743-1753.
4. Del Valle, E. M. M. *Process Biochemistry* **2004,** 39, (9), 1033-1046.
5. Irie, T.; Uekama, K. *Journal of Pharmaceutical Sciences* **1997,** 86, (2), 147-162.
6. Kurkov, S. V.; Loftsson, T. *International Journal of Pharmaceutics* **2013,** 453, (1), 167-180.
7. French, D.; Levine, M. L.; Pazur, J. H.; Norberg, E. *Journal of the American Chemical Society* **1949,** 71, (1), 353-356.
8. Cramer, F.; Hettler, H. *Die Naturwissenschaften* **1967,** 54, (24), 625-632.
9. W., S., Organische Einschluß-Verbindungen. In *Fortschritte der Chemischen Forschung* Springer, Ed. Springer Berlin Heidelberg: 1951; Vol. 2, pp 92-145.
10. Ikeda, K.; Uekama, K.; Otagiri, M. *Chemical and Pharmaceutical Bulletin* **1975,** 23, (1), 201-208.
11. Schlenk, H.; Sand, D. M.; Tillotson, J. A. *Journal of the American Chemical Society* **1955,** 77, (13), 3587-3590.
12. Challa, R.; Ahuja, A.; Ali, J.; Khar, R. K. *AAPS PharmSciTech [electronic resource].* **2005,** 6, (2), E329-357.
13. Loftsson, T.; Brewster, M. E. *Journal of Pharmaceutical Sciences* **1996,** 85, (10), 1017-1025.
14. Brewster, M. E.; Loftsson, T. *Advanced Drug Delivery Reviews* **2007,** 59, (7), 645-666.
15. Salustio, P. J.; Pontes, P.; Conduto, C.; Sanches, I.; Carvalho, C.; Arrais, J.; Marques, H. M. C. *AAPS PharmSciTech* **2011,** 12, (4), 1276-1292.
16. Uekama, K.; Hirayama, F.; Irie, T. *Chemical Reviews* **1998,** 98, (5), 2045-2076.
17. Steed, J. W.; Atwood, J.L., *Supramolecular chemistry* John Wiley and Sons Ltd: 2009.
18. Connors, K. A. *Chemical Reviews* **1997,** 97, (5), 1325-1357.
19. Cheppudira, B.; Fowler, M.; McGhee, L.; Greer, A.; Mares, A.; Petz, L.; Devore, D.; Loyd, D. R.; Clifford, J. L. *Expert Opinion on Investigational Drugs* **2013,** 22, (10), 1295-1303.
20. Srimal, R. C. *Fitoterapia* **1997,** 68, (6), 483-493.
21. Elion, R. A.; Cohen, C. *Primary Care - Clinics in Office Practice* **1997,** 24, (4), 905-919.
22. Seiler, N.; Atanassov, C. L.; Raul, F. *International Journal of Oncology* **1998,** 13, (5), 993-1006.
23. Huang, M. T.; Newmark, H. L.; Frenkel, K. *Journal of Cellular Biochemistry* **1997,** 67, (SUPPL. 27), 26-34.
24. Radjaram, A.; Fuad Hafid, A.; Setyawan, D. *International Journal of Pharmacy and Pharmaceutical Sciences* **2013,** 5, (SUPPL 3), 401-405.
25. Tang, B.; Ma, L.; Wang, H. Y.; Zhang, G. Y. *Journal of Agricultural and Food Chemistry* **2002,** 50, (6), 1355-1361.

26. Mohan, P. R. K.; Sreelakshmi, G.; Muraleedharan, C. V.; Joseph, R. *Vibrational Spectroscopy* **2012,** 62, 77-84.

27. Yallapu, M. M.; Jaggi, M.; Chauhan, S. C. *Colloids and Surfaces B: Biointerfaces* **2010,** 79, (1), 113-125.

28. Yadav, V. R.; Suresh, S.; Devi, K.; Yadav, S. *AAPS PharmSciTech* **2009,** 10, (3), 752-762.

29. Boztas, A. O.; Karakuzu, O.; Galante, G.; Ugur, Z.; Kocabas, F.; Altuntas, C. Z.; Yazaydin, A. O. *Molecular Pharmaceutics* **2013,** 10, (7), 2676-2683.

30. Sun, X. Z.; Williams, G. R.; Hou, X. X.; Zhu, L. M. *Carbohydrate Polymers* **2013,** 94, (1), 147-153.

31. Pinheiro, A. C.; Bourbon, A. I.; Quintas, M. A. C.; Coimbra, M. A.; Vicente, A. A. *Innovative Food Science and Emerging Technologies* **2012,** 16, 227-232.

32. Shen, Y.; Liu, S.; Wang, L.; Yin, P.; He, Y. *Luminescence* **2014,** 29, (7), 884-892.

33. Ge, X.; Li, C.; Fan, C.; Feng, X.; Cao, B. *Applied Physics A: Materials Science and Processing* **2013,** 113, (3), 583-589.

34. Martin, A.; Tabary, N.; Leclercq, L.; Junthip, J.; Aubert-Viard, F.; Chai, F.; Blanchemain, N.; Martel, B. In *Controlled release of encapsulated methylene blue in a multilayered textile coating*, MATEC Web of Conferences, 2013; 2013.

35. Mahmood, T. A., F. ; Mahmood, I. ; Kishwar F. ; Wahab, A.;. *European Academic research* **2013,** 1, (6), 1100 - 1109.

36. Zhang, G.; Shuang, S.; Dong, C.; Pan, J. *Spectrochimica Acta - Part A: Molecular and Biomolecular Spectroscopy* **2003,** 59, (13), 2935-2941.

37. Zhao, G. C.; Zhu, J. J.; Zhang, J. J.; Chen, H. Y. *Analytica Chimica Acta* **1999,** 394, (2-3), 337-344.

38. Huang, J.; Feng, Z.; Yang, L.; Qian, Y.; Zhang, Q.; Li, F. *Analytical Methods* **2012,** 4, (12), 4264-4268.

39. Yuan, Z.; Zhu, M.; Han, S. *Analytica Chimica Acta* **1999,** 389, (1-3), 291-298.

40. Chen, D. W.; Hsu, Y.-H.; Liao, J.-Y.; Liu, S.-J.; Chen, J.-K.; Ueng, S. W.-N. *International Journal of Pharmaceutics* **2012,** 430, (1-2), 335-341.

41. Ketonis, C.; Barr, S.; Adams, C. S.; Shapiro, I. M.; Parvizi, J.; Hickok, N. J. *Antimicrobial Agents and Chemotherapy* **2011,** 55, (2), 487-494.

42. Thatiparti, T. R.; Von Recum, H. A. *Macromolecular Bioscience* **2010,** 10, (1), 82-90.

43. Forster, H.; Marotta, J. S.; Heseltine, K.; Milner, R.; Jani, S. *Journal of Orthopaedic Research* **2004,** 22, (3), 671-677.

44. Jia, Y.; Joly, H.; Omri, A. *International Journal of Pharmaceutics* **2008,** 359, (1-2), 254-263.

45. Hoang Thi, T. H.; Chai, F.; Leprêtre, S.; Blanchemain, N.; Martel, B.; Siepmann, F.; Hildebrand, H. F.; Siepmann, J.; Flament, M. P. *International Journal of Pharmaceutics* **2010,** 400, (1-2), 74-85.

46. Blanchemain, N.; Laurent, T.; Chai, F.; Neut, C.; Haulon, S.; Krump-konvalinkova, V.; Morcellet, M.; Martel, B.; Kirkpatrick, C. J.; Hildebrand, H. F. *Acta Biomaterialia* **2008,** 4, (6), 1725-1733.

47. Simoes, S. M. N.; Veiga, F.; Torres-Labandeira, J. J.; Ribeiro, A. C. F.; Sandez-Macho, M. I.; Concheiro, A.; Alvarez-Lorenzo, C. *European Journal of Pharmaceutics and Biopharmaceutics* **2012,** 80, (1), 103-112.

48. Ferrari, F.; Sorrenti, M.; Rossi, S.; Catenacci, L.; Sandri, G.; Bonferoni, M. C.; Caramella, C.; Bettinetti, G. *Pharmaceutical Development and Technology* **2008,** 13, (1), 65-73.

49. Jean-Baptiste, E.; Blanchemain, N.; Martel, B.; Neut, C.; Hildebrand, H. F.; Haulon, S. *European Journal of Vascular and Endovascular Surgery* **2012,** 43, (2), 188-197.

50. Zarif, M. S.; Afidah, A. R.; Abdullah, J. M.; Shariza, A. R. *Biomedical Research (India)* **2012,** 23, (4), 513-520.

51. Wenz, G.; Keller, B. *Angewandte Chemie (International Edition in English)* **1992,** 31, (2), 197-199.

52. Harada, A.; Li, J.; Nakamitsu, T.; Kamachi, M. *Journal of Organic Chemistry* **1993,** 58, (26), 7524-7528.

53. Ogata, N.; Sanui, K.; Wada, J. *J Polym Sci Part B Polym Lett* **1976,** 14, (8), 459-462.

54. Harada, A.; Furue, M.; Nozakura, S. I. *Macromolecules* **1976,** 9, (5), 701-704.

55. Harada, A.; Furue, M.; Nozakura, S. I. *Macromolecules* **1976,** 9, (5), 705-710.

56. Uemura, T.; Moro, T.; Komiyama, J.; Iijima, T. *Macromolecules* **1979,** 12, (4), 737-739.

57. Vohlídal, J.; Wilks, E. S.; Yerin, A.; Fradet, A.; Hellwich, K. H.; Hodge, P.; Kahovec, J.; Mormann, W.; Stepto, R. F. T. *Pure and Applied Chemistry* **2012,** 84, (10), 2135-2165.

58. Harada, A., Design and Construction of Supramolecular Architectures Consisting of Cyclodextrins and Polymers. In *Advances in Polymer Science*, 1997; Vol. 133, pp 141-191.

59. Travelet, C.; Schlatter, G.; Hébraud, P.; Brochon, C.; Lapp, A.; Hadziioannou, G. *Langmuir* **2009,** 25, (15), 8723-8734.

60. Harada, A. *Accounts of Chemical Research* **2001,** 34, (6), 456-464.

61. Schmidt, B. V. K. J.; Hetzer, M.; Ritter, H.; Barner-Kowollik, C. *Progress in Polymer Science* **2014,** 39, (1), 235-249.

62. Huang, L.; Allen, E.; Tonelli, A. E. *Polymer* **1998,** 39, (20), 4857-4865.

63. Williamson, B. R.; Tonelli, A. E. *Journal of Inclusion Phenomena and Macrocyclic Chemistry* **2012,** 72, (1-2), 71-78.

64. Fujita, H.; Ooya, T.; Yui, N. *Macromolecules* **1999,** 32, (8), 2534-2541.

65. Collins, C. J.; McCauliff, L. A.; Hyun, S. H.; Zhang, Z.; Paul, L. N.; Kulkarni, A.; Zick, K.; Wirth, M.; Storch, J.; Thompson, D. H. *Biochemistry* **2013,** 52, (19), 3242-3253.

66. Perry, C.; Hébraud, P.; Gernigon, V.; Brochon, C.; Lapp, A.; Lindner, P.; Schlatter, G. *Soft Matter* **2011,** 7, (7), 3502-3512.

67. Wenz, G.; Han, B. H.; Muller, A. *Chemical Reviews* **2006,** 106, (3), 782-817.

68. Samitsu, S.; Araki, J.; Kataoka, T.; Ito, K. *Journal of Polymer Science Part B: Polymer Physics* **2006,** 44, (14), 1985-1994.

69. Harata, K. *Chemical Reviews* **1998,** 98, (5), 1803-1827.

70. Kawaguchi, Y.; Nishiyama, T.; Okada, M.; Kamachi, M.; Harada, A. *Macromolecules* **2000,** 33, (12), 4472-4477.

71. Lu, J.; Mirau, P. A.; Tonelli, A. E. *Macromolecules* **2001,** 34, (10), 3276-3284.

72. Rusa, C. C.; Fox, J.; Tonelli, A. E. *Macromolecules* **2003,** 36, (8), 2742-2747.

73. Wang, P. J.; Ye, L.; Zhang, A. Y.; Feng, Z. G. *Polymer International* **2013,** 63, 1025-1034.

74. Harada, A.; Kawaguchi, Y.; Nishiyama, T.; Kamachi, M. *Macromolecular Rapid Communications* **1997,** 18, (7), 535-539.

75. Shin, K. M.; Dong, T.; He, Y.; Taguchi, Y.; Oishi, A.; Nishida, H.; Inoue, Y. *Macromolecular Bioscience* **2004,** 4, (12), 1075-1083.

76. Wang, P. j.; Wang, J.; Ye, L.; Zhang, A. y.; Feng, Z. g. *Polymer* **2012,** 53, 2361-2368.

77. Wang, L. U.; Wang, J. L.; Dong, C. M. *Journal of Polymer Science, Part A: Polymer Chemistry* **2005,** 43, (20), 4721-4730.

78. Dai, X.-H.; Dong, C.-M.; Fa, H.-B.; Yan, D.; Wei, Y. *Biomacromolecules* **2006,** 7, (12), 3527-3533.

79. Dong, T.; Mori, T.; Pan, P.; Kai, W.; Zhu, B.; Inoue, Y. *Journal of Applied Polymer Science* **2009,** 112, (4), 2351-2357.

80. Ito, K. *Current Opinion in Solid State and Materials Science* **2010,** 14, (2), 28-34.

81. Zhang, S.; Yu, Z.; Govender, T.; Luo, H.; Li, B. *Polymer* **2008,** 49, (15), 3205-3210.

82. Arunachalam, M.; Gibson, H. W. *Progress in Polymer Science* **2014,** 39, (6), 1043-1073.

83. Harada, A.; Takashima, Y.; Nakahata, M. *Accounts of Chemical Research* **2014,** 47, (7), 2128-2140.

84. Yui, N., Emerging biomedical functions through 'mobile' polyrotaxanes. In *Supramolecular Polymer Chemistry*, Wiley-VCH, Ed. 2012; pp 195-204.

85. Li, J.; Li, X.; Ni, X.; Wang, X.; Li, H.; Leong, K. W. *Biomaterials* **2006,** 27, (22), 4132-4140.

86. Adeli, M.; Kalantari, M.; Parsamanesh, M.; Sadeghi, E.; Mahmoudi, M. *Nanomedicine: Nanotechnology, Biology and Medicine* **2011,** 7, (6), 806-817.

87. Li, Y. Y.; Dong, H. Q.; Liu, Y.; Cheng, H.; Li, C.; Xiao, W.; Chang, C.; Hua, S. H.; Zeng, X.; Cheng, S. X.; Zhang, X. Z.; Zhuo, R. X. *Soft Matter* **2011,** 7, (10), 4839-4844.

88. Zhu, J. L.; Liu, K. L.; Zhang, Z.; Zhang, X. Z.; Li, J. *Chemical Communications* **2011,** 47, (48), 12849-12851.

89. Liu, K. L.; Zhang, Z.; Li, J. *Soft Matter* **2011,** 7, (24), 11290-11297.

90. Collins, C. J.; McCauliff, L. A.; Hyun, S. H.; Zhang, Z.; Paul, L. N.; Kulkarni, A.; Zick, K.; Wirth, M.; Storch, J.; Thompson, D. H. *Biochemistry* **2013,** 52, (19), 3242-3253.

91. Chen, Y.; Zhang, Y. M.; Liu, Y. *Chemical Communications* **2010,** 46, (31), 5622-5633.

92. Nostro, P. L.; Fratoni, L.; Ridi, F.; Baglioni, P. *Journal of Applied Polymer Science* **2003,** 88, (3), 706-715.

93. Jazkewitsch, O.; Mondrzyk, A.; Staffel, R.; Ritter, H. *Macromolecules* **2011,** 44, (6), 1365-1371.

94. Ailincai, D.; Ritter, H. *Beilstein Journal of Nanotechnology* **2014,** 5, (1), 651-657.

95. Martel, B.; Ruffin, D.; Weltrowski, M.; Lekchiri, Y.; Morcellet, M. *Journal of Applied Polymer Science* **2005,** 97, (2), 433-442.

96. Blanchemain, N.; Haulon, S.; Boschin, F.; Marcon-Bachari, E.; Traisnel, M.; Morcellet, M.; Hildebrand, H. F.; Martel, B. *Biomolecular Engineering* **2007,** 24, (1 SPEC. ISS.), 149-153.

97. Kacem, I.; Laurent, T.; Blanchemain, N.; Neut, C.; Chai, F.; Haulon, S.; Hildebrand, H. F.; Martel, B. *Journal of Biomedical Materials Research - Part A* **2014,** 102, (9), 2942-2951.

98. Leprêtre, S.; Chai, F.; Hornez, J. C.; Vermet, G.; Neut, C.; Descamps, M.; Hildebrand, H. F.; Martel, B. *Biomaterials* **2009,** 30, (30), 6086-6093.

99. Blanchemain, N.; Laurent, T.; Haulon, S.; Traisnel, M.; Neut, C.; Kirkpatrick, J.; Morcellet, M.; Hildebrand, H. F.; Martel, B. *Journal of Inclusion Phenomena and Macrocyclic Chemistry* **2007,** 57, (1-4), 675-681.

100. Martel, B.; Le Thuaut, P.; Bertini, S.; Crini, G.; Bacquet, M.; Torri, G.; Morcellet, M. *Journal of Applied Polymer Science* **2002,** 85, (8), 1771-1778.

101. Ducoroy, L.; Martel, B.; Bacquet, B.; Morcellet, M. *Journal of Inclusion Phenomena and Macrocyclic Chemistry* **2007,** 57, (1-4), 271-277.

102. Lanza, R.; Langer, R.; Vacanti, J. P., *Principles of Tissue Engineering: Fourth Edition*. 2013; p 1-1887.

103. Doshi, J.; Reneker, D. H. *Journal of Electrostatics* **1995,** 35, (2-3), 151-160.

104. Bognitzki, M.; Czado, W.; Frese, T.; Schaper, A.; Hellwig, M.; Steinhart, M.; Greiner, A.; Wendorff, J. H. *Advanced Materials* **2001,** 13, (1), 70-72.

105. Bhardwaj, N.; Kundu, S. C. *Biotechnology Advances* **2010,** 28, (3), 325-347.

106. Reneker, D. H.; Yarin, A. L.; Fong, H.; Koombhongse, S. *Journal of Applied Physics* **2000,** 87, (9 I), 4531-4547.

107. Reneker, D. H.; Yarin, A. L. *Polymer* **2008,** 49, (10), 2387-2425.

108. Agarwal, S.; Greiner, A.; Wendorff, J. H. *Progress in Polymer Science* **2013,** 38, (6), 963-991.

109. Reneker, D. H.; Yarin, A. L.; Zussman, E.; Xu, H., Electrospinning of Nanofibers from Polymer Solutions and Melts. In *Advances in Applied Mechanics*, Hassan, A.; Erik van der, G., Eds. Elsevier: 2007; Vol. Volume 41, pp 43-346.

110. Park, J. S. *Advances in Natural Sciences: Nanoscience and Nanotechnology* **2010,** 1, (4).

111. Lavielle, N.; Popa, A. M.; De Geus, M.; Hébraud, A.; Schlatter, G.; Thony-Meyer, L.; Rossi, R. M. *European Polymer Journal* **2013,** 49, (6), 1331-1336.

112. Lavielle, N.; Hébraud, A.; Mendoza-Palomares, C.; Ferrand, A.; Benkirane-Jessel, N.; Schlatter, G. *Macromolecular Materials and Engineering* **2012,** 297, (10), 958-968.

113. Rogers, C. M.; Morris, G. E.; Gould, T. W. A.; Bail, R.; Toumpaniari, S.; Harrington, H.; Dixon, J. E.; Shakesheff, K. M.; Segal, J.; Rose, F. R. A. J. *Biofabrication* **2014,** 6, (3).

114. Ahirwal, D.; Hébraud, A.; Kadar, R.; Wilhelm, M.; Schlatter, G. *Soft Matter* **2013,** 9, (11), 3164-3172.

115. Nedjari, S.; Eap, S.; Hébraud, A.; Wittmer, C. R.; Benkirane-Jessel, N.; Schlatter, G. *Macromolecular Bioscience* **2014,** 10.1002/mabi.201400226.

116. Wittmer, C. R. H., A. ; Nedjari, S.; Schlatter, G. *Polymer* **2014,** 55, (22), 5781-5787.

117. Goh, Y. F.; Shakir, I.; Hussain, R. *Journal of Materials Science* **2013,** 48, (8), 3027-3054.

118. Holmes, B.; Castro, N. J.; Zhang, L. G.; Zussman, E. *Tissue Engineering - Part B: Reviews* **2012,** 18, (6), 478-486.

119. Ghasemi-Mobarakeh, L.; Prabhakaran, M. P.; Balasubramanian, P.; Jin, G.; Valipouri, A.; Ramakrishna, S. *Journal of Nanoscience and Nanotechnology* **2013,** 13, (7), 4656-4671.

120. Braghirolli, D. I.; Steffens, D.; Pranke, P. *Drug Discovery Today* **2014,** 19, (6), 743-753.

121. Agarwal, S.; Wendorff, J. H.; Greiner, A. *Advanced Materials* **2009,** 21, (32-33), 3343-3351.

122. Khadka, D. B.; Haynie, D. T. *Nanomedicine: Nanotechnology, Biology, and Medicine* **2012,** 8, (8), 1242-1262.

123. Ji, W.; Sun, Y.; Yang, F.; Van Den Beucken, J. J. J. P.; Fan, M.; Chen, Z.; Jansen, J. A. *Pharmaceutical Research* **2011,** 28, (6), 1259-1272.

124. Ferrand, A.; Eap, S.; Richert, L.; Lemoine, S.; Kalaskar, D.; Demoustier-Champagne, S.; Atmani, H.; Mély, Y.; Fioretti, F.; Schlatter, G.; Kuhn, L.; Ladam, G.; Benkirane-Jessel, N. *Macromolecular Bioscience* **2014,** 14, (1), 45-55.

125. Zamani, M.; Prabhakaran, M. P.; Ramakrishna, S. *International Journal of Nanomedicine* **2013,** 8, 2997-3017.

126. Agarwal, S.; Wendorff, J. H.; Greiner, A. *Macromolecular Rapid Communications* **2010,** 31, (15), 1317-1331.

127. Cipitria, A.; Skelton, A.; Dargaville, T. R.; Dalton, P. D.; Hutmacher, D. W. *Journal of Materials Chemistry* **2011,** 21, (26), 9419-9453.

128. Engelberg, I.; Kohn, J. *Biomaterials* **1991,** 12, (3), 292-304.
129. Woodruff, M. A.; Hutmacher, D. W. *Progress in Polymer Science (Oxford)* **2010,** 35, (10), 1217-1256.
130. Domb, A. J. K., N.; Ezra, A., *Biodegradable polymers in Clinical use and Clinical Development*. John Wiley and Sons Inc.: Hoboken, New Jersey (USA), 2011; p 581.
131. Ravichandran, R.; Sundarrajan, S.; Venugopal, J. R.; Mukherjee, S.; Ramakrishna, S. *Macromolecular Bioscience* **2012,** 12, (3), 286-311.
132. Seo, Y. A.; Pant, H. R.; Nirmala, R.; Lee, J. H.; Song, K. G.; Kim, H. Y. *Journal of Porous Materials* **2012,** 19, (2), 217-223.
133. Koepsell, L.; Remund, T.; Bao, J.; Neufeld, D.; Fong, H.; Deng, Y. *Journal of Biomedical Materials Research - Part A* **2011,** 99 A, (4), 564-575.
134. Barnes, C. P.; Sell, S. A.; Boland, E. D.; Simpson, D. G.; Bowlin, G. L. *Advanced Drug Delivery Reviews* **2007,** 59, (14), 1413-1433.
135. Lin, H. M.; Lin, Y. H.; Hsu, F. Y. *Journal of Materials Science: Materials in Medicine* **2012,** 23, (11), 2619-2630.
136. Place, E. S.; George, J. H.; Williams, C. K.; Stevens, M. M. *Chemical Society Reviews* **2009,** 38, (4), 1139-1151.
137. Sarvestani, A. S.; He, X.; Jabbari, E. *European Biophysics Journal* **2008,** 37, (2), 229-234.
138. Beachley, V.; Wen, X. *Progress in Polymer Science (Oxford)* **2010,** 35, (7), 868-892.
139. Pereira, I. H. L.; Ayres, E.; Averous, L.; Schlatter, G.; Hebraud, A.; De Paula, A. C. C.; Viana, P. H. L.; Goes, A. M.; Oréfice, R. L. *Journal of Materials Science: Materials in Medicine* **2014,** 25, (4), 1137-1148.
140. Goddard, J. M.; Hotchkiss, J. H. *Progress in Polymer Science (Oxford)* **2007,** 32, (7), 698-725.
141. Oyane, A.; Uchida, M.; Choong, C.; Triffitt, J.; Jones, J.; Ito, A. *Biomaterials* **2005,** 26, (15), 2407-2413.
142. Yu, H. S.; Jang, J. H.; Kim, T. I.; Lee, H. H.; Kim, H. W. *Journal of Biomedical Materials Research - Part A* **2009,** 88, (3), 747-754.
143. Serrano, M. C.; Pagani, R.; Vallet-Regí, M.; Peña, J.; Comas, J. V.; Portolés, M. T. *Acta Biomaterialia* **2009,** 5, (6), 2045-2053.
144. Lam, C. X.; Hutmacher, D. W.; Schantz, J. T.; Woodruff, M. A.; Teoh, S. H. *Journal of biomedical materials research. Part A* **2009,** 90, (3), 906-919.
145. Ma, Z.; Mao, Z.; Gao, C. *Colloids and Surfaces B: Biointerfaces* **2007,** 60, (2), 137-157.
146. Gupta, B.; Krishnanand, K.; Deopura, B. L.; Atthoff, B. *Journal of Applied Polymer Science* **2013,** 127, (3), 1744-1750.
147. Martins, A.; Pinho, E. D.; Faria, S.; Pashkuleva, I.; Marques, A. P.; Reis, R. L.; Neves, N. M. *Small* **2009,** 5, (10), 1195-1206.
148. Prabhakaran, M. P.; Venugopal, J.; Chan, C. K.; Ramakrishna, S. *Nanotechnology* **2008,** 19, 455102.
149. Lancuski, A.; Fort, S.; Bossard, F. *ACS Applied Materials and Interfaces* **2012,** 4, (12), 6499-6504.
150. Lancuski, A.; Bossard, F.; Fort, S. *Biomacromolecules* **2013,** 14, (6), 1877-1884.
151. Uyar, T.; Havelund, R.; Hacaloglu, J.; Zhou, X.; Besenbacher, F.; Kingshott, P. *Nanotechnology* **2009,** 20, (12).
152. Uyar, T.; Besenbacher, F. *European Polymer Journal* **2009,** 45, (4), 1032-1037.
153. Uyar, T.; Balan, A.; Toppare, L.; Besenbacher, F. *Polymer* **2009,** 50, (2), 475-480.

154. Uyar, T.; Havelund, R.; Nur, Y.; Hacaloglu, J.; Besenbacher, F.; Kingshott, P. *Journal of Membrane Science* **2009,** 332, (12), 129-137.
155. Uyar, T.; Havelund, R.; Hacaloglu, J.; Besenbacher, F.; Kingshott, P. *ACS Nano* **2010,** 4, (9), 5121-5130.
156. Uyar, T.; Hacaloglu, J.; Besenbacher, F. *Reactive and Functional Polymers* **2009,** 69, (3), 145-150.
157. Canbolat, M. F.; Celebioglu, A.; Uyar, T. *Colloids and Surfaces B: Biointerfaces* **2014,** 115, 15-21.
158. Aytac, Z.; Dogan, S. Y.; Tekinay, T.; Uyar, T. *Colloids and Surfaces B: Biointerfaces* **2014,** 120, 125-131.
159. Celebioglu, A.; Uyar, T. *Chemical Communications* **2010,** 46, (37), 6903-6905.
160. Celebioglu, A.; Uyar, T. *Langmuir* **2011,** 27, (10), 6218-6226.
161. Celebioglu, A.; Umu, O. C. O.; Tekinay, T.; Uyar, T. *Colloids and Surfaces B: Biointerfaces* **2014,** 116, 612-619.
162. Araki, J.; Kataoka, T.; Katsuyama, N.; Teramoto, A.; Ito, K.; Abe, K. *Polymer* **2006,** 47, (25), 8241-8246.
163. Uyar, T.; Kingshott, P.; Besenbacher, F. *Angewandte Chemie - International Edition* **2008,** 47, (47), 9108-9111.
164. Katsuyama, N.; Shimizu, K.; Sato, S.; Kuroiwa, J.; Teramoto, A.; Abe, K.; Araki, J.; Ito, K. *Textile Research Journal* **2010,** 80, (9), 834-840.
165. Katsuyama, N.; Shimizu, K.; Sato, S.; Araki, J.; Teramoto, A.; Abe, K.; Ito, K. *Textile Research Journal* **2010,** 80, (12), 1131-1137.
166. Sakai, Y.; Ueda, K.; Katsuyama, N.; Shimizu, K.; Sato, S.; Kuroiwa, J.; Araki, J.; Teramoto, A.; Abe, K.; Yokoyama, H.; Ito, K. *Journal of Physics Condensed Matter* **2011,** 23, (28), 284108.
167. Dubois, P.; Coulembier, O.; Raquez, J.-M., *Handbook of Ring-Opening Polymerization*. Wiley-VCH ed.; WILEY-VCH Verlag GmbH & Co. KGaA: Weinheim, Germany, 2009.
168. Van Natta, F. J.; Hill, J. W.; Carothers, W. H. *Journal of the American Chemical Society* **1934,** 56, (2), 455-457.
169. Raquez, J. M.; Mincheva, R.; Coulembier, O.; Dubois, P., Ring-Opening Polymerization of Cyclic Esters: Industrial Synthesis, Properties, Applications, and Perspectives. In *Polymer Science: A Comprehensive Reference, 10 Volume Set*, 2012; Vol. 4, pp 761-778.
170. Tanzi, M. C.; Verderio, P.; Lampugnani, M. G.; Resnati, M.; Dejana, E.; Sturani, E. *Journal of Materials Science: Materials in Medicine* **1994,** 5, (6-7), 393-396.
171. Connor, E. F.; Nyce, G. W.; Myers, M.; Möck, A.; Hedrick, J. L. *Journal of the American Chemical Society* **2002,** 124, (6), 914-915.
172. Kamber, N. E.; Jeong, W.; Waymouth, R. M.; Pratt, R. C.; Lohmeijer, B. G. G.; Hedrick, J. L. *Chemical Reviews* **2007,** 107, (12), 5813-5840.
173. Pratt, R. C.; Lohmeijer, B. G. G.; Long, D. A.; Waymouth, R. M.; Hedrick, J. L. *Journal of the American Chemical Society* **2006,** 128, (14), 4556-4557.
174. Simon, L.; Goodman, J. M. *Journal of Organic Chemistry* **2007,** 72, (25), 9656-9662.
175. Lang, M.; Chu, C. C. *Journal of Applied Polymer Science* **2002,** 86, (9), 2296-2306.
176. Araki, J. *Journal of Polymer Science, Part A: Polymer Chemistry* **2010,** 48, (22), 5258-5264.
177. Harada, A.; Okada, M.; Li, J.; Kamachi, M. *Macromolecules* **1995,** 28, (24), 8406-8411.

178. Harada, A.; Kawaguchi, Y.; Nishiyama, T.; Kamachi, M. *Macromolecular Rapid Communications* **1997,** 18, (7), 535-539.
179. Rusa, C. C.; Luca, C.; Tonelli, A. E. *Macromolecules* **2001,** 34, (5), 1318-1322.
180. Travelet, C.; Hébraud, P.; Perry, C.; Brochon, C.; Hadziioannou, G.; Lapp, A.; Schlatter, G. *Macromolecules* **2010,** 43, (4), 1915-1921.
181. Shuai, X.; Porbeni, F. E.; Wei, M.; Bullions, T.; Tonelli, A. E. *Macromolecules* **2002,** 35, (6), 2401-2405.
182. Ninan, N.; Muthiah, M.; Park, I. K.; Kalarikkal, N.; Elain, A.; Wui Wong, T.; Thomas, S.; Grohens, Y. *Materials Letters* **2014,** 132, 34-37.
183. Fathi, M.; Martín, Á.; McClements, D. J. *Trends in Food Science & Technology* **2014,** 39, (1), 18-39.
184. Mesquita, J. P.; Donnici, C. L.; Pereira, F. V. *Biomacromolecules* **2010,** 2010, 473-480.
185. Doh, S. J.; Lee, J. Y.; Lim, D. Y.; Im, J. N. *Fibers and Polymers* **2013,** 14, (12), 2176-2184.
186. Wiegand, C.; Hipler, U. C. *Journal of Wound Care* **2013,** 22, (11), 592-598.
187. Yoon, Y. N.; Im, J. N.; Doh, S. J. *Fibers and Polymers* **2013,** 14, (6), 1012-1018.
188. Domb, A. K., N. ; Ezra, A., *Biodegradable Polymers in Clinical Use and Clinical Development.* John Wiley and Sons, Inc.: New Jersey, 2011.
189. Ding, F.; Deng, H.; Du, Y.; Shi, X.; Wang, Q. *Nanoscale* **2014,** 6, (16), 9477-9493.
190. Seyrek, E.; Decher, G. *Polymer Science* **2012,** 7, 159-185.
191. Nakajima, A. *Journal of Macromolecular Science-Physics* **1980,** B17, (4), 715-721.
192. Wang, Q.; Schlenoff, J. B. *Macromolecules* **2014,** 47, (9), 3108-3116.
193. Tsuchida, E. O., Y; Ohno, H. *Journal of Macromolecular Science-Physics* **1980,** B17, (4), 683-714.
194. Lankalapalli, S.; Kolapalli, V. R. M. *Indian Journal of Pharmaceutical Sciences* **2009,** 71, (5), 481-487.
195. Pergushov, D. V.; Müller, A. H. E.; Schacher, F. H. *Chemical Society Reviews* **2012,** 41, (21), 6888-6901.
196. Hariri, H. H.; Schlenoff, J. B. *Macromolecules* **2010,** 43, (20), 8656-8663.
197. Yoon, H.; Dell, E. J.; Freyer, J. L.; Campos, L. M.; Jang, W. D. *Polymer* **2014,** 55, (2), 453-464.
198. Deeksha; Malviya, R.; Sharma, P. K. *Recent Patents on Nanotechnology* **2014,** 8, (2), 129-141.
199. Pillay, V.; Seedat, A.; Choonara, Y. E.; Du Toit, L. C.; Kumar, P.; Ndesendo, V. M. K. *AAPS PharmSciTech* **2013,** 14, (2), 692-711.
200. Krishnan, R.; Sundarrajan, S.; Ramakrishna, S. *Macromolecular Materials and Engineering* **2013,** 298, (10), 1034-1058.
201. Saquing, C. D.; Tang, C.; Monian, B.; Bonino, C. A.; Manasco, J. L.; Alsberg, E.; Khan, S. A. *Industrial and Engineering Chemistry Research* **2013,** 52, (26), 8692-8704.
202. Liu, Y.; Park, M.; Shin, H. K.; Pant, B.; Park, S. J.; Kim, H. Y. *Materials Letters* **2014,** 132, 23-26.
203. Van Hong Thien, D.; Hsiao, S.; Ho, M.; Li, C.; Shih, J. *Journal of Materials Science* **2013,** 48, (4), 1640-1645.
204. Bonino, C. A.; Krebs, M. D.; Saquing, C. D.; Jeong, S. I.; Shearer, K. L.; Alsberg, E.; Khan, S. A. *Carbohydrate Polymers* **2011,** 85, (1), 111-119.
205. Lee, K. Y.; Jeong, L.; Kang, Y. O.; Lee, S. J.; Park, W. H. *Advanced Drug Delivery Reviews* **2009,** 61, (12), 1020-1032.

206. Jeong, S. K., MD. ; Bonino, CA.; Samorezov, JE. ; Khan, SA. ; Alsberg, E. *Tissue Engineering: Part A* **2011,** 17, (1-2), 59-70.
207. Knill, C. J.; Kennedy, J. F.; Mistry, J.; Miraftab, M.; Smart, G.; Groocock, M. R.; Williams, H. J. *Carbohydrate Polymers* **2004,** 55, (1), 65-76.
208. Ma, G.; Liu, Y.; Fang, D.; Chen, J.; Peng, C.; Fei, X.; Nie, J. *Materials Letters* **2012,** 74, 78-80.
209. Hu, W.-W.; Yu, H.-N. *Carbohydrate Polymers* **2013,** 95, (2), 716-727.
210. Penchev, H.; Paneva, D.; Manolova, N.; Rashkov, I. *Macromolecular Rapid Communications* **2008,** 29, (8), 677-681.
211. Xu, J. C., N. ; Xu, W. ; Xue, Y. ; Wang, Z. ; Dai, Q. ; Yu, F. . *Nanotechnology* **2013,** 24, (2), 025701.
212. Smitha, B.; Sridhar, S.; Khan, A. A. *European Polymer Journal* **2005,** 41, (8), 1859-1866.
213. Xu, J.; Cai, N.; Xu, W.; Xue, Y.; Wang, Z.; Dai, Q.; Yu, F. *Nanotechnology* **2013,** 24, (2), 025701.
214. Verma, D.; Desai, M. S.; Kulkarni, N.; Langrana, N. *Materials Science and Engineering C* **2011,** 31, (8), 1741-1747.
215. Fernandes, S. C. M.; Freire, C. S. R.; Silvestre, A. J. D.; Neto, C. P.; Gandini, A.; Berglund, L. A.; Salmen, L. *Carbohydrate Polymers* **2010,** 81, 394-401.
216. Sklarz, B. *Quarterly Reviews, Chemical Society* **1967,** 21, (1), 3-28.
217. Mitschang, F.; Schmalz, H.; Agarwal, S.; Greiner, A. *Angewandte Chemie International Edition* **2014,** 53, (19), 4972-4975.
218. Thompson , K. F., *Modification of polymeric substrates using surface-grafted nanoscaffolds*. Georgia Institute of Technology: 2005.

Publications and Valorization

Publications and Valorization

Article in Macromolecular Rapid Communications (DOI: 10.1002/marc.201400533)

DOI: 10.1002/marc.2014#####

Article Type: Communication

Star-pseudopolyrotaxane organized in nanoplatelet micelles for poly(ε-caprolactone)-based nanofibrous scaffolds with enhanced surface reactivity

Murielle Oster[1], Anne Hébraud[1], Sébastien Gallet[1], Alain Lapp[2], Eric Pollet[1], Luc Avérous[1], Guy Schlatter[1]*

Murielle Oster, Dr. Anne Hébraud, Dr. Sébastien Gallet, Dr. Eric Pollet, Pr. Luc Avérous, Pr. Guy Schlatter
ICPEES Institut de Chimie et Procédés pour l'Energie, l'Environnement et la Santé, UMR 7515, CNRS, Université de Strasbourg, 25 Rue Becquerel, 67089 Strasbourg Cedex, France
E-mail: murielle.oster@etu.unistra.fr ; anne.hebraud@unistra.fr ; sebastien.gallet@unistra.fr ; eric.pollet@unistra.fr ; luc.averous@unistra.fr ; guy.schlatter@unistra.fr

Dr. Alain Lapp
Laboratoire Léon Brillouin, LLB, CEA Saclay, Bat 56, 91191 Gif-Sur-Yvette, France
Email : alain.lapp@cea.fr

Herein, we demonstrated that star pseudopolyrotaxanes (star-pPRs) obtained from the inclusion complexation of α-cyclodextrin (CD) and four-branched star poly(ε-caprolactone) (star-PCL) organized into nanoplatelet micelles in dimethyl sulfoxide at 35°C. This peculiar property, not observed for linear pseudopolyrotaxanes, allowed the processing of star-pPRs while preserving their supramolecular assembly. Thus, original PCL:star-pPR core:shell nanofibers were elaborated by coaxial electrospinning. The star-pPR shell ensured the presence of available CD hydroxyl functions on the fiber surface allowing its post-functionalization. As proof of concept, fluorescein isothiocyanate was grafted. Moreover, the morphology of the fibers was maintained thanks to the star-pPR shell that acted as a shield preventing the fiber dissolution during chemical modification. The proposed strategy is simple and avoids the synthesis of polyrotaxanes, i.e. the pPR end-capping to prevent the CD

dethreading. Furthermore, because PCL is widely used for biomedical applications, this strategy paves the way for simple functionalization with any bioactive molecules.

1. Introduction

Cyclodextrins, FDA aproved cyclic oligosaccharides of 6, 7 or 8 glucose units (α-, β- or γ-cyclodextrins, respectively), are well-known to form pseudopolyrotaxanes with many types of polymer chains[1]. These necklace-like supramolecular inclusion complexes are of great interest due to the possible grafting of active molecules on the hydroxyl groups carried by the cyclodextrins allowing thus the functionalization of intrinsically inert polymers[2-5]. As an example, it was demonstrated that poly(ε-caprolactone) (PCL) can form pseudopolyrotaxanes (pPRs) with α-cyclodextrins (CDs)[6-8] paving thus the way for biomedical applications. Indeed, PCL is depicted these last decades as a key material, especially for tissue engineering[9]. PCL is widely used for the elaboration by electrospinning of fibrous scaffolds mimicking living tissues[10] because it is a low cost, biocompatible, biodegradable and FDA approved[11] polyester, with suitable mechanical properties[9]. However, despite these excellent properties, PCL scaffolds do not present any specific biological surface activity and the grafting of bioactive molecules cannot be achieved easily. Therefore, a smart approach allowing the functionalization of PCL-based scaffolds could be the use of pPRs. The aim of this letter is to show that pPRs can be organized in the form of stable micelles that can be further used as building blocks to elaborate reactive PCL based fibrous nanocomposite scaffolds.

During their synthesis, pseudopolyrotaxanes generally precipitate in the form of polycrystal clusters due to favorable interactions between their rotaxane tubular portions[12-15]. These crystal domains render the pseudopolyrotaxanes insoluble in most common solvents[16-18]. Moreover, the few known solvents, such as dimethyl sulfoxide (DMSO) or ionic solvents[19], able to solubilize pseudopolyrotaxanes, generally also destabilize the supramolecular assembly due to cyclodextrin dethreading. Thus, the processing of pseudopolyrotaxanes to elaborate functional nanomaterials remains a challenge. However, by studying the recrystallization phenomenon in polar solvents of different architectures of PCL-based pPR, Chung et al.[20] showed that the polycrystal clusters reorganized in long-range microfiber monocrystals. The authors suggested that such phenomenon was possible due to the breaking of the clusters into single monocrystal rotaxane bundles before their reorganization in the form of large microfibers. Thus, this work seems to show that it is possible to prepare a suspension made of isolated small monocrystal pPR bundles in polar solvents without breaking the supramolecular assembly.

Herein, we report the synthesis and the characterization of CD/PCL pseudopolyrotaxanes with a linear or a star architecture, respectively lin-pPR or star-pPR. Then, using small angle neutron scattering (SANS) experiments, the pPR structure in DMSO-d_6 was investigated showing that isolated nanoplatelet micelles of star-pPRs could be obtained. As an application, PCL:star-pPR core:shell fibers were prepared by coaxial electrospinning. Finally, the fiber surface was subsequently modified by grafting fluorescein isothiocyanate (FITC) on the cyclodextrin hydroxyl functions to prove that functionalization of such PCL-based nanofibrous scaffolds is possible.

2. Results and Discussion

2.1. Structure of star-pPRs in DMSO

A four-branched star PCL with a molar mass M_n of 10 kg/mol and a linear PCL of same M_n were used to prepare respectively star-pPRs and lin-pPRs. The supramolecular structure of each pPR was confirmed by thermogravimetric analyses (TGA), differential scanning calorimetry (DSC) and X-ray diffraction (XRD). However, significant differences have been observed between the two types of pPRs suggesting a dense CD coverage for star-pPR and only partial complexation for lin-pPR with uncovered PCL portions. Indeed, for lin-pPR, a melting temperature of 50°C, corresponding to the melting of pure PCL was measured whereas no thermal transition was observed for star-pPR (Figures S12-S15 in the Supp. Info.). XRD analysis also confirmed these results. For star-pPR, the characteristic peak at $2\theta = 20°$ due to the CD channel-like crystals formed by the pPR rotaxane portions[7] is very sharp and is by far the prevailing peak. In contrast, for lin-pPR, the peaks corresponding to PCL crystal domains (i.e. the peaks corresponding to naked portions of lin-pPR uncovered by the CDs) are in this case the peaks which dominate the diffractogram (Figure S17 in the Supp. Info.). Additionally, ^{1}H NMR spectroscopy supported the previous observations as ε-caprolactone over α-cyclodextrin (ε-CL:α-CD) ratios of 11:1 and 2:1 were found for lin-pPR and star-pPR, respectively (Figures S3 and S5 in the Supp. Info.).

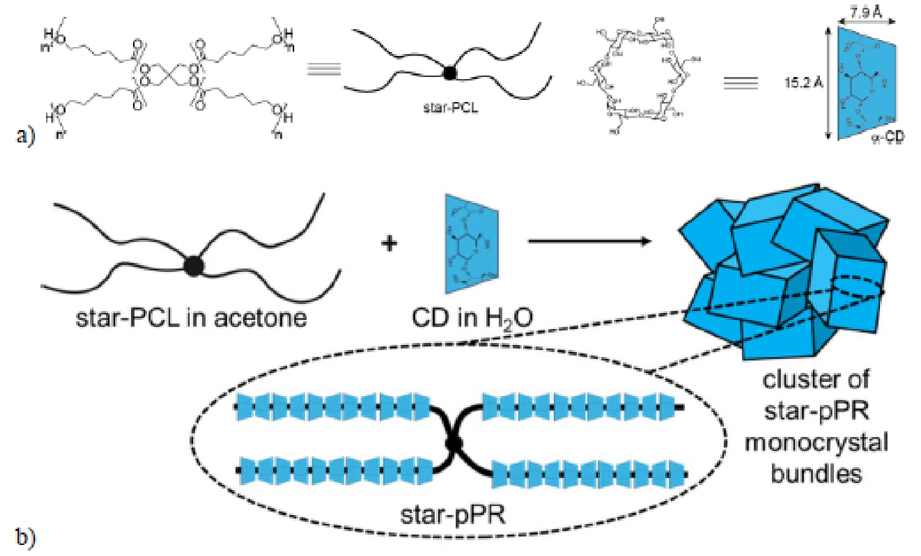

Scheme 1: a) Scheme of the used molecules. b) General scheme of the synthesis of star-pPRs in the form of clusters of randomly organized monocrystal star-pPR bundles.

The structure and the stability of the supramolecular assembly of pPRs in solvents are of prime importance for their processing by electrospinning and more generally for their use as building blocks in nanomaterials. Thus, one has to find a solvent that allows the dispersion and organization of the pPRs polycrystals clusters into nanodomains while keeping the pPR supramolecular assembly intact. Therefore, we tested different polar solvents that could potentially break the hydrogen bonding responsible for the aggregation of the pPR bundles in the clusters. Acetone, dichloromethane, chloroform, methanol, ethanol, dimethylformamide, and tetrahydrofuran were not efficient and led to white suspensions proving the presence of large aggregates. DMSO was the only solvent that led to transparent pPR suspensions without any sign of visible aggregates. However, to obtain a totally transparent solution, the mixture of pPR and DMSO needed to be heated between 30 and 35°C. Below 30°C, few aggregates were still observed. In the case of lin-pPR, a concentration $c \leq 5$ w% was necessary to achieve the transparency of the suspension. However, when these solutions were cooled down to room temperature, they became turbid within less than an hour. In the case of star-pPR, solutions up to a concentration of 10 w% were easily soluble and stayed transparent for several hours at room temperature. To elucidate the structure and the peculiar behavior of pPR in DMSO, SANS experiments were carried out in DMSO-d_6 for temperatures ranging from 35 to 50°C. In the case of lin-pPR, even at the lowest tested temperature (i.e. $T = 35$ °C), it was observed that the scattered intensity profile corresponded exactly to the sum of the profile of linear PCL chains and free CDs. This proved that CD dethreading occurred (Fig. S18 in the Supp. Info.). This behavior, generally admitted for pPRs in DMSO, explained the suspension turbidity when its temperature was decreased to 20°C due to the presence of uncovered PCL chains. Indeed, observations showed that pristine PCL was not soluble in DMSO at temperature lower than 30°C and appeared as white precipitates. Star-pPRs, pristine CDs and star-PCL, as well as a blend of CDs and star-PCL directly prepared in DMSO-d6 (i.e. without the complexation step) were then examined by SANS. The scattered intensity profiles obtained at 40 and 50°C are almost the same than the mixture of uncomplexed CD and PCL (Figures 1a and S19 in Supp. Info.). This result showed that for temperatures higher than 40 °C, a high amount of CD dethreading occurred. However, at 35°C, although the suspension of star-pPR in DMSO was transparent to the eyes, an excess of scattering intensity is shown at low *q*-range suggesting aggregation of star-pPRs. Furthermore, in agreement with macroscopic observations, the scattered intensity profile was constant during more than 7 hours showing the high stability of the structures formed in DMSO at 35°C. A similar behavior was already observed for other types of pseudopolyrotaxane[14, 15] or polyrotaxane[16] for which lateral association between the rotaxane portions led to self-organization in nano-bundles or nano-platelets. By analogy, a parallelepiped model was used to fit the SANS data. A thickness $L = 95 \pm 5$ Å and a lateral size $W = 300 \pm 100$ Å allowed the fitting (Figures 1 and S19 and details of SANS analysis in the Supp. Info). Knowing that the length of an α-CD is 7.9 Å and its outer diameter is 15.2 Å, the model suggests that star-pPRs are organized in the form of nanoplatelets with roughly 20 CDs in their width W and 11 aligned CDs in their thickness L. Furthermore, the L value is in agreement with the extended length of a star-PCL branch. As suggested in Figure 1b, the nanoplatelets have probably a micellar structure. The pPR channel organization prevented the CD dethreading of the inner part of the micelle, while CD dethreading of outer branches left naked PCL chains that stabilized the micelles.

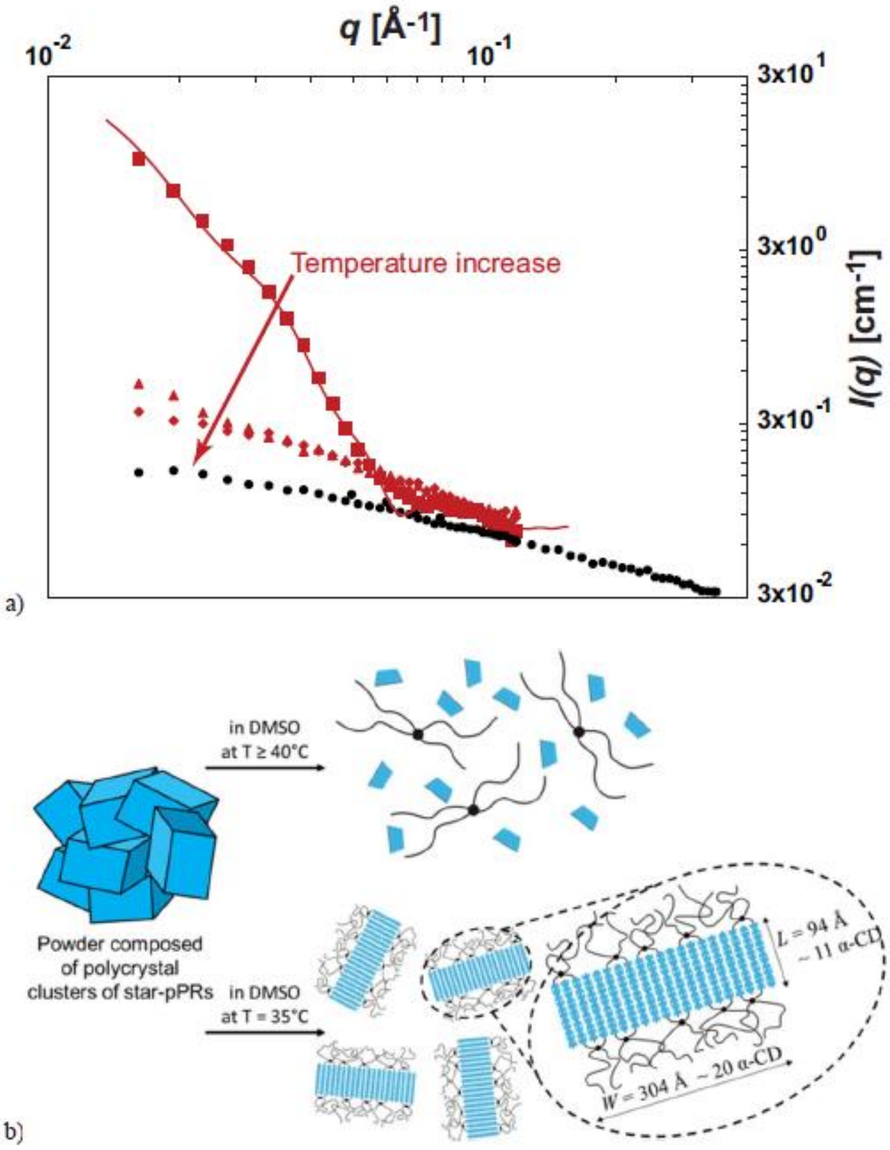

Figure 1. a) Absolute scattering intensity *I(q)* versus modulus of the scattering vector *q* obtained by SANS of star-pPR in DMSO-d6. ■ star-pPR at 35°C and its fitting by a parallelepiped model with $L = 94$ Å and $W = 300$ Å (red solid line), ▲ star-pPR at 40°C, ♦ star-pPR at 50°C, • mixture of star-PCL and free α-CD at 35°C. b) Proposed structure of the star-pPR in DMSO as a function of the temperature.

2.2. Elaboration of functional star-pPR based nanofibers

To the best of our knowledge, only poly(ethylene oxyde)-based pseudopolyrotaxanes were processed by electrospinning to elaborate nanofibers[21] but no functionalization was carried out. Here, PCL:pPR core:shell fibers were produced by coaxial electrospinning. When using a PCL core solution, the resulting fibers were ensured to present suitable mechanical properties regarding potential biomedical applications while by using pPR solutions for the shell, the reactive CD hydroxyl groups are expected to be on the fiber surface in order to facilitate the post-functionalization. Furthermore, knowing that electrospinning needs homogeneous polymer solutions and well-dispersed suspensions for the preparation of composite nanofibers[22], coaxial electrospinning appeared as the best strategy allowing to adapt the solvent for each polymer. Thus, for the core solution, 15w% of PCL was solubilized in a 60/40 w/w mixture of DCM/DMF whereas concentrations of 5, 10 and 15w% of pPRs in DMSO were prepared and resulted in PCL:pPR solid weight ratios in the fibers of respectively 10:1, 10:2 and 10:3. Observations by scanning electron microscopy (SEM) revealed two populations of fibers with average diameters d_S and d_L (Table S2 and Figures S22-S25 in the Supp. Info.). This morphology may be due to the lower solubility of PCL in DMF which, however, was added to DCM for continuous and stable production[23]. It is worth noting that because the lin-pPR shell solutions were not homogeneous for periods of production shorter than one hour, scaffolds with numerous thick fibers were obtained. For star-pPR based fibers, all solutions were transparent for several hours leading to stable production. XRD carried out on the 10:3 PCL:star-pPR fibers showed a distinct peak at $2\theta=20°$ due to rotaxane crystals (Figure S20a in the Supp. Info.). This pPR peak was small compared to the peaks of PCL crystal as the PCL/star-pPR weight ratio was at least 3.33 if one assumes that no CD dethreading occurred. No peak at $2\theta=20°$ was observed for the two lowest concentrations of star-pPR. Nevertheless, it is safe to assume that as a distinct peak can be seen for the 10:3 PCL:star-pPR membrane, star-pPRs are also still intact in the 10:1 and 10:2 PCL:star-pPR membranes.

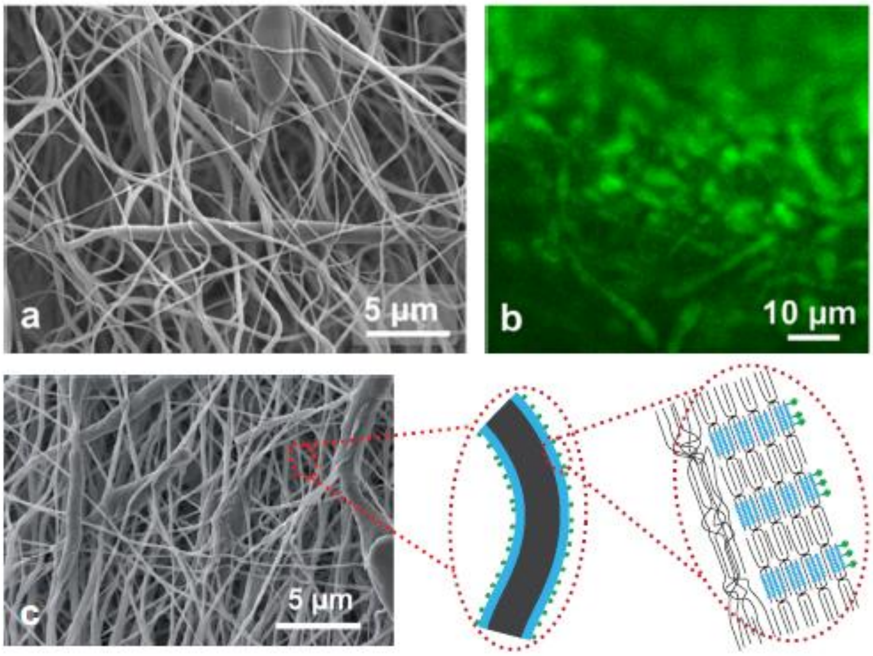

Figure 2. a) SEM images of PCL:star-pPR 10:2 core:shell fibers after FITC grafting. b) Fluorescent confocal images of the same fibers. c) Hierarchical structure of the PCL:star-pPR core:shell fibers modified with FITC. The figure shows also a SEM picture of PCL:star-pPR 10:1 core:shell fibers.

To prove the presence of CD hydroxyl groups at the fiber surface, FITC was grafted after the electrospinning step. All pPR based membranes as well as a neat PCL membrane were let to react for 4 hours with an FITC solution of 10^{-6} mol.L^{-1} in a 1:1 mixture of $CH_3CN:H_20$. SEM images revealed that the reaction mixture and the FITC grafting did not affect the morphology of star-pPR based coaxial fibers (Figure 2a and S26 in the Supp. Info.) whereas the fibrous structure of the neat PCL membrane and those elaborated from lin-pPR were completely destroyed by the chemical treatment (Figures S27-S28 in the Supp. Info.). As revealed by confocal fluorescent microscopy (Figures 2b and S29 in the Supp. Info.), only membranes presenting a shell of star-pPR showed fluorescence. The absence of fluorescence for lin-pPR membranes could be explained by the CD dethreading in DMSO during electrospinning leading to the CD leaching during the FITC grafting. Furthermore, stronger fluorescent intensity was observed for the highest star-pPR amount in the shell fibers due to higher number of accessible and reactive hydroxyl functions. Hence, these results demonstrated that only star-pPR can be successfully used to produce functional fibers. Moreover, star-pPRs acted as a shield toward solvents by protecting the fibers during chemical treatments.

3. Conclusions

In conclusion, star-pPRs based on α-CDs and four branched star-PCL were successfully synthesized. As opposed to lin-pPRs, the supramolecular structure of star-pPRs is stable in DMSO due to their organization in nanoplatelet micelles. It was hypothesized that naked PCL branches stabilized the external part of the micelle whereas rotaxane branches were localized in the central part of the micelle and blocked by the core of the star PCL. The star-pPR organization allowed their processing by coaxial electrospinning for several hours under stable conditions. PCL:star-pPR core:shell fibers were then produced and their surface was subsequently modified by FITC grafting onto the cyclodextrin hydroxyl functions leading to the hierarchical structure as shown in Figure 2c. The star-pPR shell of the fibers acted as a shield during the chemical treatment ensuring the stability of the membrane morphology. This original strategy paves the way to any easy functionalization reaction with various bioactive molecules onto PCL-based scaffolds for biomedical applications.

Acknowledgments: The authors thank the French Agence Nationale de la Recherche (ANR) (ANR Blanc 2011 Project FibRotaxanes) for the financial support. Michel Schmitt and Lydie Séon are also acknowledged for the NMR analysis and fluorescent confocal microscopy respectively.

Received: Month XX, XXXX; Revised: Month XX, XXXX; Published online:
((For PPP, use "Accepted: Month XX, XXXX" instead of "Published online")); DOI: 10.1002/marc.((insert number)) ((or ppap., mabi., macp., mame., mren., mats.))

Keywords: polyrotaxane; cyclodextrin; self-assembling; electrospinning;

The table of contents entry

Star pseudo-polyrotaxanes (star-pPR) of α-cyclodextrin (CD) and star poly(ε-caprolactone) (star-PCL) formed stable nanoplatelet micelles in dimethyl sulfoxide (DMSO) and were subsequently processed by coaxial electrospinning to obtain PCL:star-pPR core:shell fibers. The star-pPR shell ensured the presence of CD hydroxyl functions on the fiber surface allowing efficient post-functionalization while keeping intact the entire morphology of the fibrous scaffold in solvents.

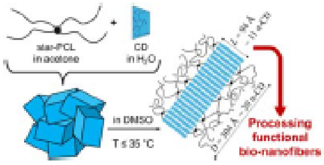

FIGURE FOR ToC_ABSTRACT

[1] G. Wenz, B.-H. Han, A. Müller, *Chemical Review* **2006**, *106*, 782.
[2] H. Hyun, N. Yui, *Macromolecular Rapid Communications* **2011**, *32*, 326.
[3] S. Yu, Y. Zhang, X. Wang, X. Zhen, Z. Zhang, W. Wu, X. Jiang, *Angew. Chem. Int. Ed.* **2013**, *52*, 7272.
[4] J. Li, C. Yang, H. Li, X. Wang, S. H. Goh, J. L. Ding, D. Y. Wang, K. W. Leong, *Advanced Materials* **2006**, *18*, 2969.
[5] J. Araki, *Journal of Polymer Science, Part A: Polymer Chemistry* **2011**, *49*, 2199.
[6] A. Harada, Y. Kawaguchi, T. Nishiyama, M. Kamachi, *Macromolecular Rapid Communications* **1997**, *18*, 535.
[7] L. Huang, E. Allen, A. E. Tonelli, *Polymer* **1998**, *39*, 4857.
[8] L. U. Wang, J. L. Wang, C.-M. Dong, *Journal of Polymer Science, Part A: Polymer Chemistry* **2005**, *43*, 4721.
[9] A. Cipitria, A. Skelton, T. R. Dargaville, P. D. Dalton, D. W. Hutmacher, *Journal of Materials Chemistry* **2011**, *21*, 9419.
[10] I. Engelberg, J. Kohn, *Biomaterials* **1991**, *12*, 292.
[11] M. A. Woodruff, D. W. Hutmacher, *Progress in Polymer Science (Oxford)* **2010**, *35*, 1217.
[12] J. Lu, P. A. Mirau, A. E. Tonelli, *Macromolecules* **2001**, *34*, 3276.
[13] C. C. Rusa, J. Fox, A. E. Tonelli, *Macromolecules* **2003**, *36*, 2742.
[14] C. Travelet, G. Schlatter, P. Hébraud, C. Brochon, A. Lapp, G. Hadziioannou, *Langmuir* **2009**, *25*, 8723.
[15] C. Perry, P. Hébraud, V. Gernigon, C. Brochon, A. Lapp, P. Lindner, G. Schlatter, *Soft Matter* **2011**, *7*, 3502.
[16] C. Travelet, P. Hébraud, C. Perry, C. Brochon, G. Hadziioannou, A. Lapp, G. Schlatter, *Macromolecules* **2010**, *43*, 1915.

[17] A. Harada, J. Li, M. Kamachi, *Nature* **1994**, *370*, 126.

[18] A. Harada, J. Li, T. Nakamitsu, M. Kamachi, *Journal of Organic Chemistry* **1993**, *58*, 7524.

[19] S. Samitsu, J. Araki, T. Kataoka, K. Ito, *Journal of Polymer Science, Part B: Polymer Physics* **2006**, *44*, 1985.

[20] J. W. Chung, T. J. Kang, S.-Y. Kwak, *Macromolecules* **2007**, *40*, 4225.

[21] T. Uyar, P. Kingshott, F. Besenbacher, *Angew. Chem. Int. Ed.* **2008**, *47*, 9108.

[22] F. Mitschang, H. Schmalz, S. Agarwal, A. Greiner, *Angew. Chem. Int. Ed.* **2014**, *53*, 4972.

[23] D. Ahirwal, A. Hébraud, R. Kadar, M. Wilhelm, G. Schlatter, *Soft Matter* **2013**, *9*, 3164.

Articles

- Oster M., Hébraud A., Pollet E., Gallet S., Lapp A., Avérous L., Schlatter G., *" Star pseudopolyrotaxanes organized in nanoplatelet micelles for poly(ε-caprolactone)-based nanofibrous scaffolds with enhanced surface reactivity"*, submitted in Macromolecular Rapid Communications

- Oster M., Hébraud A., Pollet E., Gallet S., Avérous L, Schlatter G., *" Miktoarm star pseudo-polyrotaxanes for the elaboration of functional nanofibres"*, to be submitted in Polymer.

- Oster M., Séon L., Ouerghemmi S., Hébraud A., Boulmedais F., Lavalle P., Schaaf P., Schlatter G., *"Antimicrobial nanofibres based on polyelectrolyte complexes of natural polysaccharides", in preparation.*

International Communications

2014 Murielle Oster, Anne Hébraud, Christophe Fajolles, Guy Schlatter, *α-cyclodextrin/poly(ε-caprolactone) star and miktoarm star pseudo-polyrotaxanes for nanofibrous scaffolds with enhanced surface reactivity*, ***International Cyclodextrin Symposium***, ***ICS17***, Saarbrücken, Germany, May 2014

2013 Murielle Oster, Anne Hébraud, Eric Pollet, Sébastien Gallet, Alain Lapp, Luc Avérous, Guy Schlatter, *Elaboration of PCL-based pseudo-polyrotaxanes fibrous membranes for potential biomedical applications* ***European Congress of Polymer***, Pisa, Italy, June 2013

2012 Murielle Oster, Anne Hébraud, Eric Pollet, Alain Lapp, Luc Avérous, Guy Schlatter, *Elaboration of electrospun nanoporous fibres based on poly(ε-caprolactone) and α- or β-cyclodextrin pseudo-polyrotaxanes for bone regeneration*, ***Suprachem***, Strasbourg, September 2012

Murielle Oster, Anne Hébraud, Eric Pollet, Luc Avérous, Guy Schlatter, *Elaboration of electrospun nanoporous fibres based on poly(ε-caprolactone) and α-cyclodextrin pseudo-polyrotaxanes****, IOP conference***, London, England, March 2012

National Communication

2012 Murielle Oster, Anne Hébraud, Eric Pollet, Alain Lapp, Luc Avérous, Guy Schlatter, *Elaboration of pseudo-polyrotaxane based fibrous membranes for bone regeneration,* ***Groupe Français des Polymères***, Grenoble, France, November 2012

Note. For the oral communications, the person who presented the work is underligned.

Elaboration de nanofibres fonctionnelles à base de cyclodextrines pour des applications biomédicales

Les membranes nanofibreuses obtenues par électro-filage sont couramment utilisées pour diverses applications biomédicales telles que les pansements ou la régénération tissulaire, en raison de leur grande porosité et de leur morphologie mimant la structure des tissus humains. Au cours de cette thèse, nous avons étudié deux stratégies différentes, toutes deux basées sur l'utilisation de la cyclodextrine, pour fonctionnaliser ces membranes avec des molécules d'intérêt biologique.

Dans un premier temps, des membranes nanofibreuses à base de complexe de polyélectrolyte ont été élaborées à partir de carboxyméthylcellulose et de chitosane pour des applications de type pansements. Du bleu de méthylène, connu pour son activité antibactérienne, a été incorporé dans les fibres, seul ou en tant que complexe d'inclusion avec la cyclodextrine. Les tests préliminaires sont très prometteurs quant à l'efficacité bactéricide de ces matériaux. Une seconde approche visant à élaborer des nanofibres fonctionnelles à base de poly(ε-caprolactone) (PCL) a également été étudiée. Le PCL étant très peu fonctionnalisable, des complexes d'inclusion entre ce polyester et les cyclodextrines, appelés pseudo-polyrotaxanes (pPR), ont été préparés. Des fibres cœur:peau ont ensuite été produites en ajoutant les pPR en surface des fibres. Afin de vérifier la réactivité et l'accessibilité des fonctions hydroxyles des cyclodextrines, un fluorophore a été greffé sur les fibres. Ce type de réaction ouvre de nouvelles voies de fonctionnalisation des fibres de PCL jusqu'alors inexplorées.

Elaboration of cyclodextrin based functional nanofibres for biomedical applications

Electrospun nanofibrous membranes have proven to be ideal scaffolds for biomedical applications such as wound dressing and tissue engineering, mostly due to their high porosity and their morphology that mimics the structure of human tissues. In this work, we investigated two different strategies based on the use of cyclodextrins to functionalize these scaffolds with molecules of interest.

Scaffolds made of polyelectrolyte complexes of carboxymethylcellulose and chitosan were first prepared by blend or coaxial electrospinning for wound dressing applications. Methylene blue, a molecule known to present antibiotic activity, was added, alone or as an inclusion complex with cyclodextrin, in the polymer solution before electrospinning. The preliminary biological assessment suggested that the fibrous membranes exhibited good antibacterial activity. In a second part, electrospun poly(ε-caprolactone) (PCL) scaffolds were prepared for tissue engineering applications. As this polyester can not easily be functionalized, PCL and cyclodextrins were combined to form pseudo-polyrotaxanes (pPRs) with various architectures. Core:shell PCL:pPR fibres were prepared by coaxial electrospinning. Fluorescein isothiocyanate was then grafted onto the fibre surface to prove the presence of available and reactive cyclodextrin hydoxyl groups at the surface of the PCL fibres. This reaction opens the way for innovative and versatile biofunctionalization of PCL.